

Investigation of the Steric and/or Electronic Effects  
Associated with the (1,5)-Sigmatropic Rearrangement of  
1-substituted-2,3,4,5-tetraphenyl-2,4-cyclopentadien-1-ols

by

Robert Lee Eagan

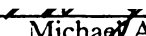
Dissertation submitted to the Faculty of the  
Virginia Polytechnic Institute and State University  
in partial fulfillment of the requirements for the degree of

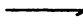
Doctor of Philosophy

in

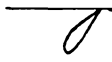
Chemistry


APPROVED:

  
Michael A. Ogliaruso, Chairman

  
Harold M. Bell

  
David G.I. Kingston

  
John G. Mason

  
James P. Wightman

May, 1986

Blacksburg, Virginia

**Investigation of the Steric and/or Electronic Effects  
Associated with the (1,5)-Sigmatropic Rearrangement of  
1-Substituted-2,3,4,5-tetraphenyl-2,4-cyclopentadien-1-ols**

by

Robert Lee Eagan

Michael A. Ogliaruso, Chairman

Chemistry

(ABSTRACT)

A series of eight 1-substituted-2,3,4,5-tetraphenyl-2,4-cyclopentadien-1-ols were efficiently synthesized by the addition of the appropriate organometallic reagent to tetracyclone. It was determined that the steric and electronic nature of the migrating groups played a predictable role in the [1,5]-sigmatropic rearrangement of these compounds. Electron donating groups increased the rate of migration whereas electron withdrawing substituents were responsible for slowing the migration. Likewise, smaller groups accelerated the rate while bulky groups deterred the migration. Consequently, the experimental evidence supports the originally proposed charge separated transition state.

The Michael addition of potassium cyanide to tetracyclone afforded upon protonation a diastereomeric mixture of the *cis* (kinetic product) and the *trans* (thermodynamic product) 4-cyano-2,3,4,5-tetraphenyl-2-cyclopenten-1-ones. Finally an efficient synthesis of 2,3,4,5-tetraphenyl-2(1H)-pyridinone (90%) resulted from the acid promoted addition of sodium azide to tetracyclone. The presence of an intermediate bicyclic triazoline eliminated the Schmitt mechanism as a viable reaction pathway.

## Acknowledgements

I would like to thank Dr. Ogliaruso ( Dean "O" ) for his encouragement throughout this project and for all the invaluable advice he has given me while at Virginia Tech.

I am grateful to Dr.'s Bell, Kingston, McNair, Mason and Wightman for donating their time to serve on my committee and for their comments and suggestions concerning this dissertation.

I would like to thank my friend, \_\_\_\_\_, for all the help, encouragement and advice he has given me since I became a member of \_\_\_\_\_ research group. It would be an honor and a pleasure to be able to work with him again in the future.

Many thanks to \_\_\_\_\_ for their friendship and encouragement throughout this ordeal.

I would like to thank analytical services (especially \_\_\_\_\_) for their help in obtaining NMR spectra and I am very grateful to \_\_\_\_\_ (Merck, Sharp and Dohme research laboratories) for doing the X-ray crystal structures mentioned in this dissertation.

I would like to thank \_\_\_\_\_ and \_\_\_\_\_ for all the in-depth discussions of chemistry (as well as other topics) that we have shared on the golf links. Perhaps our best ideas originated while trying to break par.

I would like to acknowledge \_\_\_\_\_ for showing me how to do chemistry the right way. Many of the lab techniques that I have learned are a direct result of observing him in action.

I am eternally grateful to my parents for their continuing support throughout my lengthy pursuit for my Ph.D. in chemistry. I'm sorry it's taken so long. Perhaps the next one will be quicker.

Last, I am very thankful to have a cousin like . Without her help and support this dissertation may never have been finished. I only hope that someday I can repay her.

# Table of Contents

<b>Introduction</b> .....	<b>1</b>
<b>Historical</b> .....	<b>3</b>
<b>Results and Discussion</b> .....	<b>16</b>
Synthesis of 1-Substituted tetraphenylcyclopentadienols .....	16
Synthesis of 2-substituted tetraphenylcyclopentenones .....	18
Kinetic Investigation .....	21
Reactions with potassium cyanide and Triton B .....	104
Reactions with sodium azide .....	112
<b>Summary</b> .....	<b>118</b>
<b>Experimental</b> .....	<b>120</b>
General Procedures .....	120
Synthesis of 1-substituted tetraphenylcyclopentadienols .....	121
Synthesis of 2-substituted tetraphenylcyclopentenones .....	126

Kinetic investigation .....	130
Reactions with potassium cyanide and triton B .....	131
Reactions with sodium azide .....	136
Crystallographic Analysis .....	141
<b>Literature Cited .....</b>	<b>143</b>
<b>Appendix .....</b>	<b>145</b>
<b>Vita .....</b>	<b>169</b>

# List of Figures

<u>Figure</u>		<u>Page</u>
1	[1,5]-Sigmatropic Shift of Carbon .....	6
2	First-order plot of the isomerization of 1,2,3,4,5-pentaphenyl-2,4-cyclopentadien-1-ol (2) @ 175.0 ± 0.4 °C .....	50
3	First-order plot of the isomerization of 1,2,3,4,5-pentaphenyl-2,4-cyclopentadien-1-ol (2) @ 190.0 ± 0.4 °C .....	51
4	First-order plot of the isomerization of 1,2,3,4,5-pentaphenyl-2,4-cyclopentadien-1-ol (2) @ 205.0 ± 0.4 °C .....	52
5	First-order plot of the isomerization of 1,2,3,4,5-pentaphenyl-2,4-cyclopentadien-1-ol (2) @ 175.0 - 205.0 °C .....	53
6	Arrhenius plot of the isomerization of 1,2,3,4,5-pentaphenyl-2,4-cyclopentadien-1-ol (2) .....	54
7	Eyring plot of the isomerization of 1,2,3,4,5-pentaphenyl-2,4-cyclopentadien-1-ol (2) .....	55
8	First-order plot of the isomerization of 1-(1-naphthyl)-2,3,4,5-tetraphenyl-2,4-cyclopentadien-1-ol (24) @ 205.0 ± 0.4 °C .....	56
9	First-order plot of the isomerization of 1-(1-naphthyl)-2,3,4,5-tetraphenyl-2,4-cyclopentadien-1-ol (24) @ 220.0 ± 0.4 °C .....	57
10	First-order plot of the isomerization of 1-(1-naphthyl)-2,3,4,5-tetraphenyl-2,4-cyclopentadien-1-ol (24) @ 235.0 ± 0.4 °C .....	58
11	First-order plot of the isomerization of 1-(1-naphthyl)-2,3,4,5-tetraphenyl-2,4-cyclopentadien-1-ol (24) @ 205.0 - 235.0 °C .....	59
12	Arrhenius plot of the isomerization of 1-(1-naphthyl)-2,3,4,5-tetraphenyl-2,4-cyclopentadien-1-ol (24) .....	60
13	Eyring plot of the isomerization of 1-(1-naphthyl)-2,3,4,5-tetraphenyl-2,4-cyclopentadien-1-ol (24) .....	61

<u>Figure</u>	<u>Page</u>
14 First-order plot of the isomerization of 1-(2-pyridyl)-2,3,4,5-tetraphenyl-2,4-cyclopentadien-1-ol ( <b>25</b> ) @ 145.0 ± 0.4 °C .....	62
15 First-order plot of the isomerization of 1-(2-pyridyl)-2,3,4,5-tetraphenyl-2,4-cyclopentadien-1-ol ( <b>25</b> ) @ 160.0 ± 0.4 °C .....	63
16 First-order plot of the isomerization of 1-(2-pyridyl)-2,3,4,5-tetraphenyl-2,4-cyclopentadien-1-ol ( <b>25</b> ) @ 175.0 ± 0.4 °C .....	64
17 First-order plot of the isomerization of 1-(2-pyridyl)-2,3,4,5-tetraphenyl-2,4-cyclopentadien-1-ol ( <b>25</b> ) @ 145.0 - 175.0 °C .....	65
18 Arrhenius plot of the isomerization of 1-(2-pyridyl)-2,3,4,5-tetraphenyl-2,4-cyclopentadien-1-ol ( <b>25</b> ) .....	66
19 Eyring plot of the isomerization of 1-(2-pyridyl)-2,3,4,5-tetraphenyl-2,4-cyclopentadien-1-ol ( <b>25</b> ) .....	67
20 First-order plot of the isomerization of 1-(2-furyl)-2,3,4,5-tetraphenyl-2,4-cyclopentadien-1-ol ( <b>26</b> ) @ 175.0 ± 0.4 °C .....	68
21 First-order plot of the isomerization of 1-(2-furyl)-2,3,4,5-tetraphenyl-2,4-cyclopentadien-1-ol ( <b>26</b> ) @ 190.0 ± 0.4 °C .....	69
22 First-order plot of the isomerization of 1-(2-furyl)-2,3,4,5-tetraphenyl-2,4-cyclopentadien-1-ol ( <b>26</b> ) @ 205.0 ± 0.4 °C .....	70
23 First-order plot of the isomerization of 1-(2-furyl)-2,3,4,5-tetraphenyl-2,4-cyclopentadien-1-ol ( <b>26</b> ) @ 175.0 - 205.0 °C .....	71
24 Arrhenius plot of the isomerization of 1-(2-furyl)-2,3,4,5-tetraphenyl-2,4-cyclopentadien-1-ol ( <b>26</b> ) .....	72
25 Eyring plot of the isomerization of 1-(2-furyl)-2,3,4,5-tetraphenyl-2,4-cyclopentadien-1-ol ( <b>26</b> ) .....	73
26 First-order plot of the isomerization of 1-(2-thienyl)-2,3,4,5-tetraphenyl-2,4-cyclopentadien-1-ol ( <b>27</b> ) @ 175.0 ± 0.4 °C .....	74
27 First-order plot of the isomerization of 1-(2-thienyl)-2,3,4,5-tetraphenyl-2,4-cyclopentadien-1-ol ( <b>27</b> ) @ 190.0 ± 0.4 °C .....	75
28 First-order plot of the isomerization of 1-(2-thienyl)-2,3,4,5-tetraphenyl-2,4-cyclopentadien-1-ol ( <b>27</b> ) @ 205.0 ± 0.4 °C .....	76
29 First-order plot of the isomerization of 1-(2-thienyl)-2,3,4,5-tetraphenyl-2,4-cyclopentadien-1-ol ( <b>27</b> ) @ 175.0 - 205.0 °C .....	77
30 Arrhenius plot of the isomerization of 1-(2-thienyl)-2,3,4,5-tetraphenyl-2,4-cyclopentadien-1-ol ( <b>27</b> ) .....	78
31 Eyring plot of the isomerization of 1-(2-thienyl)-2,3,4,5-tetraphenyl-2,4-cyclopentadien-1-ol ( <b>27</b> ) .....	79



<u>Figure</u>	<u>Page</u>
32 First-order plot of the isomerization of 1-phenylethynyl-2,3,4,5-tetraphenyl-2,4-cyclopentadien-1-ol ( <b>28</b> ) @ 145.0 ± 0.4 °C ...	80
33 First-order plot of the isomerization of 1-phenylethynyl-2,3,4,5-tetraphenyl-2,4-cyclopentadien-1-ol ( <b>28</b> ) @ 160.0 ± 0.4 °C ...	81
34 First-order plot of the isomerization of 1-phenylethynyl-2,3,4,5-tetraphenyl-2,4-cyclopentadien-1-ol ( <b>28</b> ) @ 175.0 ± 0.4 °C ...	82
35 First-order plot of the isomerization of 1-phenylethynyl-2,3,4,5-tetraphenyl-2,4-cyclopentadien-1-ol ( <b>28</b> ) @ 145.0 - 175.0 °C .	83
36 Arrhenius plot of the isomerization of 1-phenylethynyl-2,3,4,5-tetraphenyl-2,4-cyclopentadien-1-ol ( <b>28</b> ) .....	84
37 Eyring plot of the isomerization of 1-phenylethynyl-2,3,4,5-tetraphenyl-2,4-cyclopentadien-1-ol ( <b>28</b> ) .....	85
38 First-order plot of the isomerization of 1-vinyl-2,3,4,5-tetraphenyl-2,4-cyclopentadien-1-ol ( <b>29</b> ) @ 90.0 ± 0.4 °C .....	86
39 First-order plot of the isomerization of 1-vinyl-2,3,4,5-tetraphenyl-2,4-cyclopentadien-1-ol ( <b>29</b> ) @ 105.0 ± 0.4 °C .....	87
40 First-order plot of the isomerization of 1-vinyl-2,3,4,5-tetraphenyl-2,4-cyclopentadien-1-ol ( <b>29</b> ) @ 120.0 ± 0.4 °C .....	88
41 First-order plot of the isomerization of 1-vinyl-2,3,4,5-tetraphenyl-2,4-cyclopentadien-1-ol ( <b>29</b> ) @ 90.0 - 120.0 °C .....	89
42 Arrhenius plot of the isomerization of 1-vinyl-2,3,4,5-tetraphenyl-2,4-cyclopentadien-1-ol ( <b>29</b> ) .....	90
43 Eyring plot of the isomerization of 1-vinyl-2,3,4,5-tetraphenyl-2,4-cyclopentadien-1-ol ( <b>29</b> ) .....	91
44 First-order plot of the isomerization of 1- <i>tert</i> -butyl-2,3,4,5-tetraphenyl-2,4-cyclopentadien-1-ol ( <b>30</b> ) @ 145.0 ± 0.4 °C .....	92
45 First-order plot of the isomerization of 1- <i>tert</i> -butyl-2,3,4,5-tetraphenyl-2,4-cyclopentadien-1-ol ( <b>30</b> ) @ 160.0 ± 0.4 °C .....	93
46 First-order plot of the isomerization of 1- <i>tert</i> -butyl-2,3,4,5-tetraphenyl-2,4-cyclopentadien-1-ol ( <b>30</b> ) @ 175.0 ± 0.4 °C .....	94
47 First-order plot of the isomerization of 1- <i>tert</i> -butyl-2,3,4,5-tetraphenyl-2,4-cyclopentadien-1-ol ( <b>30</b> ) @ 145.0 - 175.0 °C .....	95
48 Arrhenius plot of the isomerization of 1- <i>tert</i> -butyl-2,3,4,5-tetraphenyl-2,4-cyclopentadien-1-ol ( <b>30</b> ) .....	96
49 Eyring plot of the isomerization of 1- <i>tert</i> -butyl-2,3,4,5-tetraphenyl-2,4-cyclopentadien-1-ol ( <b>30</b> ) .....	97

<u>Figure</u>	<u>Page</u>
50 Arrhenius plot of the isomerization of 1-substituted-2,3,4,5-tetraphenyl-2,4-cyclopentadien-1-ols .....	98
51 Eyring plot of the isomerization of 1-substituted-2,3,4,5-tetraphenyl-2,4-cyclopentadien-1-ols .....	99
52 $E_a$ and precision estimates for the rearrangement of 1-substituted-2,3,4,5-tetraphenyl-2,4-cyclopentadien-1-ols .....	101
53 $\Delta S^\ddagger$ and precision estimates for the rearrangement of 1-substituted-2,3,4,5-tetraphenyl-2,4-cyclopentadien-1-ols .....	102
54 Computer generated drawing derived from the X-ray coordinates of <i>trans</i> -4-cyano-2,3,4,5-tetraphenyl-2-cyclopenten-1-one ( <b>40a</b> ) .....	108
55 Computer generated drawing derived from the X-ray coordinates of <i>cis</i> -2,3,4,5-tetraphenyl-4-cyano-5-methyl-2-cyclopenten-1-one ( <b>41</b> ) .....	109
56 Computer generated drawing derived from the X-ray coordinates of 1,5,8-triphenyl-7-methyl-2,3,4-triazabicyclo[3.3.0]octa-2,7-dien-6-one ( <b>45b</b> ) .....	116

# List of Tables

<u>Table</u>	<u>Page</u>
I Selection Rules for Thermal [1, j]-Sigmatropic Rearrangements .....	7
II Synthesis of 1-Substituted Tetraphenylcyclopentadienols .....	17
III Synthesis of 2-Substituted Tetraphenylcyclopentenones .....	20
IV The Isomerization of 1,2,3,4,5-Pentaphenyl-2,4-cyclopentadien-1-ol ( <b>2</b> ) @ 175.0 ± 0.4 °C .....	26
V The Isomerization of 1,2,3,4,5-Pentaphenyl-2,4-cyclopentadien-1-ol ( <b>2</b> ) @ 190.0 ± 0.4 °C .....	27
VI The Isomerization of 1,2,3,4,5-Pentaphenyl-2,4-cyclopentadien-1-ol ( <b>2</b> ) @ 205.0 ± 0.4 °C .....	28
VII The Isomerization of 1-(1-Naphthyl)-2,3,4,5-tetraphenyl-2,4-cyclopentadien-1-ol ( <b>24</b> ) @ 205.0 ± 0.4 °C ..	29
VIII The Isomerization of 1-(1-Naphthyl)-2,3,4,5-tetraphenyl-2,4-cyclopentadien-1-ol ( <b>24</b> ) @ 220.0 ± 0.4 °C ..	30
IX The Isomerization of 1-(1-Naphthyl)-2,3,4,5-tetraphenyl-2,4-cyclopentadien-1-ol ( <b>24</b> ) @ 235.0 ± 0.4 °C ..	31
X The Isomerization of 1-(2-Pyridyl)-2,3,4,5-tetraphenyl-2,4-cyclopentadien-1-ol ( <b>25</b> ) @ 145.0 ± 0.4 °C .....	32
XI The Isomerization of 1-(2-Pyridyl)-2,3,4,5-tetraphenyl-2,4-cyclopentadien-1-ol ( <b>25</b> ) @ 160.0 ± 0.4 °C .....	33
XII The Isomerization of 1-(2-Pyridyl)-2,3,4,5-tetraphenyl-2,4-cyclopentadien-1-ol ( <b>25</b> ) @ 175.0 ± 0.4 °C .....	34
XIII The Isomerization of 1-(2-Furyl)-2,3,4,5-tetraphenyl-2,4-cyclopentadien-1-ol ( <b>26</b> ) @ 175.0 ± 0.4 °C .....	35

<u>Table</u>	<u>Page</u>
XIV The Isomerization of 1-(2-Furyl)-2,3,4,5-tetraphenyl-2,4-cyclopentadien-1-ol (26) @ 190.0 ± 0.4 °C .....	36
XV The Isomerization of 1-(2-Furyl)-2,3,4,5-tetraphenyl-2,4-cyclopentadien-1-ol (26) @ 205.0 ± 0.4 °C .....	37
XVI The Isomerization of 1-(2-Thienyl)-2,3,4,5-tetraphenyl-2,4-cyclopentadien-1-ol (27) @ 175.0 ± 0.4 °C .....	38
XVII The Isomerization of 1-(2-Thienyl)-2,3,4,5-tetraphenyl-2,4-cyclopentadien-1-ol (27) @ 190.0 ± 0.4 °C .....	39
XVIII The Isomerization of 1-(2-Thienyl)-2,3,4,5-tetraphenyl-2,4-cyclopentadien-1-ol (27) @ 205.0 ± 0.4 °C .....	40
XIX The Isomerization of 1-Phenylethynyl-2,3,4,5-tetraphenyl-2,4-cyclopentadien-1-ol (28) @ 145.0 ± 0.4 °C .	41
XX The Isomerization of 1-Phenylethynyl-2,3,4,5-tetraphenyl-2,4-cyclopentadien-1-ol (28) @ 145.0 ± 0.4 °C .	42
XXI The Isomerization of 1-Phenylethynyl-2,3,4,5-tetraphenyl-2,4-cyclopentadien-1-ol (28) @ 175.0 ± 0.4 °C .	43
XXII The Isomerization of 1-Vinyl-2,3,4,5-tetraphenyl-2,4-cyclopentadien-1-ol (29) @ 90.0 ± 0.4 °C .....	44
XXIII The Isomerization of 1-Vinyl-2,3,4,5-tetraphenyl-2,4-cyclopentadien-1-ol (29) @ 105.0 ± 0.4 °C .....	45
XXIV The Isomerization of 1-Vinyl-2,3,4,5-tetraphenyl-2,4-cyclopentadien-1-ol (29) @ 120.0 ± 0.4 °C .....	46
XXV The Isomerization of 1- <i>tert</i> -Butyl-2,3,4,5-tetraphenyl-2,4-cyclopentadien-1-ol (30) @ 145.0 ± 0.4 °C .....	47
XXVI The Isomerization of 1- <i>tert</i> -Butyl-2,3,4,5-tetraphenyl-2,4-cyclopentadien-1-ol (30) @ 160.0 ± 0.4 °C .....	48
XXVII The Isomerization of 1- <i>tert</i> -Butyl-2,3,4,5-tetraphenyl-2,4-cyclopentadien-1-ol (30) @ 175.0 ± 0.4 °C .....	49
XXVIII $E_a$ , $\Delta H^\ddagger$ and $\Delta S^\ddagger$ for the [1,5]-Sigmatropic Rearrangement of 1-Substituted-2,3,4,5-tetraphenyl-2,4-cyclopentadien-1-ols .....	100
XXIX $k$ , $-\Delta G^\ddagger$ and $-E_a$ for the [1,5]-Sigmatropic Rearrangement of 1-Substituted-2,3,4,5-tetraphenyl-2,4-cyclopentadien-1-ols @ 175.0 °C .....	103
XXX Effect of Temperature and Solvent on Protonation of Enolates 38a and 38b .....	110
XXXI Thermodynamic Isomerization of Ketones 39 and 40 .....	111

# Introduction

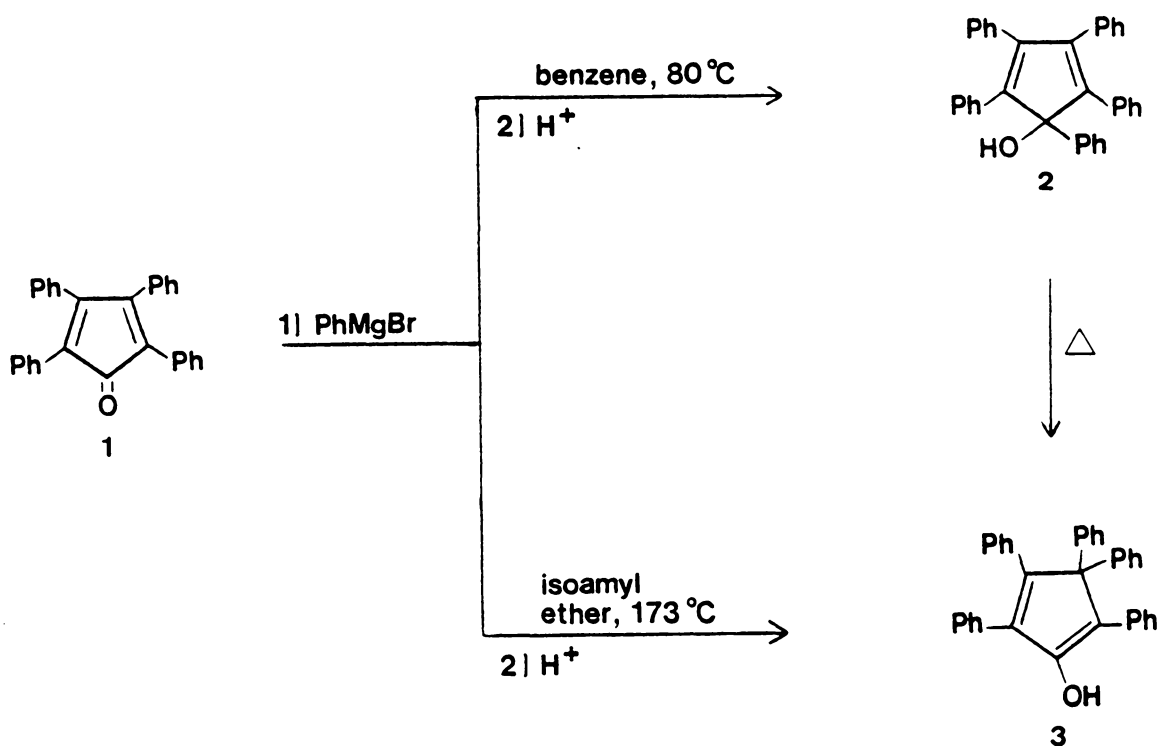
The thermally induced isomerization of 1,2,3,4,5-pentaphenyl-2,4-cyclopentadien-1-ol to 2,2,3,4,5-pentaphenyl-3-cyclopenten-1-one has been shown by Youssef and Ogliaruso<sup>1</sup> to be an example of a symmetry allowed [1,5]-sigmatropic phenyl rearrangement. In order to obtain more insight into the true nature of the transition state for this rearrangement, investigations were undertaken by Perfetti,<sup>2</sup> Oldaker<sup>2</sup> and Brubaker<sup>3</sup> to determine if the rearrangement was sensitive to electronic effects. Various *p*-substituted phenyl derivatives of 1,2,3,4,5-pentaphenyl-2,4-cyclopentadien-1-ol were evaluated in which the *p*-substituent was positioned at either the migration origin (migrating group), migration terminus or along the  $\pi$ -backbone of the cyclopentadienol ring system. They concluded from their results that there was no detectable linear free energy relationship with respect to the substituents at these positions. Consequently they proposed a transition state devoid of charge separation for the phenyl migration in this system.

The crux of this dissertation was a kinetic investigation of the [1,5]-sigmatropic rearrangement of a series of 1-substituted-2,3,4,5-tetraphenyl-2,4-cyclopentadien-1-ols. These compounds were prepared by the addition of a variety of organometallic reagents to tetracyclone. The nature of the migrating group was greatly varied in order to maximize any steric and/or electronic effects associated with the transition state of this rearrangement. Once the rates of rearrangement were experimentally determined, the activation energies ( $E_a$ ) and entropies of activation ( $\Delta S^\ddagger$ ) were calculated.

The results of this investigation are explained in terms of these parameters. However in the process of synthesizing the 1-substituted alcohols, it was determined that two nucleophiles (cyanide and azide) react with tetracyclone by a different mode of addition. Consequently, these reactions were studied to provide more insight into the chemistry of tetracyclone.

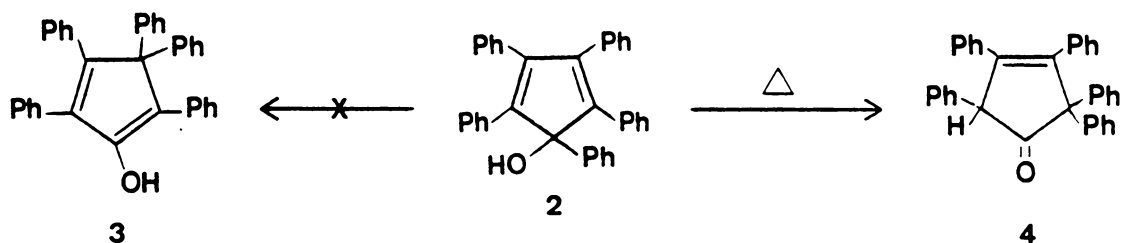
# Historical

In 1943, Allen and VanAllan<sup>4</sup> reported that the reaction of 2,3,4,5-tetraphenyl-2,4-cyclopentadien-1-one (1) with phenylmagnesium bromide produced different products depending upon the temperature at which the reaction was run. In refluxing benzene (ca. 80 °C), the product obtained from this reaction was 1,2,3,4,5-pentaphenyl-2,4-cyclopentadien-1-ol (2) resulting from 1,2-addition of the Grignard reagent. However at elevated temperatures (i.e. refluxing isoamyl

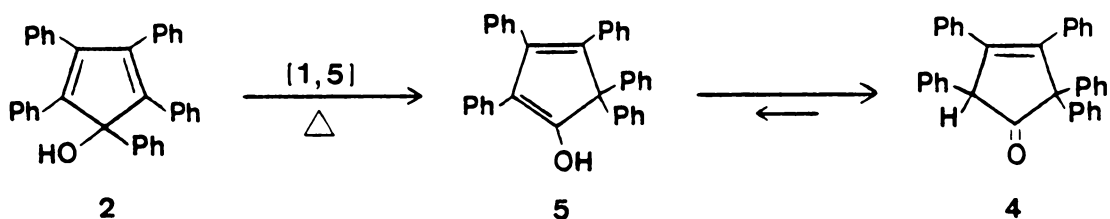


ether; ca. 173 °C), the product obtained was 2,3,3,4,5-pentaphenyl-1,4-cyclopentadien-1-ol (**3**) resulting from 1,4-addition of phenylmagnesium bromide. Furthermore, the 1,2-addition product (**2**) could be isomerized to the stable enol form (**3**) by heating at 290-300 °C in the absence of solvent or in refluxing isoamyl ether.

In 1961, Dufraisse, Rio and Ranjon<sup>5</sup> reinvestigated the thermal isomerization of **2** in the absence of solvent and found that, in addition to two minor products formed, the correct structure of the major product was not **3**, as previously reported, but rather 2,2,3,4,5-pentaphenyl-3-cyclopenten-1-one (**4**). They proposed that the formation of **4** from **2** was the result of a thermally induced pinacol rearrangement.



In 1972, Youssef and Ogliaruso<sup>1</sup> reinvestigated both the 1,4-addition of phenylmagnesium bromide to **1** and the thermal isomerization of **2**. However by this time, the rules concerning the conservation of orbital symmetry had been published by Woodward and Hoffmann<sup>6</sup> which provided a new mechanistic interpretation for this phenomenon. This rearrangement could now be classified as a thermally-allowed [1,5]-sigmatropic phenyl rearrangement followed by a rapid tautomerization of the initially formed enol structure (**5**) to the observed keto form (**4**).

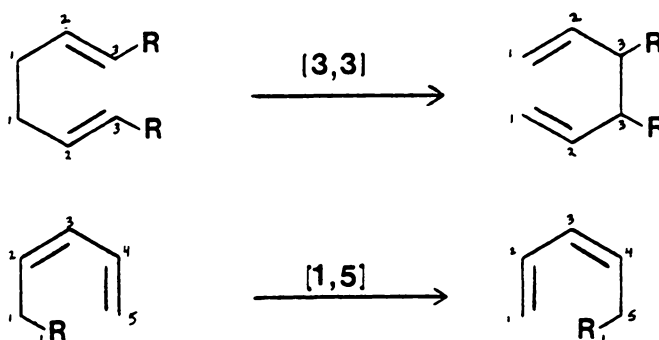


A sigmatropic rearrangement is an uncatalyzed, intramolecular process by which a  $\sigma$  bond, adjacent to one or more  $\pi$  systems, migrates to a new position in the molecule with the  $\pi$  system becoming reorganized in the process.<sup>7</sup> The rearrangement requires either thermal or photochemical initiation and the  $\sigma$  and  $\pi$  bonds shift in a concerted fashion with conservation of orbital



symmetry.<sup>8</sup> In a concerted process both bond-making and bond-breaking contribute to the structure of the transition state, although not necessarily to the same degree.<sup>9</sup>

The order of a sigmatropic rearrangement is designated by a pair of numbers in square brackets. The numbers refer to the change (if any) in the position of attachment of the ends of the  $\sigma$  bond in question. They can be determined by simply counting the atoms over which each end of the  $\sigma$  bond has moved in the rearrangement.<sup>7</sup> For example:



There are two geometrical pathways by which a sigmatropic rearrangement can take place. If the migrating group remains associated with the same face of the  $\pi$  system throughout the rearrangement, the migration is denoted as a suprafacial rearrangement. Alternatively, if the migrating group moves from one face of the  $\pi$  system to the opposite face during the rearrangement, this is termed an antarafacial rearrangement.<sup>7</sup>

However, in any given sigmatropic rearrangement, only one of the two pathways is allowed by the orbital symmetry rules; the other is forbidden. To determine whether a particular system will rearrange suprafacially or antarafacially, one must use a modified frontier orbital approach. The transition state is treated as if the  $\sigma$  bond was broken and the migrating group and the  $\pi$  system are free radicals.<sup>7</sup> In the transition state there is overlap between the highest occupied molecular orbital (HOMO) of one of the components and the HOMO of the other. Each HOMO is singly occupied and together they provide a pair of electrons<sup>10</sup>.

These rules are illustrated in Figure 1. In a [1,5]-migration of carbon, the symmetry of the HOMO of the allylic radical in the ground state (thermal rearrangement) dictates that the rearrangement occurs suprafacially with retention of configuration in the migrating group or antarafacially with inversion. However, in the excited state (photochemical rearrangement) the

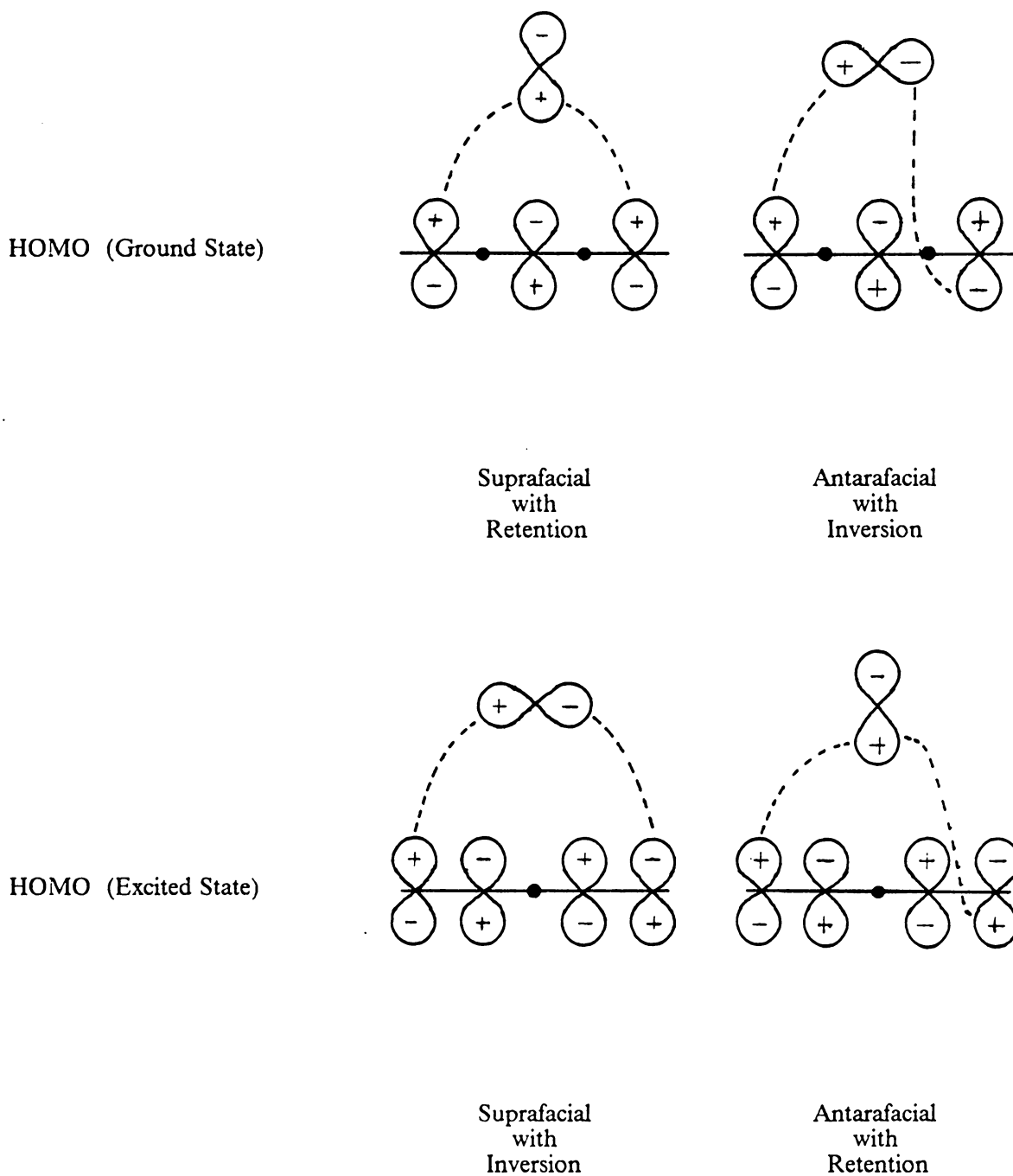


Figure 1. [1,5]-Sigmatropic Shift of Carbon.

symmetry of the HOMO is reversed and the migration occurs antarafacially with inversion or suprafacially with retention. The selection rules for neutral [1,j] thermal sigmatropic rearrangements are shown in Table I.

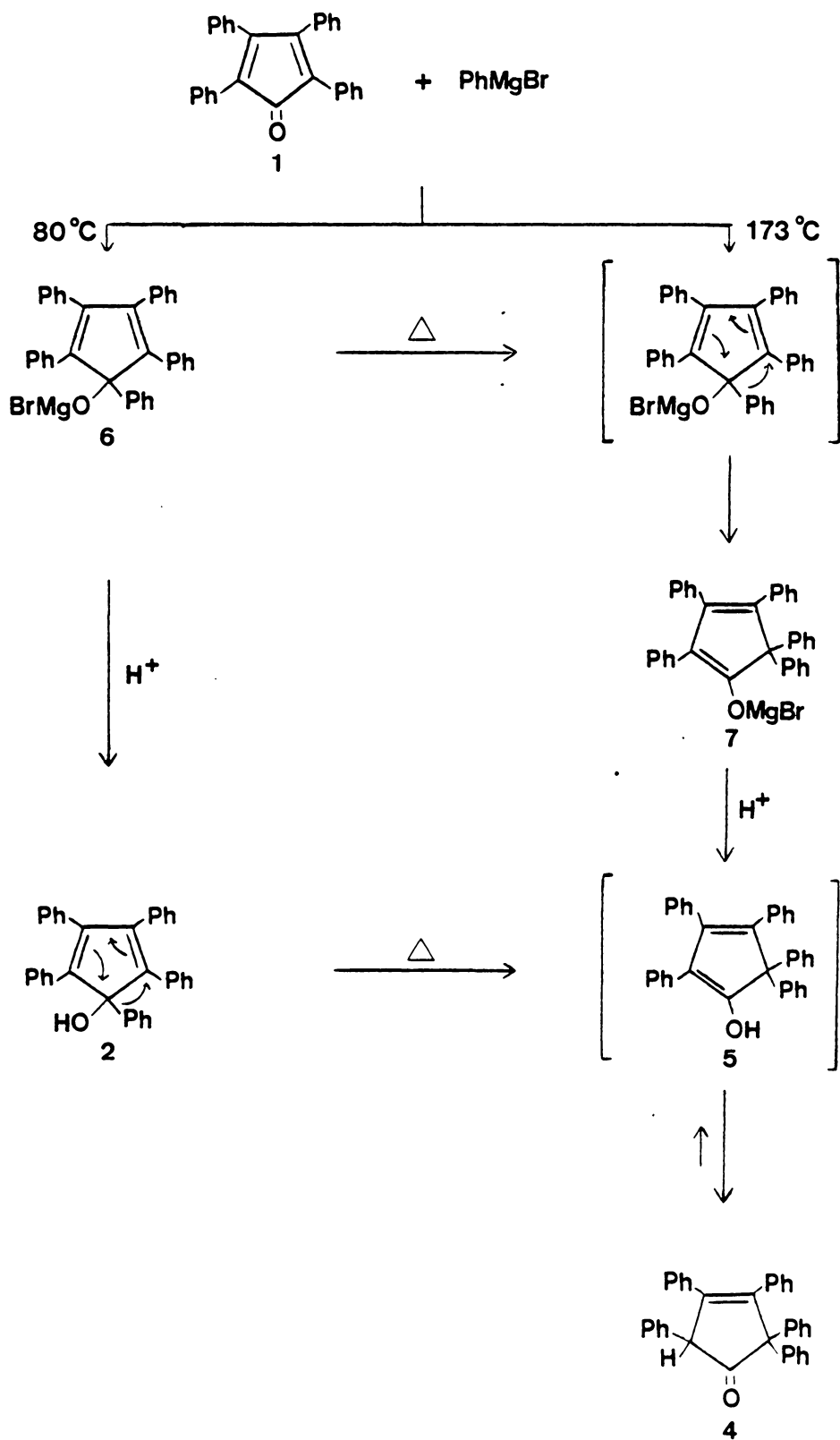
**Table I. Selection Rules for Thermal [1, j]-Sigmatropic Rearrangements**

j	Allowed	Forbidden
3	Antara - Retention Supra - Inversion	Antara - Inversion Supra - Retention
5	Antara - Inversion Supra - Retention	Antara - Retention Supra - Inversion
7	Antara - Retention Supra - Inversion	Antara - Inversion Supra - Retention

However in order to establish the rearrangement of **2** to **4** as proceeding by an initial [1,5]-sigmatropic rearrangement followed by a keto-enol tautomerization, Youssef and Ogliaruso<sup>1</sup> performed the following series of experiments as illustrated in Scheme I. When the addition of phenylmagnesium bromide to **1** was carried out in refluxing benzene (ca. 80 °C), the 1,2-addition product (**6**) was formed since quenching an aliquot of this solution afforded the dienol (**2**). This eliminated the possibility of a 1,6-addition of the organometallic to tetracyclone (**1**) to produce **7** directly by showing **6** to be an intermediate in the reaction. The dienol (**2**) could then be isomerized in refluxing isoamyl ether (ca. 173 °C) to the enol form (**5**) which rapidly tautomerizes to the keto structure (**4**). Alternatively, the Grignard salt (**6**), formed by addition of phenylmagnesium bromide to **1** in either refluxing benzene or refluxing isoamyl ether, could be thermally rearranged to **7** which upon hydrolysis also yields the ketone **4**.

To establish the concertedness of the phenyl shift, the possibility of ionic or free-radical pathways had to be eliminated. The ionic pathway was eliminated by heating **2** in both isoamyl ether ( $\epsilon = 2.8$ ) and dimethyl sulfoxide ( $\epsilon = 46.6$ ) for identical periods of time at the same temperature (i.e., 3 hours @ 173 °C). In spite of the great differences in the dielectric constants of these solvents, the extent of rearrangement (as determined by chromatography) was the same. A free-radical

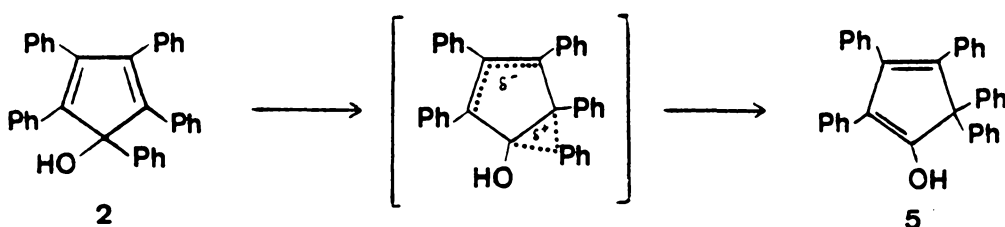
Scheme I



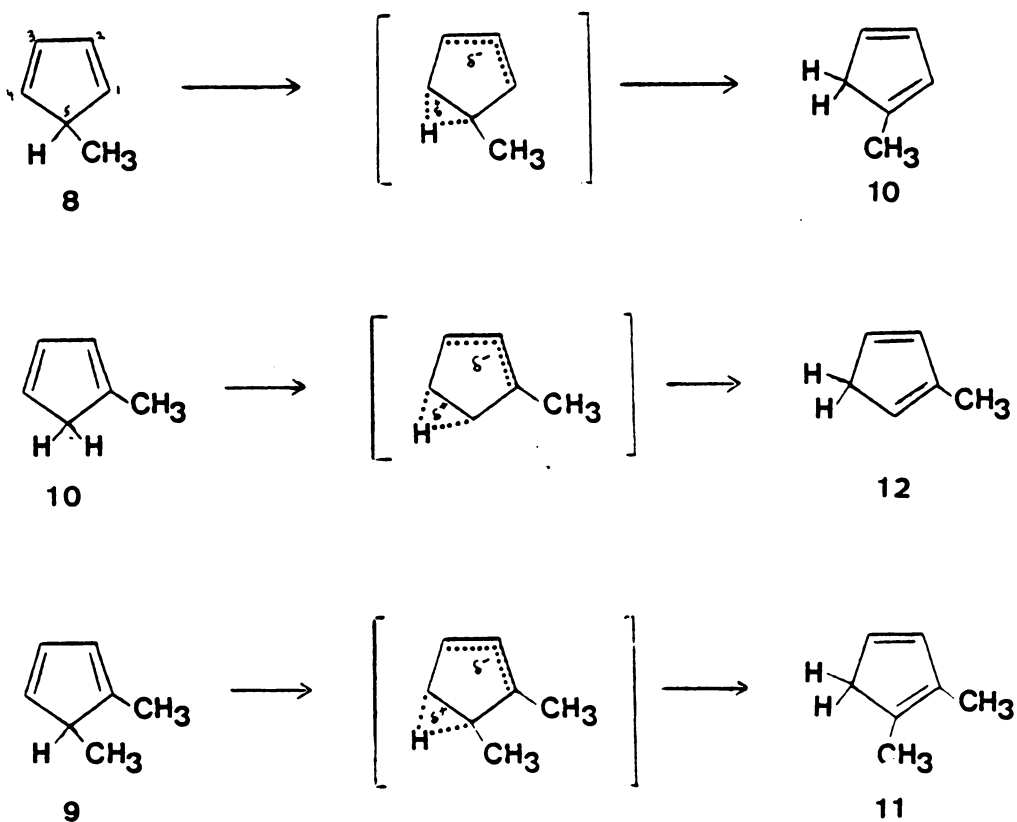
pathway was eliminated in the following manner. **2** was refluxed in isoamyl ether with a stream of oxygen bubbling continuously through the solution. The yield of **4** was identical to that obtained when the reaction was run in the absence of oxygen. Since the presence of a radical inhibitor had no effect on the yield of **4**, the reaction must not be free-radical in nature. By eliminating these possibilities, the reaction was characterized as a thermally-induced [1,5]-sigmatropic phenyl rearrangement and as such must proceed by a suprafacial shift in accordance with the Woodward-Hoffmann rules.<sup>6</sup>

In 1973, Youssef and Ogliaruso<sup>11</sup> also investigated the kinetics of the conversion of **2** to **4**. The rearrangement demonstrated first-order kinetics which is consistent with a sigmatropic rearrangement. The activation energy ( $E_a$ ) for this process was demonstrated to be  $36.1 \pm 3.6$  kcal/mol with an entropy of activation ( $\Delta S^\ddagger$ ) of -7.5 eu. The only other known values at this time for a [1,5]-sigmatropic phenyl shift were those reported by Miller<sup>12</sup> in the indene system. Miller obtained values for the  $E_a$  and  $\Delta S^\ddagger$  to be 27.2 kcal/mol and -27.2 eu respectively.

Youssef and Ogliaruso proposed a transition state for the phenyl migration which was analogous to the transition state put forth by McLean and Haynes<sup>13</sup> and Breslow<sup>14</sup> for [1,5]-hydrogen migrations in substituted cyclopentadienols.



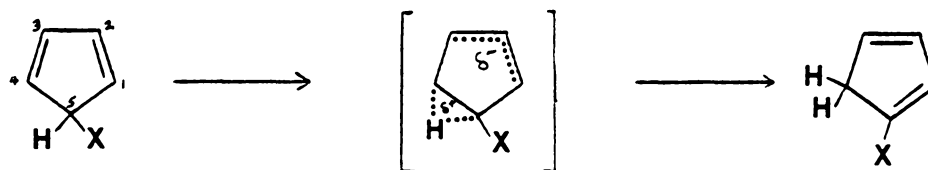
In the studies using methyl substituted cyclopentadienes, McLean and Haynes<sup>13</sup> synthesized 5-methyl cyclopentadiene (**8**), 1,5-dimethyl cyclopentadiene (**9**) and 1-methyl cyclopentadiene (**10**) then measured the rates of hydrogen migration. The rearrangement of **8** to **10** was found to be the fastest of the three; **9** to **11** proceeded at an intermediary rate, while **10** to **12** was the slowest. The rearrangement of **8** to **10** proceeded fastest due to stabilization of the partial positive charge experienced at C5 in the transition state. Presumably the methyl group stabilizes the  $\delta^+$  by its inductive effect and by facilitating rehybridization of the  $sp^3$  carbon (C5) to the more electronegative  $sp^2$ . In the conversion of **10** to **12**, the methyl substituent lies along the  $\pi$ -backbone, an area which bears



a partial negative charge in the transition state. In this case the electron-donating inductive effect of the methyl substituent destabilizes the transition state by intensifying the build-up of electron density. As a result, this rearrangement was the slowest of the three. Finally, in the conversion of 9 to 11, the methyl groups are situated at both a  $\delta^+$  (C5) and a  $\delta^-$  (C1) site which effectively cancels any electronic effect. Consequently an intermediate rate of rearrangement was observed for this system.

Breslow<sup>14</sup> also observed a definite substituent effect for the [1,5]-hydrogen migration in halogen substituted cyclopentadienes. The rates of rearrangement of C5-halogen substituted cyclopentadienes were compared to the rate of hydrogen migration for the parent compound. In all cases halogen substitution slowed the rearrangement relative to the parent compound. This was consistent with the proposed transition state, since the electron-withdrawing halogen at C5 effectively destabilizes the  $\delta^+$  charge in the transition state. Hence the destabilizing electron withdrawal

through induction must be predominating over the ability to stabilize through  $\pi$ -donation via resonance.



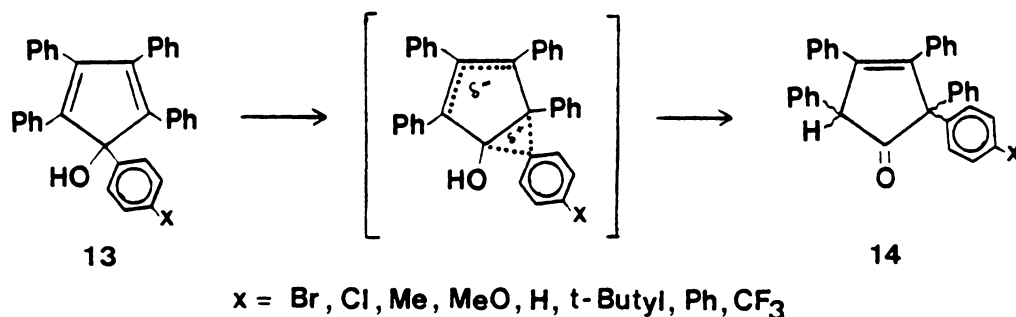
X	Relative Rates
H	1.00
Cl	0.67
Br	0.64
I	0.17

Additional evidence supporting the proposed transition state for hydrogen migration in 5-substituted cyclopentadienes was provided by Shchembelov and Ustynyuk.<sup>15</sup> Calculations performed on this system showed an area of low electron density ( $\delta^+$ ) on the migrating hydrogen and an area of high electron density ( $\delta^-$ ) on the cyclopentadienyl ring in the transition state.

In view of the results above, the 1,2,3,4,5-pentaphenyl-2,4-cyclopentadien-1-ol (2) system seemed especially well suited for an investigation into the possibility that the rearrangement could be sensitive to electronic effects. Any of the phenyl rings could be utilized to examine electronic effects operating on the cyclopentadienol ring.

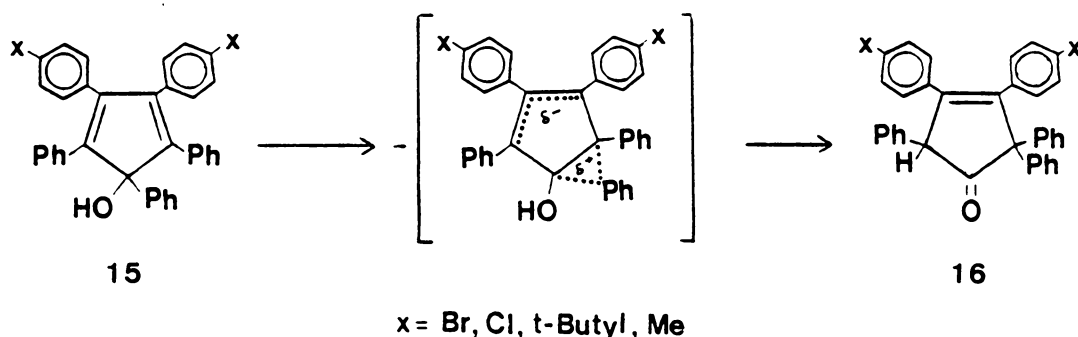
Youssef<sup>16</sup> initiated this study with the synthesis and isomerization of a series of 1-(*p*-substituted phenyl)-2,3,4,5-tetraphenyl-2,4-cyclopentadien-1-ols (13). The existence (or non-existence) of a linear free energy relationship was to be determined by comparing the relative rates of rearrangement. The substituents initially examined included *p*-bromo, *p*-chloro, *p*-methoxy and *p*-*tert*-butyl. Unfortunately the results of this study were inconclusive in that while the rates differed, a linear free energy relationship was not observed. However there was concern that the gas chromatographic analysis employed in this study may have affected the results. It was theorized that further rearrangement of the alcohol (13) to the ketone (14) would occur on the heated column

of the GC during the 30 minutes required for elution of the compounds. This would yield measured rates greater than the true rates and activation energies less than the actual values.



In 1975, Berg, Ogliaruso and McNair<sup>17</sup> developed a liquid chromatographic procedure for the analysis of the alcohol(13)/ketone(14) reaction mixtures. This enabled Oldaker<sup>2</sup> to extend the series initiated by Youssef concerning the kinetics of the rearrangement of 1-(*p*-substituted phenyl) alcohols (13). In this series the substituents are exerting their electronic effects upon an area which bears a  $\delta^+$  charge in the proposed transition state. Thus, electron-donating substituents should increase the rates of rearrangement through stabilization of the transition state while electron-withdrawing substituents should slow the rates of migration. The results of Oldaker's study indicated that the rates of rearrangement were nearly identical and linear free energy correlations were not observed.

Concurrently, Perfetti<sup>2</sup> was investigating the kinetics of the rearrangement of 3,4-bis(*p*-substituted phenyl)-1,2,5-triphenyl-2,4-cyclopentadien-1-ols (15) to the corresponding ketones (16) for possible electronic effects. In this series the substituted phenyls are located along the  $\pi$ -backbone

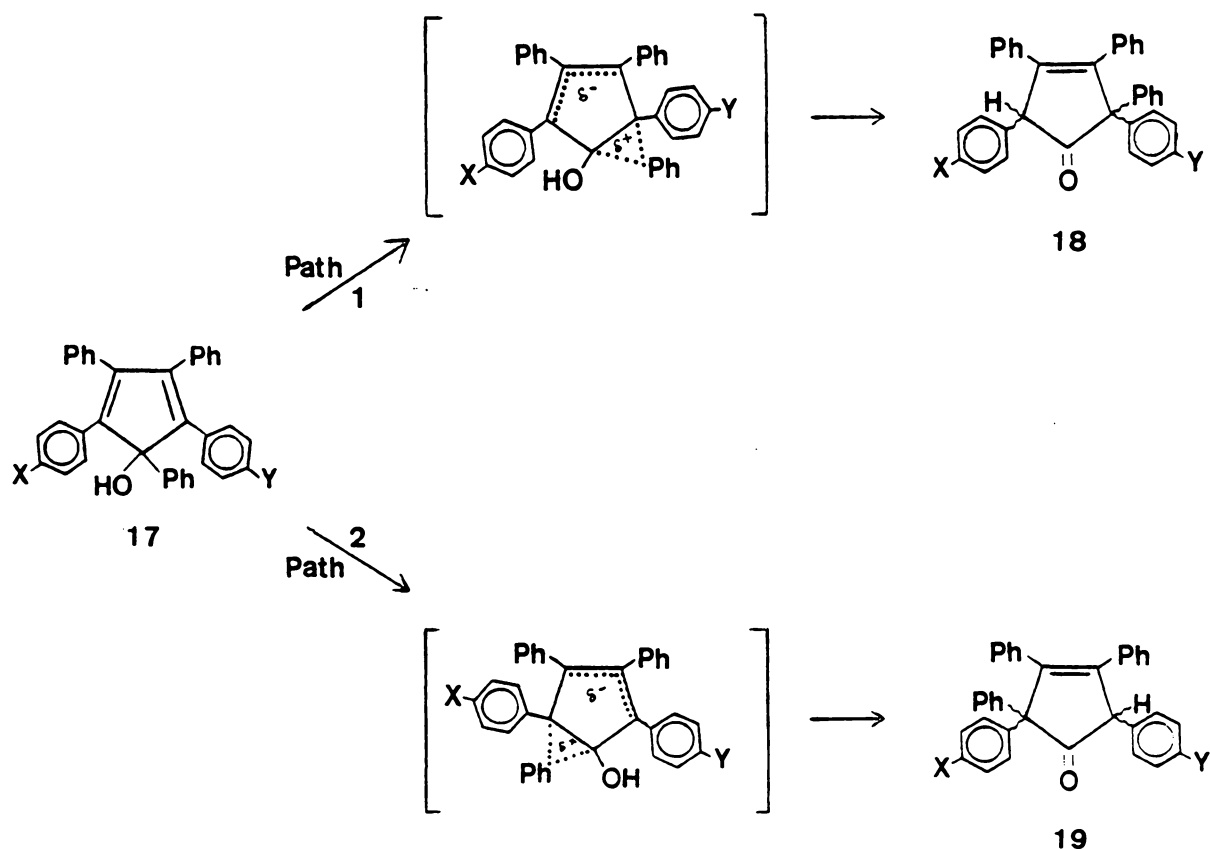


of the cyclopentadienyl ring, an area which bears a  $\delta^-$  charge in the proposed transition state. As a result, electron-donating substituents would be expected to decrease the rates of rearrangement



through destabilization of the transition state. Conversely, electron-withdrawing substituents should increase the rates of rearrangement. Unfortunately, Perfetti found the rates to be essentially the same and no correlation of rate to substituent could be established for this series.

Subsequent work by Brubaker<sup>3</sup> involved the synthesis and thermal isomerization of a series of 2- and/or 5-(*p*- or *m*-substituted phenyl)-1,3,4-triphenyl-2,4-cyclopentadien-1-ols (17). In this system, in which more than one migration pathway is available, substituents should interact with the transition state in a manner which would influence the direction of migration.



Thus, where Y is electron-donating and X = H, pathway 1 leading to 18 should be preferred since the Y-substituent is stabilizing the  $\delta^+$  in the proposed transition state relative to the unsubstituted phenyl. However if the phenyl migrates toward the side where X = H (pathway 2), the electron-donating effect of the Y-substituent is forced to interact with a  $\delta^-$  charge, resulting in destabilization of the transition state. Conversely, when Y is electron-withdrawing and X = H, pathway 2, leading to 19, would be favored since the substituent stabilizes the build-up of the  $\delta^-$  charge

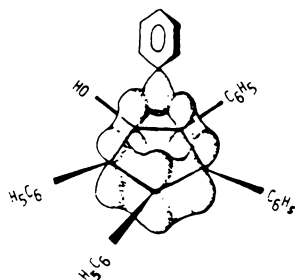
in the transition state. Migration toward the Y-substituent (path 1) would produce a transition state in which the electron-withdrawing substituents would intensify, thus destabilize, the developing  $\delta^+$  charge.

These effects would be even more pronounced for the case where X is electron-withdrawing and Y is electron-donating, since path 1 allows the Y-substituent to stabilize the  $\delta^+$  in the transition state while the X-substituent can simultaneously stabilize the  $\delta^-$  charge. An attempt by phenyl to migrate by path 2 would require a transition state in which both the  $\delta^+$  and  $\delta^-$  charges are destabilized by the electronic effects of the substituents.

Since the rearrangement is considered irreversible, parallel path first order kinetics leading from the reactant (17) to the two products (18+19) would be observed. Therefore the product distribution ratio (18/19) at  $t = \infty$  would also be a measure of the ratio of the rates leading to their formation (path 1/ path 2). If the product distribution correlates with the nature of the substituent, then support would be given to the  $\delta^-$  charge separated transition state. However if no preference is shown resulting in a product ratio of 50/50, then the strictly neutral transition state would be implied.

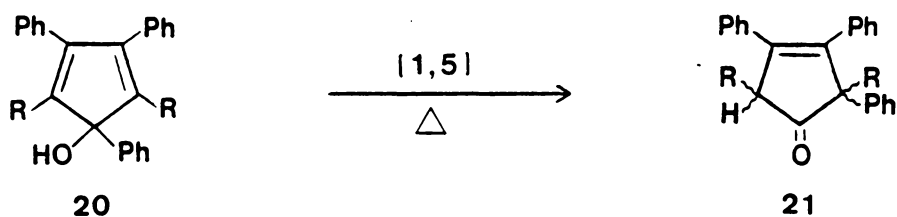
Unfortunately Brubaker's results indicated that the slight differences (if any) in the product ratios observed for this series of rearrangements are random in nature and not attributable to either resonance or inductive effects due to the substituents. According to Brubaker<sup>17</sup>: "The effects are at best, marginal; at worst, imaginary."

The results of Oldaker,<sup>2</sup> Perfetti<sup>2</sup> and Brubaker<sup>3</sup> led them to the conclusion that the originally proposed transition state was not applicable in the pentaphenylcyclopentadienol system. A transi-

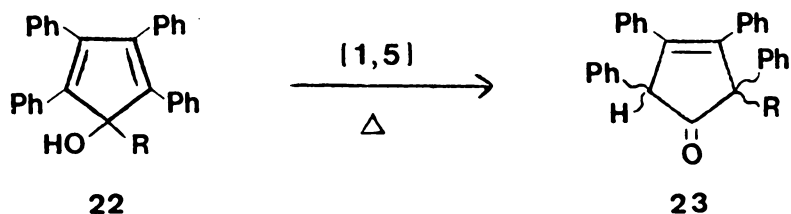


tion state devoid of charge separation was consistent with their findings. Thus they concluded that this system rearranges by a truly neutral mechanism as shown above.

Recently, Davis<sup>18</sup> investigated the thermal rearrangement of 2,5-dialkyl-1,3,4-triphenyl-2,4-cyclopentadien-1-ols (**20**) to the corresponding ketones (**21**) with regard to the effect that steric interactions at the migration terminus would have on the energy of activation for the phenyl migration. His results indicated that the activation energy for this process remained essentially the same regardless of the nature of the alkyl substituent.



However it can be argued that the substituents used by Oldaker, Perfetti and Brubaker do not interact to a significant degree with the  $\delta^+$  and  $\delta^-$  areas of the proposed transition state because of the distances involved between the substituents and the cyclopentadienol ring system. Since inductive effects fall off with the square of the distance<sup>19</sup>, it would be more desirable to have the substituents as close as possible to the sites of interaction.



Thus the subject of this dissertation is the synthesis of a wide variety of 1-substituted-2,3,4,5-tetraphenyl-2,4-cyclopentadien-1-ols (**22**) in which the nature of the migrating group is greatly varied in order to maximize any steric and/or electronic effects associated with the transition state of the [1,5]-sigmatropic rearrangement leading to **23**. The syntheses of these compounds as well as the kinetic study of their rearrangements are presented herein.

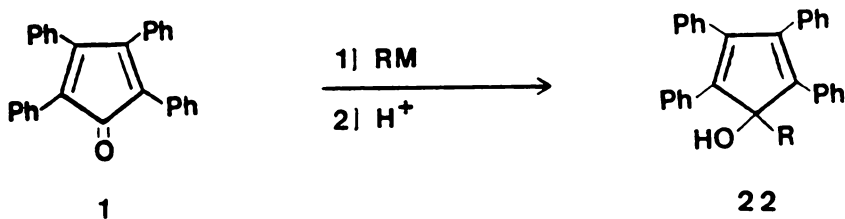
## Results and Discussion


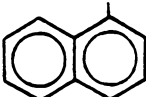
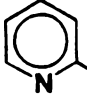
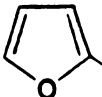
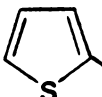
### *Synthesis of 1-Substituted tetraphenylcyclopentadienols*

For the purposes of this investigation, eight 1-substituted-2,3,4,5-tetraphenyl-2,4-cyclopentadien-1-ols were prepared by the addition of the appropriate organometallic reagent to tetracyclone (1) followed by quenching with a dilute acid solution. These results are summarized in Table II. Although the isolated yields ranged from 48% to 85%, the reactions were essentially quantitative with respect to the consumption of tetracyclone. The disappearance of the intense purple-black color of tetracyclone effectively serves as an indicator for the end-point of the reaction. In addition, IR and  $^1\text{H}$  NMR spectral data of the crude reaction mixtures, indicated that there were little or no impurities present. The low isolated yields for some of these compounds were probably due to losses in chromatographic and/or recrystallization procedures employed during the work-up procedure.

Table II.

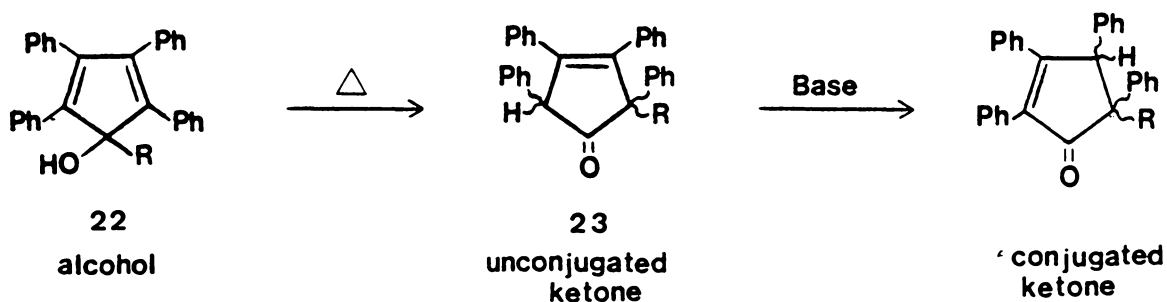
Synthesis of 1-Substituted Tetraphenylcyclopentadienols.



R	Alcohol	% Yield (isolated)	MP (°C)
	2	73	175-177
	24	53	182-183
	25	62	217-219
	26	81	176-177
	27	85	155-157
Ph - C $\equiv$ C -	28	77	201-203
CH <sub>2</sub> = CH -	29	85	138-140
(CH <sub>3</sub> ) <sub>3</sub> C -	30	48	167-169

## Synthesis of 2-substituted tetraphenylcyclopentenones

The investigation of the thermal isomerization of 1-substituted tetraphenylcyclopentadienols (**22**) to the corresponding 2-substituted tetraphenylcyclopentenones (**23**) is the crux of this dissertation. Although the isomerization is quantitative with respect to the disappearance of alcohol, the reaction is highly sensitive to the presence of base. If base is present, this results in the conversion of the initially formed 2-substituted-2,3,4,5-tetraphenyl-3-cyclopenten-1-one ("unconjugated ketone") to the isomeric 5-substituted-2,3,4,5-tetraphenyl-2-cyclopenten-1-one ("conjugated ketone").

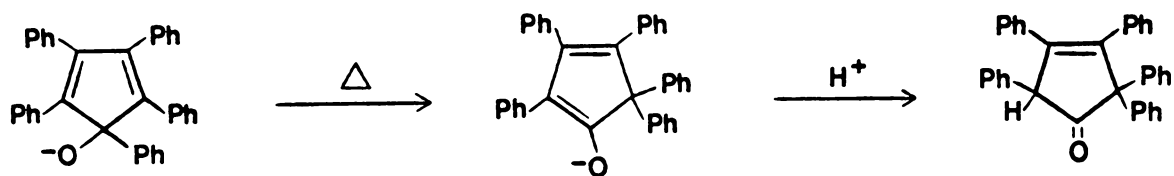


As a result, caution must be observed in excluding basic contaminants from glassware, alcohols and solvents. Cutshaw<sup>20</sup> and Brubaker<sup>3</sup> observed that even when extreme care was taken, approximately five to ten percent of the rearranged product consisted of the conjugated ketone.

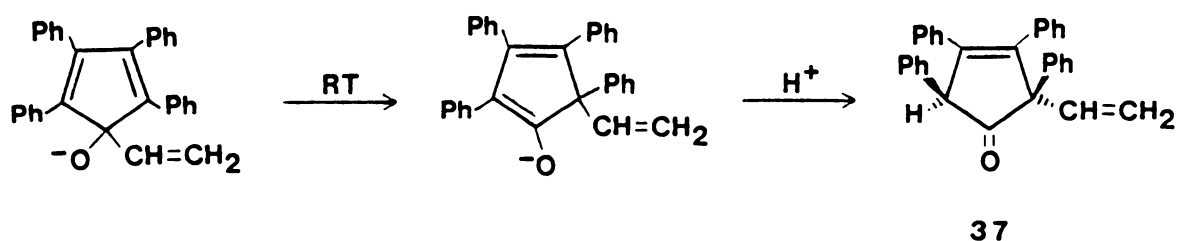
This observation was especially true in the case of the thermal rearrangement of the 2-furyl (**26**), 2-thienyl (**27**) and 2-pyridyl (**25**) alcohols. Even if extreme care is taken to remove basic impurities, these alcohols are plagued by the fact that they inherently contain basic heteroatoms. The result of this being the formation of considerable amounts of the conjugated ketones. In fact, the conjugated ketones are the predominate species produced from the 2-furyl and 2-thienyl rearrangements and is the only species observed in the rearrangement of the 2-pyridyl alcohol.

Based on these observations, it was determined that the thermal isomerization of the corresponding alcohol was not the most efficient way of generating the unconjugated ketones. However Youssef<sup>21</sup> demonstrated that the sodium salt of the phenyl alcohol (alkoxide) rearranged at a faster

rate than the neutral alcohol, and that the unconjugated ketone could be obtained in high yields (ca. 99%) by a kinetic protonation of the resulting enolate.



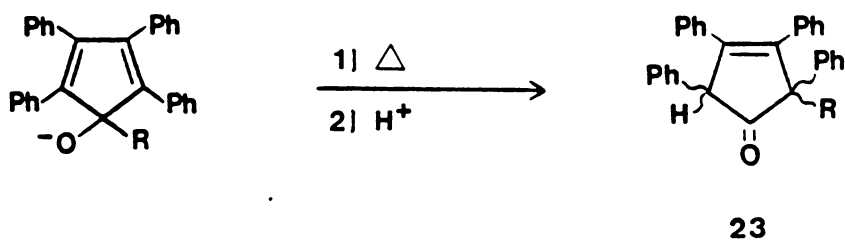
Likewise, Beak<sup>22</sup> postulated that the formation of the unconjugated vinyl ketone (37) from the addition of vinyl lithium to tetracyclone (1) was the result of a rearrangement of the initially formed 1,2-adduct. The results of our investigation demonstrated that if the initially formed 1,2-adduct (alkoxide) was not immediately protonated to form the alcohol, the alkoxide rearranged at room temperature to the stabilized enolate system which upon kinetic protonation generated the unconjugated vinyl ketone. Although Beak did not specify the stereochemistry of the vinyl ketone, our results of a <sup>1</sup>H-<sup>1</sup>H difference NOE NMR experiment suggest that the unconjugated vinyl ketone obtained in this manner has a *cis* relationship with respect to the methine proton and the vinyl group. The *cis* isomer represents the kinetic product, since it is the product obtained by protonation from the least hindered side.


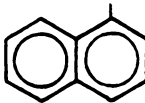
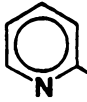
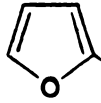
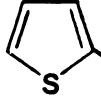


Consequently, it was determined that the most efficient way of generating the unconjugated ketones was a rearrangement of the appropriate alkoxides followed by a kinetic protonation to form the unconjugated ketones as the major isomers. The alkoxides were generated by the addition of one equivalent of *n*-butyllithium to a solution containing the alcohol or by the addition of the appropriate organometallic reagent to tetracyclone (1). After heating for the desired time, the solutions were cooled then quenched with a proton source. These results are summarized in Table III.

Table III.

Synthesis of 2-Substituted Tetraphenylcyclopentenones.



R	Ketone	% Yield (isolated)	MP (°C)
	<b>4</b>	52	191-193
	<b>31</b>	50	175-177
	<b>32</b>	71	153-155
	<b>33</b>	43	170-172
	<b>34</b>	80	189-191
Ph - C $\equiv$ C -	<b>35</b>	50	180-181
CH <sub>2</sub> = CH -	<b>36</b>	46	163-164
(CH <sub>3</sub> ) <sub>3</sub> C -	<b>37</b>	50	148-149



## *Kinetic Investigation*

The results of the thermal isomerization of 1-substituted tetraphenylcyclopentadienols are summarized in Tables IV-XXVII and graphically displayed in Figures 2-51. When the log of the alcohol concentration (expressed in terms of % concentration) was plotted versus time, a linear relationship was observed. This indicated that the rearrangement followed first-order kinetics<sup>23</sup> which is consistent for sigmatropic rearrangements. As a result, the rate constant for this process is equal to  $-2.303(\text{slope})$  (Appendix A). In addition, the initial concentration (2.00 (log 100%) @  $t = 0$ ) should agree with the values obtained for the y-intercept of this plot.

Once the individual rates were obtained, the Arrhenius activation energy ( $E_a$ ) was calculated by plotting  $\log k$  versus  $1/T$  (Appendix B).<sup>23</sup> The activation energy is equal to  $-4.576 \text{ cal mol}^{-1} \text{ K}^{-1}$  (*slope*). The enthalpy of activation ( $\Delta H^\ddagger$ ) and entropy of activation ( $\Delta S^\ddagger$ ) were obtained from the Eyring equation (Appendix C)<sup>23</sup> by plotting  $\log (k/T)$  versus  $1/T$ . The enthalpy of activation,  $\Delta H^\ddagger$ , is equal to  $-4.576 \text{ cal mol}^{-1} \text{ K}^{-1}$  (*slope*) and the entropy of activation,  $\Delta S^\ddagger$ , is equal to  $4.576 \text{ cal mol}^{-1} \text{ K}^{-1}$  ( $y_{\text{intercept}} - 10.32$ ). The calculations for each alcohol are shown in the Appendix (D-K). The results are summarized in Table XXVIII and the  $E_a$  and  $\Delta S^\ddagger$  for each alcohol are graphically displayed in Figures 52 and 53. The uncertainties (precision estimates) in the rates, activation energies, enthalpies of activation and entropies of activation were obtained graphically by the method of limiting slopes.<sup>24</sup>

The results in Table XXVIII show the phenyl alcohol (2) has an activation energy of  $31.7 \pm 1.4 \text{ kcal mol}^{-1}$  with an entropy of activation of  $-10.0 \pm 3.1 \text{ eu}$ . These values are in close agreement to those recently obtained by Davis<sup>18</sup> ( $31.0 \pm 1.0 \text{ kcal mol}^{-1}$  and  $-12.0 \pm 3.0 \text{ eu}$  respectively).

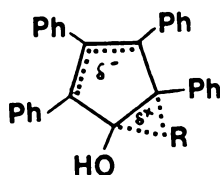
In analyzing Table XXVIII and Figure 53, it appears that the entropies of activation ( $\Delta S^\ddagger$ ) can be divided into three groups: -3.7, -6.2 to -10.0, and -13.7 eu. The -3.7 value represents the linear acetylene group ( $sp$  hybridized), the intermediate values coincide with the planar  $sp^2$  hybridized substituents while the -13.7 value is attributable to the bulky *t*-butyl group ( $sp^3$ ). Thus,

going from the smaller to larger substituents resulted in a greater negative value for the entropy of activation ( $\Delta S^\ddagger$ ).

Likewise, it appears that the activation energies ( $E_a$ ) for the thermal rearrangement can also be divided into three categories: 27.5-29.7, 31.7-32.9, and 34.8 kcal/mol (Figure 52). In analyzing this figure, a steric argument can be made to explain the differences in the activation energies for the rearrangement of the vinyl (**29**), phenyl (**2**) and 1-naphthyl (**24**) alcohols. The vinyl group is the smallest substituent and as a result has the lowest activation energy. The naphthyl group is the bulkiest of the three and consequently has the largest activation energy. The phenyl substituent gives the intermediate value.

However, in comparing the heterocyclic alcohols to the phenyl system, some interesting observations are made. First, the activation energy for the migration of the pyridine ring in the 2-pyridyl alcohol (**25**) is lower than the activation energy for the corresponding migration of a phenyl ring in the phenyl alcohol (**2**). Second, rearrangement of the 5-membered furan and thiophene rings results in essentially the same activation energy (within experimental error) if not slightly higher than does that required for migration of a phenyl ring. Third, the rates of rearrangement of the phenyl alcohol versus the 2-thienyl alcohol are essentially the same (within experimental error) whereas both are significantly higher than those determined for the 2-furyl alcohol.

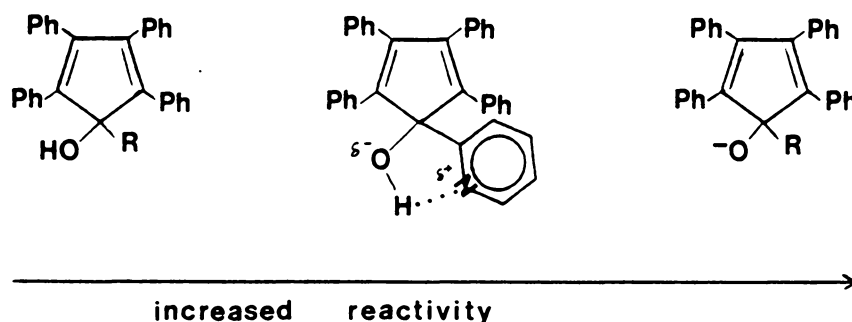
Obviously a steric argument can not be employed to explain these observations. Disregarding any electronic influences, it is logical for one to assume that the five membered rings would rearrange at a comparable if not faster rate than the six membered rings, thus resulting in equal if not lower activation energies. It is possible however, although not experimentally proven, that electronic effects of atoms alpha to the migrating carbon can influence the rates of rearrangement as well as the activation energies. According to the originally proposed transition state for the rearrangement,<sup>13,14,16</sup> the migrating carbon attains  $\delta^+$  charge in the transition state. Electron withdrawing groups alpha to this carbon should destabilize this transition state by increasing the  $\delta^+$  charge on this site. In fact, the stronger the ability to withdraw electron density, the larger the  $\delta^+$  and presumably the slower the rate of rearrangement. This is possibly why the 2-furyl alcohol has



a slower rate of rearrangement than the 2-thienyl or phenyl alcohol. Oxygen has an electronegativity value of 4.0 versus 2.5 for sulfur and carbon.<sup>25</sup> In using this argument, one would expect the 2-pyridyl alcohol (nitrogen electronegativity of 3.0) to rearrange at a rate between that of the 2-furyl and 2-thienyl alcohols, assuming only a minor effect of the larger ring size.

However the 2-pyridyl alcohol differs from the other two heterocycles in that the pyridine ring forms an intramolecular hydrogen bond to the alcohol proton. This statement is supported by both IR and <sup>1</sup>H NMR data. All alcohols except the 2-pyridyl alcohol show a OH stretch in the IR at 3650-3600 cm<sup>-1</sup>. In the 2-pyridyl case, the absorbance occurs at 3360 cm<sup>-1</sup> and is quite broad. In the <sup>1</sup>H NMR of the pyridyl alcohols, the alcohol proton is observed at δ 6.36 (and rapidly exchanges with D<sub>2</sub>O). The hydroxyl protons of the other alcohols used in this study are located at δ 2.7-2.2.

Since the alcohol is hydrogen bonded, the oxygen atom has a δ<sup>-</sup> charge. It was observed by Youssef<sup>21</sup> that the alkoxides rearranged at a faster rate than the corresponding alcohols. Thus in the 2-pyridyl system, the alcohol is positioned between the neutral alcohol and the alkoxide in terms of reactivity resulting in the faster rates and the lower activation energy for this compound. It appears possible that the electronic effects associated with the oxygen atom of the alcohol play a more



important role than those alpha to the migrating carbon.

From Table XXVIII, the phenylethynyl alcohol (28) is found to have essentially the same activation energy as does the phenyl alcohol. This is quite surprising since the rate of migration of the phenylethynyl substituent is 15 times faster than the phenyl group at 175 °C. However there is a significant difference in the entropy of activation (-3.7 for (28) versus -10.0 for (2)). It is this difference which accounts for the differences in rates.

According to the Gibbs free energy equation:<sup>26</sup>

$$\Delta G^\ddagger = \Delta H^\ddagger - T \Delta S^\ddagger$$

At the temperatures used in this study ( $T = 363 - 508 \text{ K}$ ), the  $T \Delta S^\ddagger$  term becomes significant and is responsible for the observed differences.

Since<sup>23</sup>

$$k = \frac{RT}{N_A h} \exp^{-\Delta G^\ddagger / RT}$$

and

$$k = A \exp^{-E_a / RT}$$

the rates are directly related to  $-\Delta G^\ddagger$  whereas they may differ from  $-E_a$  because the pre-exponential factor ( $A$ ) is not constant throughout the alcohol series and because of the entropy term. In other words, if the  $\Delta S^\ddagger$  are essentially the same, the rates of rearrangement should follow the same trend as does  $-E_a$ . However if the  $\Delta S^\ddagger$  are significantly different, this trend will not be observed. This is illustrated in Table XXIX.

In analyzing the *tert*-butyl alcohol (32), it is observed that the very sterically hindered *t*-butyl group rearranges faster than would be expected based solely upon a steric argument. Perhaps the electronic nature of the *t*-butyl group is responsible for the increase in the rate of rearrangement. The electron donating ability of this group is capable of stabilizing the  $\delta^+$  charge in the originally proposed transition state. Thus opposing factors appear to be present in this system, an electronic

influence which accelerates the rate and a steric factor which is responsible for slowing the rearrangement.

Likewise a similar situation exists for the phenylethynyl alcohol (28), a steric influence counteracted by an electronic factor. However in this case, the steric influence is responsible for accelerating the rearrangement whereas the electronic nature of the substituent is capable of slowing the rate. The electronegative  $sp$  hybridized carbon of the acetylene group should destabilize the proposed transition state by intensifying the  $\delta^+$  charge on this carbon. As a result, a slower rate should result.

The results of this investigation differ from those obtained by other researchers studying the [1,5]-sigmatropic rearrangement in the cyclopentadienol series. Oldaker,<sup>2</sup> Perfetti<sup>2</sup> and Brubaker<sup>3</sup> concluded that electronic effects of *para*-phenyl substituents were found to have no discernible effect upon either the rate of rearrangement or the direction of migration. The results of this study suggest that the electronic nature of the migrating group does effect the rate of migration in a predictable manner. Electron donating substituents accelerate the rate while electron withdrawing substituents slow the rearrangement.

In the investigation of the thermal rearrangement of 2,5-dialkyl-1,3,4-triphenyl-2,4-cyclopentadien-1-ols (20), Davis<sup>18</sup> observed that the activation energy for the phenyl migration was essentially the same regardless of the steric nature of the alkyl substituents at the migration terminus. However, it was shown in our investigation that the steric bulk of the migrating group affects the rates of migration. Smaller groups rearrange faster than larger groups, assuming the electronic nature of the groups are comparable.

Consequently, the results of this investigation support the originally proposed transition state involving the partial charge separation. A truly neutral, concerted mechanism with a transition state devoid of charge as proposed by Oldaker,<sup>2</sup> Perfetti<sup>2</sup> and Brubaker<sup>3</sup> is not consistent with the experimental results obtained by this investigation. It is indeed possible that the *para*-substituents used by these investigators cannot effectively transmit their electronic effects to the cyclopentadienol ring because of the the distances involved. As a result, the substituents are reduced to equivalency with no differences being observed.

**Table IV. The Isomerization of  
1,2,3,4,5-Pentaphenyl-2,4-cyclopentadien-1-ol (2) @ 175.0 ± 0.4 °C**

Aliquot #	Time (sec)	% Concentration	log (% Conc.)
0	0	100.0	2.00
1	2,700	84.9	1.93
2	5,397	74.6	1.87
3	8,100	61.4	1.79
4	10,797	52.1	1.72
5	13,498	43.2	1.64
6	16,199	36.4	1.56
7	18,960	30.5	1.48
8	21,602	26.3	1.42

k

Plotting log (% Conc.) versus Time

$$k = -2.303 (\text{slope})$$

$$k = 6.30 \pm 0.18 \times 10^{-5} \text{ sec}^{-1}$$

$$\text{slope} = -2.74 \times 10^{-5}$$

$$y_{\text{intercept}} = 2.01$$

$$\text{corr} = -0.999$$

**Table V. The Isomerization of  
1,2,3,4,5-Pentaphenyl-2,4-cyclopentadien-1-ol (2) @ 190.0 ± 0.4 °C**

Aliquot #	Time (sec)	% Concentration	log (% Conc.)
0	0	100.0	2.00
1	958	81.1	1.91
2	1,801	65.7	1.82
3	2,699	55.1	1.74
4	3,602	48.3	1.68
5	4,500	40.4	1.61
6	5,400	35.7	1.55
7	6,300	26.6	1.42
8	7,142	21.3	1.33

*k*

Plotting log (% Conc.) versus Time

$$k = -2.303 (\text{slope})$$

$$k = 2.07 \pm 0.13 \times 10^{-4} \text{ sec}^{-1}$$

$$\text{slope} = -8.99 \times 10^{-5}$$

$$y_{\text{intercept}} = 2.00$$

$$\text{corr} = -0.996$$

**Table VI. The Isomerization of  
1,2,3,4,5-Pentaphenyl-2,4-cyclopentadien-1-ol (2) @ 205.0 ± 0.4 °C**

Aliquot #	Time (sec)	% Concentration	log (% Conc.)
0	0	100.0	2.00
1	302	83.2	1.92
2	600	65.7	1.82
3	896	55.5	1.74
4	1,203	47.3	1.67
5	1,498	40.2	1.60
6	1,799	34.2	1.53
7	2,099	29.0	1.46
8	2,399	24.2	1.38

k

Plotting log (% Conc.) versus Time

$$k = -2.303 (\text{slope})$$

$$k = 5.86 \pm 0.41 \times 10^{-4} \text{ sec}^{-1}$$

$$\text{slope} = -2.54 \times 10^{-4}$$

$$y_{\text{intercept}} = 1.99$$

$$\text{corr} = -0.999$$



**Table VII. The Isomerization of  
1-(1-Naphthyl)-2,3,4,5-tetraphenyl-2,4-cyclopentadien-1-ol (24) @ 205.0 ± 0.4 °C**

Aliquot #	Time (sec)	% Concentration	log (% Conc.)
0	0	100.0	2.00
1	70	99.6	2.00
2	3,660	80.5	1.91
3	8,100	59.5	1.77
4	12,599	43.2	1.64
5	17,410	32.8	1.52
6	21,600	25.5	1.41
7	25,199	20.5	1.31
8	28,925	17.1	1.23
9	32,405	13.2	1.12

k

Plotting log (% Conc.) versus Time

$$k = -2.303 (\text{slope})$$

$$k = 6.24 \pm 0.30 \times 10^{-5} \text{ sec}^{-1}$$

$$\text{slope} = -2.71 \times 10^{-5}$$

$$y_{\text{intercept}} = 2.00$$

$$\text{corr} = -1.000$$

**Table VIII. The Isomerization of  
1-(1-Naphthyl)-2,3,4,5-tetraphenyl-2,4-cyclopentadien-1-ol (24) @ 220.0 ± 0.4 °C**

Aliquot #	Time (sec)	% Concentration	log (% Conc.)
0	0	100.0	2.00
1	61	98.4	1.99
2	1,200	80.5	1.91
3	2,400	62.9	1.80
4	3,599	49.5	1.69
5	4,814	39.2	1.59
6	6,000	30.5	1.48
7	7,201	24.2	1.38
8	8,400	19.1	1.28
9	9,600	15.4	1.19

$k$

Plotting log (% Conc.) versus Time

$$k = -2.303 (\text{slope})$$

$$k = 1.97 \pm 0.07 \times 10^{-4} \text{ sec}^{-1}$$

$$\text{slope} = -8.55 \times 10^{-5}$$

$$y_{\text{intercept}} = 2.00$$

$$\text{corr} = -1.000$$

**Table IX. The Isomerization of  
1-(1-Naphthyl)-2,3,4,5-tetraphenyl-2,4-cyclopentadien-1-ol (24) @ 235.0 ± 0.4 °C**

Aliquot #	Time (sec)	% Concentration	log (% Conc.)
0	0	100.0	2.00
1	59	96.8	1.99
2	358	80.7	1.91
3	719	70.3	1.85
4	1,083	55.7	1.75
5	1,440	49.3	1.69
6	1,799	38.8	1.59
7	2,160	31.7	1.50
8	2,520	25.9	1.41
9	2,881	21.5	1.33

k

Plotting log (% Conc.) *versus* Time

$$k = -2.303 (\text{slope})$$

$$k = 5.37 \pm 0.23 \times 10^{-4} \text{ sec}^{-1}$$

$$\text{slope} = -2.33 \times 10^{-4}$$

$$y_{\text{intercept}} = 2.01$$

$$\text{corr} = -0.999$$

**Table X. The Isomerization of  
1-(2-Pyridyl)-2,3,4,5-tetraphenyl-2,4-cyclopentadien-1-ol (25) @ 145.0 ± 0.4 °C**

Aliquot #	Time (sec)	% Concentration	log (% Conc.)
0	0	100.0	2.00
1	61	99.6	2.00
2	3,300	81.5	1.91
3	6,599	64.0	1.81
4	10,050	48.8	1.69
5	13,199	42.9	1.63
6	16,500	37.1	1.57
7	19,831	32.1	1.51
8	23,100	26.1	1.42

k

Plotting log (% Conc.) versus Time

$$k = -2.303 (\text{slope})$$

$$k = 5.78 \pm 0.51 \times 10^{-5} \text{ sec}^{-1}$$

$$\text{slope} = -2.51 \times 10^{-5}$$

$$y_{\text{intercept}} = 1.99$$

$$\text{corr} = -0.995$$

**Table XI. The Isomerization of  
1-(2-Pyridyl)-2,3,4,5-tetraphenyl-2,4-cyclopentadien-1-ol (25) @ 160.0 ± 0.4 °C**

Aliquot #	Time (sec)	% Concentration	log (% Conc.)
0	0	100.0	2.00
1	60	99.9	2.00
2	1,080	83.5	1.92
3	2,160	65.6	1.82
4	3,240	57.0	1.76
5	4,320	45.1	1.65
6	5,400	37.1	1.57
7	6,480	29.4	1.47
8	7,559	25.0	1.40
9	8,642	20.1	1.30

k

Plotting log (% Conc.) versus Time

$$k = -2.303 (\text{slope})$$

$$k = 1.87 \pm 0.07 \times 10^{-4} \text{ sec}^{-1}$$

$$\text{slope} = -8.12 \times 10^{-5}$$

$$y_{\text{intercept}} = 2.00$$

$$\text{corr} = -0.999$$

**Table XII. The Isomerization of  
1-(2-Pyridyl)-2,3,4,5-tetraphenyl-2,4-cyclopentadien-1-ol (25) @ 175.0 ± 0.4 °C**

Aliquot #	Time (sec)	% Concentration	log (% Conc.)
0	0	100.0	2.00
1	59	97.3	1.99
2	362	79.8	1.90
3	753	64.5	1.81
4	1,078	47.8	1.68
5	1,500	37.2	1.57
6	1,803	31.1	1.49
7	2,196	25.7	1.41
8	2,519	20.3	1.31
9	2,889	16.1	1.21

k

Plotting log (% Conc.) versus Time

$$k = -2.303 (\text{slope})$$

$$k = 6.33 \pm 0.37 \times 10^{-4} \text{ sec}^{-1}$$

$$\text{slope} = -2.75 \times 10^{-4}$$

$$y_{\text{intercept}} = 2.00$$

$$\text{corr} = -0.999$$

**Table XIII. The Isomerization of  
1-(2-Furyl)-2,3,4,5-tetraphenyl-2,4-cyclopentadien-1-ol (26) @ 175.0 ± 0.4 °C**

Aliquot #	Time (sec)	% Concentration	log (% Conc.)
0	0	100.0	2.00
1	3,901	81.6	1.91
2	7,799	71.0	1.85
3	11,699	61.0	1.79
4	15,600	53.6	1.73
5	19,500	42.0	1.62
6	23,401	35.5	1.55
7	27,299	30.5	1.48
8	31,202	26.0	1.41

k

Plotting log (% Conc.) versus Time

$$k = -2.303 (\text{slope})$$

$$k = 4.35 \pm 0.23 \times 10^{-5} \text{ sec}^{-1}$$

$$\text{slope} = -1.89 \times 10^{-5}$$

$$y_{\text{intercept}} = 2.00$$

$$\text{corr} = -0.998$$

**Table XIV. The Isomerization of  
1-(2-Furyl)-2,3,4,5-tetraphenyl-2,4-cyclopentadien-1-ol (26) @ 190.0 ± 0.4 °C**

Aliquot #	Time (sec)	% Concentration	log (% Conc.)
0	0	100.0	2.00
1	906	86.9	1.94
2	1,800	79.4	1.90
3	2,699	69.4	1.84
4	3,599	56.6	1.75
5	4,504	50.6	1.70
6	5,399	43.0	1.63
7	6,300	41.4	1.62
8	7,200	35.3	1.55
9	9,000	25.2	1.40
10	10,861	20.4	1.31

k

Plotting log (% Conc.) versus Time

$$k = -2.303 (\text{slope})$$

$$k = 1.49 \pm 0.17 \times 10^{-4} \text{ sec}^{-1}$$

$$\text{slope} = -6.47 \times 10^{-5}$$

$$y_{\text{intercept}} = 2.00$$

$$\text{corr} = -0.997$$



**Table XV. The Isomerization of  
1-(2-Furyl)-2,3,4,5-tetraphenyl-2,4-cyclopentadien-1-ol (26) @ 205.0 ± 0.4 °C**

Aliquot #	Time (sec)	% Concentration	log (% Conc.)
0	0	100.0	2.00
1	840	65.0	1.81
2	1,260	55.0	1.74
3	1,681	42.8	1.63
4	2,100	38.5	1.59
5	2,520	31.3	1.50
6	2,939	24.6	1.39
7	3,360	20.8	1.32

$k$

Plotting log (% Conc.) versus Time

$$k = -2.303 (\text{slope})$$

$$k = 4.60 \pm 0.28 \times 10^{-4} \text{ sec}^{-1}$$

$$\text{slope} = -2.00 \times 10^{-4}$$

$$y_{\text{intercept}} = 1.99$$

$$\text{corr} = -0.998$$

**Table XVI. The Isomerization of  
1-(2-Thienyl)-2,3,4,5-tetraphenyl-2,4-cyclopentadien-1-ol (27) @ 175.0 ± 0.4 °C**

Aliquot #	Time (sec)	% Concentration	log (% Conc.)
0	0	100.0	2.00
1	60	99.3	2.00
2	2,700	80.7	1.91
3	5,401	65.5	1.82
4	8,100	57.0	1.76
5	13,560	38.3	1.58
6	16,200	34.3	1.54
7	18,900	28.9	1.46
8	21,600	24.9	1.40

k

Plotting log (% Conc.) versus Time

$$k = -2.303 (\text{slope})$$

$$k = 6.46 \pm 0.37 \times 10^{-5} \text{ sec}^{-1}$$

$$\text{slope} = -2.80 \times 10^{-5}$$

$$y_{\text{intercept}} = 1.99$$

$$\text{corr} = -0.998$$

**Table XVII. The Isomerization of  
1-(2-Thienyl)-2,3,4,5-tetraphenyl-2,4-cyclopentadien-1-ol (27) @ 190.0 ± 0.4 °C**

Aliquot #	Time (sec)	% Concentration	log (% Conc.)
0	0	100.0	2.00
1	60	100.0	2.00
2	900	85.3	1.93
3	1,800	70.1	1.85
4	2,700	55.6	1.75
5	3,600	45.5	1.66
6	4,500	36.6	1.56
7	5,400	30.8	1.49
8	6,300	26.8	1.43
9	7,200	21.8	1.34

k

Plotting log (% Conc.) versus Time

$$k = -2.303 (\text{slope})$$

$$k = 2.16 \pm 0.15 \times 10^{-4} \text{ sec}^{-1}$$

$$\text{slope} = -9.38 \times 10^{-5}$$

$$y_{\text{intercept}} = 2.00$$

$$\text{corr} = -0.999$$

**Table XVIII. The Isomerization of  
1-(2-Thienyl)-2,3,4,5-tetraphenyl-2,4-cyclopentadien-1-ol (27) @ 205.0 ± 0.4 °C**

Aliquot #	Time (sec)	% Concentration	log (% Conc.)
0	0	100.0	2.00
1	59	97.4	1.99
2	300	83.0	1.92
3	601	72.6	1.86
4	899	58.3	1.77
5	1,199	49.4	1.69
6	1,500	40.4	1.61
7	1,800	30.3	1.48
8	2,161	25.4	1.40
9	2,460	21.9	1.34

k

Plotting log (% Conc.) versus Time

$$k = -2.303 (\text{slope})$$

$$k = 6.38 \pm 0.37 \times 10^{-4} \text{ sec}^{-1}$$

$$\text{slope} = -2.77 \times 10^{-4}$$

$$y_{\text{intercept}} = 2.01$$

$$\text{corr} = -0.998$$

**Table XIX. The Isomerization of  
1-Phenylethynyl-2,3,4,5-tetraphenyl-2,4-cyclopentadien-1-ol (28) @ 145.0 ± 0.4 °C**

Aliquot #	Time (sec)	% Concentration	log (% Conc.)
0	0	100.0	2.00
1	2,401	80.2	1.90
2	4,801	66.2	1.82
3	7,200	56.9	1.76
4	9,600	47.2	1.67
5	12,000	40.2	1.60
6	14,399	32.8	1.52
7	16,803	26.9	1.43
8	19,200	23.8	1.38
9	23,998	16.6	1.22

k

Plotting log (% Conc.) versus Time

$$k = -2.303 (\text{slope})$$

$$k = 7.38 \pm 0.44 \times 10^{-5} \text{ sec}^{-1}$$

$$\text{slope} = -3.20 \times 10^{-5}$$

$$y_{\text{intercept}} = 1.98$$

$$\text{corr} = -0.999$$

Table XX. The Isomerization of  
1-Phenylethynyl-2,3,4,5-tetraphenyl-2,4-cyclopentadien-1-ol (28) @ 160.0 ± 0.4 °C

Aliquot #	Time (sec)	% Concentration	log (% Conc.)
0	0	100.0	2.00
1	721	81.7	1.91
2	1,440	68.1	1.83
3	2,159	54.7	1.74
4	2,879	45.4	1.66
5	3,597	36.8	1.57
6	4,319	29.8	1.47
7	5,040	25.2	1.40
8	5,759	21.6	1.33

$k$

Plotting log (% Conc.) versus Time

$$k = -2.303 (\text{slope})$$

$$k = 2.72 \pm 0.14 \times 10^{-4} \text{ sec}^{-1}$$

$$\text{slope} = -1.18 \times 10^{-4}$$

$$y_{\text{intercept}} = 2.00$$

$$\text{corr} = -0.999$$

**Table XXI. The Isomerization of  
1-Phenylethynyl-2,3,4,5-tetraphenyl-2,4-cyclopentadien-1-ol (28) @ 175.0 ± 0.4 °C**

Aliquot #	Time (sec)	% Concentration	log (% Conc.)
0	0	100.0	2.00
1	364	68.3	1.83
2	719	48.5	1.69
3	1,079	33.3	1.52
4	1,445	23.0	1.36
5	1,799	17.3	1.24
6	2,160	12.0	1.08
7	2,521	8.0	0.90
8	2,880	6.3	0.80

k

Plotting log (% Conc.) versus Time

$$k = -2.303 (\text{slope})$$

$$k = 9.70 \pm 0.51 \times 10^{-4} \text{ sec}^{-1}$$

$$\text{slope} = -4.21 \times 10^{-4}$$

$$y_{\text{intercept}} = 1.99$$

$$\text{corr} = -0.999$$

**Table XXII. The Isomerization of  
1-Vinyl-2,3,4,5-tetraphenyl-2,4-cyclopentadien-1-ol (29) @ 90.0 ± 0.4 °C**

Aliquot #	Time (sec)	% Concentration	log (% Conc.)
0	0	100.0	2.00
1	60	100.0	2.00
2	7,209	84.0	1.92
3	14,399	68.5	1.84
4	21,601	59.2	1.77
5	28,800	47.1	1.67
6	36,002	37.6	1.58
7	43,321	29.9	1.48
8	50,400	23.2	1.37

k

Plotting log (% Conc.) versus Time

$$k = -2.303 (\text{slope})$$

$$k = 2.82 \pm 0.18 \times 10^{-5} \text{ sec}^{-1}$$

$$\text{slope} = -1.23 \times 10^{-5}$$

$$y_{\text{intercept}} = 2.01$$

$$\text{corr} = -0.998$$



**Table XXIII. The Isomerization of  
1-Vinyl-2,3,4,5-tetraphenyl-2,4-cyclopentadien-1-ol (29) @ 105.0 ± 0.4 °C**

Aliquot #	Time (sec)	% Concentration	log (% Conc.)
0	0	100.0	2.00
1	59	99.1	2.00
2	1,145	88.7	1.95
3	2,280	80.6	1.91
4	3,779	68.2	1.83
5	5,280	57.1	1.76
6	6,840	49.2	1.69
7	8,460	41.7	1.62
8	10,201	32.1	1.51
9	12,908	23.9	1.38

k

Plotting log (% Conc.) versus Time

$$k = -2.303 (\text{slope})$$

$$k = 1.10 \pm 0.10 \times 10^{-4} \text{ sec}^{-1}$$

$$\text{slope} = -4.79 \times 10^{-5}$$

$$y_{\text{intercept}} = 2.01$$

$$\text{corr} = -0.999$$

**Table XXIV. The Isomerization of  
1-Vinyl-2,3,4,5-tetraphenyl-2,4-cyclopentadien-1-ol (29) @ 120.0 ± 0.4 °C**

Aliquot #	Time (sec)	% Concentration	log (% Conc.)
0	0	100.0	2.00
1	60	97.0	1.99
2	300	85.5	1.93
3	599	73.3	1.87
4	902	61.5	1.79
5	1,199	53.9	1.73
6	1,499	42.6	1.63
7	2,113	33.0	1.52
8	2,400	27.7	1.44
9	3,180	19.0	1.28
10	3,900	13.4	1.13

k

Plotting log (% Conc.) versus Time

$$k = -2.303 (\text{slope})$$

$$k = 5.18 \pm 0.32 \times 10^{-4} \text{ sec}^{-1}$$

$$\text{slope} = -2.25 \times 10^{-4}$$

$$y_{\text{intercept}} = 1.99$$

$$\text{corr} = -0.999$$

**Table XXV. The Isomerization of  
1-tert-Butyl-2,3,4,5-tetraphenyl-2,4-cyclopentadien-1-ol (30) @ 145.0 ± 0.4 °C**

Aliquot #	Time (sec)	% Concentration	log (% Conc.)
0	0	100.0	2.00
1	3,600	84.2	1.93
2	7,200	73.7	1.87
3	10,800	62.5	1.80
4	14,400	48.5	1.69
5	18,000	42.5	1.63
6	22,200	35.6	1.55
7	25,200	28.0	1.45
8	28,800	24.1	1.38

k

Plotting log (% Conc.) versus Time

$$k = -2.303 (\text{slope})$$

$$k = 5.01 \pm 0.44 \times 10^{-5} \text{ sec}^{-1}$$

$$\text{slope} = -2.18 \times 10^{-5}$$

$$y_{\text{intercept}} = 2.01$$

$$\text{corr} = -0.998$$

**Table XXVI. The Isomerization of  
1-tert-Butyl-2,3,4,5-tetraphenyl-2,4-cyclopentadien-1-ol (30) @ 160.0 ± 0.4 °C**

Aliquot #	Time (sec)	% Concentration	log (% Conc.)
0	0	100.0	2.00
1	1,201	81.1	1.91
2	2,401	67.0	1.83
3	3,600	52.7	1.72
4	4,801	48.2	1.68
5	5,997	40.4	1.61
6	7,199	29.9	1.48
7	8,402	26.6	1.42
8	9,600	21.6	1.33

*k*

Plotting log (% Conc.) versus Time

$$k = -2.303 (\text{slope})$$

$$k = 1.59 \pm 0.12 \times 10^{-4} \text{ sec}^{-1}$$

$$\text{slope} = -6.90 \times 10^{-5}$$

$$y_{\text{intercept}} = 2.00$$

$$\text{corr} = -0.997$$

**Table XXVII. The Isomerization of  
1-tert-Butyl-2,3,4,5-tetraphenyl-2,4-cyclopentadien-1-ol (30) @ 175.0 ± 0.4 °C**

Aliquot #	Time (sec)	% Concentration	log (% Conc.)
0	0	100.0	2.00
1	361	84.0	1.92
2	721	70.5	1.85
3	1,080	58.2	1.76
4	1,439	52.1	1.72
5	1,799	43.8	1.64
6	2,163	33.6	1.53
7	2,520	30.7	1.49
8	2,880	23.9	1.38

*k*

Plotting log (% Conc.) versus Time

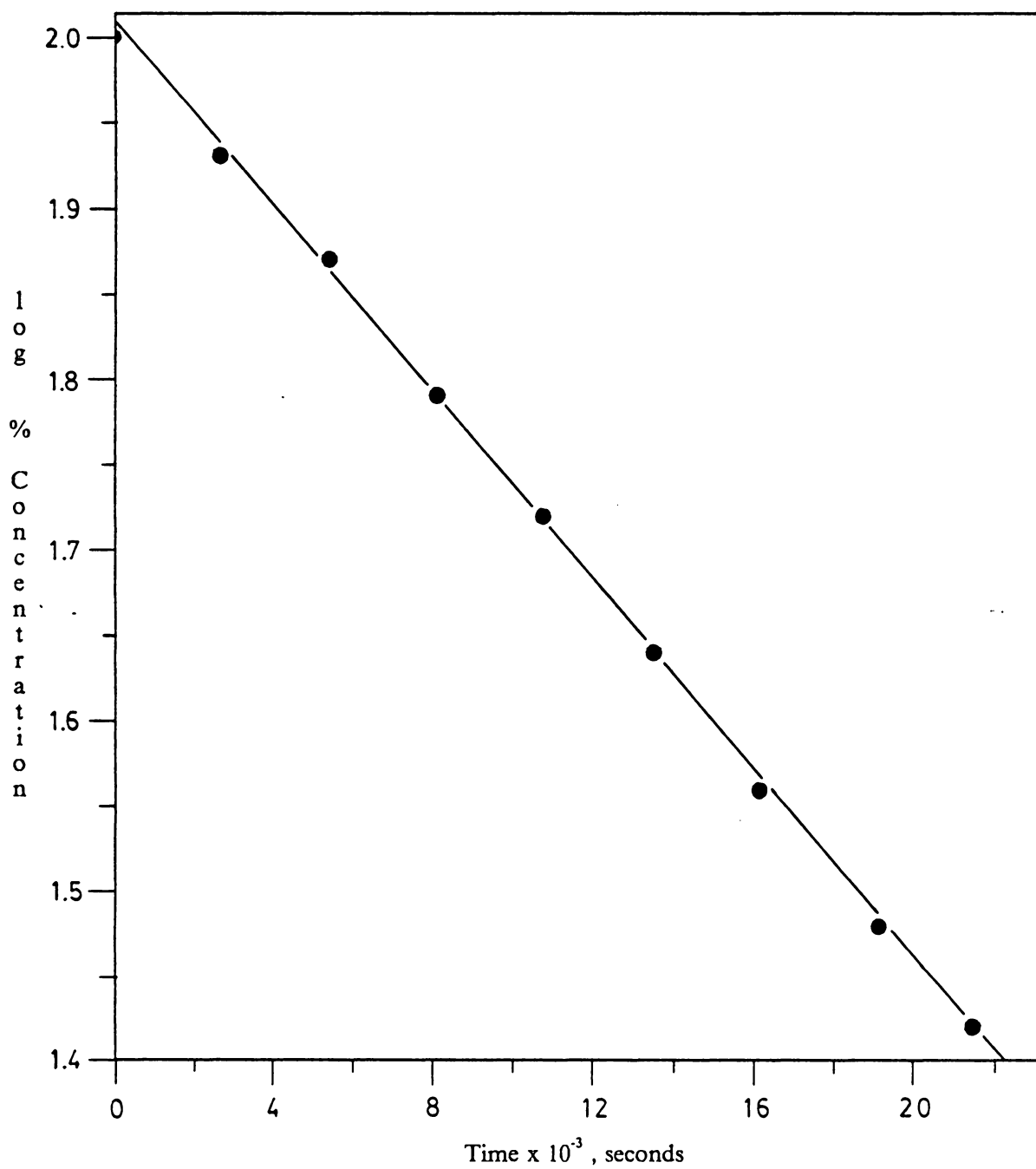
$$k = -2.303 (\text{slope})$$

$$k = 4.83 \pm 0.46 \times 10^{-4} \text{ sec}^{-1}$$

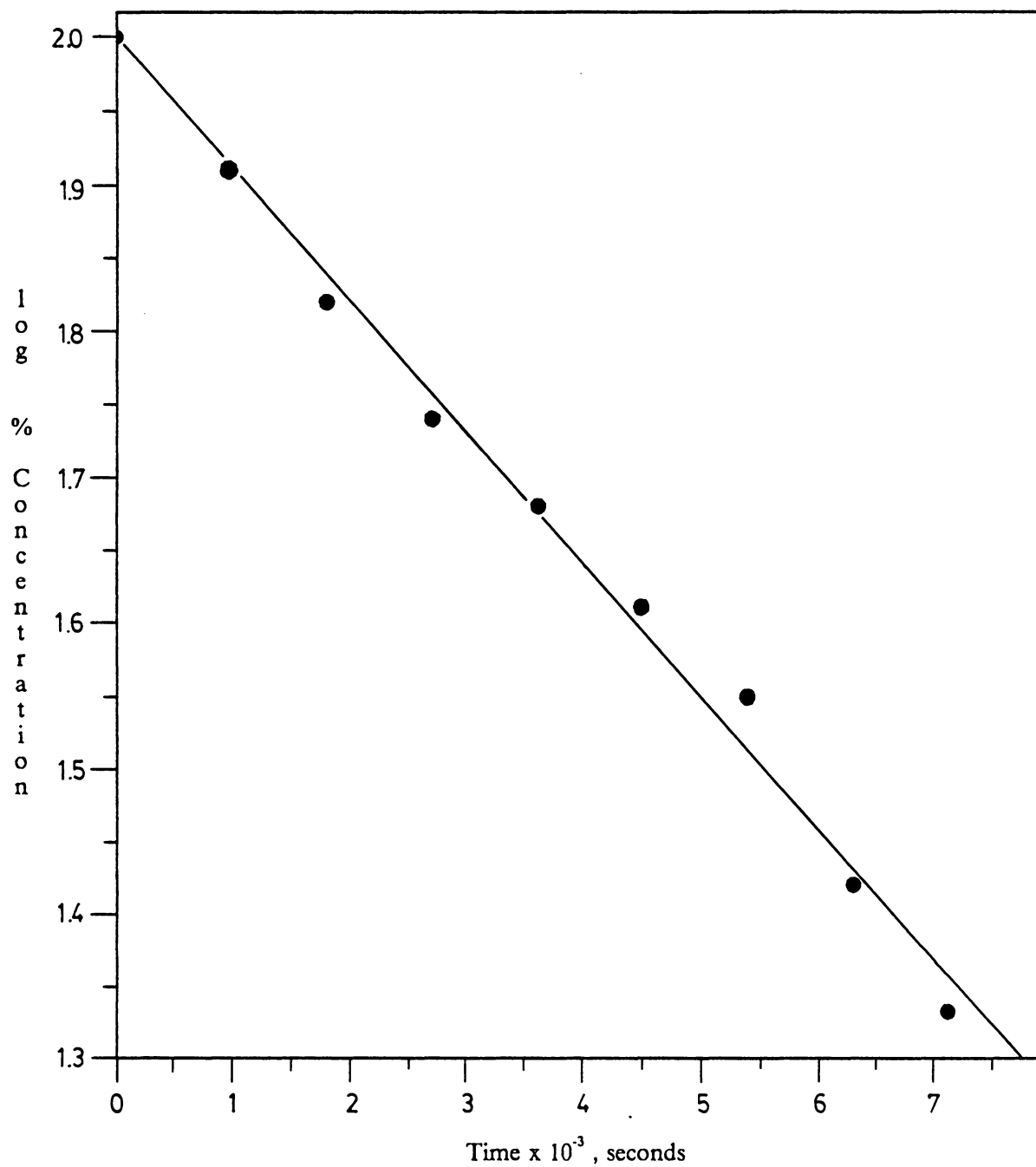
$$\text{slope} = -2.10 \times 10^{-4}$$

$$y_{\text{intercept}} = 2.00$$

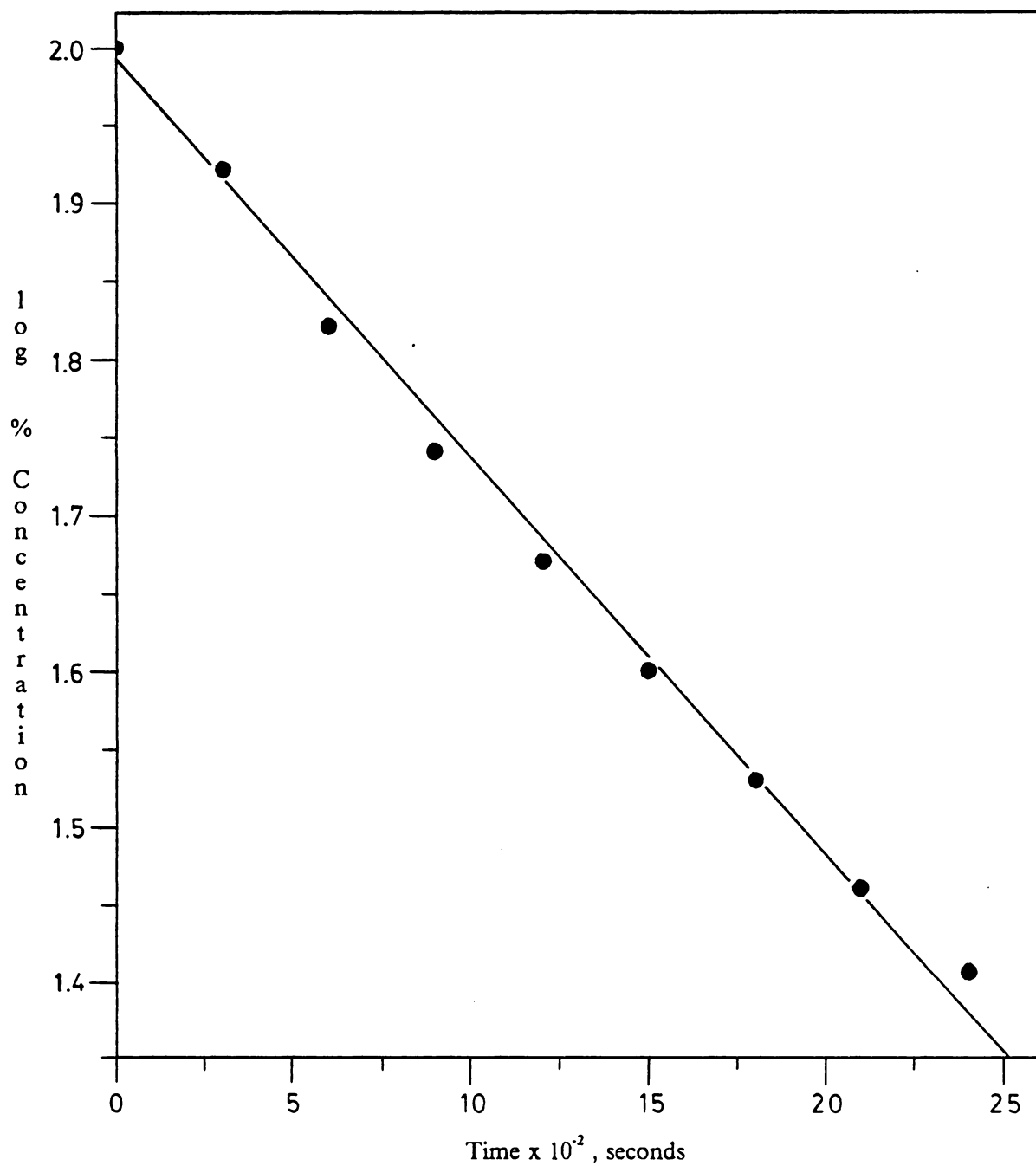
$$\text{corr} = -0.997$$



**Figure 2.** First-order plot of the isomerization of 1,2,3,4,5-pentaphenyl-2,4-cyclopentadien-1-ol (2) @ 175.0 ± 0.4 °C.



**Figure 3.** First-order plot of the isomerization of 1,2,3,4,5-pentaphenyl-2,4-cyclopentadien-1-ol (2) @ 190.0 ± 0.4 °C.



**Figure 4.** First-order plot of the isomerization of 1,2,3,4,5-pentaphenyl-2,4-cyclopentadien-1-ol (2) @ 205.0 ± 0.4 °C.



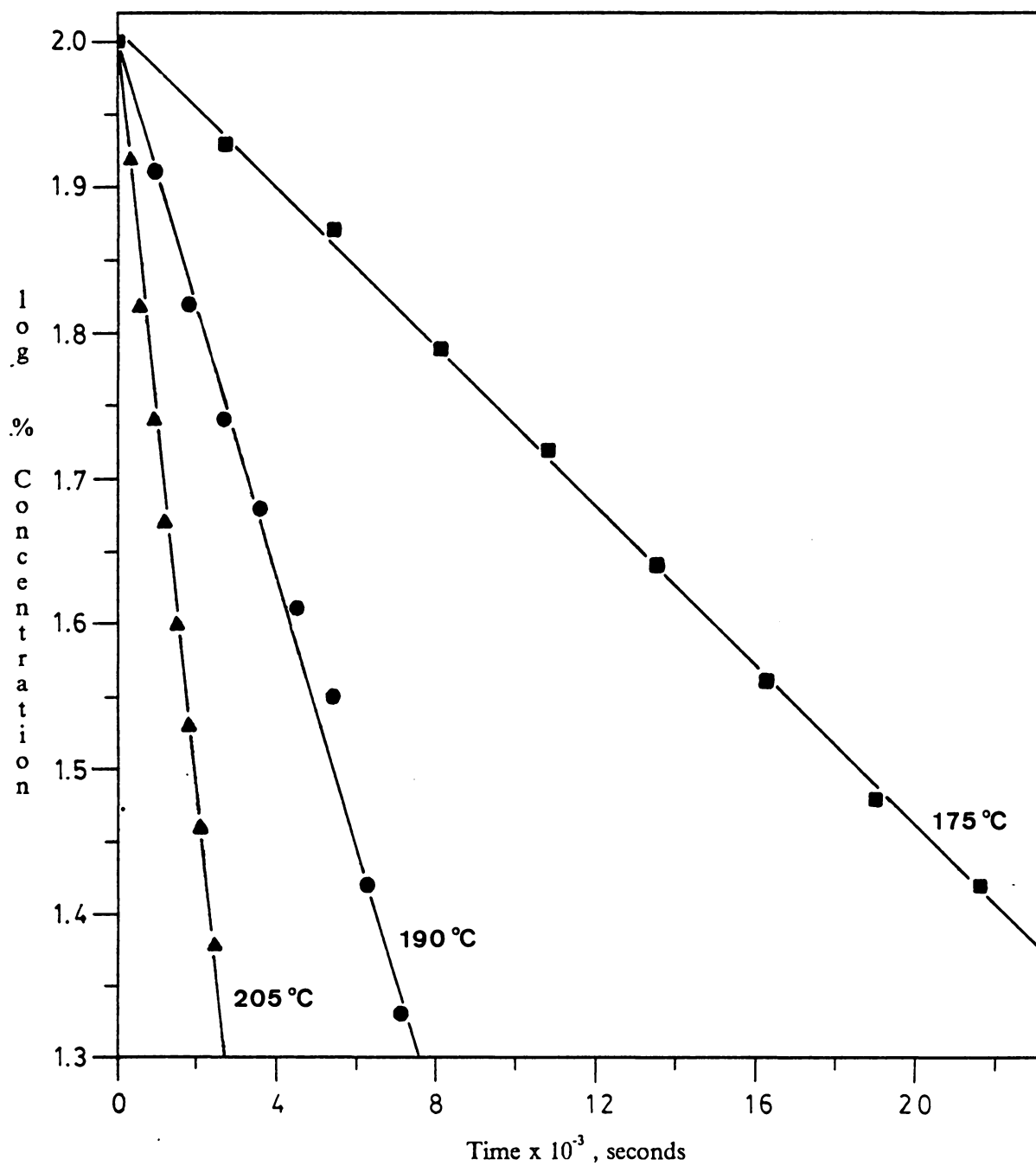
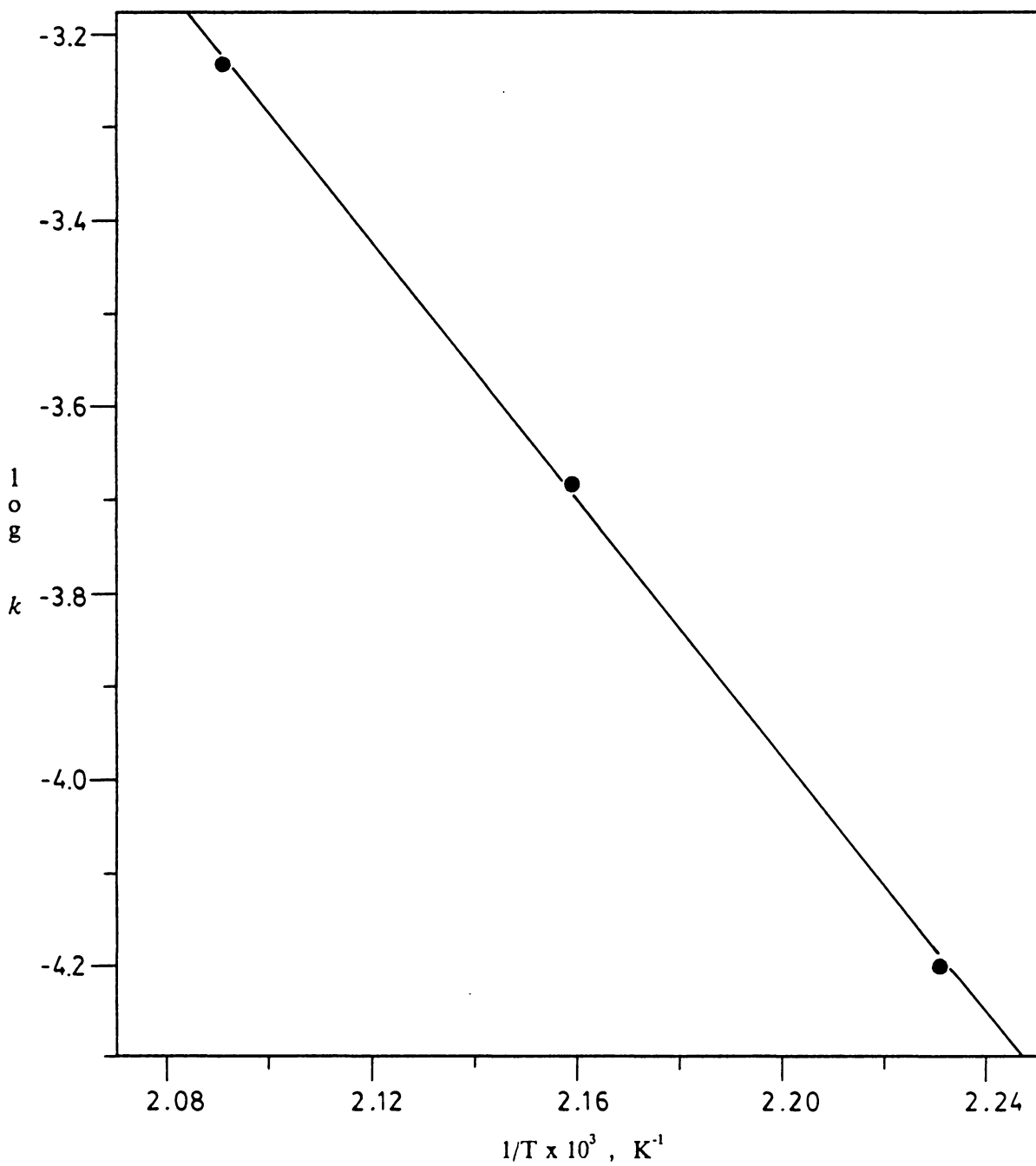
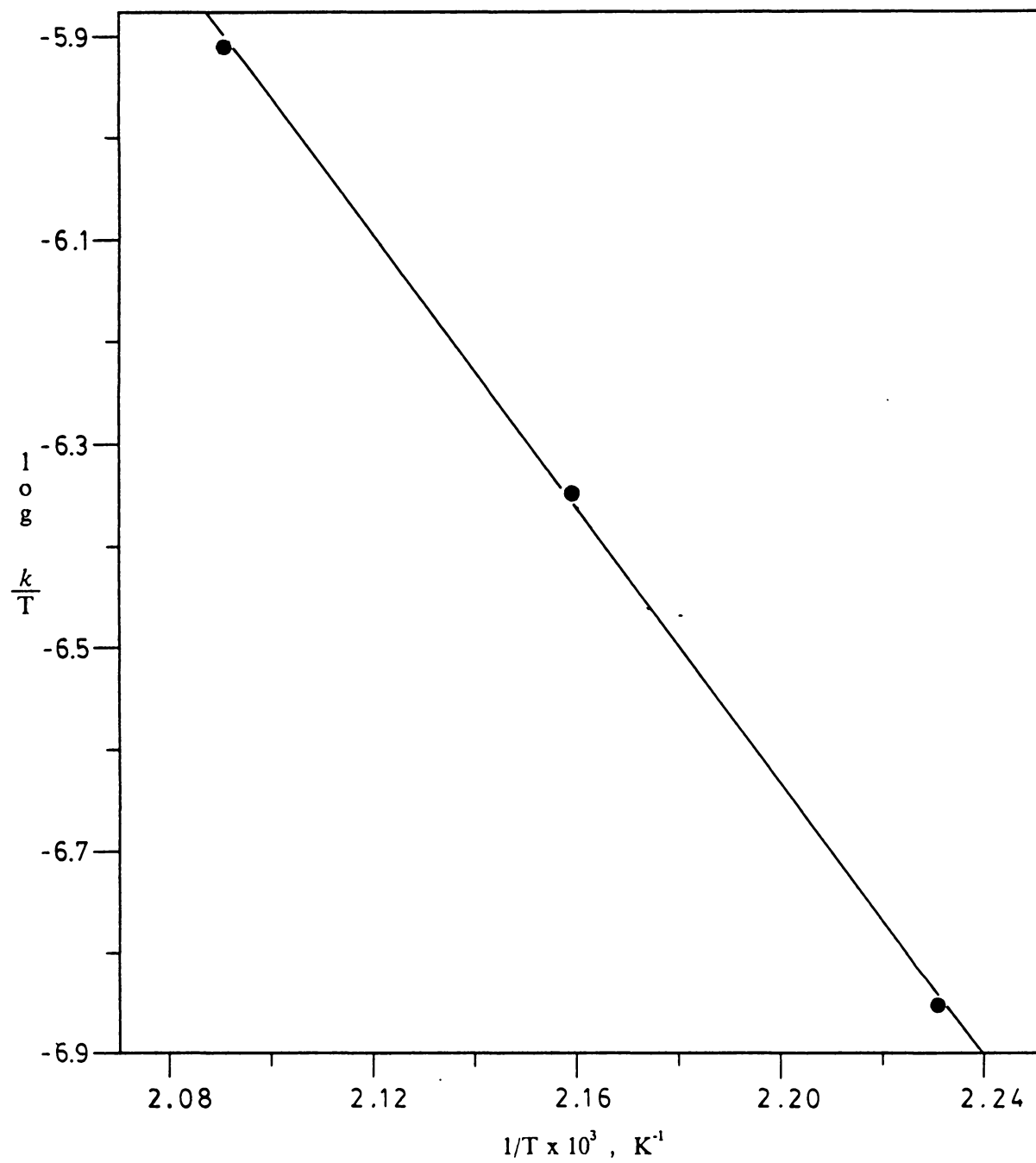


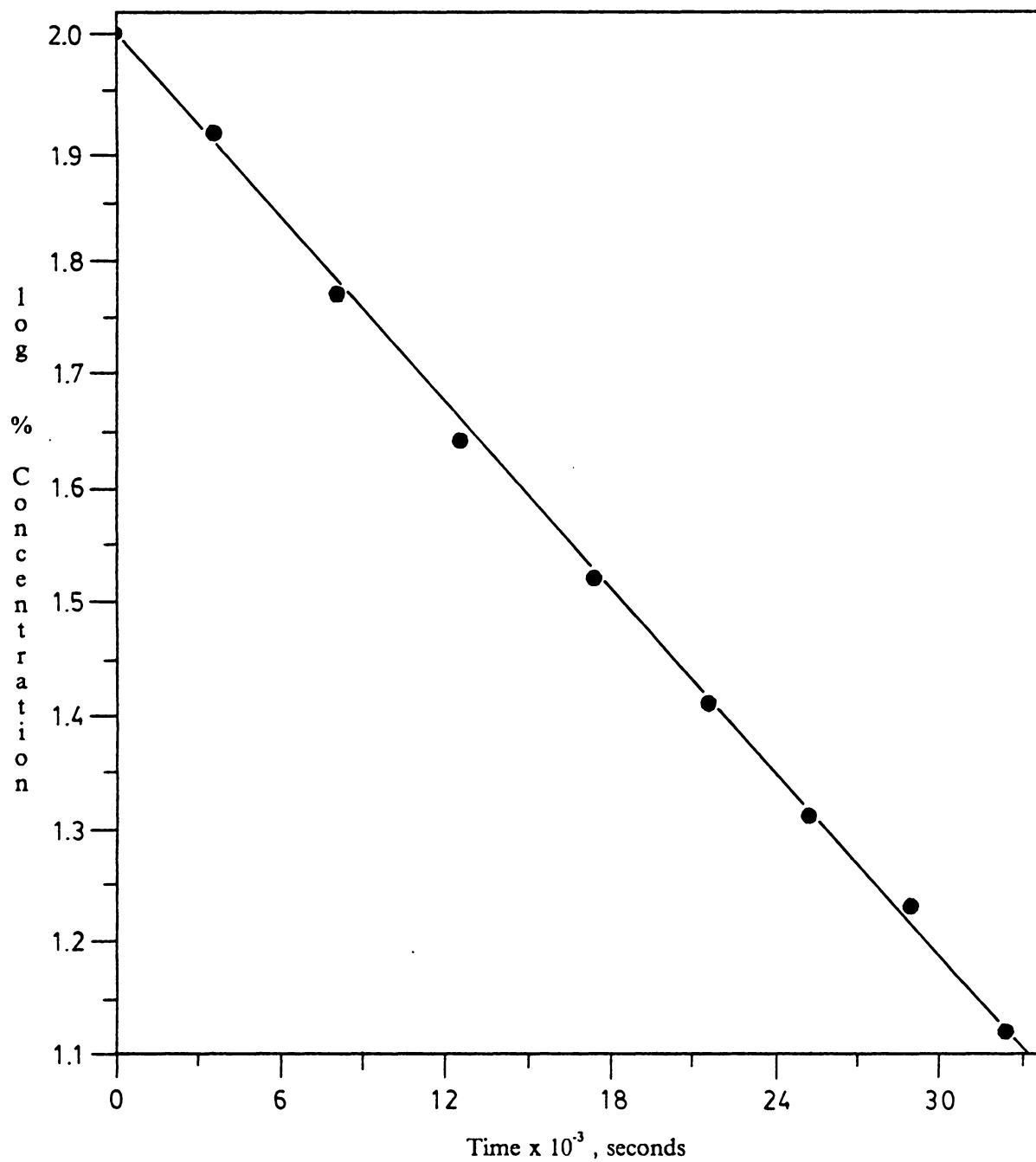
Figure 5. First-order plot of the isomerization of 1,2,3,4,5-pentaphenyl-2,4-cyclopentadien-1-ol (2) @ 175.0-205.0 °C.



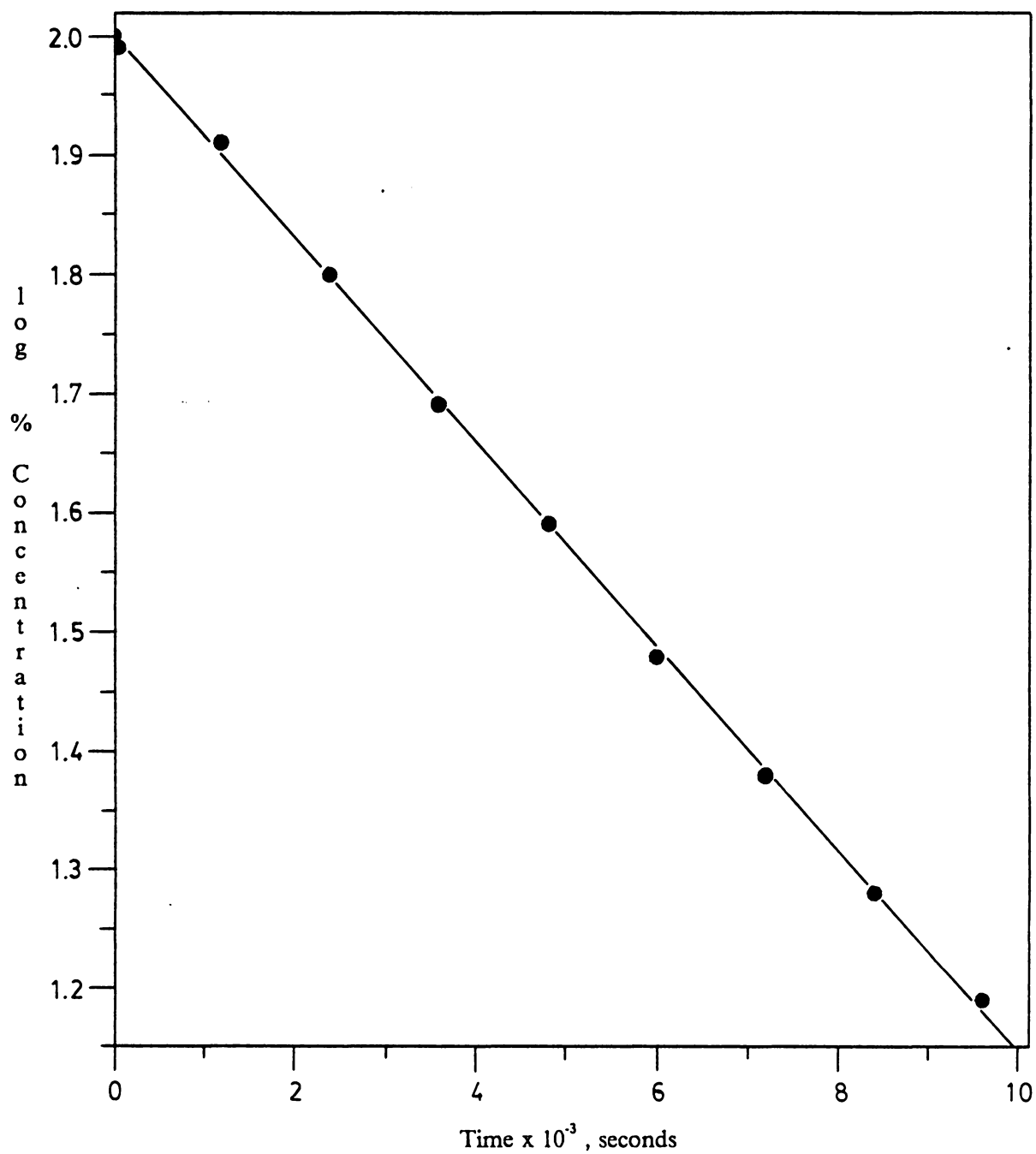
**Figure 6.** Arrhenius plot of the isomerization of 1,2,3,4,5-pentaphenyl-2,4-cyclopentadien-1-ol (2).



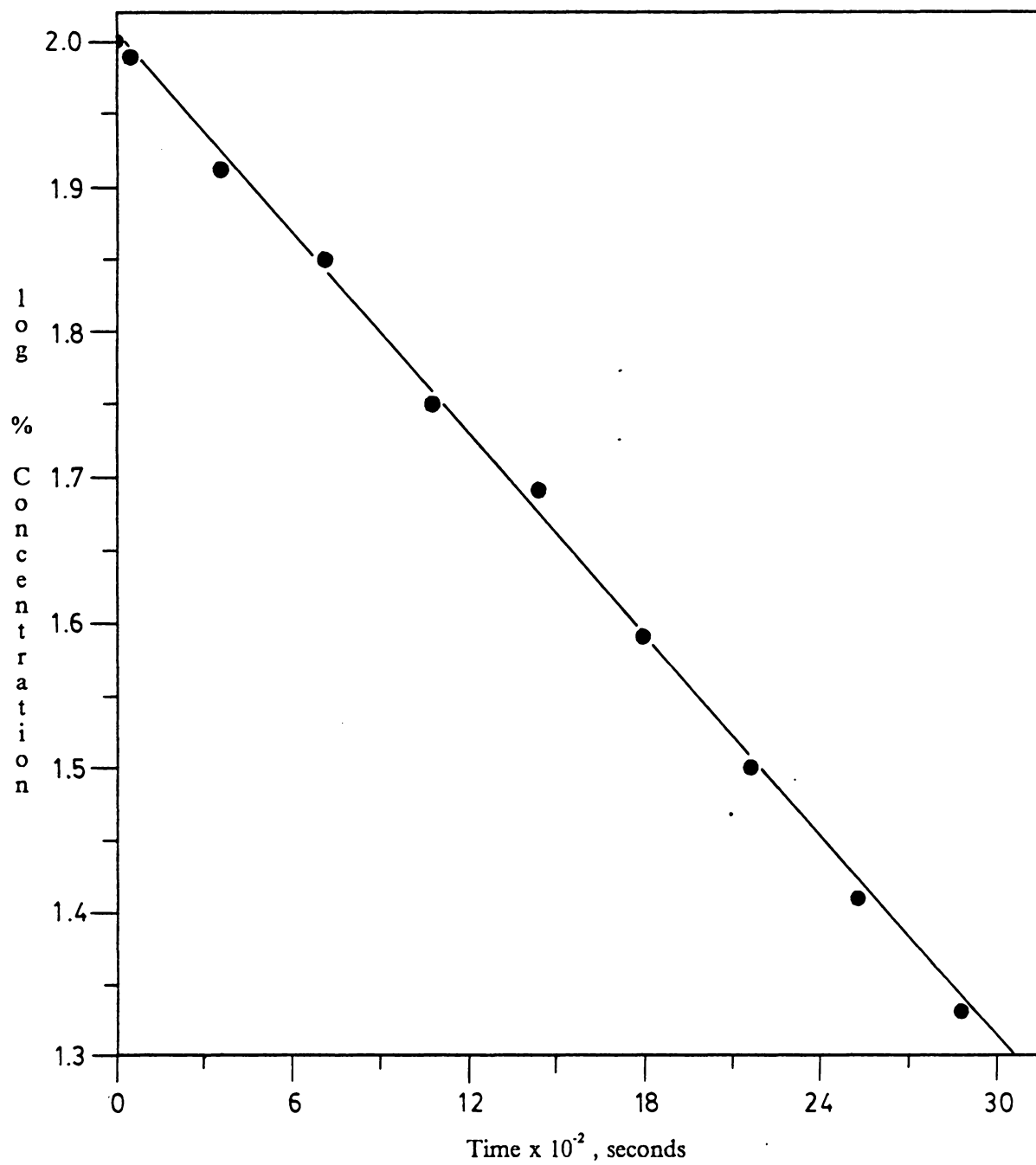
**Figure 7.** Eyring plot of the isomerization of 1,2,3,4,5-pentaphenyl-2,4-cyclopentadien-1-ol (2).



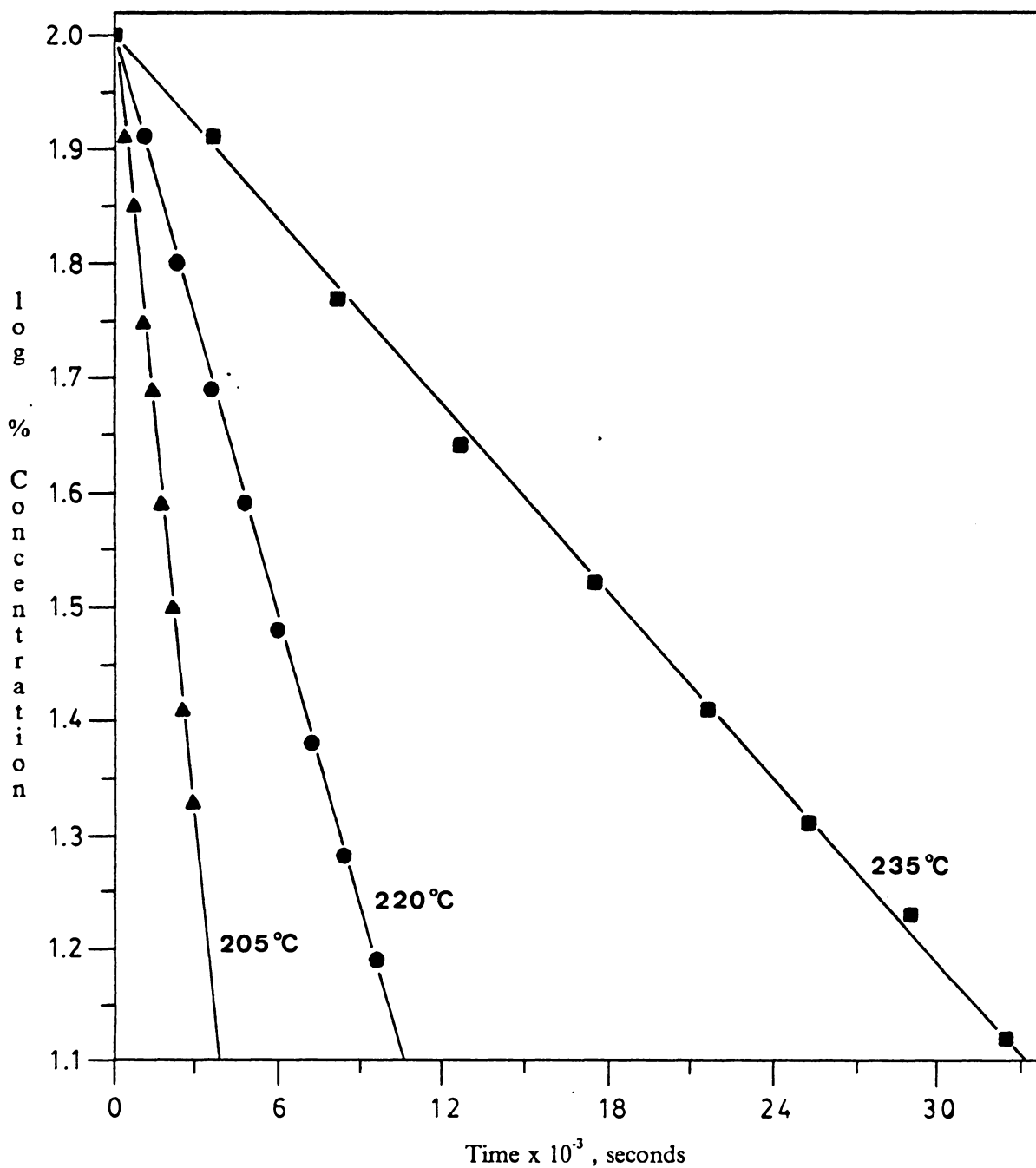
**Figure 8.** First-order plot of the isomerization of  
1-(1-naphthyl)-2,3,4,5-tetraphenyl-2,4-cyclopentadien-1-ol (**24**) @ 205.0 ± 0.4 °C.



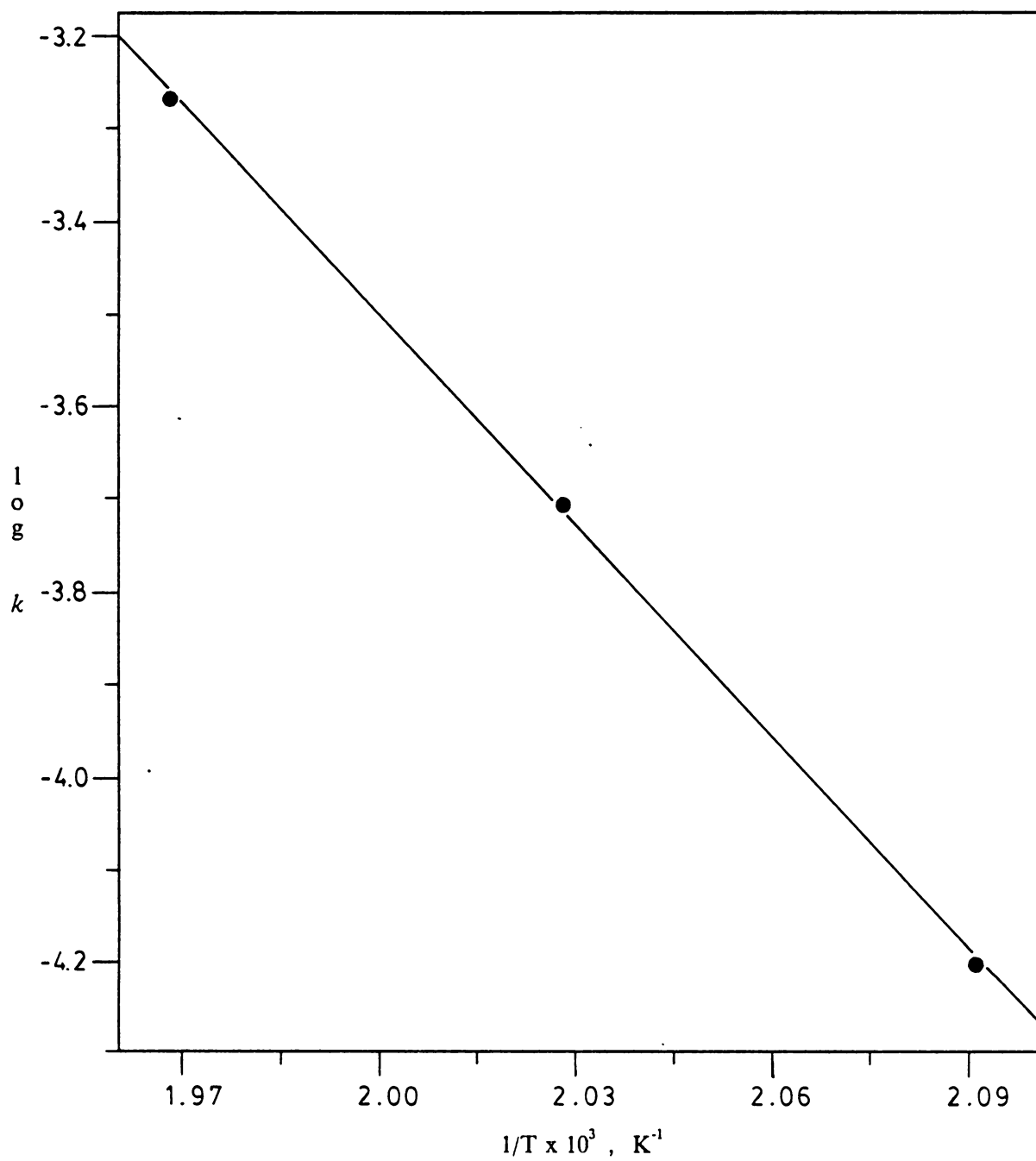
**Figure 9.** First-order plot of the isomerization of 1-(1-naphthyl)-2,3,4,5-tetraphenyl-2,4-cyclopentadien-1-ol (24) @ 220.0 ± 0.4 °C.



**Figure 10.** First-order plot of the isomerization of 1-(1-naphthyl)-2,3,4,5-tetraphenyl-2,4-cyclopentadien-1-ol (**24**) @ 235.0 ± 0.4 °C.

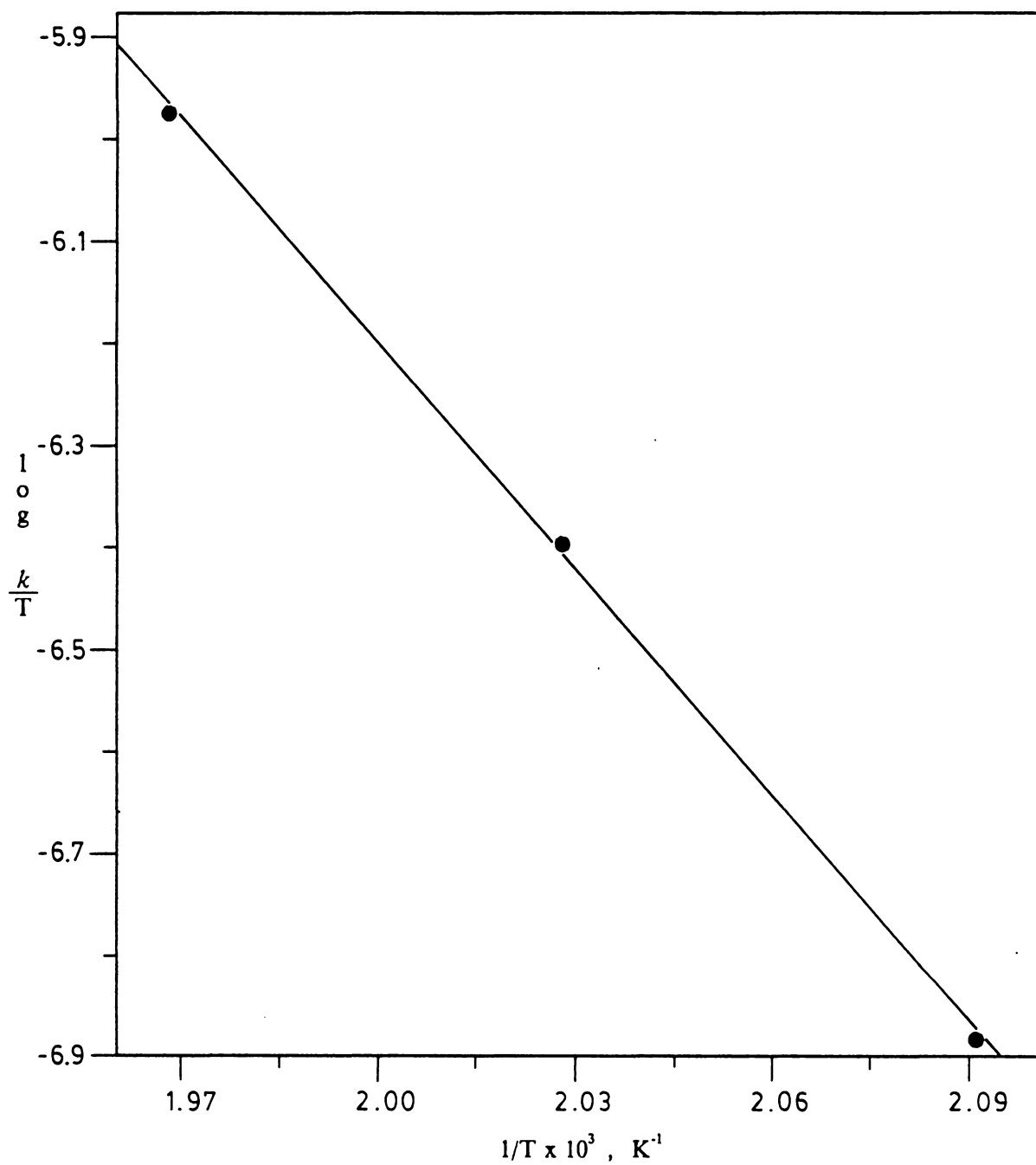


**Figure 11.** First-order plot of the isomerization of 1-(1-naphthyl)-2,3,4,5-tetraphenyl-2,4-cyclopentadien-1-ol (**24**) @ 205.0 - 235.0 °C.

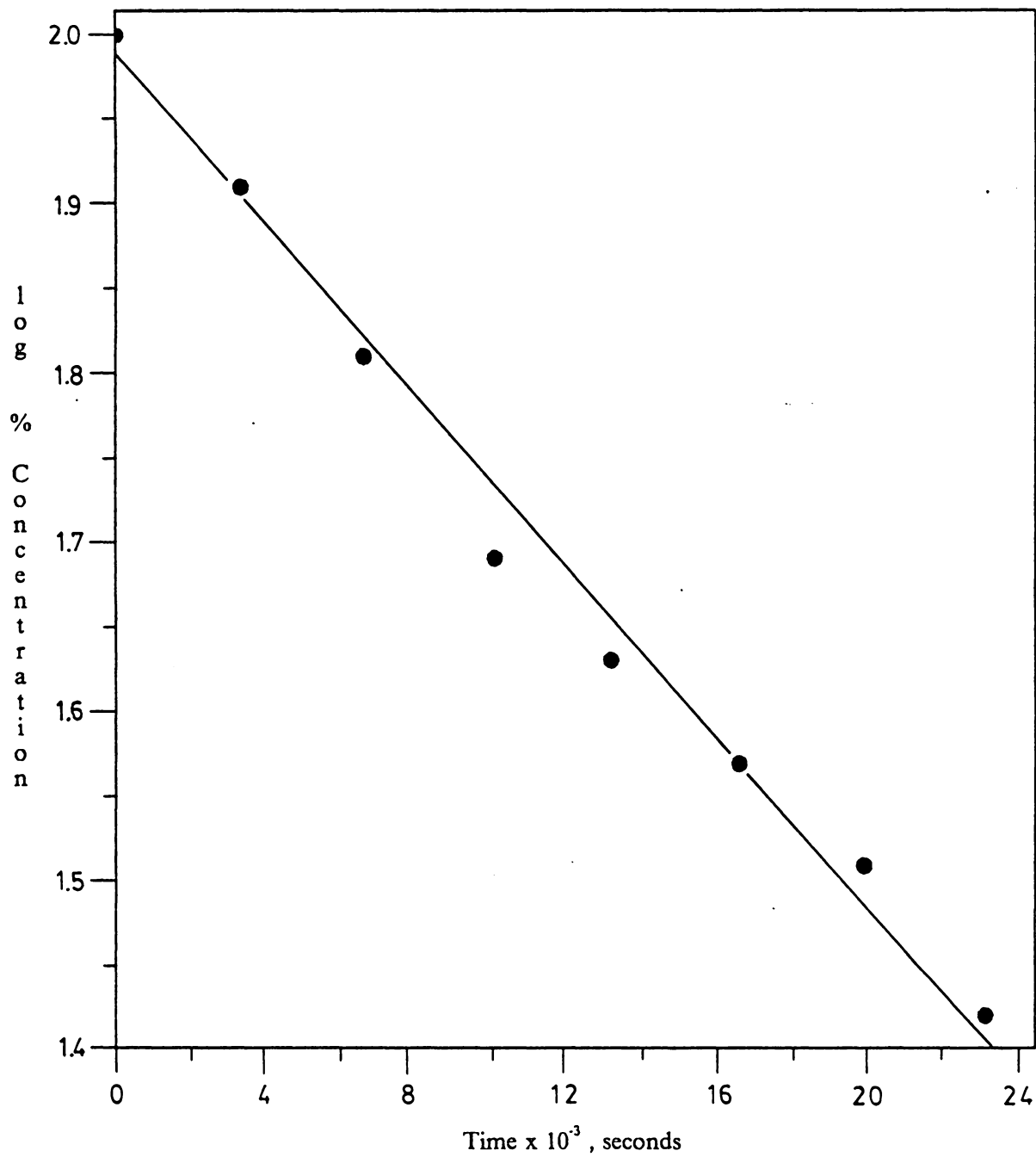


**Figure 12.** Arrhenius plot of the isomerization of 1-(1-naphthyl)-2,3,4,5-tetraphenyl-2,4-cyclopentadien-1-ol (**24**).

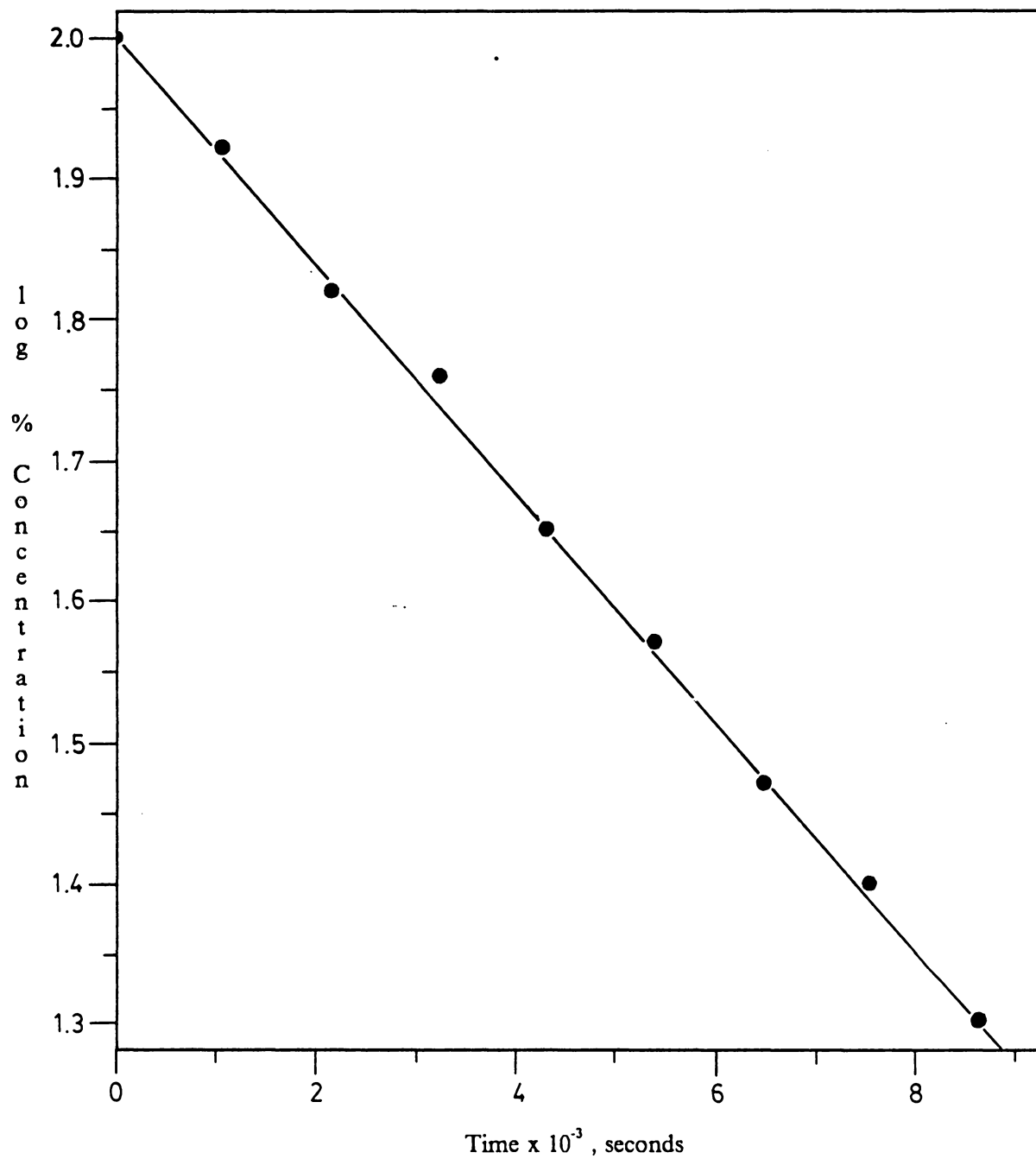




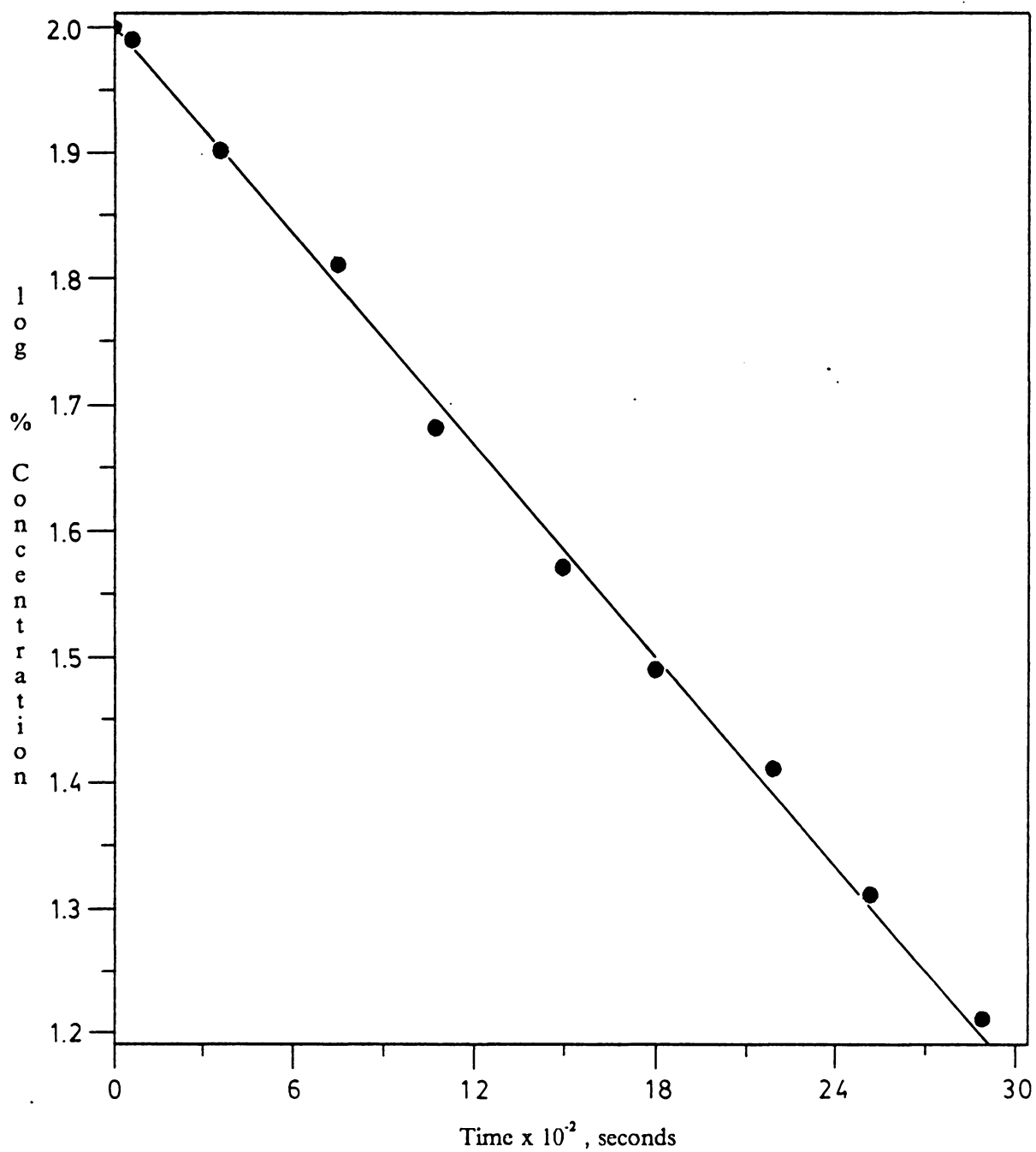
**Figure 13.** Eyring plot of the isomerization of 1-(1-naphthyl)-2,3,4,5-tetraphenyl-2,4-cyclopentadien-1-ol (**24**).



**Figure 14.** First-order plot of the isomerization of 1-(2-pyridyl)-2,3,4,5-tetraphenyl-2,4-cyclopentadien-1-ol (**25**) @ 145.0 ± 0.4 °C.



**Figure 15.** First-order plot of the isomerization of 1-(2-pyridyl)-2,3,4,5-tetraphenyl-2,4-cyclopentadien-1-ol (**25**) @ 160.0 ± 0.4 °C.



**Figure 16.** First-order plot of the isomerization of 1-(2-pyridyl)-2,3,4,5-tetraphenyl-2,4-cyclopentadien-1-ol (**25**) @ 175.0 ± 0.4 °C.

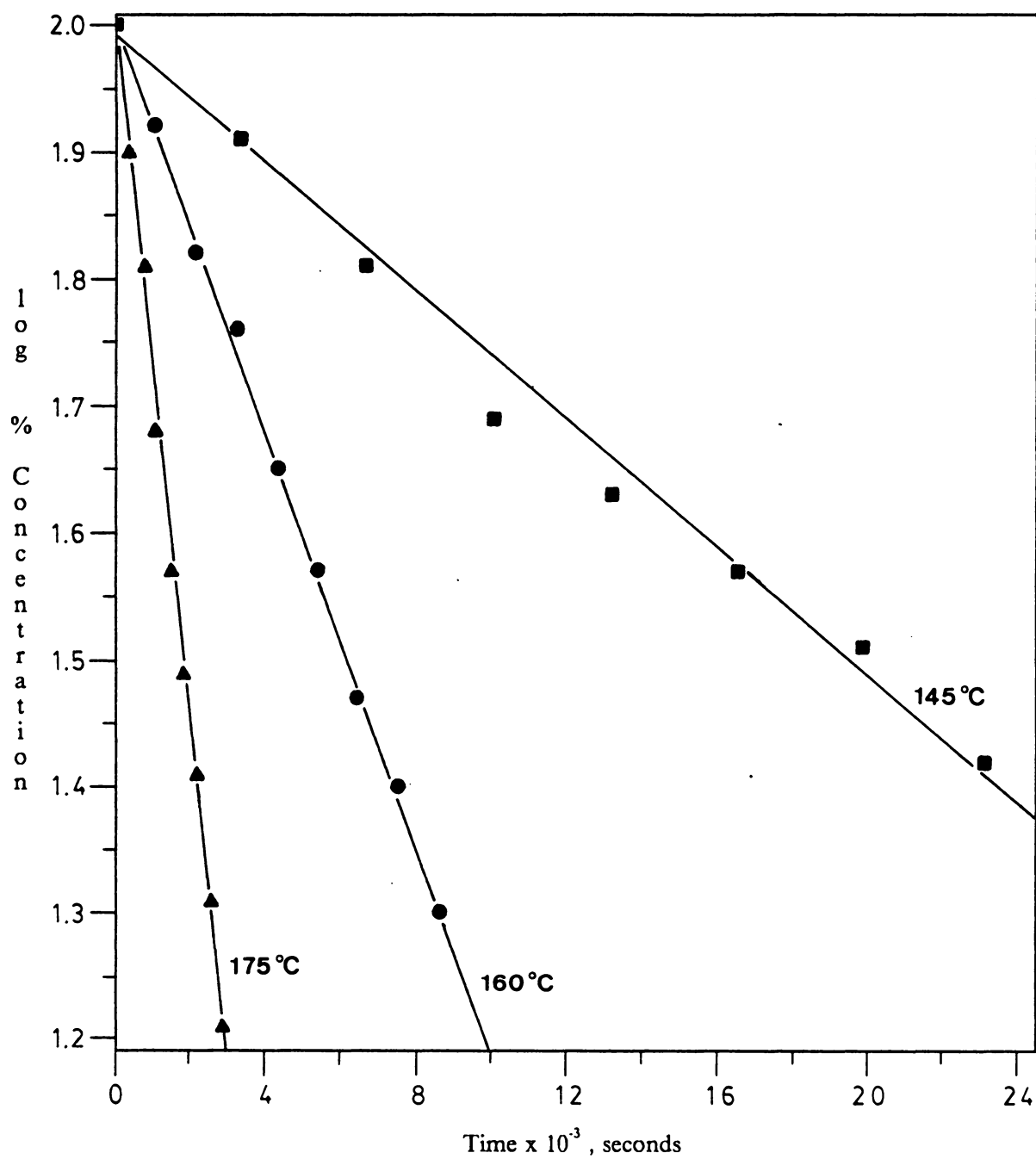
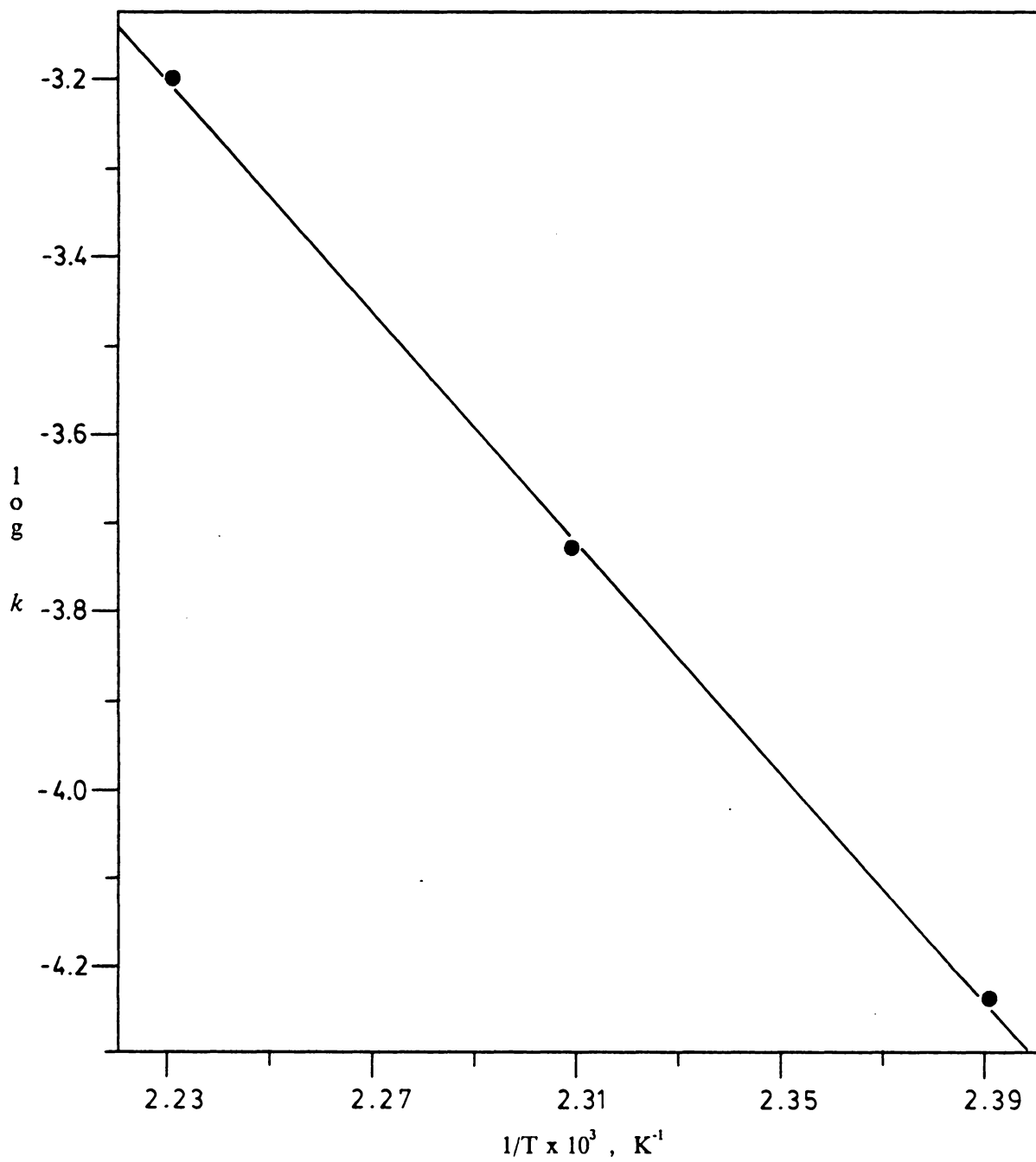
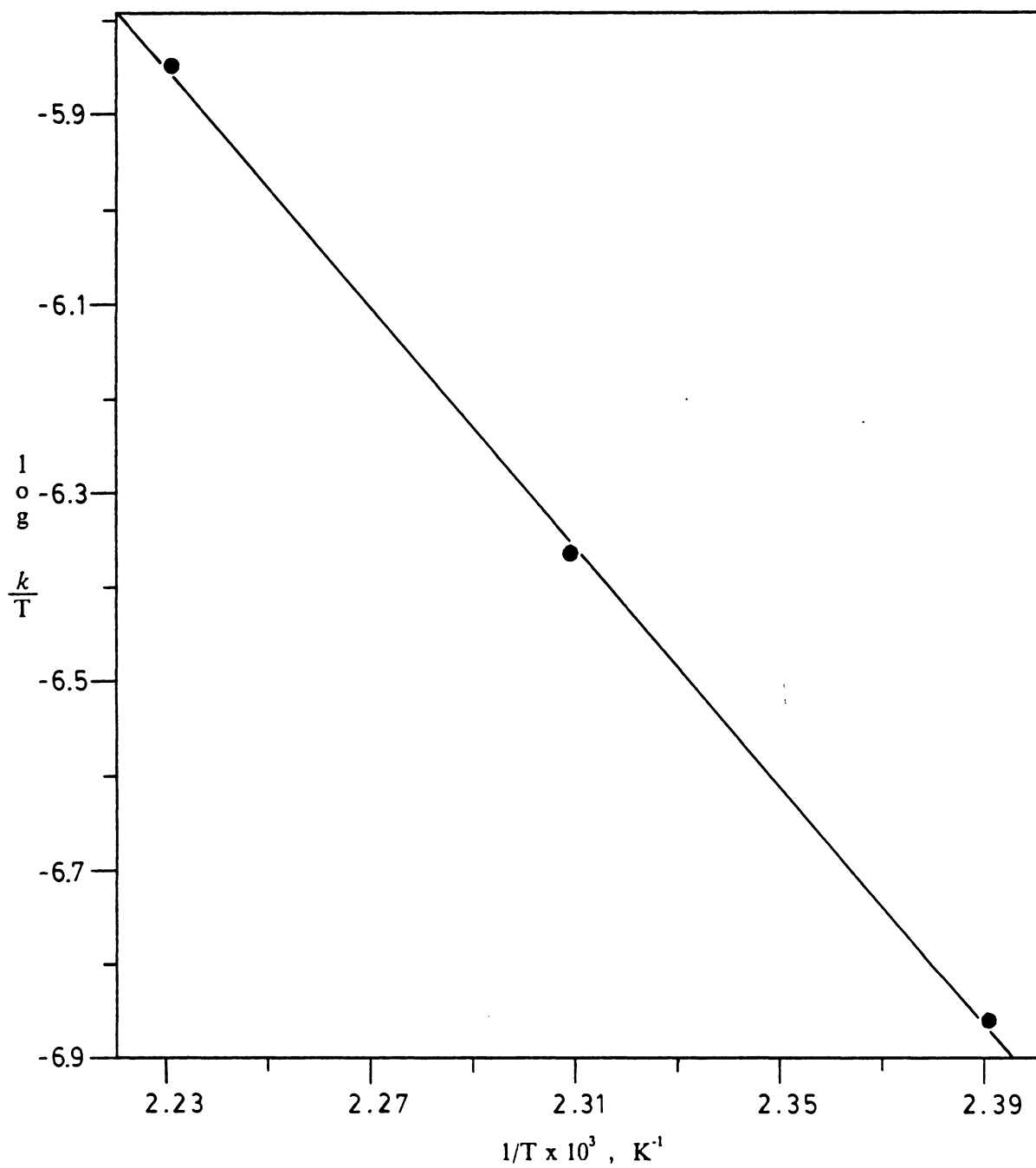


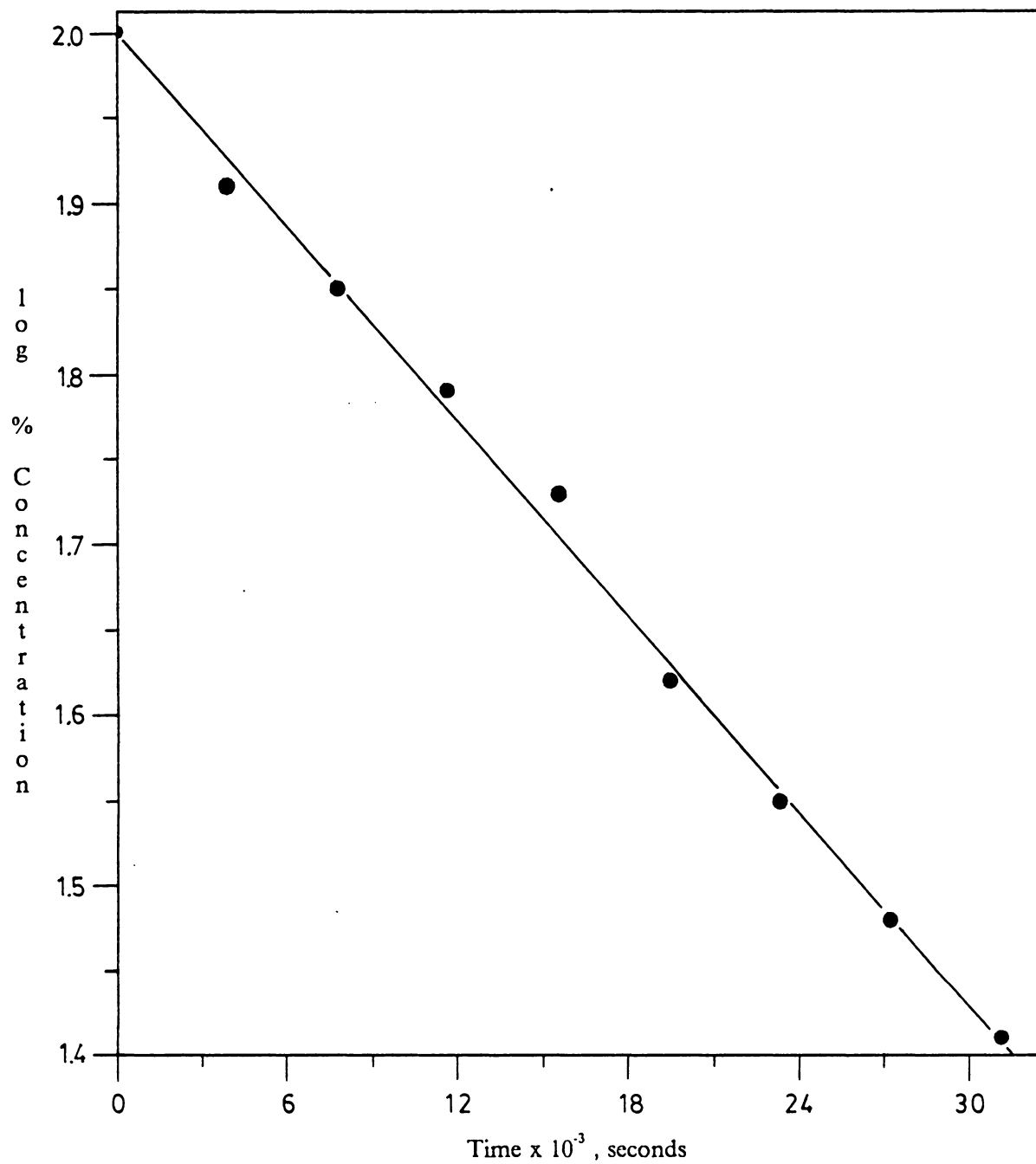
Figure 17. First-order plot of the isomerization of 1-(2-pyridyl)-2,3,4,5-tetraphenyl-2,4-cyclopentadien-1-ol (**25**) @ 145.0 - 175.0 °C.



**Figure 18.** Arrhenius plot of the isomerization of 1-(2-pyridyl)-2,3,4,5-tetraphenyl-2,4-cyclopentadien-1-ol (**25**).

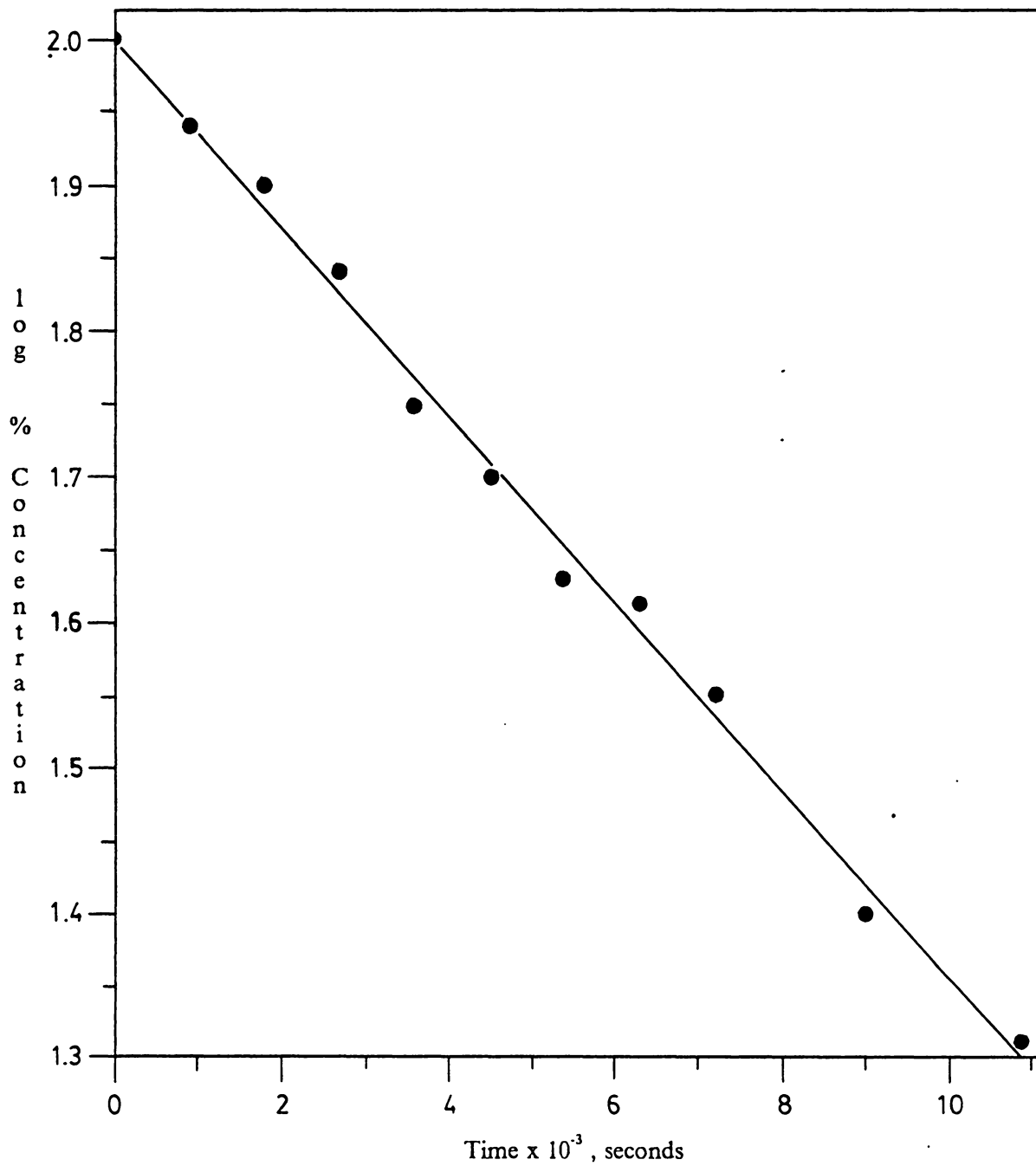


**Figure 19.** Eyring plot of the isomerization of 1-(2-pyridyl)-2,3,4,5-tetraphenyl-2,4-cyclopentadien-1-ol (25).

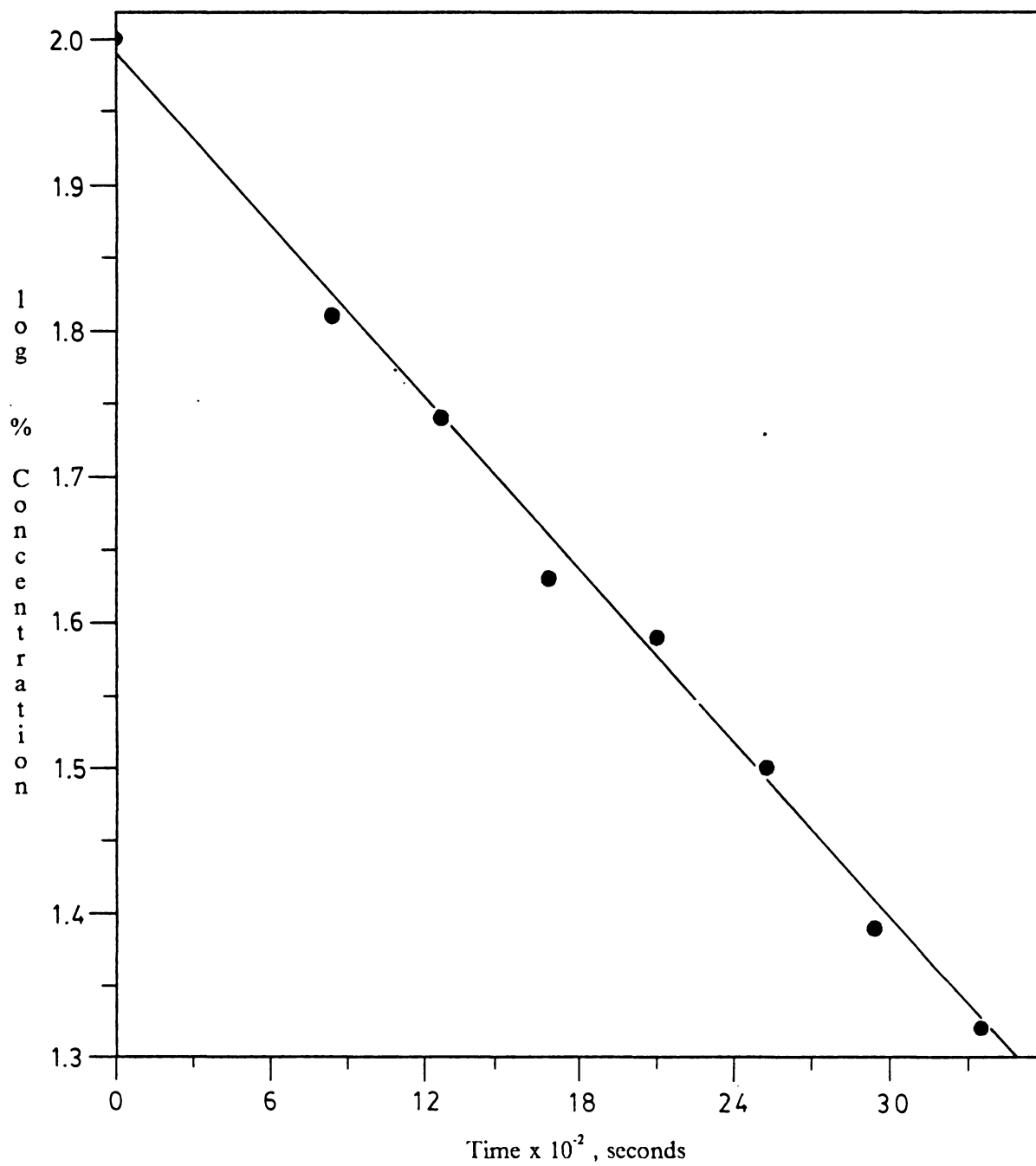


**Figure 20.** First-order plot of the isomerization of 1-(2-furyl)-2,3,4,5-tetraphenyl-2,4-cyclopentadien-1-ol (**26**) @ 175.0 ± 0.4 °C.

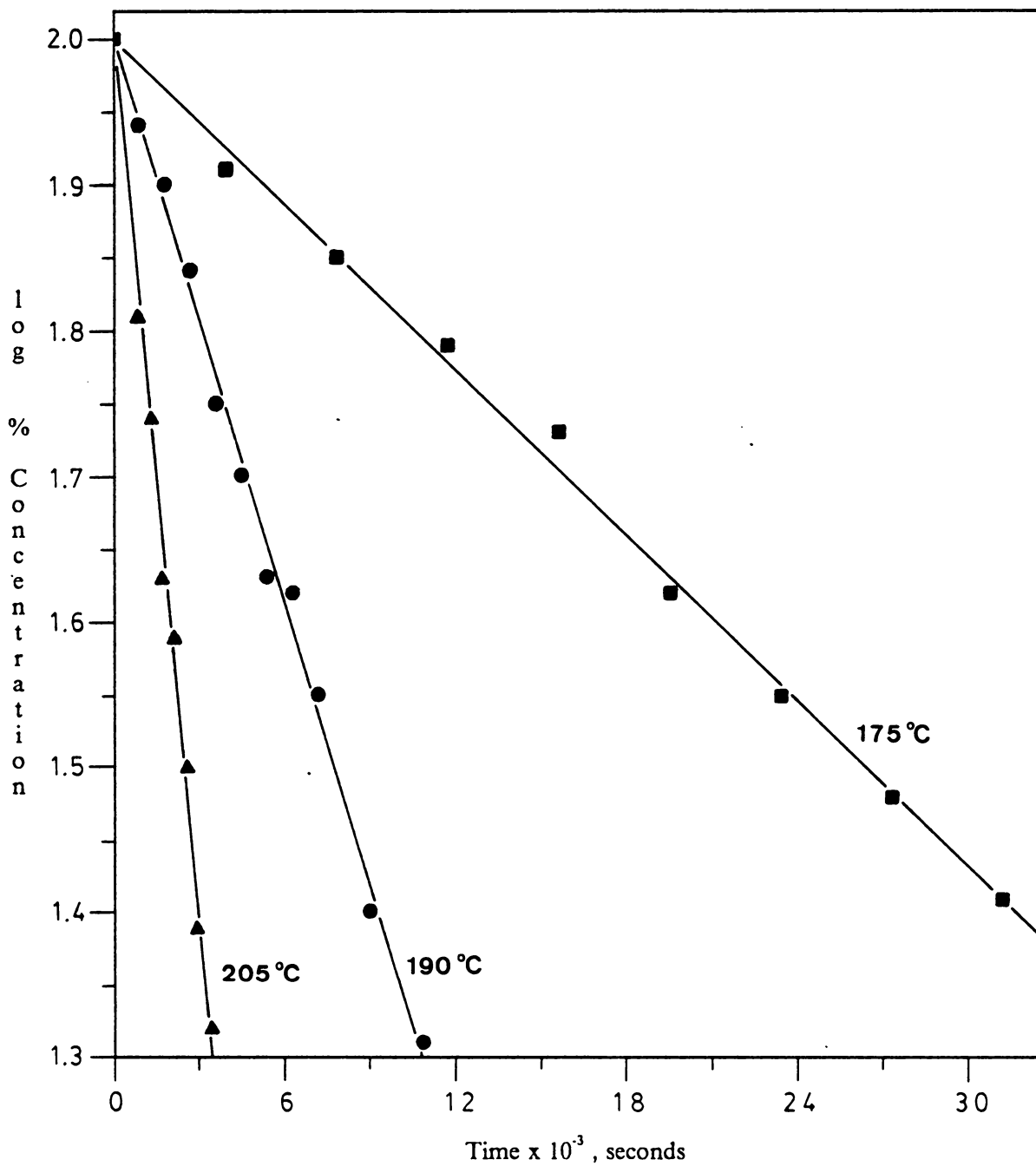




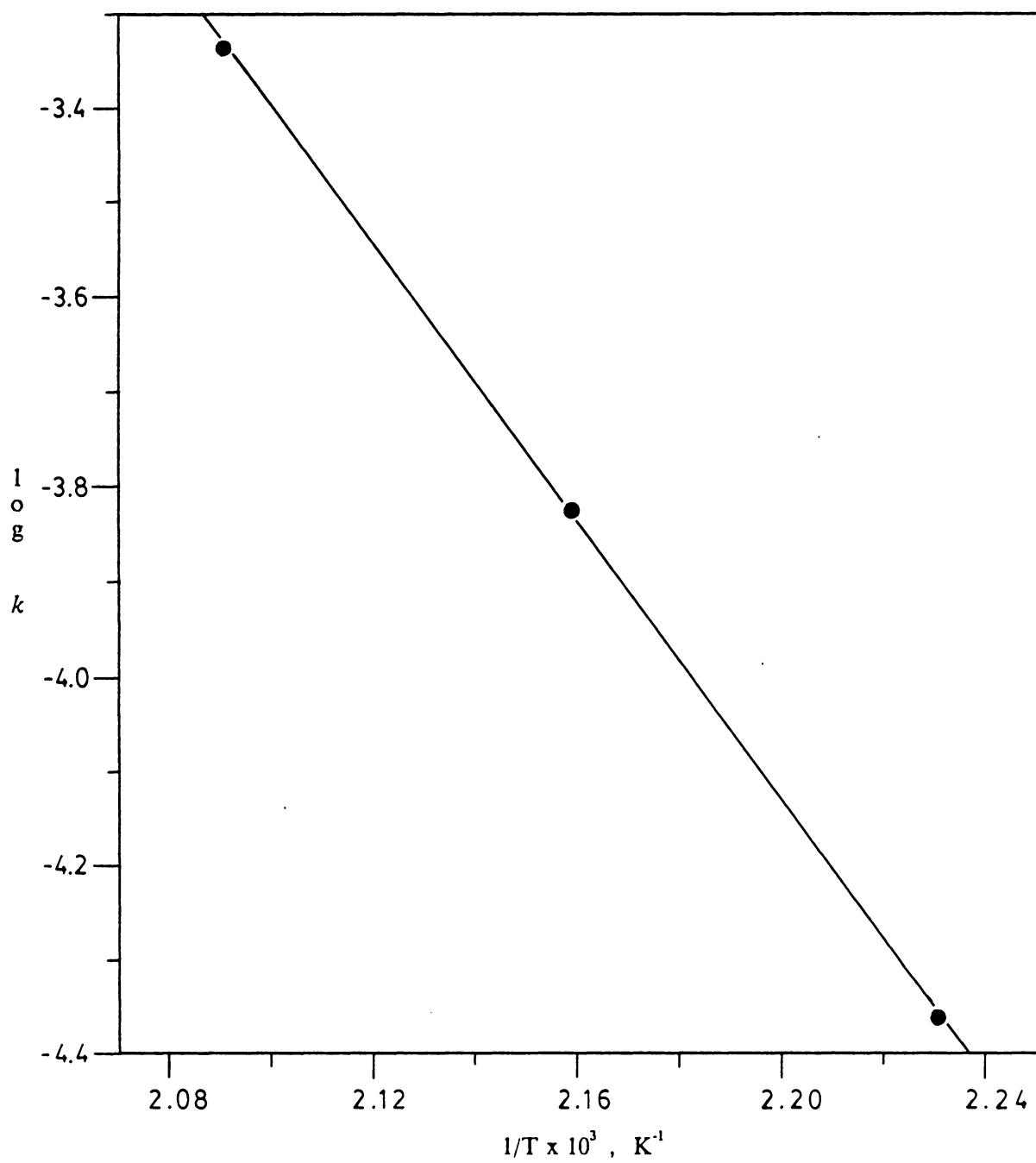
**Figure 21.** First-order plot of the isomerization of 1-(2-furyl)-2,3,4,5-tetraphenyl-2,4-cyclopentadien-1-ol (**26**) @ 190.0 ± 0.4 °C.



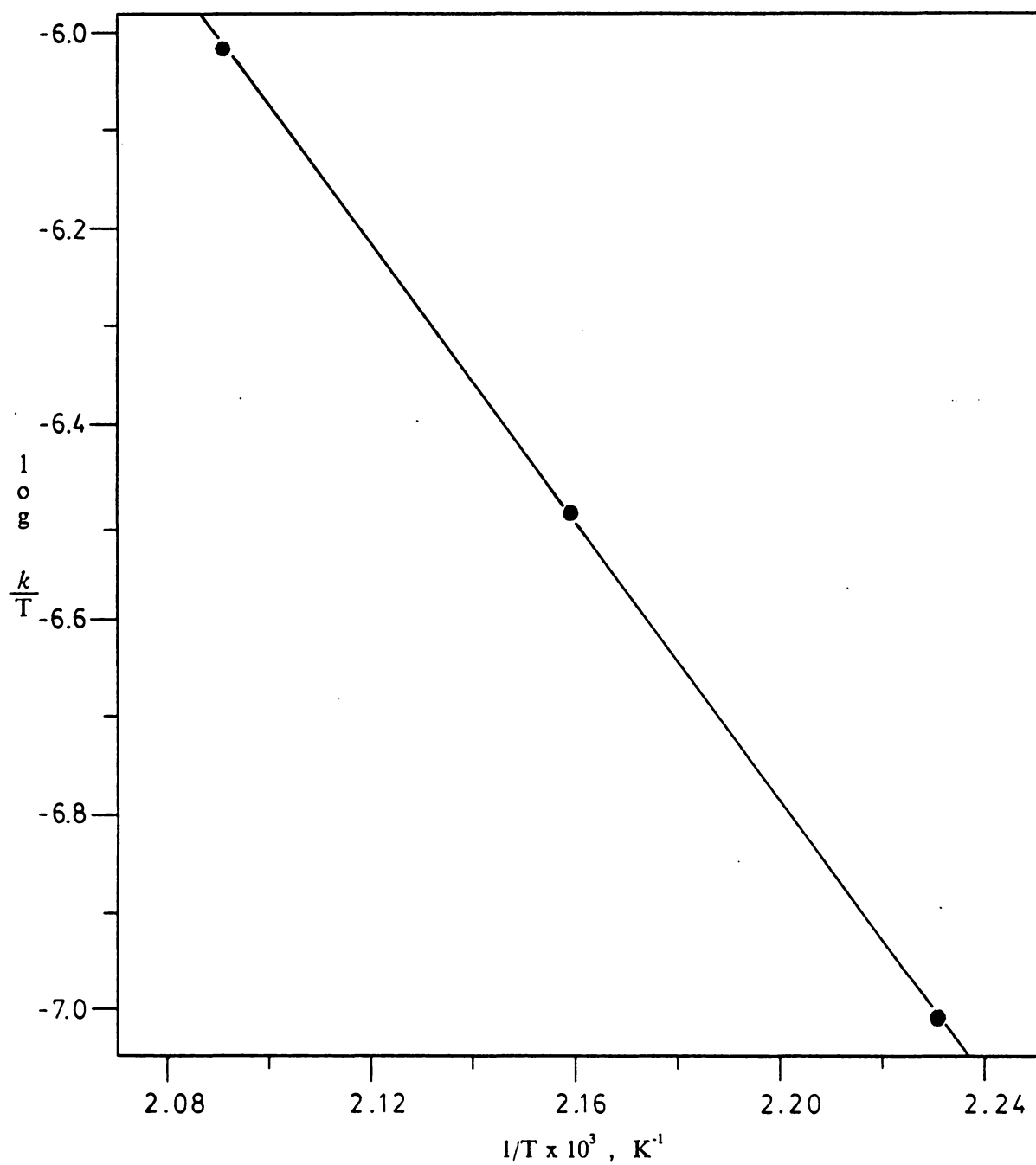
**Figure 22.** First-order plot of the isomerization of 1-(2-furyl)-2,3,4,5-tetraphenyl-2,4-cyclopentadien-1-ol (**26**) @ 205.0 ± 0.4 °C.



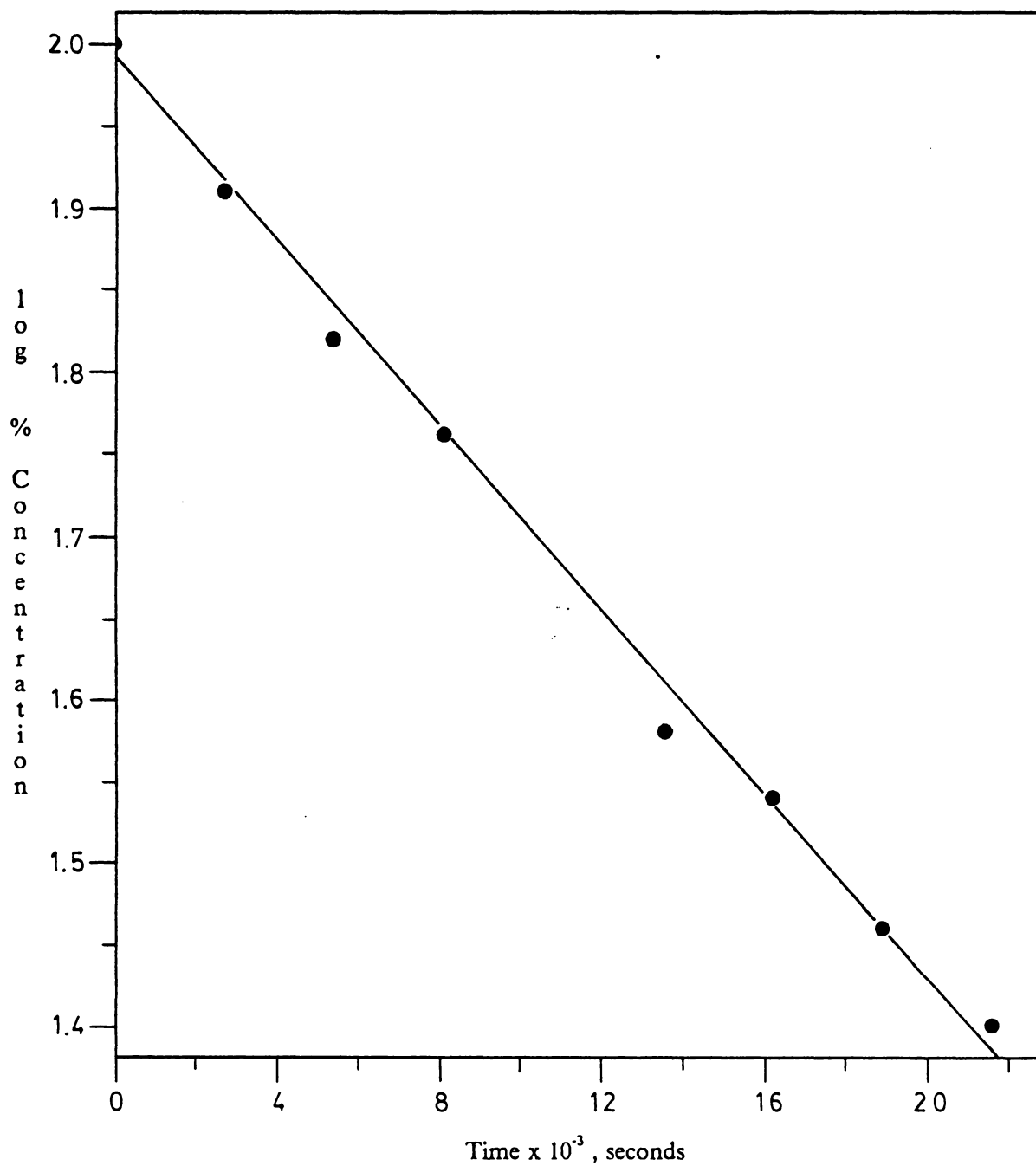
**Figure 23.** First-order plot of the isomerization of 1-(2-furyl)-2,3,4,5-tetraphenyl-2,4-cyclopentadien-1-ol (26) @ 175.0 - 205.0 °C.



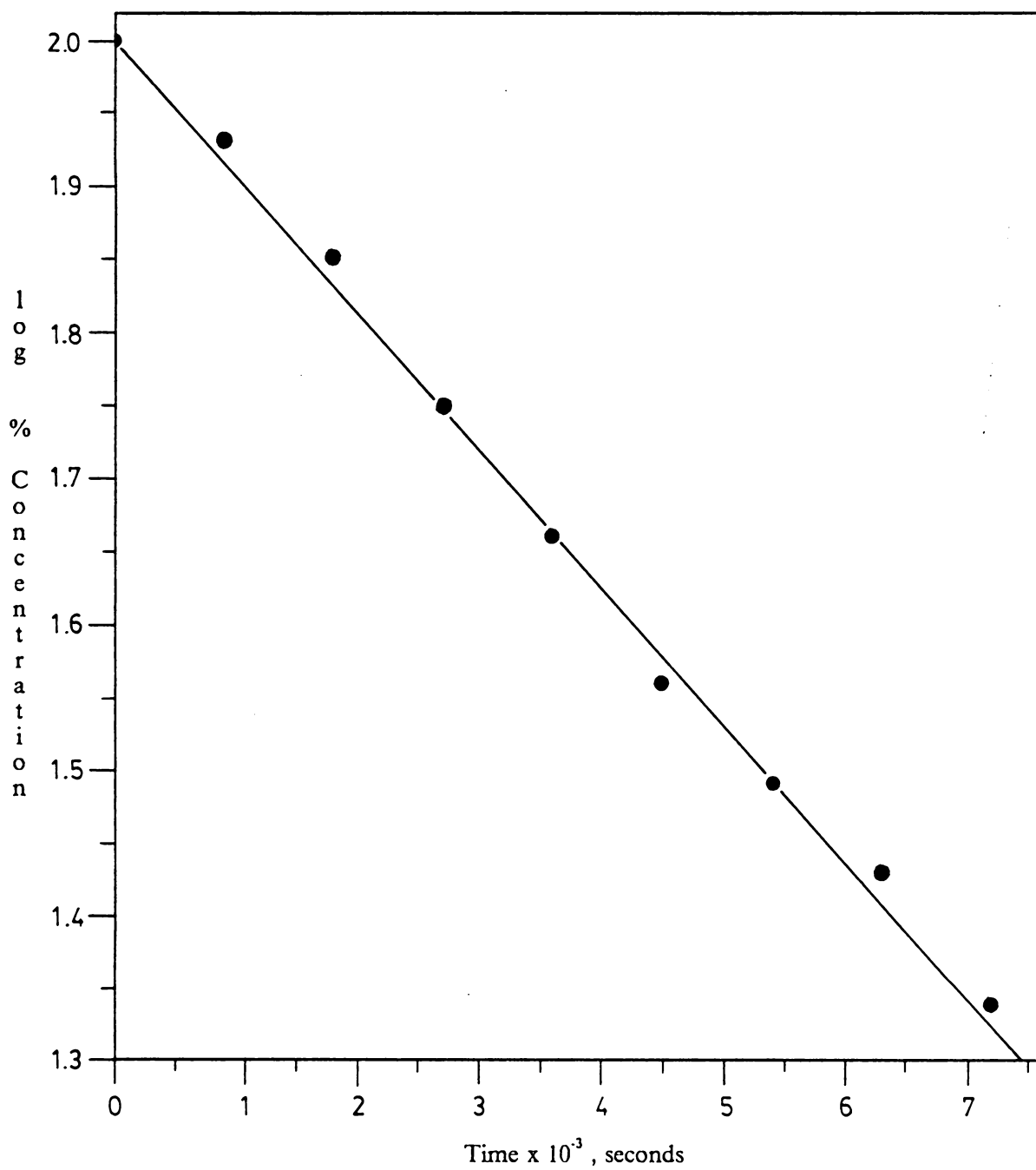
**Figure 24.** Arrhenius plot of the isomerization of 1-(2-furyl)-2,3,4,5-tetraphenyl-2,4-cyclopentadien-1-ol (26).



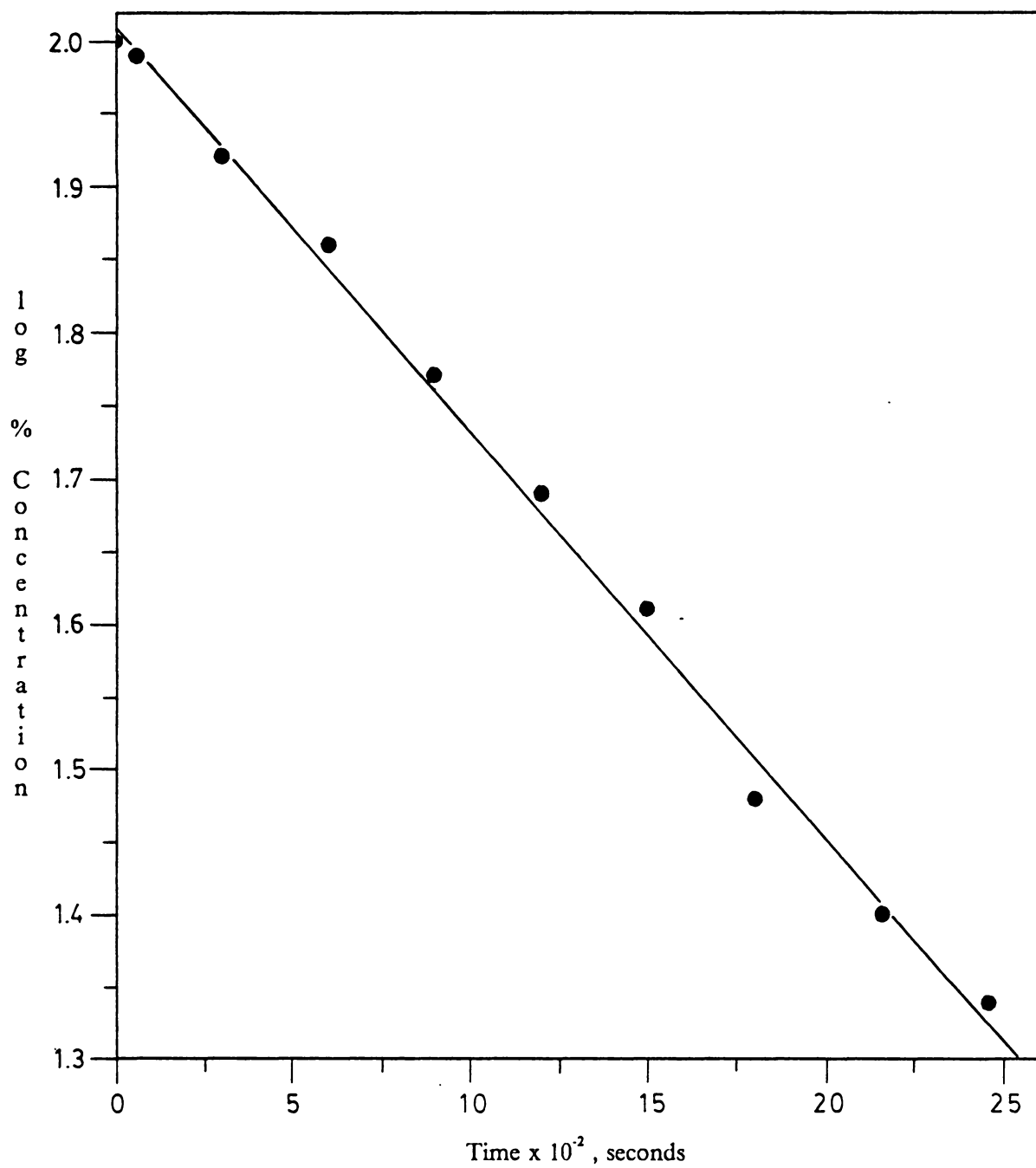
**Figure 25.** Eyring plot of the isomerization of  
1-(2-furyl)-2,3,4,5-tetraphenyl-2,4-cyclopentadien-1-ol (**26**).



**Figure 26.** First-order plot of the isomerization of 1-(2-thienyl)-2,3,4,5-tetraphenyl-2,4-cyclopentadien-1-ol (27) @ 175.0 ± 0.4 °C.

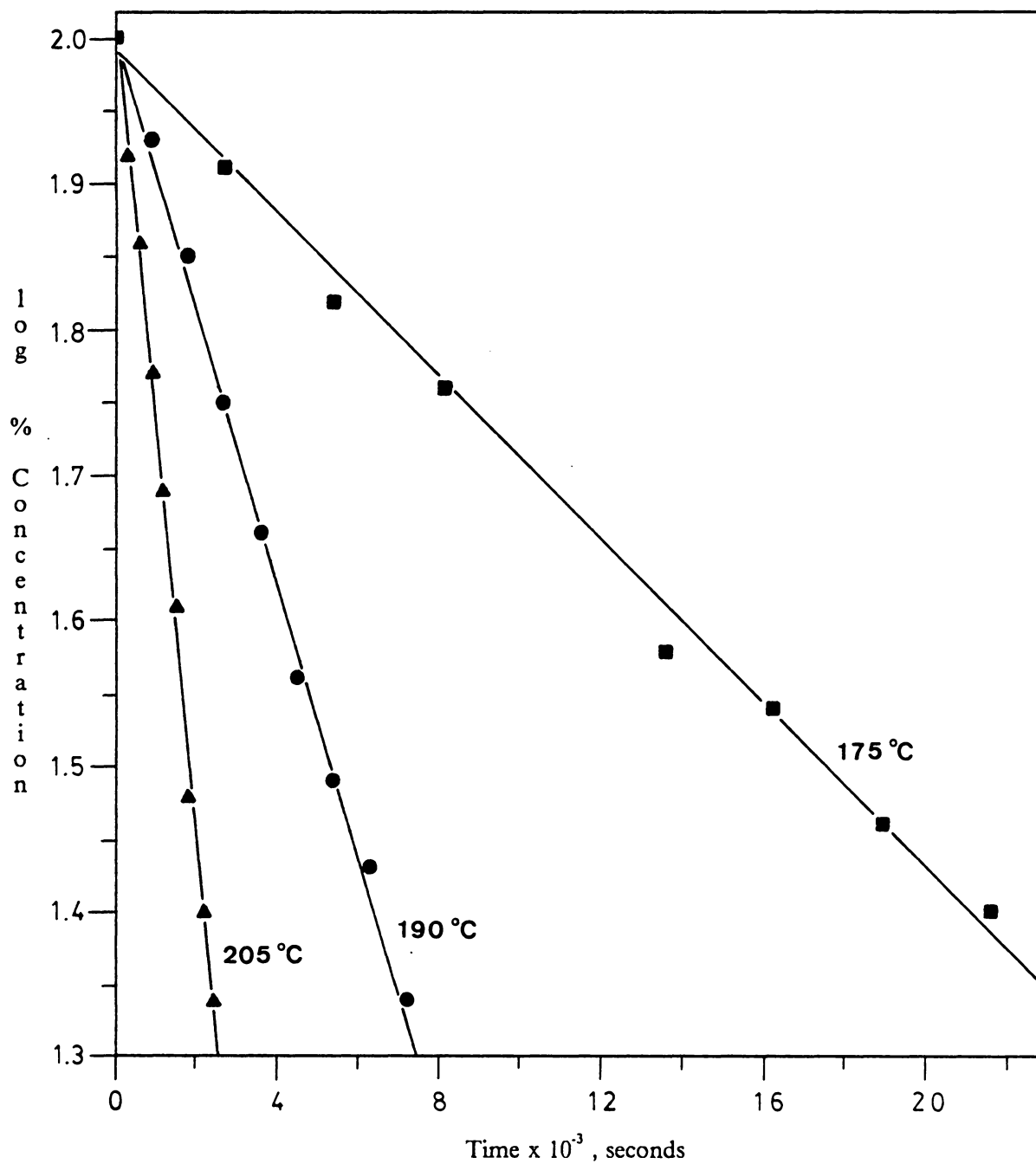


**Figure 27.** First-order plot of the isomerization of 1-(2-thienyl)-2,3,4,5-tetraphenyl-2,4-cyclopentadien-1-ol (**27**) @ 190.0 ± 0.4 °C.



**Figure 28.** First-order plot of the isomerization of 1-(2-thienyl)-2,3,4,5-tetraphenyl-2,4-cyclopentadien-1-ol (27) @ 205.0 ± 0.4 °C.





**Figure 29.** First-order plot of the isomerization of 1-(2-thienyl)-2,3,4,5-tetraphenyl-2,4-cyclopentadien-1-ol (27) @ 175.0 - 205.0 °C.

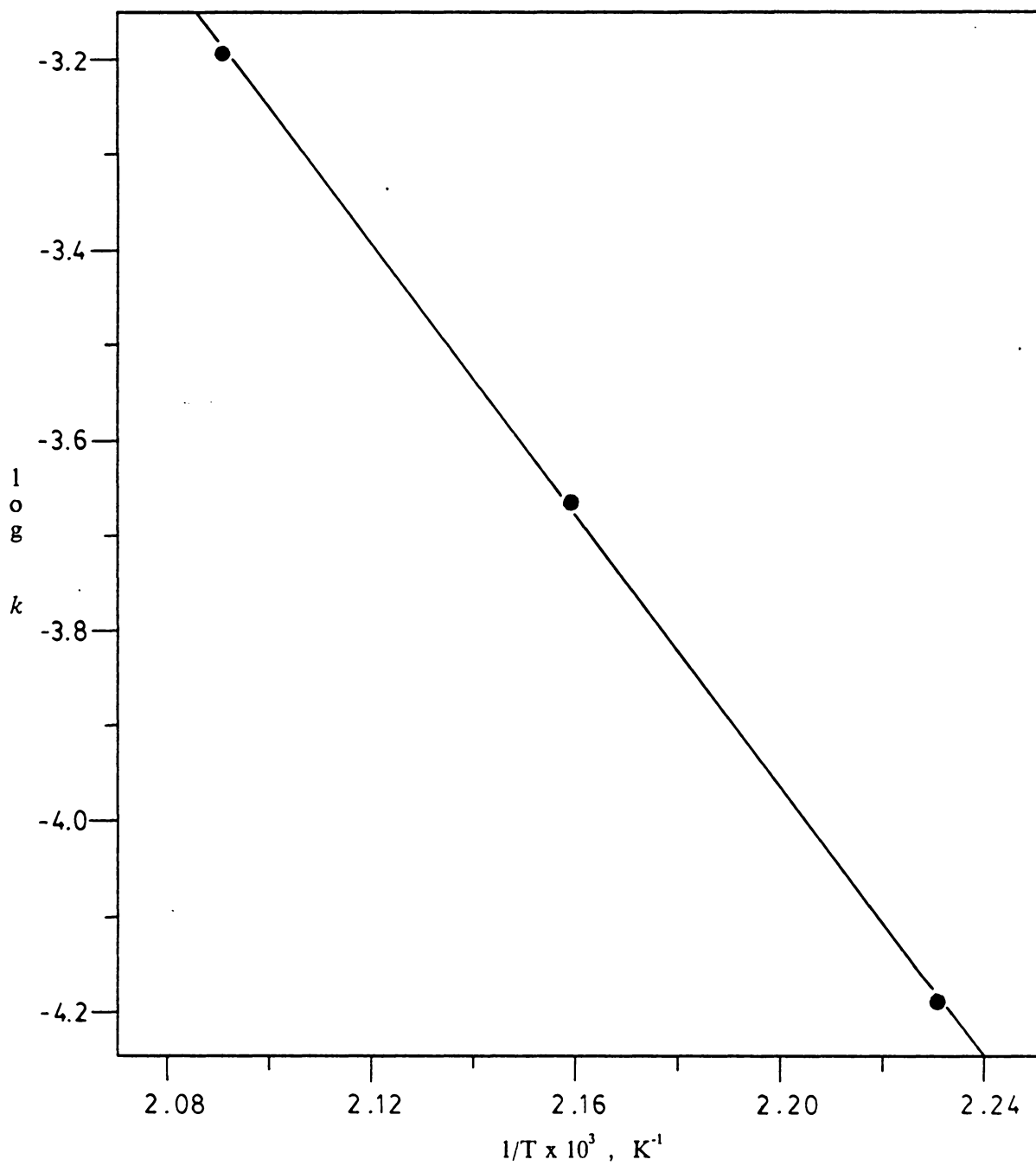
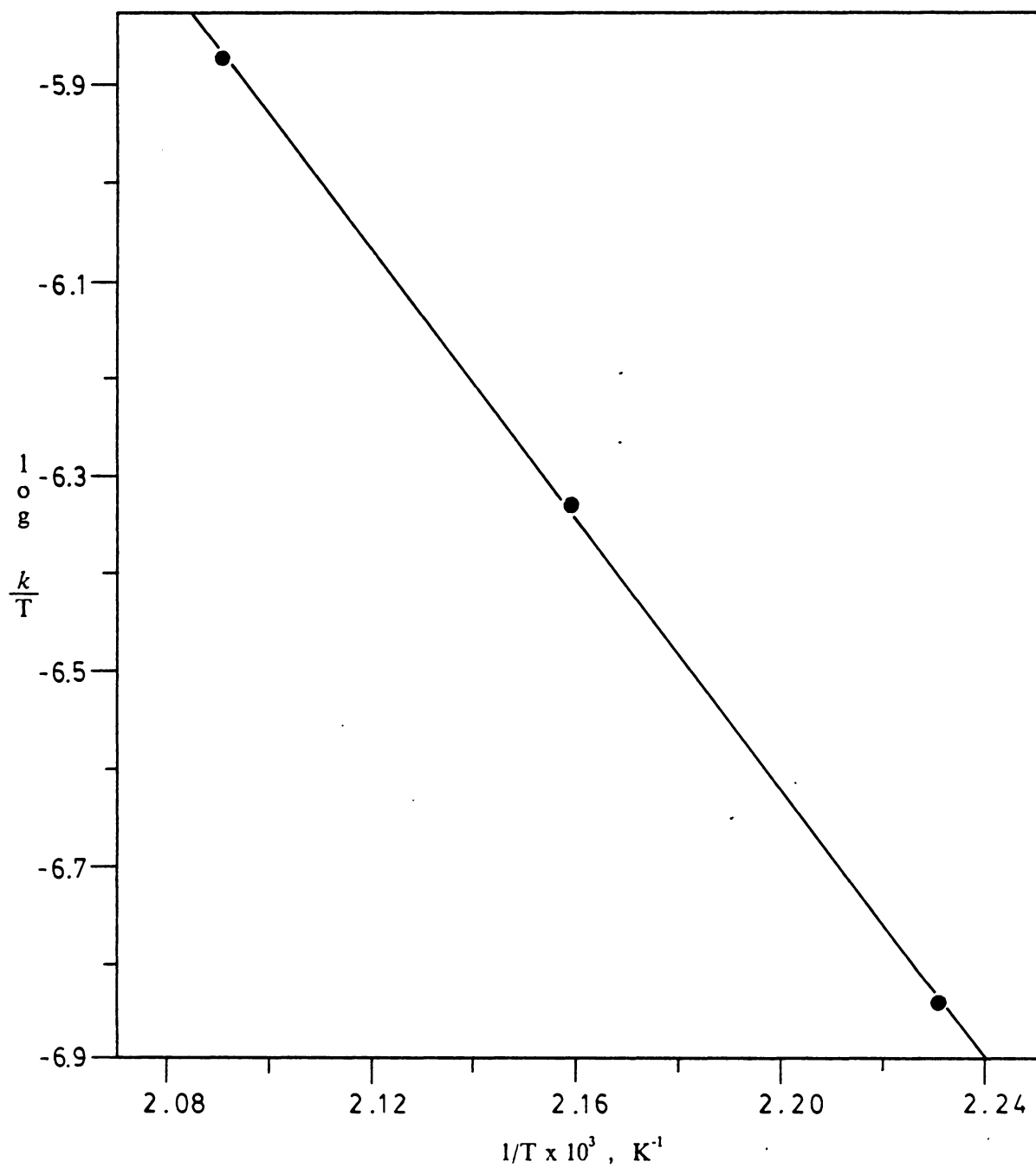
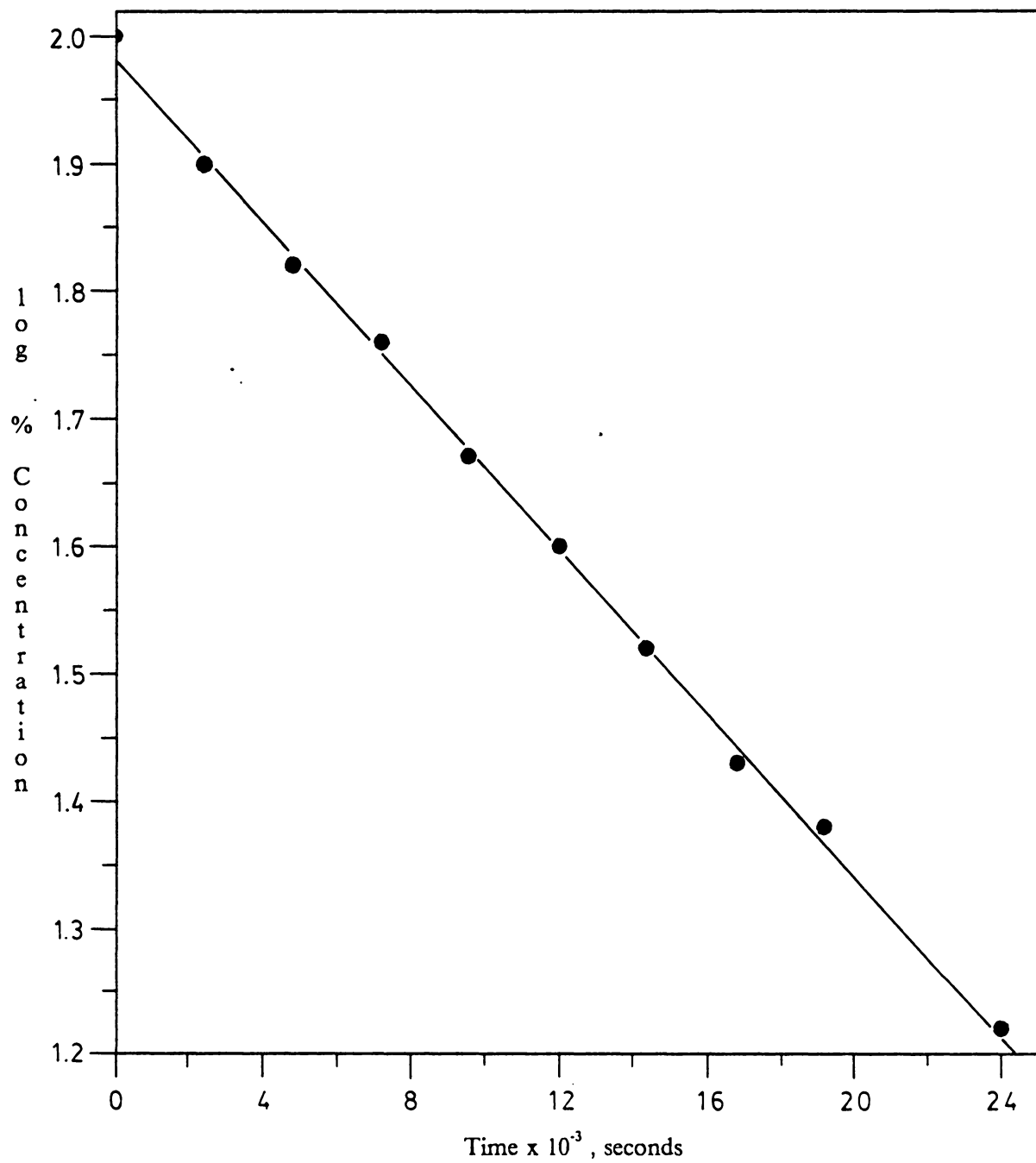


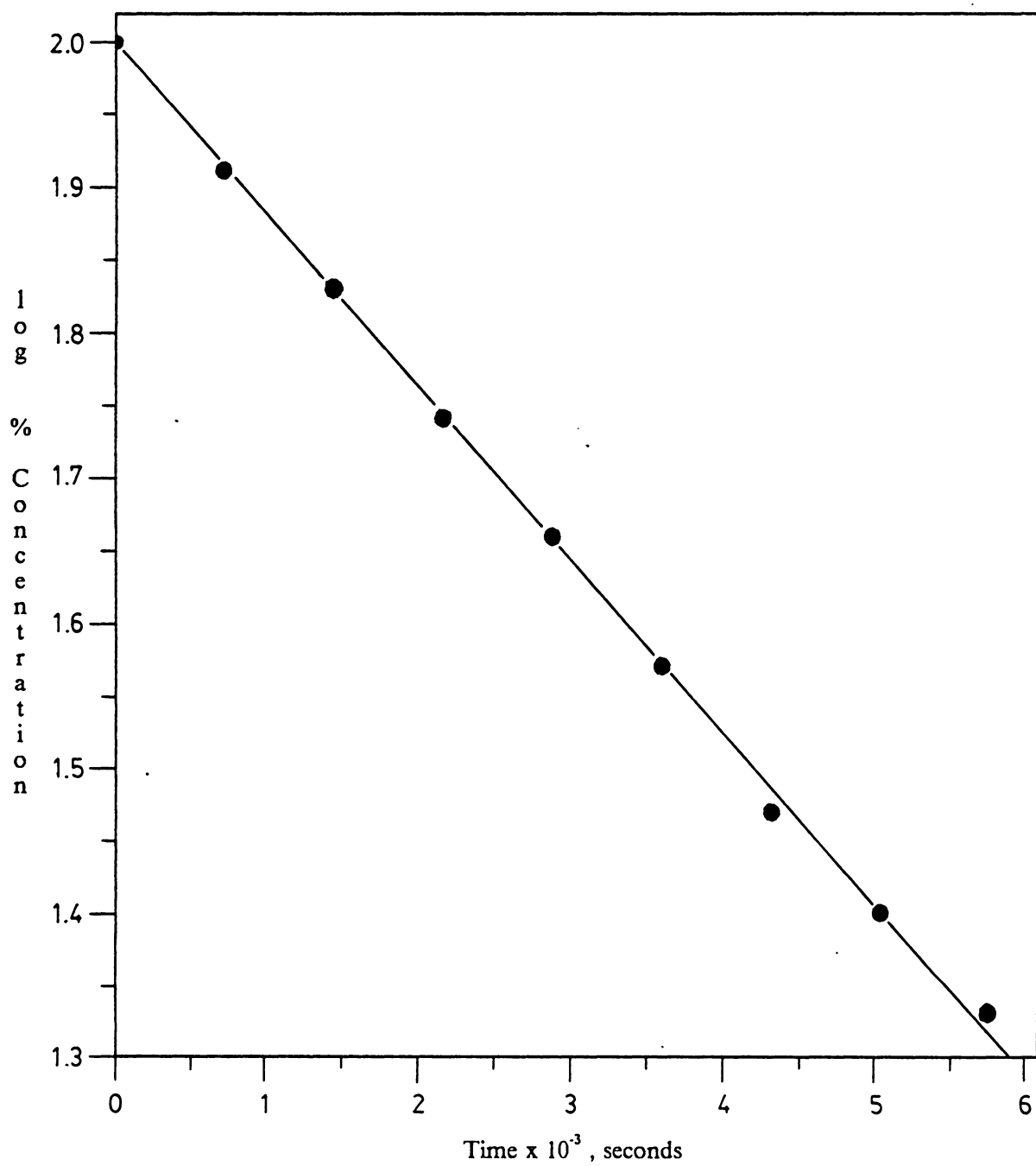
Figure 30. Arrhenius plot of the isomerization of 1-(2-thienyl)-2,3,4,5-tetraphenyl-2,4-cyclopentadien-1-ol (27).



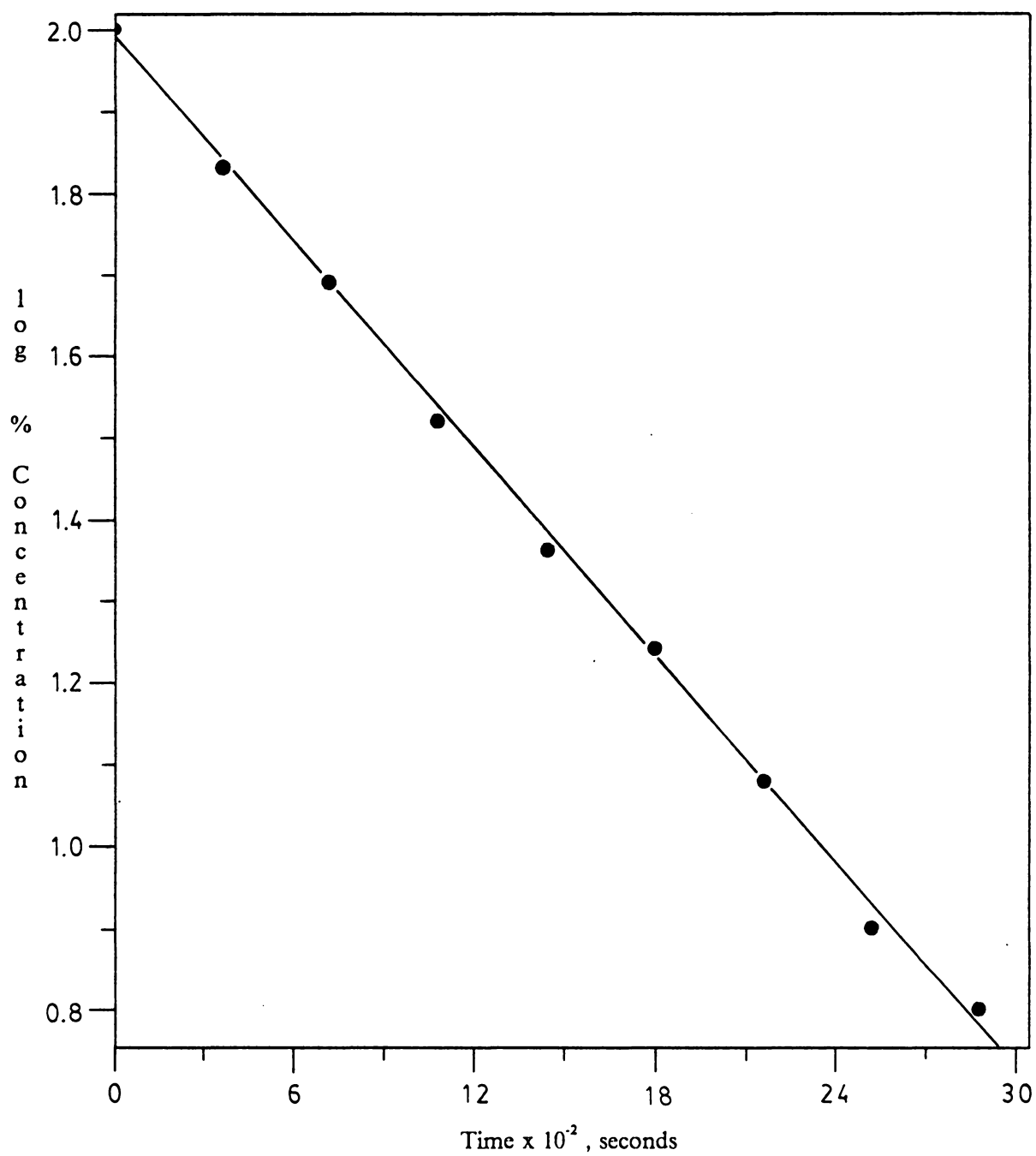
**Figure 31.** Eyring plot of the isomerization of 1-(2-thienyl)-2,3,4,5-tetraphenyl-2,4-cyclopentadien-1-ol (27).



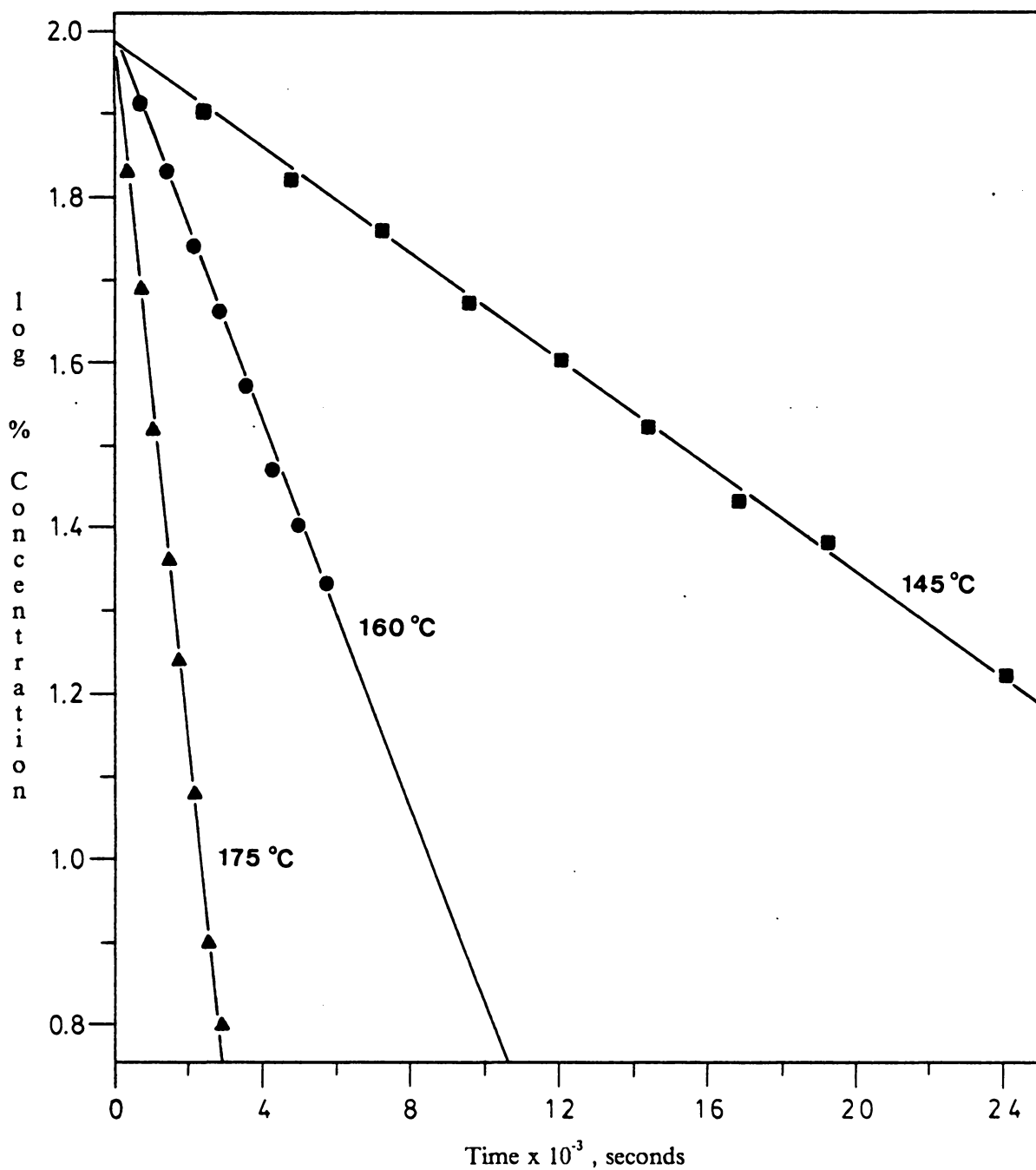
**Figure 32.** First-order plot of the isomerization of  
1-phenylethynyl-2,3,4,5-tetraphenyl-2,4-cyclopentadien-1-ol (**28**) @ 145.0 ± 0.4 °C.



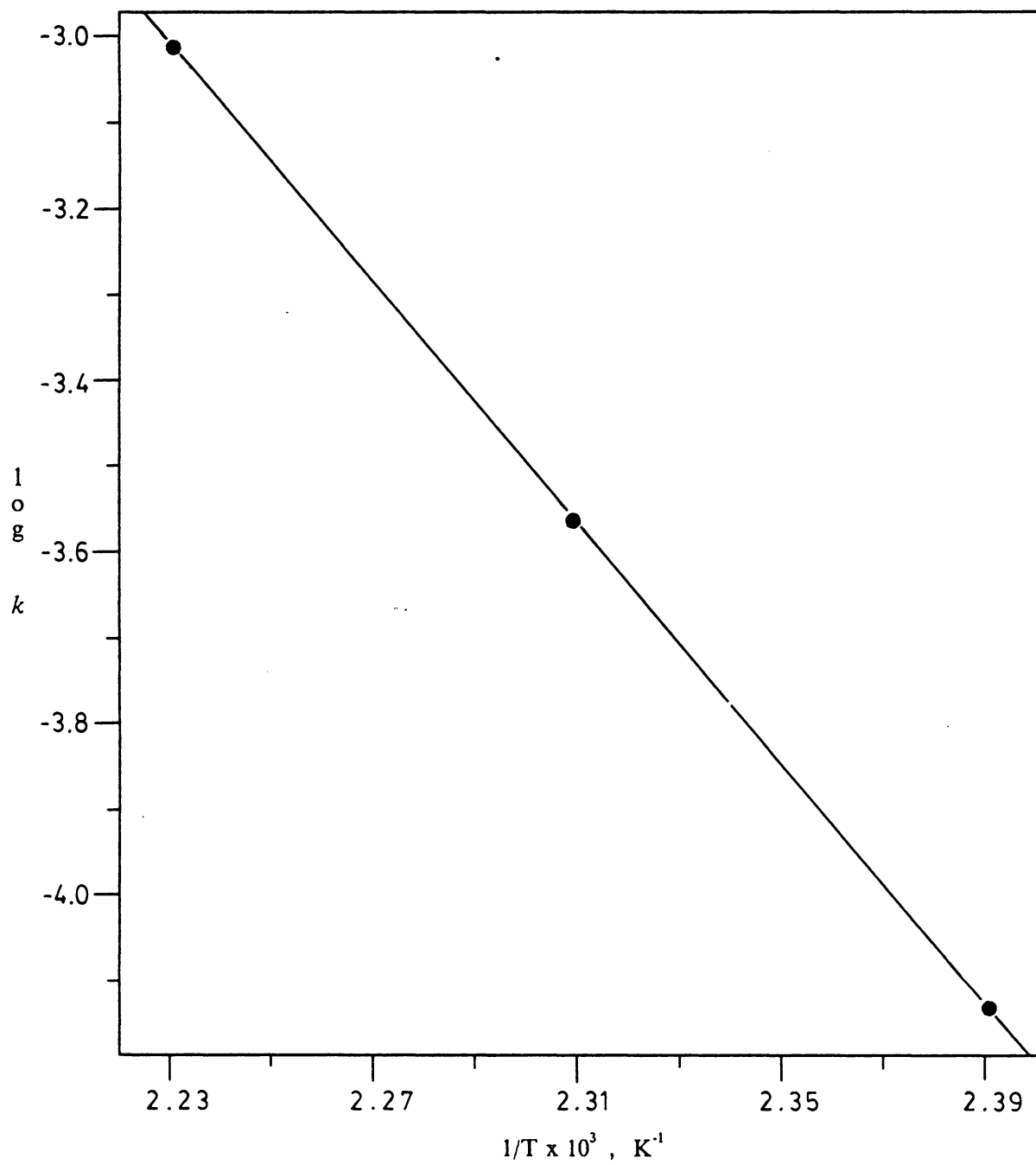
**Figure 33.** First-order plot of the isomerization of 1-phenylethynyl-2,3,4,5-tetraphenyl-2,4-cyclopentadien-1-ol (**28**) @ 160.0 ± 0.4 °C.



**Figure 34.** First-order plot of the isomerization of 1-phenylethynyl-2,3,4,5-tetraphenyl-2,4-cyclopentadien-1-ol (**28**) @ 175.0 ± 0.4 °C.

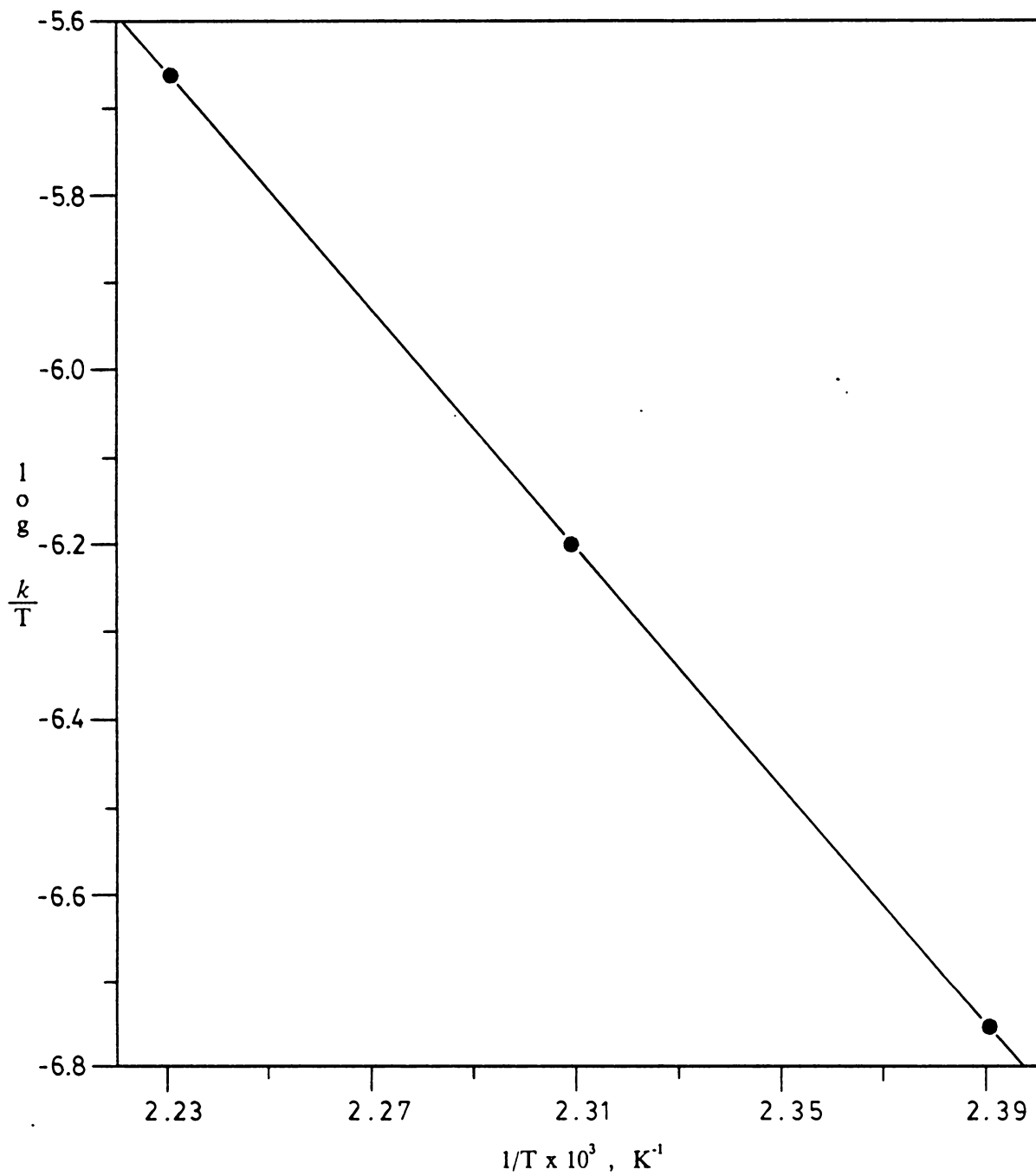


**Figure 35.** First-order plot of the isomerization of 1-phenylethynyl-2,3,4,5-tetraphenyl-2,4-cyclopentadien-1-ol (**28**) @ 145.0 - 175.0 °C.

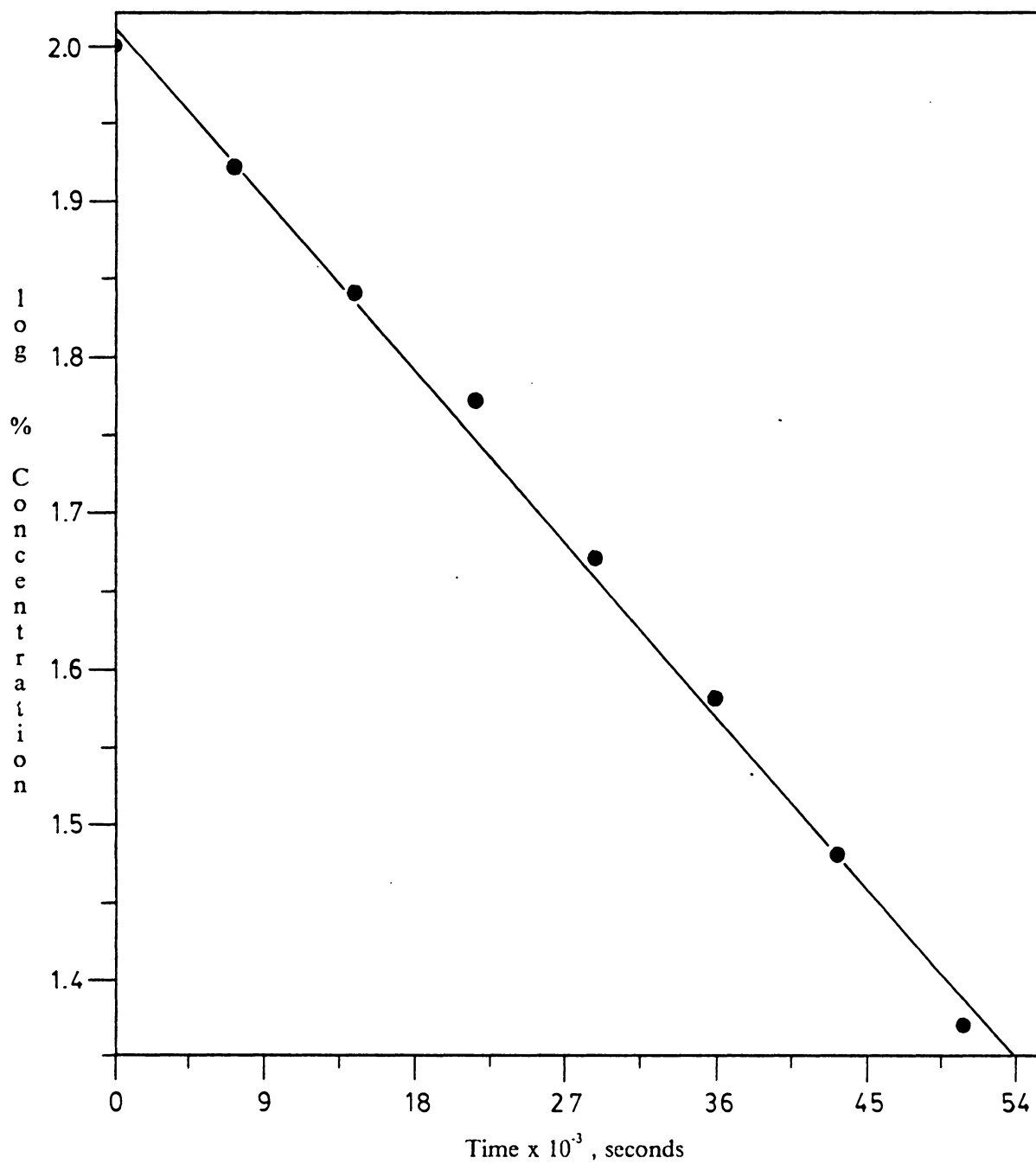


**Figure 36.** Arrhenius plot of the isomerization of 1-phenylethynyl-2,3,4,5-tetraphenyl-2,4-cyclopentadien-1-ol (**28**).

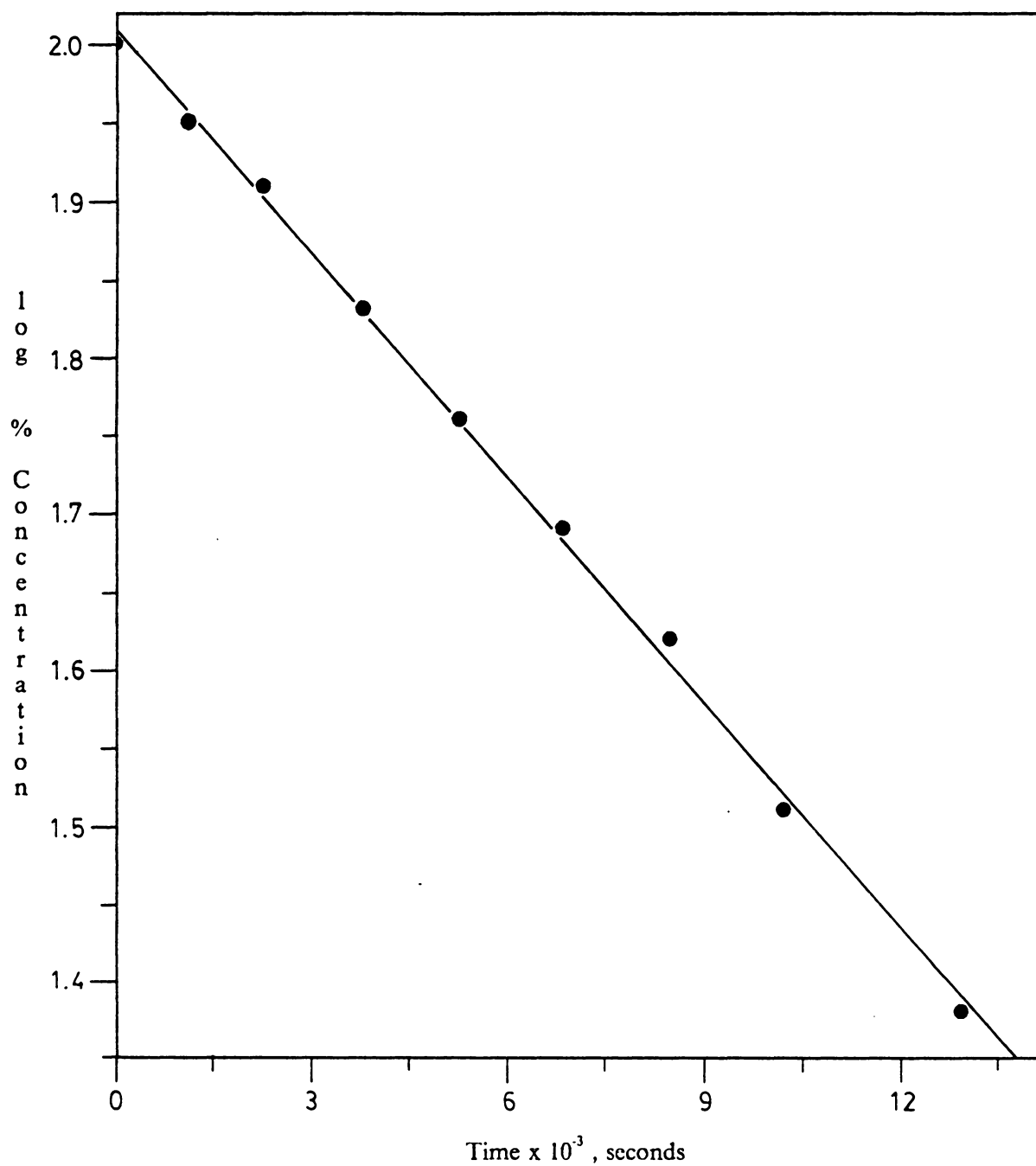




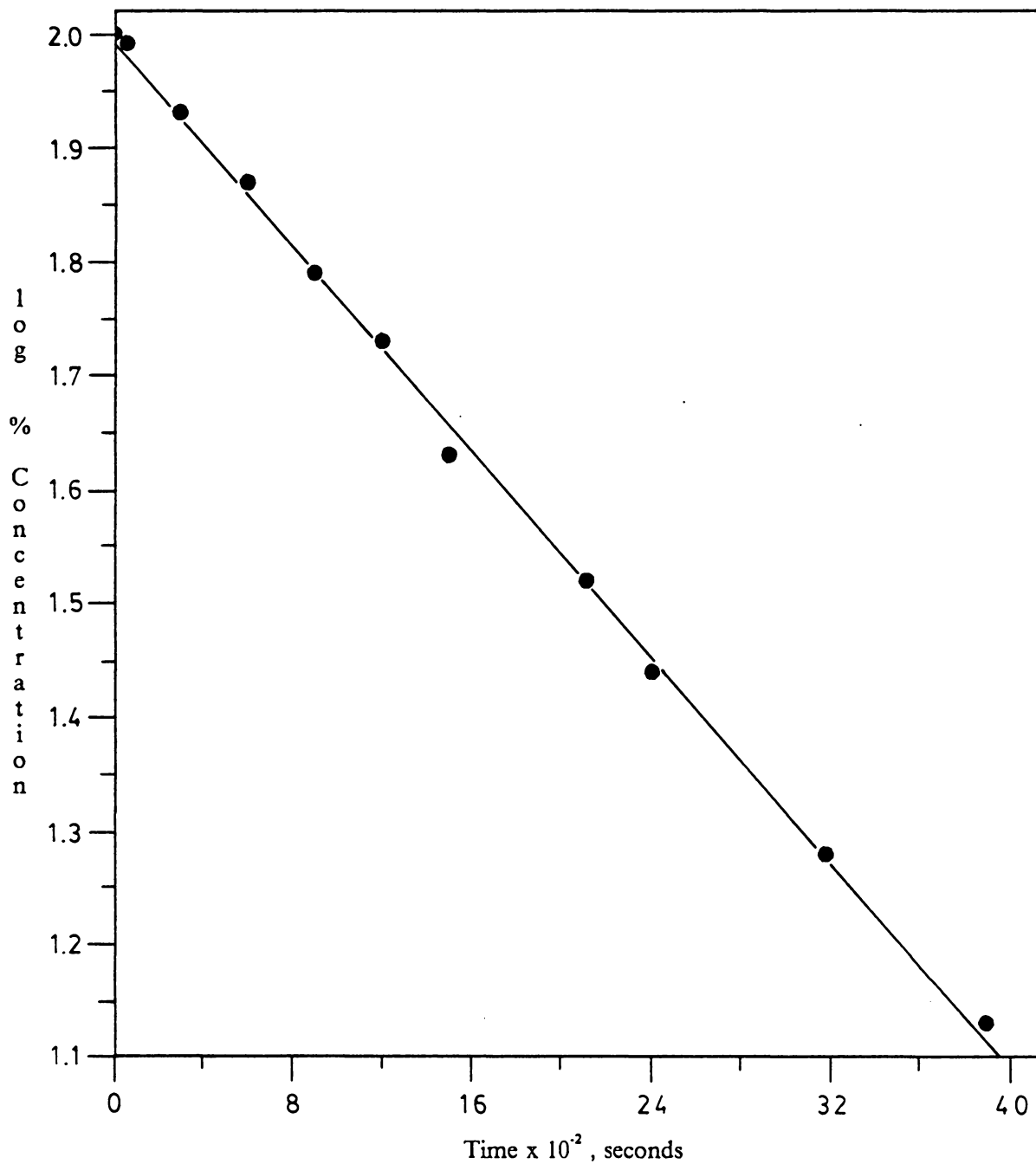
**Figure 37.** Eyring plot of the isomerization of 1-phenylethynyl-2,3,4,5-tetraphenyl-2,4-cyclopentadien-1-ol (**28**).



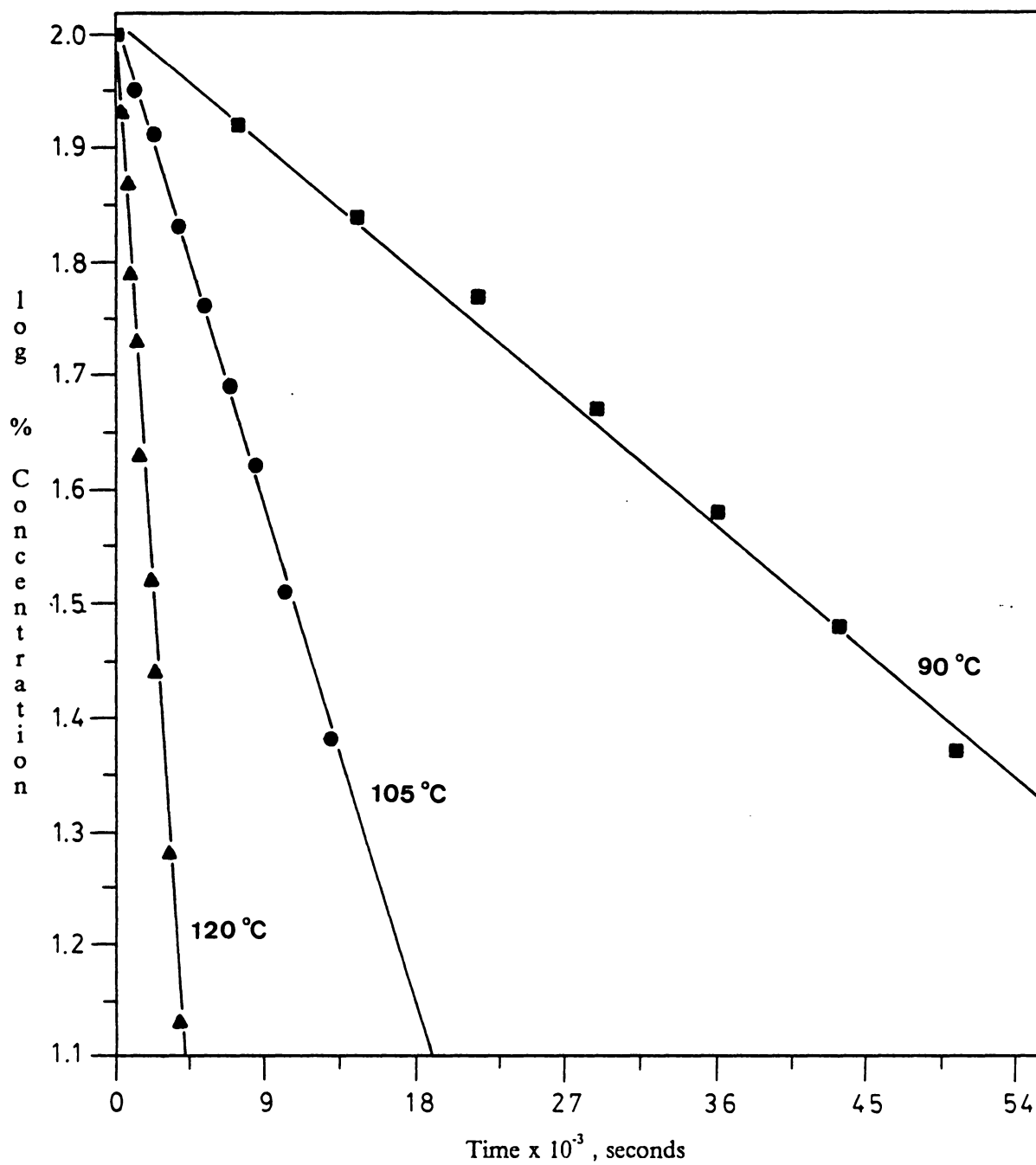
**Figure 38.** First-order plot of the isomerization of 1-vinyl-2,3,4,5-tetraphenyl-2,4-cyclopentadien-1-ol (29) @ 90.0 ± 0.4 °C.



**Figure 39.** First-order plot of the isomerization of 1-vinyl-2,3,4,5-tetraphenyl-2,4-cyclopentadien-1-ol (29) @ 105.0 ± 0.4 °C.



**Figure 40.** First-order plot of the isomerization of 1-vinyl-2,3,4,5-tetraphenyl-2,4-cyclopentadien-1-ol (29) @ 120.0 ± 0.4 °C.



**Figure 41.** First-order plot of the isomerization of 1-vinyl-2,3,4,5-tetraphenyl-2,4-cyclopentadien-1-ol (29) @ 90.0 - 120.0 °C.

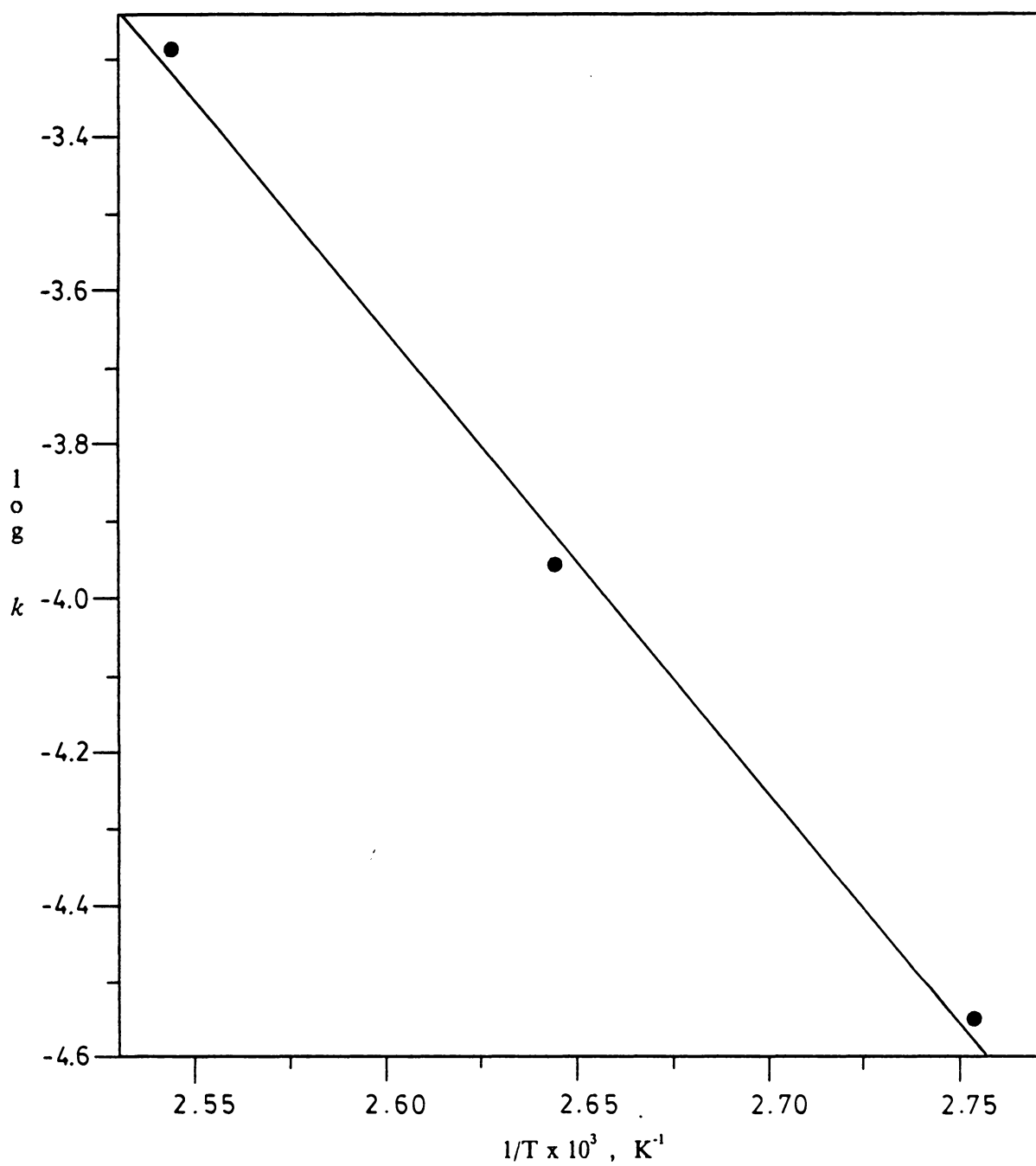
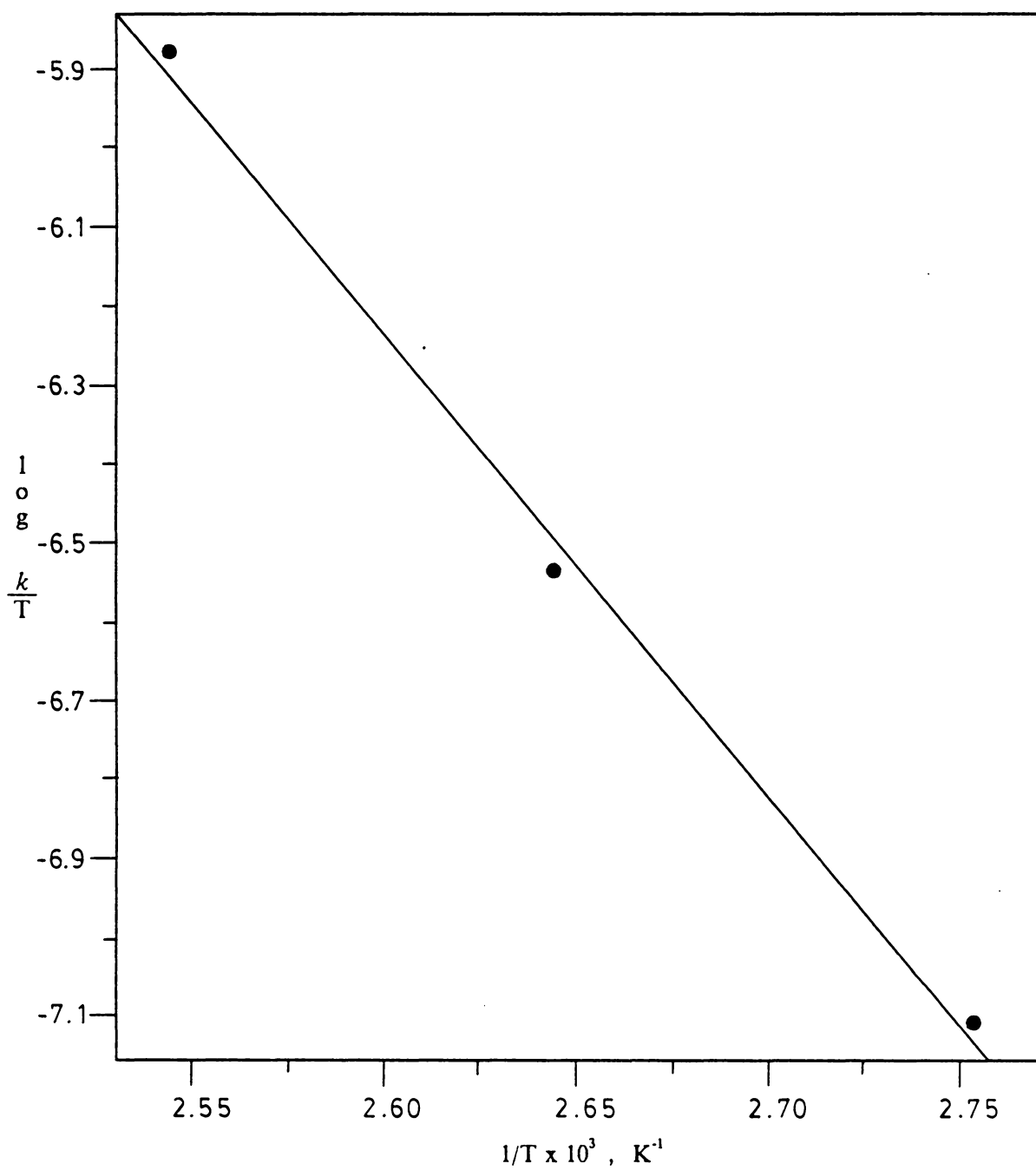
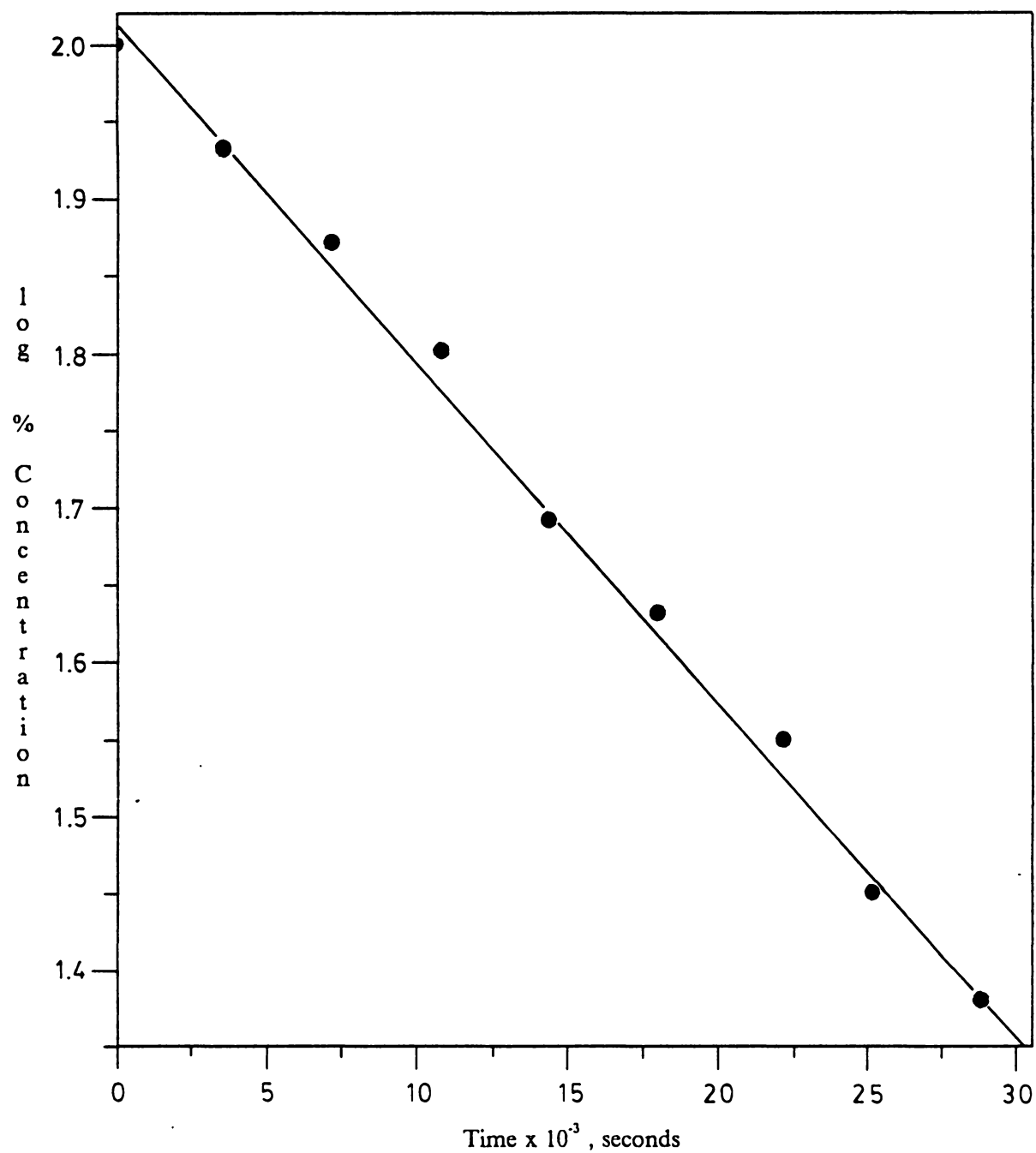


Figure 42. Arrhenius plot of the isomerization of 1-vinyl-2,3,4,5-tetraphenyl-2,4-cyclopentadien-1-ol (29).

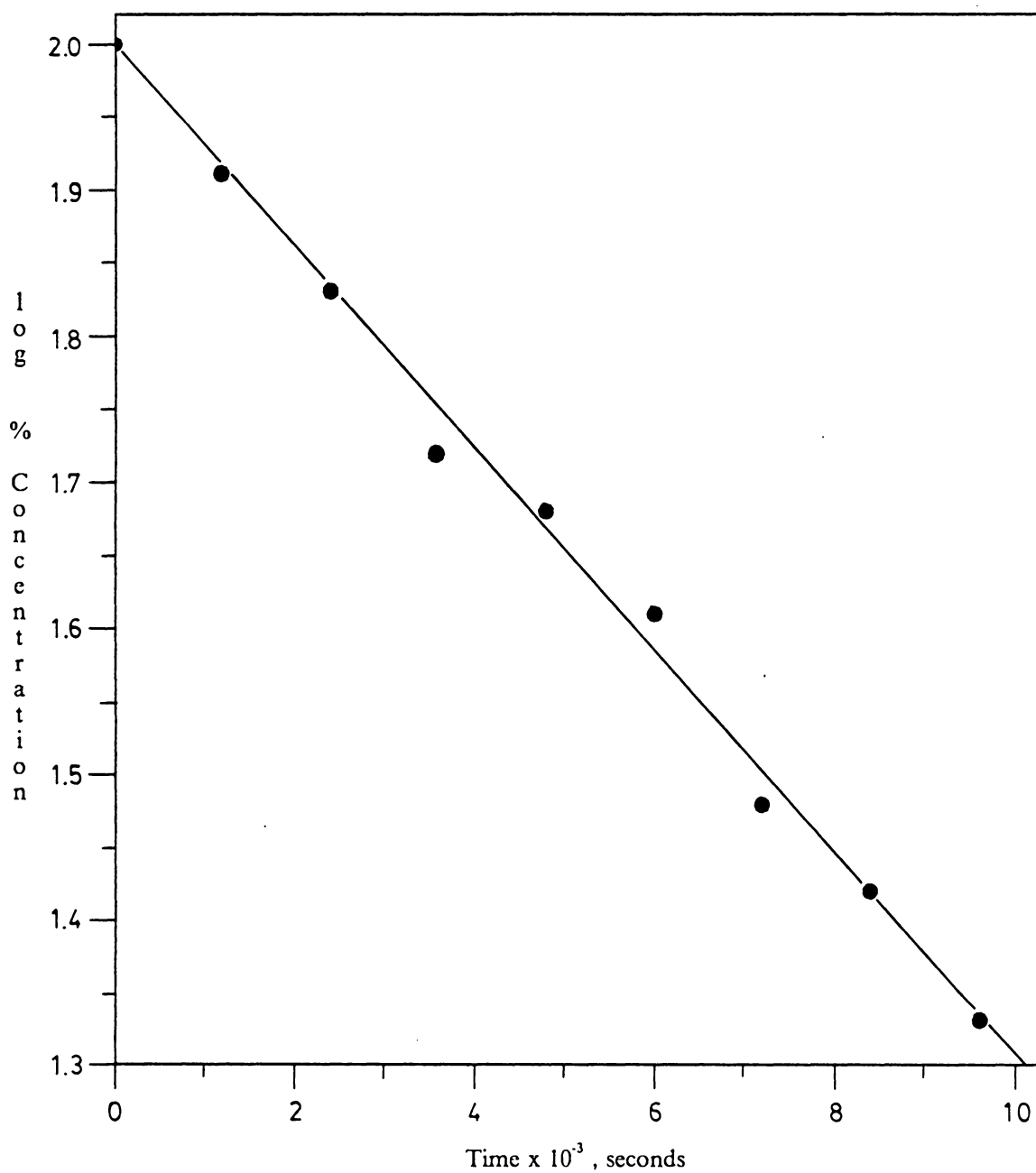


**Figure 43.** Eyring plot of the isomerization of 1-vinyl-2,3,4,5-tetraphenyl-2,4-cyclopentadien-1-ol (29).

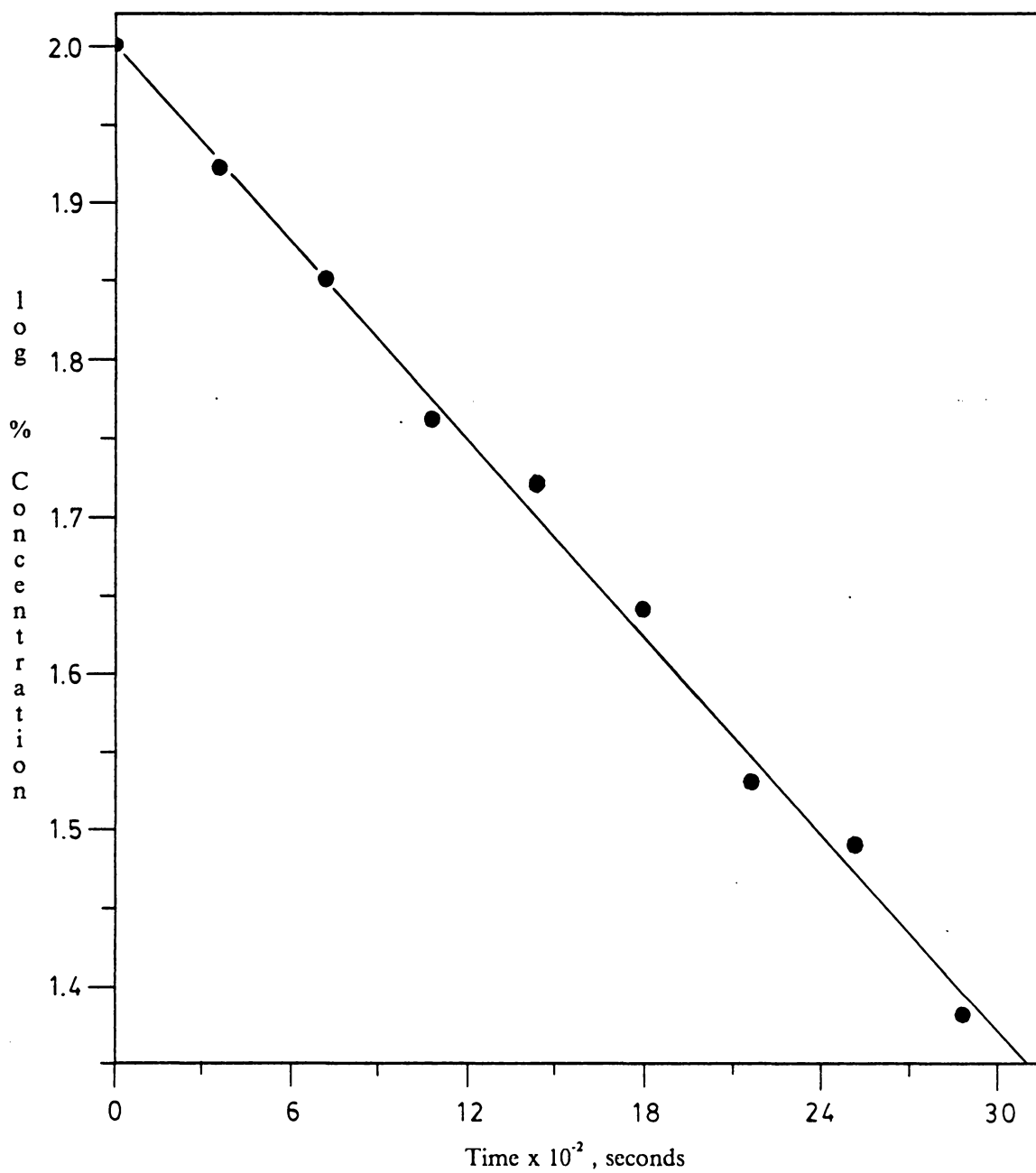


**Figure 44.** First-order plot of the isomerization of 1-*tert*-butyl-2,3,4,5-tetraphenyl-2,4-cyclopentadien-1-ol (**30**) @ 145.0 ± 0.4 °C.

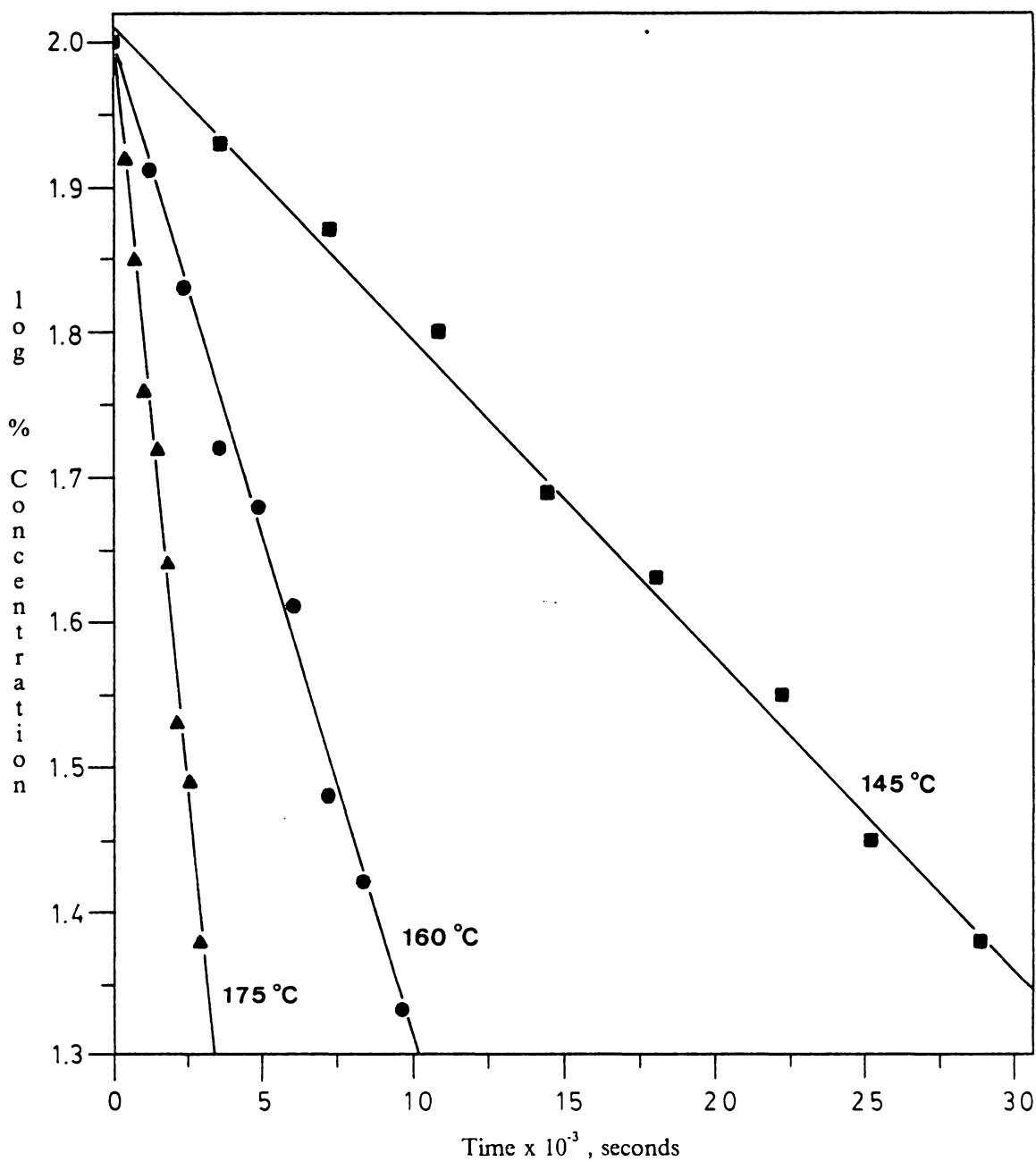




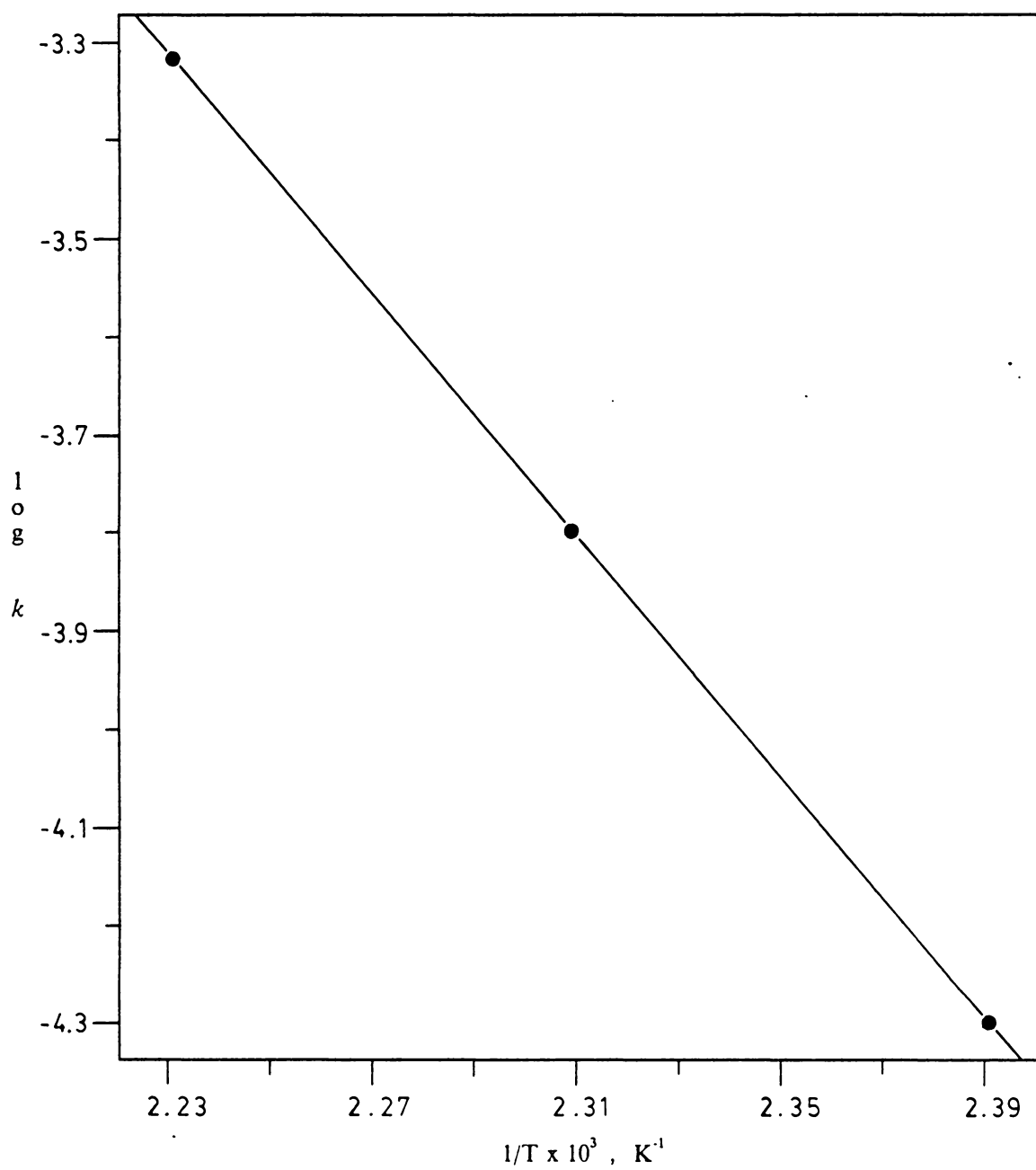
**Figure 45.** First-order plot of the isomerization of 1-*tert*-butyl-2,3,4,5-tetraphenyl-2,4-cyclopentadien-1-ol (30) @ 160.0 ± 0.4 °C.



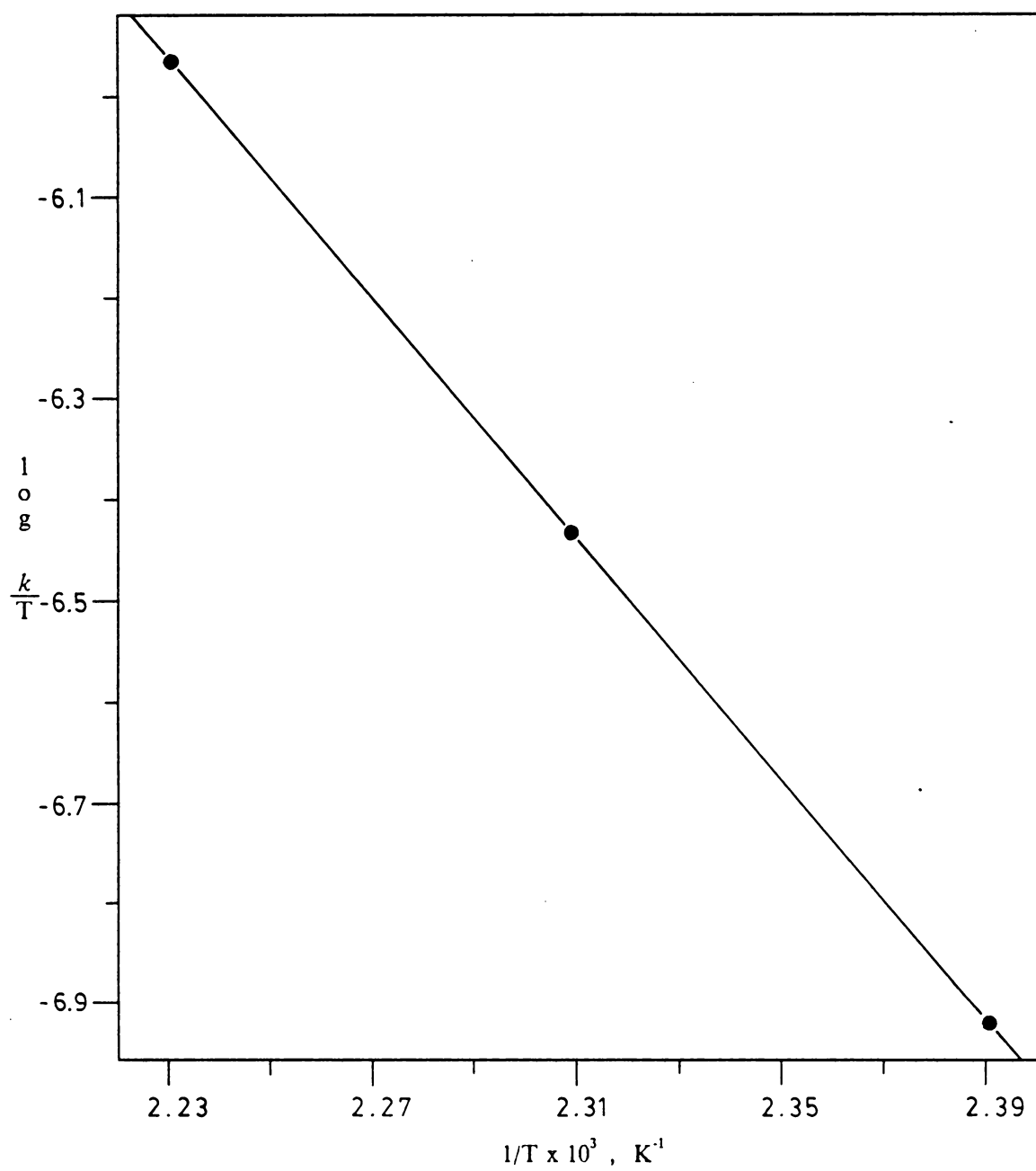
**Figure 46.** First-order plot of the isomerization of 1-*tert*-butyl-2,3,4,5-tetraphenyl-2,4-cyclopentadien-1-ol (**30**) @ 175.0 ± 0.4 °C.



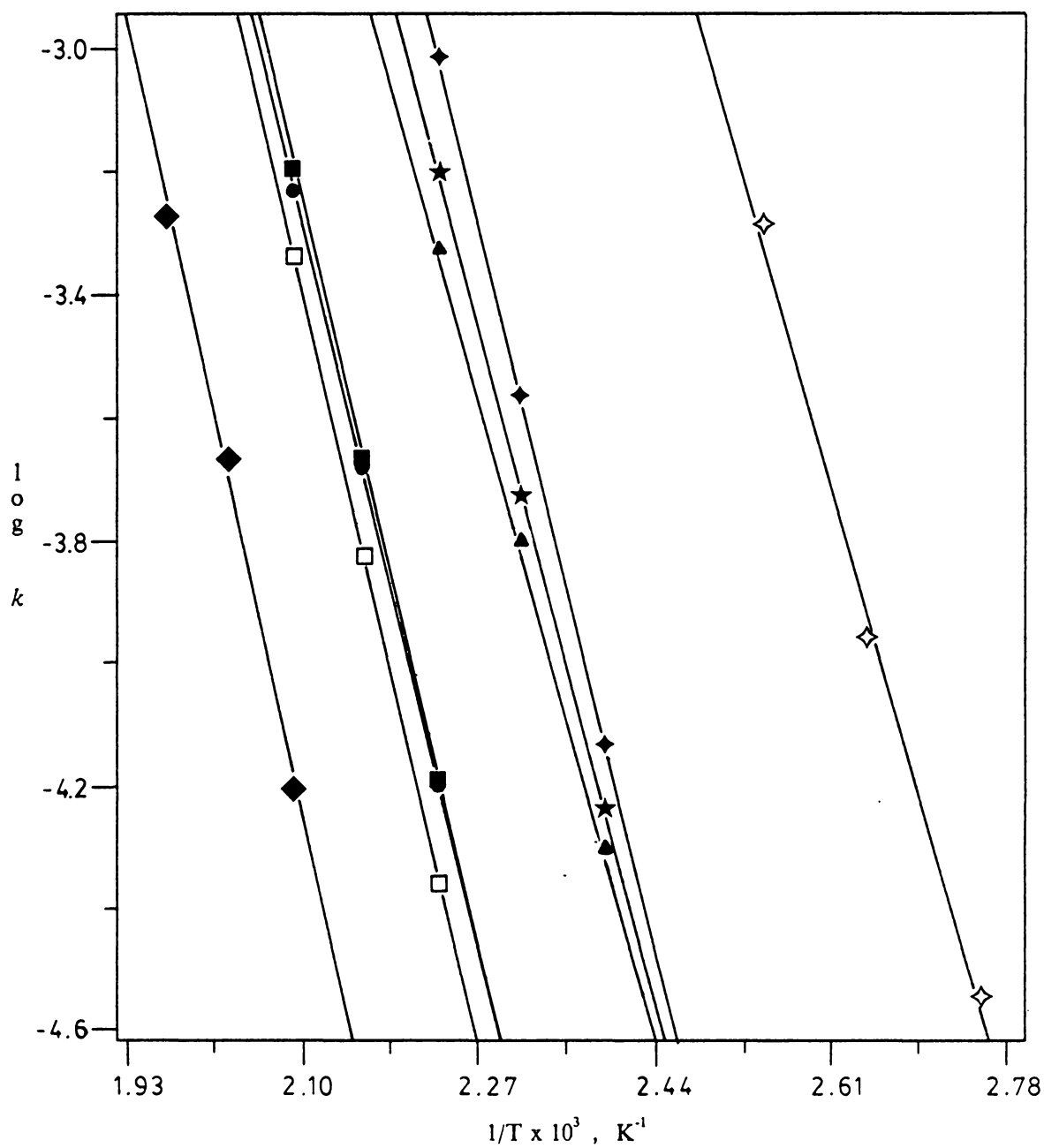
**Figure 47.** First-order plot of the isomerization of 1-*tert*-butyl-2,3,4,5-tetraphenyl-2,4-cyclopentadien-1-ol (**30**) @ 145.0 - 175.0 °C.



**Figure 48.** Arrhenius plot of the isomerization of 1-*tert*-butyl-2,3,4,5-tetraphenyl-2,4-cyclopentadien-1-ol (**30**).

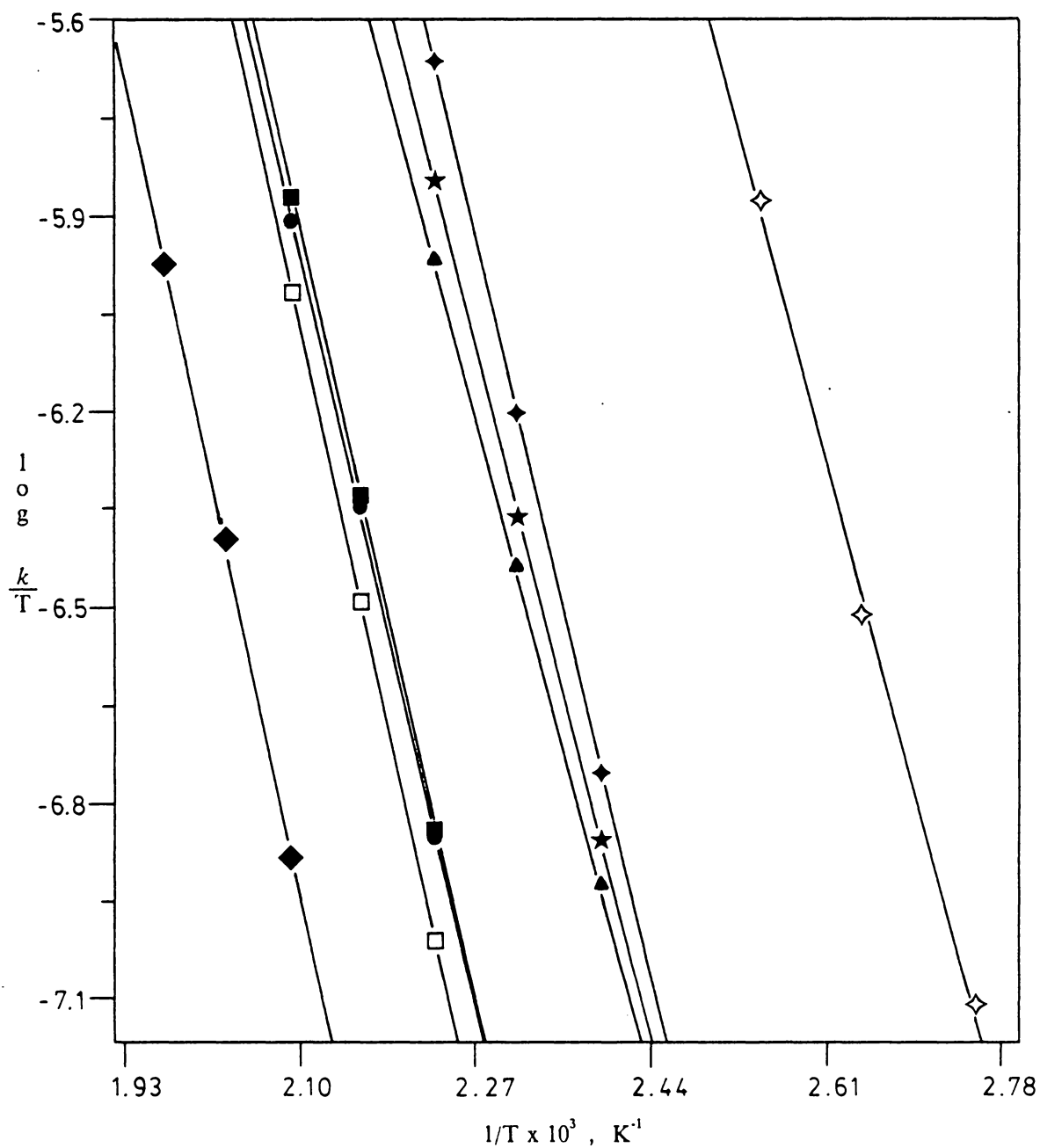


**Figure 49.** Eyring plot of the isomerization of 1-*tert*-butyl-2,3,4,5-tetraphenyl-2,4-cyclopentadien-1-ol (**30**).



**Figure 50.** Arrhenius plot of the isomerization of  
1-substituted-2,3,4,5-tetraphenyl-2,4-cyclopentadien-1-ols

(●), Phenyl (2); (◆), 1-Naphthyl (24); (★), 2-Pyridyl (25); (□), 2-Furyl (26);  
(■), 2-Thienyl (27); (◆), Phenylethynyl (28); (◇), Vinyl (29); (▲), *tert*-Butyl (30)



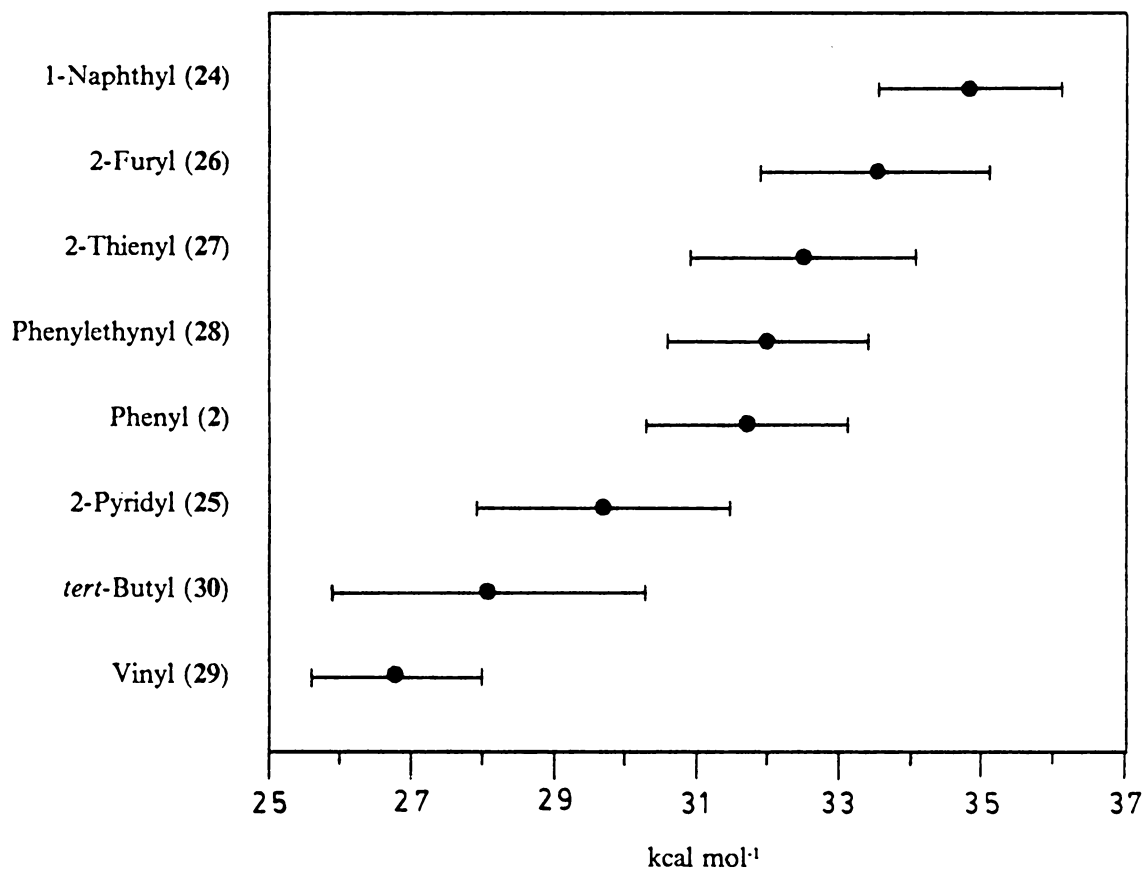
**Figure 51.** Eyring plot of the isomerization of  
1-substituted-2,3,4,5-tetraphenyl-2,4-cyclopentadien-1-ols

(●), Phenyl (2); (◆), 1-Naphthyl (24); (★), 2-Pyridyl (25); (□), 2-Furyl (26);  
(■), 2-Thienyl (27); (◆), Phenylethynyl (28); (◇), Vinyl (29); (▲), *tert*-Butyl (30)

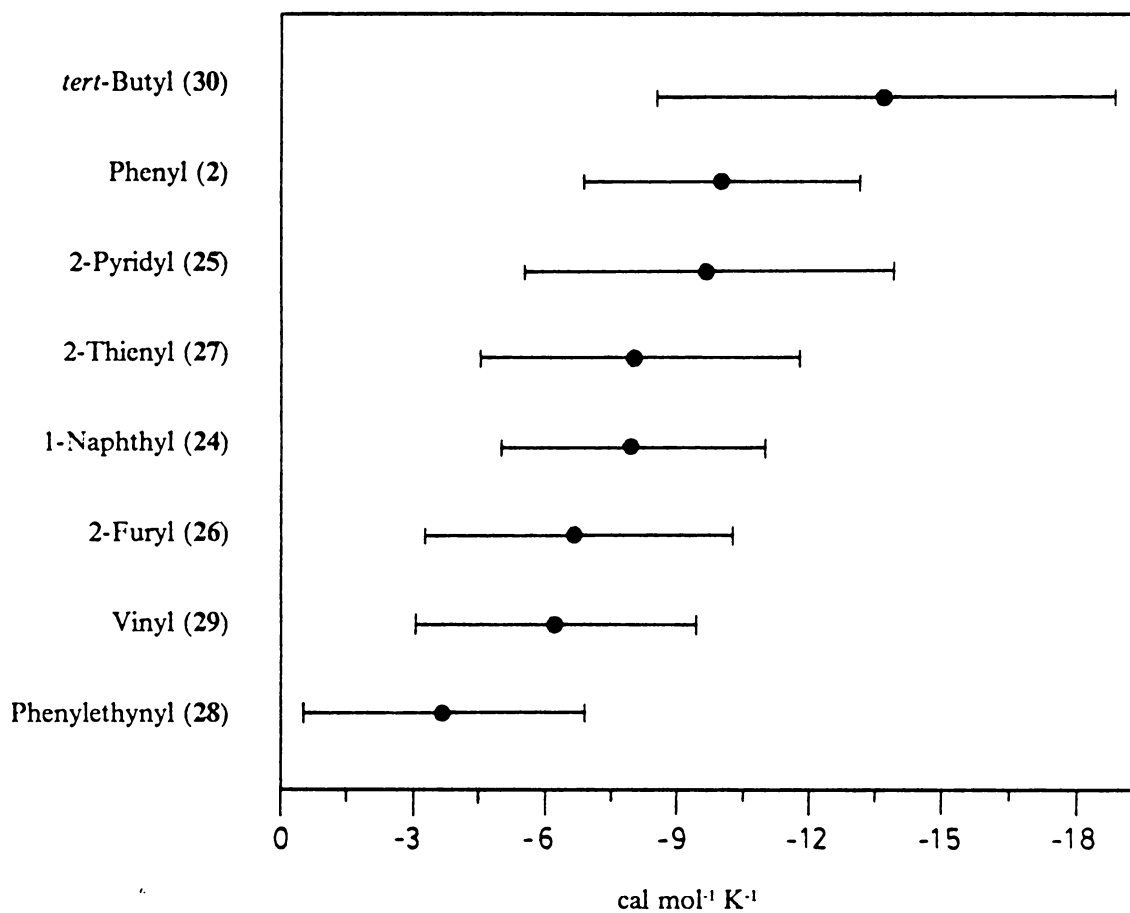
Table XXVIII.  $E_a$ ,  $\Delta H^\ddagger$  and  $\Delta S^\ddagger$  for the [1, 5]-sigmatropic rearrangement of 1-substituted-2,3,4,5-tetraphenyl-2,4-cyclopentadien-1-ols

Alcohol (1-substituent)	$E_a$ kcal mol <sup>-1</sup>	$\Delta H^\ddagger$ kcal mol <sup>-1</sup> K <sup>-1</sup>	$\Delta S^\ddagger$ cal mol <sup>-1</sup> K <sup>-1</sup>
Phenyl (2)	31.7 ± 1.4	30.7 ± 1.4	-10.0 ± 3.1
1-Naphthyl (24)	34.8 ± 1.3	33.8 ± 1.4	-8.0 ± 3.0
2-Pyridyl (25)	29.7 ± 1.8	28.8 ± 1.8	-9.7 ± 4.2
2-Furyl (26)	33.5 ± 1.6	32.6 ± 1.6	-6.7 ± 3.5
2-Thienyl (27)	32.5 ± 1.6	31.6 ± 1.6	-8.1 ± 3.6
Phenylethynyl (28)	32.0 ± 1.4	31.1 ± 1.4	-3.7 ± 3.2
Vinyl (29)	27.5 ± 1.2	26.8 ± 1.2	-6.2 ± 3.2
<i>tert</i> -Butyl (30)	28.1 ± 2.2	27.3 ± 2.3	-13.7 ± 5.2





**Figure 52.**  $E_a$  and precision estimates for the rearrangement of 1-substituted-2,3,4,5-tetraphenyl-2,4-cyclopentadien-1-ols.



**Figure 53.**  $\Delta S^\ddagger$  and precision estimates for the rearrangement of 1-substituted-2,3,4,5-tetraphenyl-2,4-cyclopentadien-1-ols.

Table XXIX.  $k$ ,  $-\Delta G^\ddagger$  and  $-E_a$  for the [1, 5]-sigmatropic rearrangement of 1-substituted-2,3,4,5-tetraphenyl-2,4-cyclopentadien-1-ols @ 175.0 °C

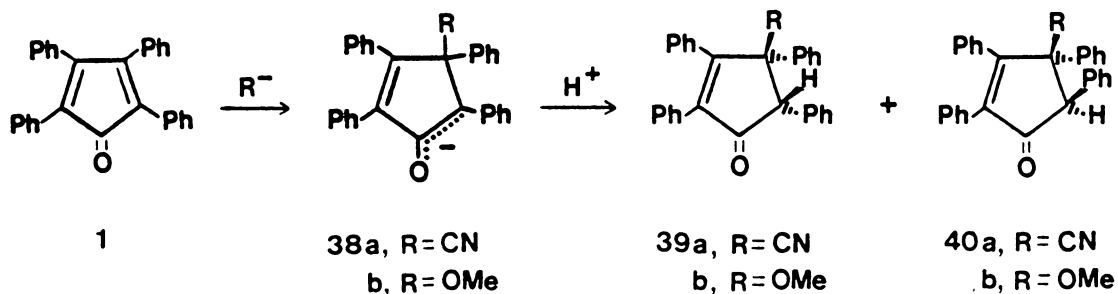
Alcohol (1-substituent)	$k$ sec <sup>-1</sup>	$-\Delta G^\ddagger$ kcal mol <sup>-1</sup> K <sup>-1</sup>	$-E_a$ kcal mol <sup>-1</sup>
Phenyl (4)	6.30 x 10 <sup>-5</sup> (3)	-35.2 (3)	-31.7 (5)
1-Naphthyl (31)*	5.51 x 10 <sup>-6</sup> (1)	-38.4 (1)	-34.8 (1)
2-Pyridyl (32)	6.33 x 10 <sup>-4</sup> (6)	-33.1 (6)	-29.7 (6)
2-Furyl (33)	4.35 x 10 <sup>-5</sup> (2)	-35.0 (2)	-33.5 (2)
2-Thienyl (34)	6.48 x 10 <sup>-5</sup> (4)	-35.2 (4)	-32.5 (3)
Phenylethynyl (35)	9.70 x 10 <sup>-4</sup> (7)	-32.8 (7)	-32.0 (4)
Vinyl (36)*	3.50 x 10 <sup>-2</sup> (8)	-30.3 (8)	-27.5 (8)
<i>tert</i> -Butyl (37)	4.83 x 10 <sup>-4</sup> (5)	-33.4 (5)	-28.1 (7)

\*Rates for these compounds were extrapolated to 175.0 °C (448.15 K)

Numbers in parentheses represent relative position with 1 = lowest and 8 = highest.

## Reactions with potassium cyanide and Triton B

Treatment of tetracyclone (1) with potassium cyanide, followed by the protonation of the intermediate enolate 38a, afforded a pair of diastereomeric enones resulting from 1,4-addition of cyanide.<sup>27</sup> The structures of the *cis*-39a and *trans*-40a isomers were assigned on the basis of their IR, <sup>1</sup>H NMR, <sup>13</sup>C NMR and X-ray spectral data (40a).



Both 39a and 40a show a carbonyl absorption at 1720 cm<sup>-1</sup> which is indicative of an α, β-unsaturated ketone in a five-membered ring. However, the isomers differ in the position of the methine proton in the <sup>1</sup>H NMR. The methine proton of 39a has a chemical shift of 4.81 ppm, while the methine proton of 40a occurs at 4.16 ppm. Likewise, in the <sup>13</sup>C NMR, the chemical shift of the nitrile carbon differs for both isomers. The <sup>13</sup>C spectrum for 39a shows a singlet at 120.4 ppm for this carbon, while 40a shows a singlet at 118.0 ppm for the same carbon.

On the basis of these observations, the assignment of *cis* and *trans* can be rationalized upon shielding and deshielding arguments.<sup>28</sup> In the *cis* case (39a), the proton is above the triple bond of the nitrile in a deshielding environment which produces the downfield chemical shift. In the *trans* case (40a), the proton and nitrile are both located above an aromatic ring in a shielding environment. This shielding effect results in an upfield chemical shift for the methine proton as well as the nitrile carbon. In addition, the structure of the *trans* isomer (40a) was confirmed by X-ray crystallographic analysis<sup>29</sup> (Figure 54).

Initial studies of the reaction of 1 with potassium cyanide resulted in varying ratios of 39a to 40a depending upon the temperature at which protonation of the enolate 38a occurred. As can be seen in Table XXX, protonation at lower temperatures (i.e., 0 or 27 °C) resulted in the *cis* isomer

(**39a**) being the major isomer, while at elevated temperatures (i.e., 90 °C), the *trans* isomer (**40a**) was the major isomer.

Clearly, what was occurring was a change from a kinetic protonation of the enolate **38a** to a thermodynamic protonation of the same enolate, affording **39a** as the kinetically controlled product. It appears logical that the *cis* isomer (**39a**) represents the kinetic product, since it is the product obtained by protonation from the least hindered side (i.e., the same side on which the cyanide group is located), while the *trans* isomer (**40a**) represents the more stable thermodynamic product which positions the two bulky phenyl groups on opposite sides of the ring.

To test the validity of this hypothesis, a series of experiments (Table XXXI) was performed to determine if **40a** was, indeed, the thermodynamically more stable isomer and the extent to which this isomer was favored when different isomerization modes were used. The three isomerization methods employed to convert a single pure isomer, either **39a** or **40a**, into its thermodynamic equilibrium composition were base (KCN), acid (HCl) and heat.

In the base-catalyzed mode, the pure isomers were separately subjected to potassium cyanide at room temperature, and regardless of which isomer was chosen as the starting material, the isomer ratio obtained was approximately 30 to 70 with the *trans* isomer (**40a**) dominating. (The 5-min entry simply demonstrates that equilibrium had not yet been established.)

Acid-catalyzed isomerization of the *cis* isomer (**39a**) at 90 °C produced an isomer ratio of 33 to 67, for **39a** to **40a**, respectively, within 5 min; while at room temperature (ca. 27 °C), equilibrium had not yet been established at the end of 3 hrs.

Finally, thermal-catalyzed isomerization of the *cis* isomer (**39a**) at 90 °C for 3 hrs resulted in a 32 to 68 ratio of **39a** to **40a**, respectively. Thus, approximately the same ratio of **39a** to **40a** was obtained by the three different modes of isomerization.

Due to the reversible nature of the protonation of enolate **38a**, it was decided to investigate the irreversible kinetic quench of the enolate using methyl iodide. As expected, methylation of enolate **38a** at either room temperature (27 °C) or 0 °C afforded the kinetic *cis* isomer (**41**) as the most abundant product (ca. 90%). Confirmation of the structure of this product was again obtained by X-ray crystallographic analysis<sup>29</sup> (Figure 55).

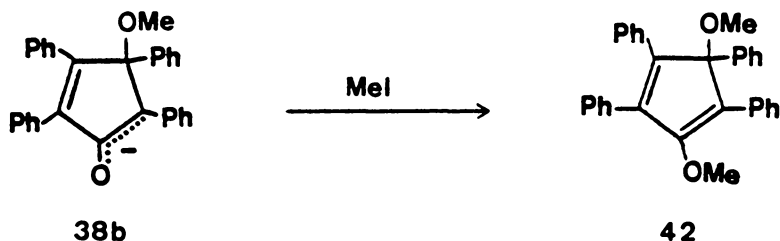
As a result of these findings, a reinvestigation of the kinetic and thermodynamic protonation of enolate **38b**, as well as study of the products obtained upon quenching enolate **38b** with methyl iodide, was undertaken. Enolate **38b** was obtained via the literature<sup>30</sup> method by treating tetracyclone (**1**) with either a solution of Triton B or potassium methoxide in a 1:1 benzene/Me<sub>2</sub>SO solvent system. Although both bases gave identical results, the products obtained from the Triton B experiments were more difficult to analyze because of the benzyl methyl ether present which interfered with the <sup>1</sup>H NMR analysis of the isomer mixtures obtained. For this reason, only reactions of potassium methoxide in methanol were used on all runs in which ratios of **39b** to **40b** were to be determined.

As can be seen from Table XXX, there appears to be no temperature dependence for protonation of enolate **38b**. All three temperatures (0, 27, and 90 °C) gave approximately the same ratio of *cis*-**39b** to *trans*-**40b** of 60 to 40. Thus, the *cis* isomer (**39b**) appears to be the kinetically favored product, but not by much, and the kinetic protonation of either enolate **38a** or **38b** resulted in the formation of the *cis* isomer (**39a** or **39b**) as the major product. The temperature dependence of the **39a** to **40a** ratio can be attributed to the ease of enol formation of this isomer pair over the **39b** and **40b** isomer pair, which shows no temperature dependence of their ratio. This ease of enolization, especially at the higher temperatures, results in the formation of the more stable thermodynamic isomer of the pair.

However, the isomerization experiments (Table XXXI) of ketones **39b** and **40b** did provide some interesting results. The base-catalyzed (KOMe) isomerization of either the *cis* isomer (**39b**) or the *trans* isomer (**40b**) resulted in the same isomer ratio (**39b** to **40b**) of 81 to 19. Likewise, the acid-catalyzed isomerization of the *trans* (**40b**) gave exactly the same ratio after equilibrating for 98 hrs. Unfortunately, both isomers decomposed to tetracyclone (**1**) and methanol under thermal conditions before equilibration could occur. As a result, the data from the thermal isomerization cannot corroborate the data obtained from the base- and acid-catalyzed rearrangements.

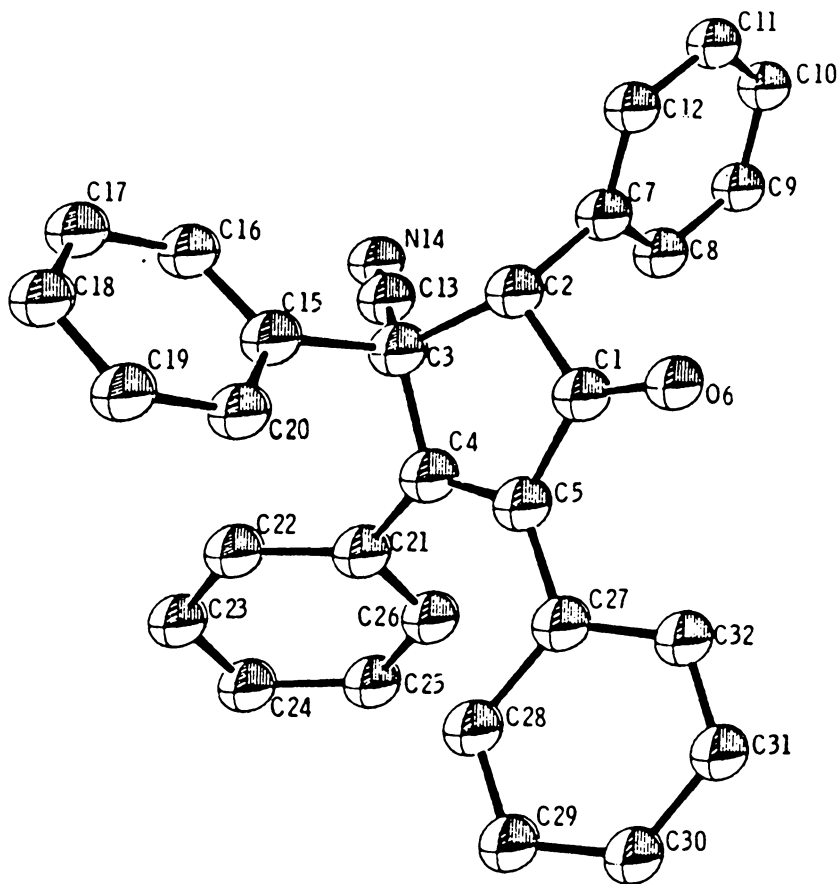
Thus the *cis* isomer (**39b**) was found to be both the kinetic and thermodynamic product from protonation of **38b**, and that the literature<sup>30</sup> claim that the ratio of **39b** to **40b** for the kinetic protonation of **38b** was identical with that obtained for thermodynamic protonation was incorrect.

Last, the methylation of **38b** was investigated. Treatment of **38b** with excess methyl iodide produced a 95% yield of the O-methylated product **42**, while methylation of **38a** afforded a



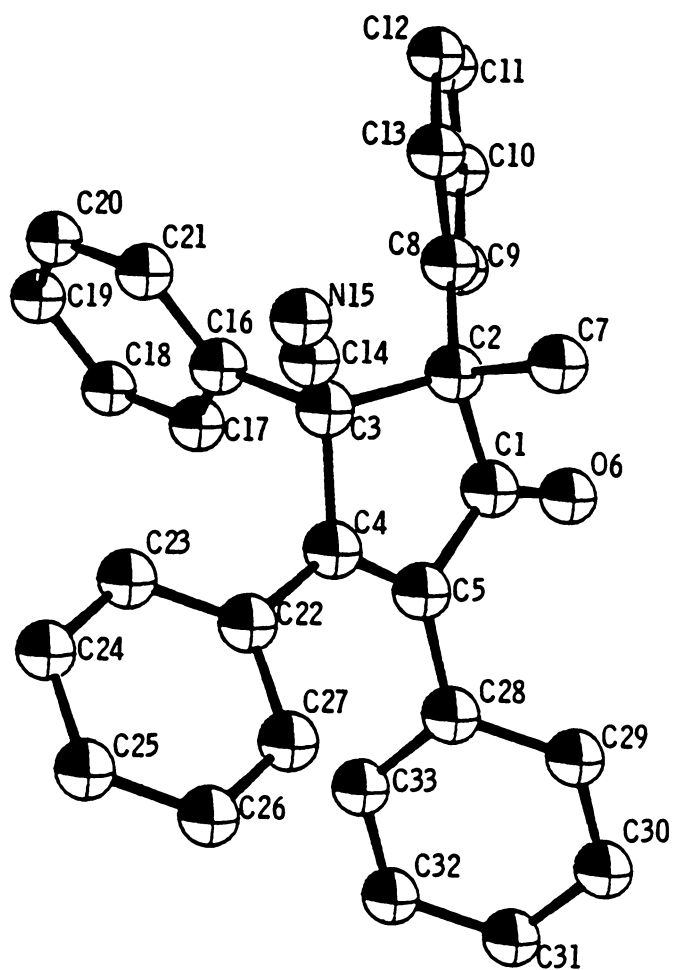
90% yield of C-methylated products. It appears that steric and/or electronic effects are responsible for this observed difference in the site of methylation, since in **38a**, it appears that there is more electron density on the carbon atom of the enolate than on the oxygen atom, while in **38b**, the electron density resides mainly on the oxygen atom of the enolate.

This can be accounted for by interaction of the methoxide oxygen lone pairs with the adjacent p orbital of the enolate, thus increasing the electron density of the enolate oxygen atom. As a result, O-methylation predominates in this system.



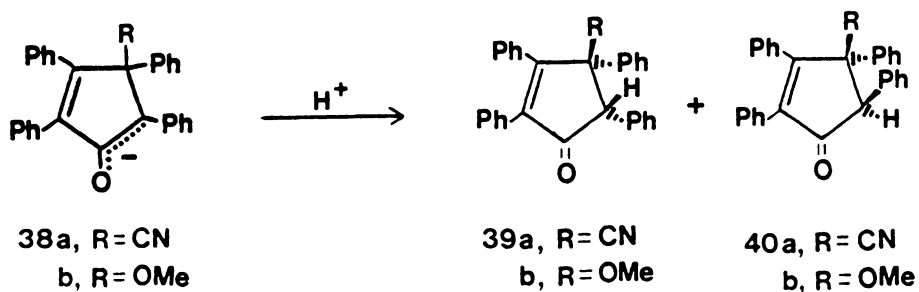
**Figure 54.** Computer generated drawing derived from the X-ray coordinates of *trans*-4-cyano-2,3,4,5-tetraphenyl-2-cyclopenten-1-one (**40a**).





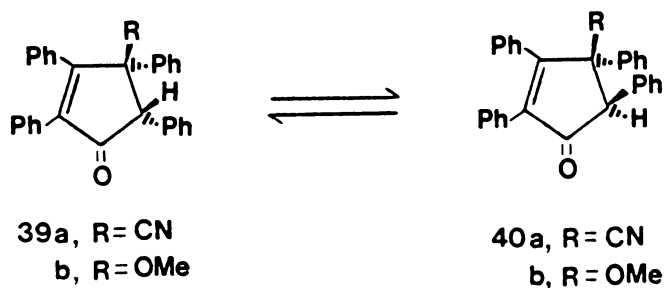
**Figure 55.** Computer generated drawing derived from the X-ray coordinates of *cis*-2,3,4,5-tetraphenyl-4-cyano-5-methyl-2-cyclopenten-1-one (41).

Table XXX. Effect of Temperature and Solvent on Protonation of Enolates 38a and 38b



enolate	temp °C	solvent	ratio 5/6
38a	0	DMF	91/9
	0	Me <sub>2</sub> SO/C <sub>6</sub> H <sub>6</sub>	91/9
	27	DMF	84/16
	27	Me <sub>2</sub> SO/C <sub>6</sub> H <sub>6</sub>	84/16
	90	Me <sub>2</sub> SO/C <sub>6</sub> H <sub>6</sub>	30/70
38b	0	Me <sub>2</sub> SO/C <sub>6</sub> H <sub>6</sub>	59/41
	27	Me <sub>2</sub> SO/C <sub>6</sub> H <sub>6</sub>	60/40
	90	Me <sub>2</sub> SO/C <sub>6</sub> H <sub>6</sub>	58/42

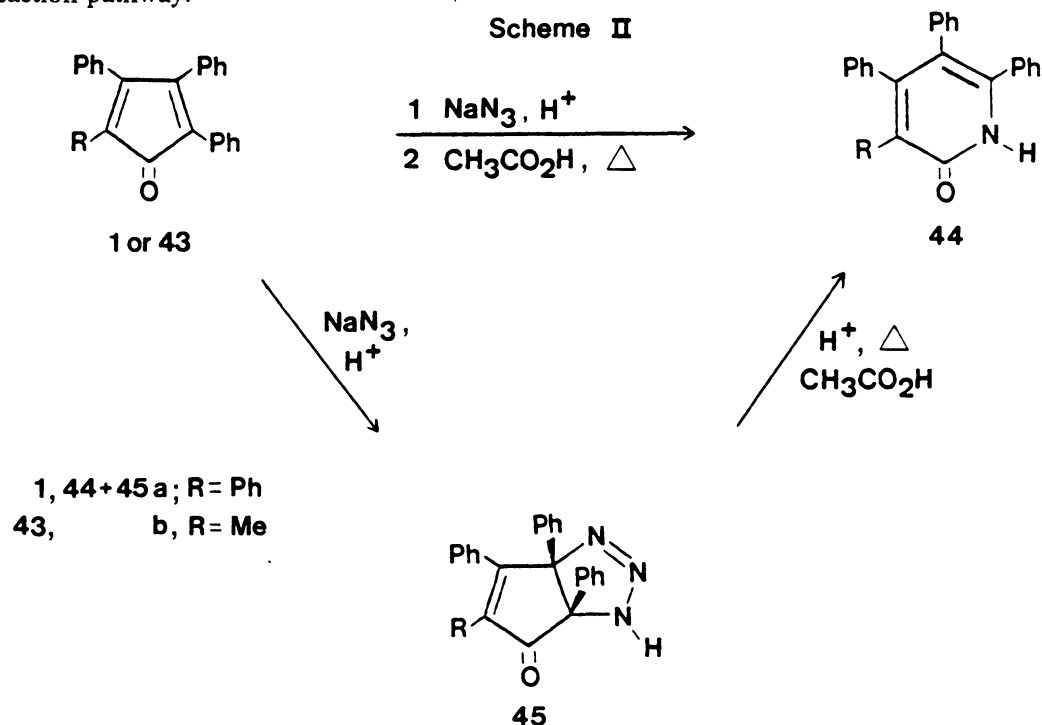
Table XXXI. Thermodynamic Isomerization of Ketones 39 and 40



isomerization mode	starting isomer	time	temp °C	ratio 39/40
base	39a	3 hrs	27	29/71
	40a	4 hrs	27	27/73
	39a	5 min	27	61/39
	39b	2 hrs	27	81/19
	40b	2 hrs	27	81/19
acid	39a	3 hrs	27	57/43
	39a	5 min	90	33/67
	40b	6 hrs	27	23/77
	40b	98 hrs	27	81/19
heat	39a	15 min	90	82/18
	39a	3 hrs	90	32/68

## Reactions with sodium azide

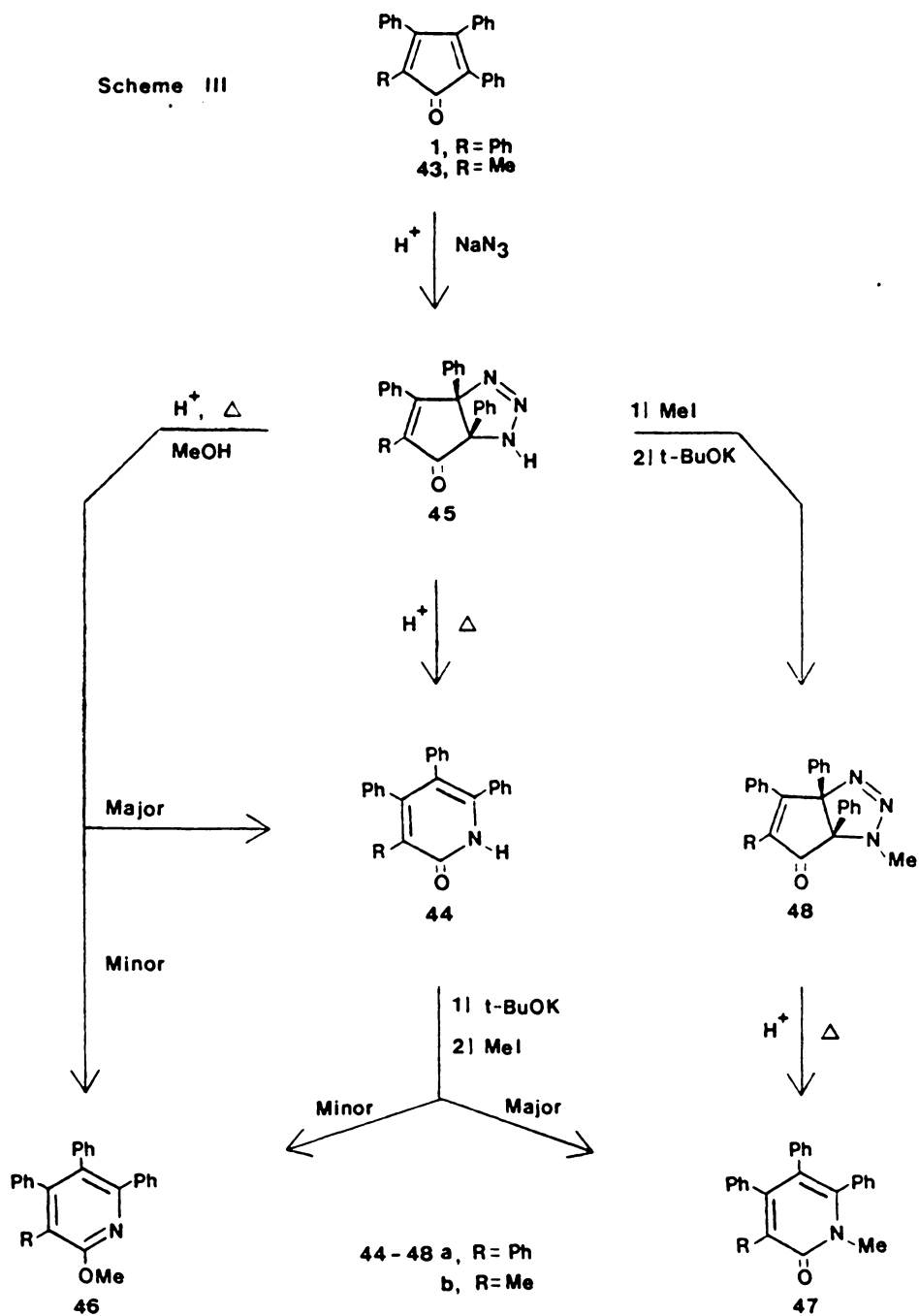
Treatment of tetracyclone (1) with sodium azide under acidic conditions resulted in a 90% isolated yield of the corresponding tetraphenylpyridinone (44a) (Scheme II).<sup>31</sup> However, when the reaction was run under milder conditions (i.e., lower temperature, shorter reaction time), the bicyclic triazolone 45a was obtained in 94% yield. Subsequent acidification of 45a resulted in elimination of nitrogen and formation of the pyridinone 44a. Thus it appears that 45a is an intermediate in the formation of 44a and that the reaction does not take place by a classical Schmitt reaction pathway.<sup>32</sup>



We postulate that the formation of 45a results from an initial acid-catalyzed Michael addition of sodium azide to tetracyclone (1), followed by protonation of the terminal nitrogen of the azide functional group and cyclization via the enol form, to generate the bicyclic structure.

It is important to note that in the unsymmetrical case 43 (Scheme II), the only bicyclic triazolone compound obtained was the one in which addition and cyclization occurred to the side

Scheme III



of the ring that contained the phenyl ring alpha to the carbonyl group. It appears that the phenyl ring at this position directs the addition to this side of the ring and stabilizes the enol structure sufficiently to allow cyclization to occur. The structure of the bicyclic triazoline **45b** was assigned on the basis of its spectral data and was confirmed by X-ray crystallographic analysis<sup>29</sup> (Figure 56).

There are many examples in the literature regarding the Michael addition of hydrazoic acid to  $\alpha$ ,  $\beta$ -unsaturated carbonyl compounds.<sup>33</sup> However, since the intermediate 1,4-addition product was not observed in this case, the possibility of a 1,3-dipolar cycloaddition<sup>34</sup> cannot be totally excluded.

As shown in Scheme III, acidification of the bicyclic triazoline structure **45** results in loss of nitrogen accompanied by ring enlargement to generate the pyridinone structure **44**. However, when the acidification takes place in methanol, an additional product is formed along with the expected pyridinone **44**. This product was identified as the appropriately substituted 2-methoxypyridine derivative **46** which was produced in about 30-35% yield from either **45a** or **45b**.

The bicyclic triazoline system **45** was derivatized to its N-methyl form **48** in order to obtain a more soluble species for spectroscopic examination. Treatment of **45** with methyl iodide followed by the addition of base resulted in acceptable yields of the desired N-methyl derivative **48**. As expected, acidification of this compound resulted in the elimination of nitrogen with formation of the N-methylpyridinone (**47**).

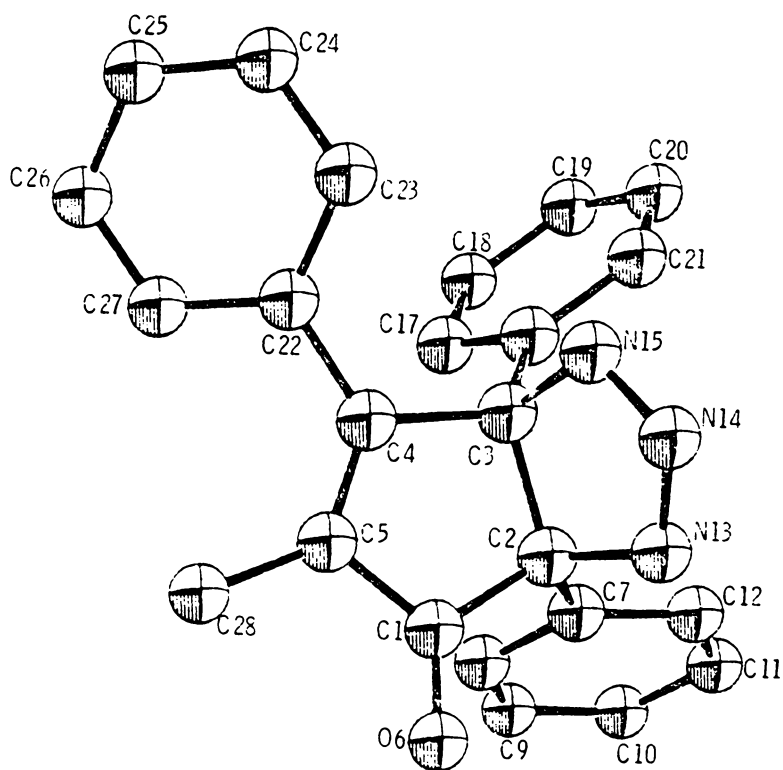
The formation of **44** from **45** and **47** from **48** is represented in Scheme IV. The conversion probably proceeds by an acid-catalyzed intramolecular attack by the amine nitrogen to produce the highly strained tricyclic ring system which can then rearrange with loss of nitrogen to generate the substituted pyridinone systems **44** and **47**.

The formation of the substituted 2-methoxypyridine **46** by acidification of **45** in methanol can be explained in a slightly different manner. Since treatment of the substituted pyridinone **44** under the identical reaction conditions did not produce any of the 2-methoxy derivative **46**, it appears that this product did not arise from **44** and therefore **46** and **44** must be derived from a common intermediate, or more likely, by separate reaction pathways.

A possible mechanism for the conversion of **45** to **46** can be envisioned as follows. Formation of the hemketal of **45**, followed by an intramolecular backside displacement of water by the amine

nitrogen generates the unstable tricyclic ether. This compound can then spontaneously and irreversibly rearrange with elimination of nitrogen to form the substituted 2-methoxypyridine (46).

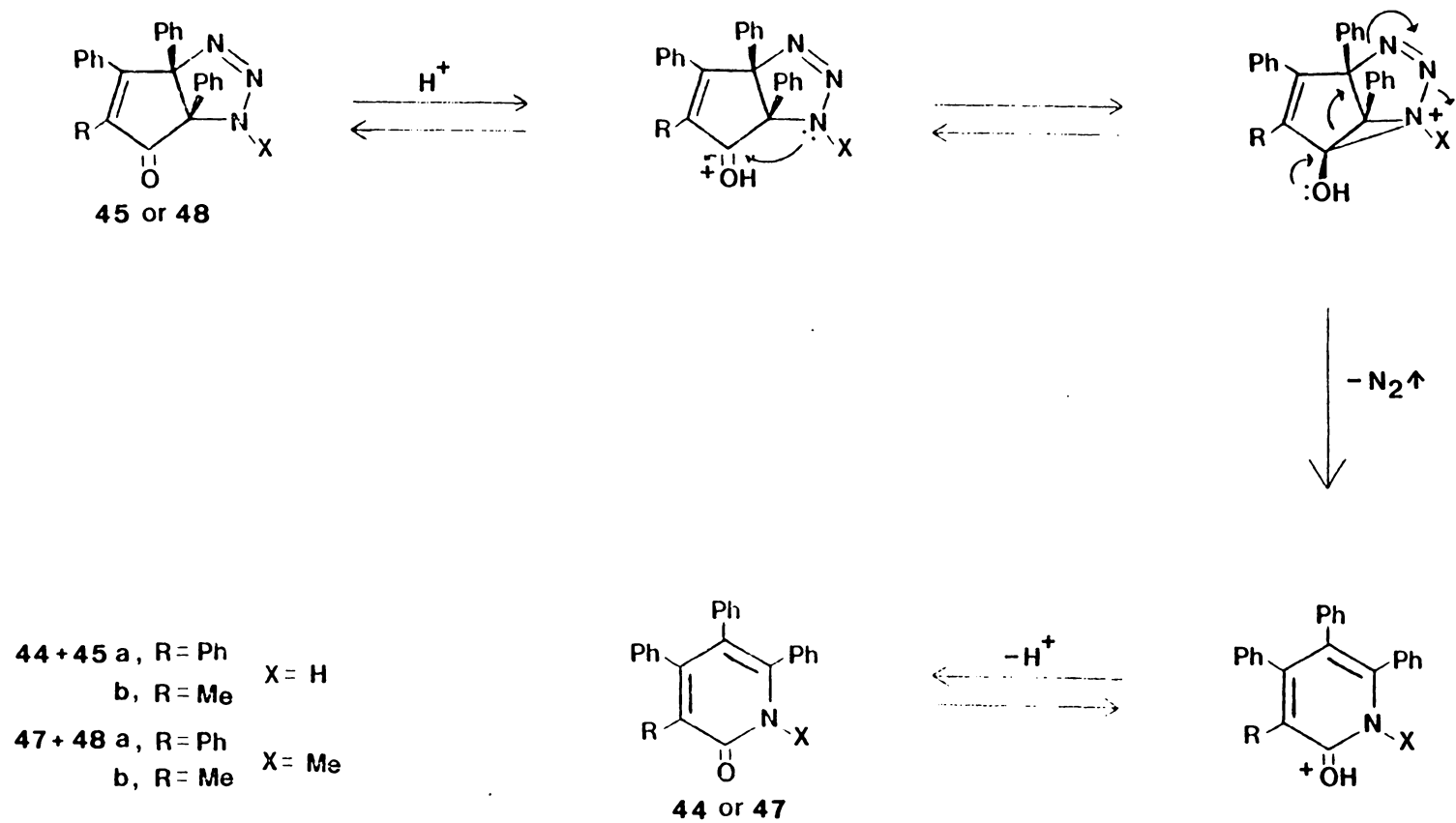
The methoxypyridine (46) and N-methylpyridinone (47) were also prepared by treatment of the pyridinone 44 with potassium *tert*-butoxide followed by quenching with methyl iodide (Scheme II). In each case (44a or 44b), the N-methyl derivative (47a or 47b) was generated as the major product. In both cases, the ratio of 47 to 46 was on the order of 65:35.



**Figure 56.** Computer generated drawing derived from the X-ray coordinates of 1,5,8-triphenyl-7-methyl-2,3,4-triazabicyclo[3.3.0]octa-2,7-dien-6-one (**45b**).



Scheme IV



## Summary

In conclusion, five major points should be emphasized.

First, syntheses of the 1-substituted tetraphenylcyclopentadienols were efficiently achieved by the addition of the appropriate organometallic reagent to tetracyclone followed by an acid quench.

Secondly, the most efficient way of generating the "unconjugated ketones" was by the anionic rearrangement of the alkoxide followed by a kinetic quench. It was found that the thermal rearrangement of the alcohols resulted in considerable amounts of the undesired "conjugated" isomers.

Third, steric and electronic effects of the migrating group were determined to play a role in the [1,5]-sigmatropic rearrangement of 1-substituted tetraphenylcyclopentadienols. Electron donating groups are believed to increase the rate of migration whereas electron withdrawing substituents are responsible for slowing the rearrangement. Likewise, smaller substituents accelerate the rate while bulky groups deter the migration. As a result, the experimental evidence supports the originally proposed charge separated transition state.

Fourth, the Michael addition of potassium cyanide to tetracyclone afforded upon protonation a diastomeric mixture of *cis* and *trans* 4-cyano-2,3,4,5-tetraphenyl-2-cyclopenten-1-ones. The *cis* isomer was determined to be the kinetic product while the *trans* isomer represents the thermodynamically more stable product.

Finally, an extremely efficient synthesis of 2,3,4,5-tetraphenyl-2(1H)-pyridinone (90%) resulted from the acid promoted addition of sodium azide to tetracyclone. By changing the reaction conditions, an intermediate bicyclic triazoline could be isolated in high yield. The presence of this compound eliminated the Schmitt mechanism as a viable reaction pathway.

# Experimental

## *General Procedures*

Melting points were determined on a Thomas-Hoover melting point apparatus and are uncorrected. The infrared spectra were recorded on a Perkin-Elmer 710B spectrophotometer using NaCl salt windows.  $^1\text{H}$  NMR spectra were determined at 90 MHz on a Varian EM-390 and at 270 MHz on a Bruker WP-270SY while  $^{13}\text{C}$  NMR spectra were recorded at 50 MHz on a JEOL FX-200 and on a Bruker NP200 and at 67.5 MHz on the Bruker WP-270SY. NMR chemical shifts are reported in parts per million (ppm) relative to tetramethylsilane ( $\text{Me}_4\text{Si}$ ) as the internal standard. Mass spectra were obtained on a Varian MAT 112 or VG 7070E-HF mass spectrometer at 70 eV. Elemental analyses were performed by Multi Chem Laboratories, Inc., Lowell, MA. All solvents were purified by standard methods prior to use.<sup>35</sup> Tetracyclone (**1**) was prepared by the method of Johnson and Grummitt<sup>36</sup> and was used without further purification. 2-Methyl-3,4,5-triphenyl-2,4-cyclopentadien-1-one (**43**) was prepared by the method of Allen and VanAllan<sup>37</sup> and used without further purification.

### *Synthesis of 1-substituted tetraphenylcyclopentadienols*

**1,2,3,4,5-Pentaphenyl-2,4-cyclopentadien-1-ol (2).** Into a 250-mL three-necked flask equipped with a magnetic stirring bar, nitrogen inlet and septum inlet adapter were placed 4.1 g (10.7 mmol) of tetracyclone (1), 60 mL of ethyl ether and 60 mL of benzene. The flask was placed in an ice-water bath and 20 mL (2.0 M, 40 mmol) of phenyllithium (Aldrich Chemical Co.) was added via a syringe to the flask. During the addition the color changed from dark purple to light orange. After stirring for 15 minutes at this temperature, the contents of the flask were transferred to a separatory funnel containing a solution of 100 mL of cold water and 5 mL of concentrated HCl. The organic layer was separated, washed three times with 100 mL portions of water and dried over anhydrous magnesium sulfate. The solvent was removed on a rotary evaporator and the resulting yellow-orange oil was redissolved in 20 mL of hot benzene followed by the addition of 80 mL of petroleum ether (bp 30-60 °C). This afforded 3.6 g (7.8 mmol, 73%) of the phenyl alcohol in the form of yellow crystals: mp 175-177 °C (lit<sup>1</sup> mp 176-177 °C); IR (CDCl<sub>3</sub>) 3640 cm<sup>-1</sup> (O-H); <sup>1</sup>H NMR (CDCl<sub>3</sub>) δ 6.8-7.7 (m, 25 H), 2.45 (s, 1 H); <sup>13</sup>C NMR (CDCl<sub>3</sub>) δ 90.2 (C-OH); mass spectrum, *m/z* 462 (M<sup>+</sup>). Anal. Calcd for C<sub>35</sub>H<sub>26</sub>O: C, 90.88; H, 5.67. Found: C, 90.80; H, 5.55.

**1-(1-naphthyl)-2,3,4,5-tetraphenyl- 2,4-cyclopentadien-1-ol (24).** Into a 250-mL three-necked flask equipped with a magnetic stirring bar, nitrogen inlet, reflux condenser and addition funnel were placed 11 mL of ethyl ether and 0.37 g (53 mmol) of Li metal which had been cut into numerous small pieces. 1-Bromonaphthlene (5.45 g, 26 mmol) dissolved in 25 mL of ether was placed in the addition funnel and several drops of the undiluted bromonaphthlene were placed in the flask to initiate the reaction. Once the reaction had started, the bromonaphthlene-ether solution was added dropwise in such a way as to maintain a vigorous reaction as determined by observing the rate of the refluxing ether. After the addition was complete, the purple solution was refluxed for 45 minutes via an electrical heating mantle then cooled to room temperature. At this time, a solution of 3.84 g (10 mmol) of tetracyclone (1) in 100 mL of benzene was added dropwise to the naphthyllithium solution. The solution was stirred for 45 minutes at room temperature then transferred to a separatory funnel containing 200 mL of a 10% NH<sub>4</sub>Cl solution. The aqueous layer

was extracted with 100 mL of benzene and the organic layers were combined, washed with 200 mL of a 10%  $\text{NH}_4\text{Cl}$  solution, then dried over anhydrous magnesium sulfate. The solvent was removed on a rotary evaporator which afforded a yellow-brown oily residue which was redissolved in 40 mL of benzene and chromatographed over silica gel (120 g) using benzene as eluant. Like fractions, as determined by TLC analysis, were combined and the solvent was removed on a rotary evaporator. The residue was redissolved in 35 mL of hot benzene and treated with 80 mL of petroleum ether (bp 30-60 °C). This afforded 2.7 g (5.3 mmol, 53%) of the naphthyl alcohol in the form of yellow crystals: mp 182-183 °C; IR ( $\text{CCl}_4$ ) 3600 + 3630  $\text{cm}^{-1}$  (O-H);  $^1\text{H}$  NMR ( $\text{CDCl}_3$ )  $\delta$  6.6-8.8 (m, 27 H), 2.63 (s, 1 H);  $^{13}\text{C}$  NMR ( $\text{CDCl}_3$ )  $\delta$  89.8 (C-OH); mass spectrum,  $m/z$  512 ( $\text{M}^+$ ). Anal. Calcd for  $\text{C}_{39}\text{H}_{28}\text{O}$ : C, 91.37; H, 5.51. Found: C, 91.30; H, 5.66.

**1-(2-Pyridyl)-2,3,4,5-tetraphenyl-2,4-cyclopentadien-1-ol (25).** Into a 250-mL three-necked flask equipped with a magnetic stirring bar, nitrogen inlet and addition funnel were placed 50 mL of ethyl ether and 8.0 mL (2.4 M, 19.2 mmol) of *n*-butyllithium (Aldrich Chemical Co.). After cooling to 0 °C in an ice-water bath, a solution of 3.12 g (19.7 mmol) of 2-bromopyridine in 10 mL of ether was slowly added to the flask. The resulting dark red-brown solution was stirred for 10 minutes at this temperature while a solution of 2.5 g (6.5 mmol) of tetracyclone (**1**) in 50 mL of benzene was transferred to the addition funnel. The tetracyclone solution was added dropwise over a 20 minute interval during which time the color changed to a dark murky green. The solution was stirred for 5 additional minutes at 0 °C then transferred to a separatory funnel containing a solution of 100 mL of cold water and 5 mL of concentrated HCl. The benzene layer was separated and the aqueous layer was re-extracted twice with 15 mL-portions of benzene. The benzene layers were combined, washed twice with 100 mL-portions of water and dried over anhydrous magnesium sulfate. The solvent was removed on a rotary evaporator and the resulting yellow-brown oil was crystallized from 15 mL of hot benzene followed by the addition of 25 mL of petroleum ether (bp 30-60 °C). This afforded 1.87 g (4.0 mmol, 62%) of the pyridyl alcohol in the form of white needles: mp 217-218.5 °C; IR ( $\text{CDCl}_3$ ) 3360  $\text{cm}^{-1}$  (O-H);  $^1\text{H}$  NMR ( $\text{CDCl}_3$ )  $\delta$  6.8-8.4 (m, 24 H), 6.36 (s, 1 H, exchangeable with  $\text{D}_2\text{O}$ );  $^{13}\text{C}$  NMR ( $\text{CDCl}_3$ )  $\delta$  89.4 (C-OH); mass spectrum,  $m/z$  463 ( $\text{M}^+$ ). Anal. Calcd for  $\text{C}_{34}\text{H}_{25}\text{NO}$ : C, 88.09; H, 5.44; N, 3.02. Found: C, 88.10; H, 5.66; N, 3.02.

**1-(2-Furyl)-2,3,4,5-tetraphenyl-2,4-cyclopentadien-1-ol (26).** Into a 100-mL three-necked flask equipped with a magnetic stirring bar, nitrogen inlet, addition funnel and reflux condenser were placed 15 mL of ethyl ether and 0.9 mL (0.94 g/mL, 0.85 g, 12 mmol) of furan. To the stirred solution was slowly added 3.0 mL (2.6 M, 7.8 mmol) of *n*-butyllithium (Aldrich Chemical Co.). The solution was refluxed for 1 hr then placed in an ice-water bath. To the cold solution was added a solution of 2.00 g (5.2 mmol) of tetracyclone (1) in 40 mL of benzene. The solution was stirred for 1 hr at this temperature then transferred to a separatory funnel containing a solution of 50 mL of cold water and 1 mL of concentrated HCl. The organic layer was separated, washed twice with 50-mL portions of water then dried over anhydrous magnesium sulfate. The solvent was removed on a rotary evaporator and the yellow residue was redissolved in 15 mL of hot benzene and treated with 35 mL of petroleum ether (bp 30-60 °C). This afforded 1.9 g (4.2 mmol, 81%) of the furyl alcohol in the form of yellow crystals: mp 176-177 °C; IR (CHCl<sub>3</sub>) 3640 cm<sup>-1</sup> (O-H); <sup>1</sup>H NMR (CDCl<sub>3</sub>) δ 6.8-7.2 (m, 20 H), 7.28 (dd, 1 H, J = 0.9, 1.9 Hz), 6.35 (dd, 1 H, J = 0.9, 3.1 Hz), 6.25 (dd, 1 H, J = 1.9, 3.1 Hz), 2.64 (s, 1 H); <sup>13</sup>C NMR (CDCl<sub>3</sub>) δ 87.1 (C-OH); mass spectrum, *m/z* 452 (M<sup>+</sup>). Anal. Calcd for C<sub>33</sub>H<sub>24</sub>O<sub>2</sub>: C, 87.58; H, 5.35. Found: C, 87.78; H, 5.45.

**1-(2-Thienyl)-2,3,4,5-tetraphenyl-2,4-cyclopentadien-1-ol (27).** Into a 250-mL three-necked flask equipped with a magnetic stirring bar, nitrogen inlet and addition funnel were placed 75 mL of ethyl ether and 6.0 mL (1.05 g/mL, 6.3 g, 75 mmol) of thiophene. To the stirred solution was slowly added 19.5 mL (2.6 M, 51 mmol) of *n*-butyllithium (Aldrich Chemical Co.). The solution was stirred for 15 min at room temperature then placed in an ice-water bath. To the cold solution was added a solution of 5.54 g (14.4 mmol) of tetracyclone (1) in 90 mL of benzene. The solution was stirred for 1 hr at this temperature then transferred to a separatory funnel containing 100 mL of a 20% NH<sub>4</sub>Cl solution. The organic layer was separated and washed again with 100 mL of a 20% NH<sub>4</sub>Cl solution. The aqueous layers were combined and extracted with 50 mL of benzene. The organic layers were combined and dried over anhydrous magnesium sulfate. The solvent was removed on a rotary evaporator and the oil was redissolved in 30 mL of a benzene/carbon tetrachloride solution (80/20) and chromatographed on silica gel (70 g) using the same solvent as eluant. Like fractions, as determined by TLC analysis, were combined and the solvent was removed

on a rotary evaporator. The resulting yellow oil was dissolved in 20 mL of hot benzene and treated with 80 mL of petroleum ether (bp 30-60 °C). This afforded 5.7 g (12.2 mmol, 85%) of the thienyl alcohol in the form of yellow-green crystals: mp 155-157 °C; IR (CDCl<sub>3</sub>) 3630 cm<sup>-1</sup> (O-H); <sup>1</sup>H NMR (CDCl<sub>3</sub>) δ 6.7-7.3 (m, 23 H), 2.65 (s, 1 H); <sup>13</sup>C NMR (CDCl<sub>3</sub>) δ 88.8 (C-OH) ; mass spectrum, *m/z* 468 (M<sup>+</sup>). Anal. Calcd for C<sub>33</sub>H<sub>24</sub>OS : C, 84.58; H, 5.16; S, 6.84. Found: C, 84.54; H, 5.68; S, 6.25.

**1-Phenylethynyl-2,3,4,5-tetraphenyl-2,4-cyclopentadien-1-ol (28).** Into a 250-mL three-necked flask equipped with a magnetic stirring bar, nitrogen inlet and addition funnel were placed 40 mL of ethyl ether, 0.54 g (23 mmol) of sodium metal and 3.6 g (35 mmol) of phenylacetylene. The solution was stirred for 8 hrs at room temperature then placed in a cooling bath with the temperature regulated to 10-15 °C. To the creamy white solution was slowly added over 6 hrs a solution of 3.55 g (9.2 mmol) of tetracyclone (1) in 50 mL of benzene. The resulting green solution was stirred for 30 additional minutes at this temperature then transferred to a separatory funnel containing 200 mL of a 10% NH<sub>4</sub>Cl solution. The organic layer was separated and washed with 200 mL of a 10% NH<sub>4</sub>Cl solution and dried over anhydrous magnesium sulfate. The solvent was removed on a rotary evaporator which afforded a yellow-brown solid. The crude solid was dissolved in 30 mL of chloroform and chromatographed on silica gel (50 g) using chloroform as eluant. Like fractions, as determined by TLC analysis, were combined and the solvent was removed on a rotary evaporator. The residue was redissolved in 50 mL of hot benzene and treated with 100 mL of petroleum ether (bp 30-60 °C). This afforded 3.44 g (7.1 mmol, 77%) of the phenylethynyl alcohol in the form of yellow needles: mp 201.5-203 °C; IR (CDCl<sub>3</sub>) 3600 cm<sup>-1</sup> (O-H); <sup>1</sup>H NMR (CDCl<sub>3</sub>) δ 6.7-7.7 (m, 25 H), 2.55 (s, 1 H); <sup>13</sup>C NMR (CDCl<sub>3</sub>) δ 88.9 (C-OH); mass spectrum, *m/z* 486 (M<sup>+</sup>). Anal. Calcd for C<sub>37</sub>H<sub>22</sub>O : C, 91.33; H, 5.39. Found: C, 91.39; H, 5.69.

**1-Vinyl-2,3,4,5-tetraphenyl-2,4-cyclopentadien-1-ol (29).** Into a 250-mL three-necked flask equipped with a magnetic stirring bar, nitrogen inlet and septum inlet adapter were placed 2.06 g (5.4 mmol) of tetracyclone (1), 40 mL of benzene and 50 mL of ethyl ether. The flask was placed in an ice-water bath and 10 mL (0.75 M, 7.5 mmol) of vinylolithum (previously prepared by the addition of *tert*-butyllithium to vinyl bromide in ether) was added via a syringe. The resulting



yellow solution was stirred for 5 minutes at this temperature then transferred to a separatory funnel containing a solution of 100 mL of cold water and 2 mL of concentrated HCl. The organic layer was separated, washed twice with 100 mL portions of water and dried over anhydrous magnesium sulfate. The solvent was removed on a rotary evaporator and 50 mL of petroleum ether (bp 30-60 °C) was added to the orange oil. Upon standing overnight at room temperature under a nitrogen atmosphere the oil crystallized into an off-white solid which upon suction filtration afforded 1.8 g (4.6 mmol, 85%) of the vinyl alcohol: mp 138-140 °C; IR (CDCl<sub>3</sub>) 3630 cm<sup>-1</sup> (O-H); <sup>1</sup>H NMR (CDCl<sub>3</sub>) δ 6.5-7.5 (m, 20 H), 5.94 (dd, 1 H, J = 16.5, 10.0 Hz), 5.54 (dd, 1 H, J = 16.5, 1.5 Hz), 5.22 (dd, 1 H, J = 10.0, 1.5 Hz), 2.2 (s, 1 H); <sup>13</sup>C NMR (CDCl<sub>3</sub>) δ 89.4 (C-OH); mass spectrum, *m/z* 412 (M<sup>+</sup>). Anal. Calcd for C<sub>31</sub>H<sub>24</sub>O: C, 90.26; H, 5.86. Found: C, 89.58; H, 6.26.

**1-*tert*-Butyl-2,3,4,5-tetraphenyl-2,4-cyclopentadien-1-ol (30).** Into a 100-mL three-necked flask equipped with a magnetic stirring bar, nitrogen inlet and septum inlet adapter were placed 2.0 g (5.2 mmol) of tetracyclone (1) and 50 mL of ethyl ether. The flask was placed in an ice-water bath and 8.0 mL (2.0 M, 16 mmol) of *tert*-butylmagnesium chloride (Aldrich Chemical Co.) was slowly added via a syringe to the flask during which time the color changed from dark purple to a light yellow. After stirring for 15 additional minutes at this temperature, the contents of the flask were transferred to a separatory funnel containing a solution of 40 mL of cold water and 4 mL of concentrated HCl. The organic layer was separated, washed twice with 50-mL portions of water and dried over anhydrous magnesium sulfate. The ether was removed on a rotary evaporator and the resulting yellow oil was dissolved in 10 mL of hexanes and placed in an ice-water bath. This afforded 1.1 g (2.5 mmol, 48%) of the *tert*-butyl alcohol in the form of an off white powder. Recrystallization from benzene/petroleum ether (bp 30-60 °C) (1/20) afforded the analytically pure compound in the form of yellow-green crystals: mp 167-169 °C; IR (CHCl<sub>3</sub>) 3640 cm<sup>-1</sup> (O-H); <sup>1</sup>H NMR (CDCl<sub>3</sub>) δ 6.8-7.6 (m, 20 H), 2.43 (s, 1 H), 0.87 (s, 9 H); <sup>13</sup>C NMR (CDCl<sub>3</sub>) δ 95.3 (C-OH); mass spectrum, *m/z* 442 (M<sup>+</sup>). Anal. Calcd for C<sub>33</sub>H<sub>30</sub>O: C, 89.55; H, 6.83. Found: C, 89.59; H, 7.06.

### *Synthesis of 2-substituted tetraphenylcyclopentenones*

**2,2,3,4,5-Pentaphenyl-3-cyclopenten-1-one (4).** Into a 100-mL 3-necked flask equipped with a magnetic stirring bar, nitrogen inlet, reflux condenser and septum inlet adapter were placed 1.6 g (4.2 mmol) of tetracyclone (1) and 40 mL of benzene. To the dark purple solution was added 8.0 mL (2.0 M, 16 mmol) of phenyllithium (Aldrich Chemical Co.). The resulting yellow-orange solution was refluxed for 24 hrs, cooled to 5 °C in an ice-water bath then quenched with 2 mL of concentrated HCl. The contents of the flask were transferred to a separatory funnel containing 50 mL of water. The benzene layer was separated, washed twice with 50 mL-portions of water then dried over anhydrous magnesium sulfate. The solvent was removed on a rotary evaporator and the residue was redissolved in 7 mL of hot benzene and treated with 25 mL of petroleum ether (bp 30-60 °C). This afforded 1.0 g (2.2 mmol, 52%) of the phenyl ketone in the form of white crystals: mp 191-193 °C (lit<sup>1</sup>mp 194-195 °C); IR (CDCl<sub>3</sub>) 1770 cm<sup>-1</sup> (C = O); <sup>1</sup>H NMR (CDCl<sub>3</sub>) δ 6.6-7.6 (m, 25 H), 4.9 (s, 1 H); mass spectrum, *m/z* 462 (M<sup>+</sup>). Anal. Calcd for C<sub>35</sub>H<sub>26</sub>O: C, 90.88; H, 5.67. Found: C, 91.05; H, 5.61.

**2-(1-naphthyl)-2,3,4,5-tetraphenyl-3-cyclopenten-1-one (31).** Into a 250-mL three-necked flask equipped with a magnetic stirring bar, nitrogen inlet, reflux condenser, and septum inlet adapter were placed 2.7 g (5.3 mmol) of the 1-naphthyl alcohol (24) and 75 mL of toluene. To this solution was added 2.0 mL (2.5 M, 5.0 mmol) of *n*-butyllithium (Aldrich Chemical Co.). The resulting solution was refluxed for 48 hrs; cooled to 0 °C in an ice-water bath and quenched with 1 mL of concentrated HCl. The contents of the flask were transferred to a separatory funnel and washed with 100 mL of water. The organic layer was separated and dried over anhydrous magnesium sulfate. The solvent was removed on a rotary evaporator and the residue was redissolved in 20 mL of CCl<sub>4</sub> and chromatographed over silica gel using CCl<sub>4</sub> as eluant. Like fractions, as determined by TLC analysis, were combined and the solvent was removed on a rotary evaporator. The resulting oil was dissolved in 10 mL of hot benzene and treated with 30 mL of petroleum ether (bp 30-60 °C). This afforded 1.8 g (3.5 mmol, 66%) of the 1-naphthyl ketone (31) in the form of white crystals: mp 175-177 °C ; IR (CDCl<sub>3</sub>) 1765 cm<sup>-1</sup> (C = O); <sup>1</sup>H NMR (CDCl<sub>3</sub>) δ 6.5-8.1 (m,

27 H), 5.04 (s, 1 H); mass spectrum,  $m/z$  512 ( $M^+$ ). Anal. Calcd for  $C_{39}H_{28}O$ : C, 91.37; H, 5.51. Found: C, 91.55; H, 5.66.

**2-(2-Pyridyl)-2,3,4,5-tetraphenyl-3-cyclopenten-1-one (32).** Into a 100-mL three-necked flask equipped with a magnetic stirring bar, nitrogen inlet and septum inlet adapter were placed 2.1 g (4.5 mmol) of the pyridyl alcohol (**25**) and 40 mL of benzene. To this solution was added 1.8 mL (2.5 M, 4.5 mmol) of *n*-butyllithium (Aldrich Chemical Co.). The resulting orange solution was refluxed for 11 hrs then cooled to 0°C in an ice-water bath. The contents of the flask were transferred to a separatory funnel containing 50 mL of water and 1 mL of concentrated HCl. The organic layer was separated, washed with 50 mL of water then dried over anhydrous magnesium sulfate. The solvent was removed on a rotary evaporator and the residue was redissolved in 10 mL of hot benzene and treated with 30 mL of petroleum ether (bp 30-60 °C). This afforded 1.5 g (3.2 mmol, 71%) of the pyridyl ketone in the form of white crystals: mp 153-155 °C; IR ( $CDCl_3$ ) 1765  $cm^{-1}$  (C=O);  $^1H$  NMR ( $CDCl_3$ )  $\delta$  6.8-8.7 (m, 24 H), 5.12 (s, 1 H); mass spectrum,  $m/z$  463 ( $M^+$ ). Anal. Calcd for  $C_{34}H_{25}NO$ : C, 88.09; H, 5.44; N, 3.02. Found: C, 88.11; H, 5.76; N, 2.94.

**2-(2-Furyl)-2,3,4,5-tetraphenyl-3-cyclopenten-1-one (33).** Into a 100-mL three-necked flask equipped with a magnetic stirring bar, nitrogen inlet, reflux condenser and septum inlet adapter were placed 2.1 g (4.6 mmol) of the furyl alcohol (**26**), 40 mL of toluene and 1.8 mL (2.5 M, 4.5 mmol) of *n*-butyllithium (Aldrich Chemical Co.). The solution was refluxed for 10 hrs then cooled to 0 °C. The contents of the flask were transferred to a separatory funnel containing a solution of 50 mL of water and 1 mL of concentrated HCl. The organic layer was separated and washed once with 50 mL of water then dried over anhydrous magnesium sulfate. The solvent was removed under reduced pressure to yield the crude material which was chromatographed on a silica gel column using benzene/methylene chloride (75/25) as eluant. Like fractions, as determined by TLC analysis, were combined and the solvent was removed on a rotary evaporator. The resulting oil was dissolved in 8.5 mL of benzene and treated with 30 mL of petroleum ether (bp 30-60 °C). This afforded 0.9 g (2.0 mmol, 43%) of the furyl ketone in the form of tan needles: mp 170-172 °C; IR ( $CDCl_3$ ) 1770  $cm^{-1}$  (C=O);  $^1H$  NMR ( $CDCl_3$ )  $\delta$  6.0-7.5 (m), singlets at 4.94 and 4.82 (*cis* and

*trans* diastereomers); mass spectrum,  $m/z$  452 ( $M^+$ ). Anal. Calcd for  $C_{33}H_{24}O_2$ : C, 87.58; H, 5.35. Found: C, 87.29; H, 5.11.

**2-(2-Thienyl)-2,3,4,5-tetraphenyl-3-cyclopenten-1-one (34).** Into a 100-mL three-necked flask equipped with a magnetic stirring bar, nitrogen inlet, reflux condenser and septum inlet adapter was placed 2.1 g (4.5 mmol) of the thienyl alcohol (27), 40 mL of benzene and 1.75 mL (2.5 M, 4.5 mmol) of *n*-butyllithium (Aldrich Chemical Co.). The resulting orange-red solution was refluxed for 48 hrs, cooled to 0 °C then transferred to a separatory funnel containing a solution of 50 mL of water and 1 mL of concentrated HCl. The benzene layer was washed twice with 50 mL portions of water then dried over anhydrous magnesium sulfate. The solvent was removed on a rotary evaporator and the resulting yellow oil was redissolved in 8 mL of hot benzene and treated with 30 mL of petroleum ether (bp 30-60 °C). This afforded 1.7 g (3.6 mmol, 80%) of the thienyl ketone in the form of tan needles: mp 189-191 °C; IR ( $CDCl_3$ ) 1775  $cm^{-1}$  (C=O);  $^1H$  NMR ( $CDCl_3$ )  $\delta$  6.7-7.7 (m), singlets at 5.07 and 4.79 (*cis* and *trans* diastereomers); mass spectrum,  $m/z$  468 ( $M^+$ ). Anal. Calcd for  $C_{33}H_{24}OS$ : C, 84.58; H, 5.16; S, 6.84. Found: C, 84.35; H, 5.42; S, 6.13.

**2-Phenylethynyl-2,3,4,5-tetraphenyl-3-cyclopenten-1-one (35).** Into a 250-mL three-necked flask equipped with a magnetic stirring bar, nitrogen inlet, reflux condenser, and septum inlet adapter were placed 2.5 g (5.1 mmol) of the phenylethynyl alcohol (28) and 100 mL of benzene. To this solution was added 2 mL (2.5 M, 5.0 mmol) of *n*-butyllithium (Aldrich Chemical Co.). The resulting solution was refluxed for 3 hrs, cooled in an ice-water bath and quenched with 1 mL of concentrated HCl. The contents of the flask were transferred to a separatory funnel and washed with 100 mL of water. The benzene layer was separated and dried over anhydrous magnesium sulfate. The solvent was removed on a rotary evaporator, the residue was redissolved in 10 mL of  $CCl_4$  and chromatographed over silica gel using  $CCl_4$  as eluant. Like fractions, as determined by TLC analysis, were combined and the solvent removed on a rotary evaporator. The resulting oil was dissolved in 10 mL of hot benzene and treated with 30 mL of petroleum ether (bp 30-60 °C). This afforded 1.6 g (3.3 mmol, 65%) of the phenylethynyl ketone (35) in the form of white needles: mp 180-181 °C ; IR ( $CDCl_3$ ) 1775  $cm^{-1}$  (C=O);  $^1H$  NMR ( $CDCl_3$ )  $\delta$  6.7-7.7 (m, 25 H), 5.18 (s,

1 H); mass spectrum,  $m/z$  486 ( $M^+$ ). Anal. Calcd for  $C_{37}H_{22}O$ : C, 91.33; H, 5.39. Found: C, 91.39; H, 5.68.

**2-Vinyl-2,3,4,5-tetraphenyl-3-cyclopenten-1-one (36).** Into a 250-mL three-necked flask equipped with a magnetic stirring bar, nitrogen inlet and septum inlet adapter were placed 3.0 g (7.8 mmol) of tetracyclone (1), 75 mL of ethyl ether and 75 mL of benzene. At this time 30 mL of a previously prepared solution of vinylolithium was added via a syringe to the tetracyclone solution. During the addition the color changed from a dark purple to a bright yellow color. The solution was stirred for 24 hrs at room temperature then cooled to 0 °C in an ice water bath. The contents of the flask were then transferred to a separatory funnel containing a solution of 200 mL of cold water and 3.5 mL of concentrated HCl. The organic layer was washed twice with 200-mL portions of water then dried over anhydrous magnesium sulfate. The solvent was removed on a rotary evaporator and the resulting oil was redissolved in 25 mL of hot benzene and treated with 75 mL of petroleum ether (bp 30-60 °C). This afforded 1.5 g (3.6 mmol, 46%) of the *cis*-vinyl ketone in the form of yellow crystals: mp 163-164°C (lit<sup>22</sup>mp 162-165 °C); IR ( $CDCl_3$ ) 1765  $cm^{-1}$  (C=O);  $^1H$  NMR ( $CDCl_3$ )  $\delta$  6.8-7.4 (m, 20 H), 6.12 (dd, 1 H,  $J = 17.5, 10.6$  Hz), 5.46 (dd, 1 H,  $J = 17.5, 0.8$  Hz), 5.41 (dd, 1 H  $J = 10.6, 0.8$  Hz), 5.01 (s, 1 H); mass spectrometry,  $m/z$  412 ( $M^+$ ). Anal. Calcd for  $C_{31}H_{24}O$ : C, 90.26; H, 5.86. Found: C, 89.72; H, 6.11.

**2-*tert*-Butyl-2,3,4,5-tetraphenyl-3-cyclopenten-1-one (37).** Into a 100-mL three-necked flask equipped with a magnetic stirring bar, nitrogen inlet, reflux condenser and septum inlet adapter were placed 1.6 g (4.1 mmol) of tetracyclone (1) and 50 mL of ethyl ether. To this solution was added 6.2 mL (2.0 M, 12.4 mmol) of *tert*-butyllithium (Aldrich Chemical Co.). The solution was refluxed for 3 hrs then placed in an ice-water bath and quenched with 1 mL of concentrated HCl. The contents of the flask were transferred to a separatory funnel, washed with 100 mL of water and the organic layer was dried over anhydrous magnesium sulfate. The solvent was removed on a rotary evaporator and the resulting oil was redissolved in 4 mL of benzene and chromatographed over silica gel using benzene as eluant. Like fractions, as determined by TLC analysis, were combined and the solvent was removed on a rotary evaporator. The resulting oil was crystallized from hexanes which afforded 0.8 g (2.0 mmol, 50%) of the *tert*-butyl ketone (37) in the form of white

crystals: mp 148-149 °C; IR (CDCl<sub>3</sub>) 1760 cm<sup>-1</sup> (C=O); <sup>1</sup>H NMR (CDCl<sub>3</sub>) δ 6.5-7.5 (m, 20 H), 4.85 (s, 1 H), 1.25 (s, 9 H); mass spectrum, *m/z* 486 (M<sup>+</sup>). Anal. Calcd for C<sub>33</sub>H<sub>30</sub>O: C, 89.55; H, 6.83. Found: C, 89.73; H, 7.09.

### *Kinetic investigation*

The kinetic investigation of the thermal isomerization of the alcohols was performed in the following manner:

All glassware and accessories coming into direct contact with the solvent were acid washed (0.5 M HCl), rinsed with distilled water, oven dried (105 °C) and assembled under a nitrogen atmosphere. Due to the temperatures being used, glass joints were wrapped with teflon tape as opposed to using stopcock grease.

Into a 50-mL, three-necked round-bottomed flask equipped with a magnetic stirring bar, reflux condenser with nitrogen inlet attached at the top, septum inlet adapter, thermometer adapter with an appropriate extended range thermometer was placed 30 mL of diphenyl ether which had been previously purified by vacuum distillation. The solvent was heated to the desired temperature under a nitrogen atmosphere using a THERM-O-WATCH L7/600 temperature controller connected to an electrical heating mantle. In order to minimize heat loss from the upper half of the flask, electrical heating tape was wrapped around the exposed areas of the flask and was connected to a POWERSTAT variable autotransformer. In addition, the heating tape was further insulated with several layers of aluminum foil. The THERM-O-WATCH and POWERSTAT were adjusted in such a way as to maintain the temperature range to ± 0.4 °C. After the desired temperature had stabilized, 0.4860 mmol of the alcohol was added all at once to the heated solvent and the timer was started.

Throughout the rearrangement, 0.4 mL samples were removed from the flask via a syringe, placed in separate vials and allowed to cool to room temperature. Each sample was then analyzed by liquid chromatography using a Molecular Separations, Inc., B 500 liquid chromatograph incor-

porating an Instrumentation Specialties Co. UA-4 UV detector operating at 254 nm with a lamp current of 340 ma. The mobile phase employed was an n-hexane/methanol mixture (Appendix U) with a flow rate on the order of 1.5 mL/min in conjunction with a Micro Pak NH2-10 column (30 cm x 4 mm). Peaks were recorded on a 10-mV Linear Instrument Corp. chart recorder (scanning at 1 cm/min) and peak heights were used as a measure of concentration. The concentration of alcohol in each sample was obtained from a calibration curve constructed by plotting known concentrations of alcohol versus the corresponding peak heights. The points for the calibration curves were obtained by averaging the results of triplicate injections. The points for the kinetic runs were the result of averaging duplicate injections. These results are summarized in Tables IV-XXVII.

### *Reactions with potassium cyanide and triton B*

*cis*-2,3,4,5-tetraphenyl-4-cyano-2-cyclopenten-1-one (39a). Into a 250-mL three-necked flask equipped with a magnetic stirring bar and nitrogen inlet were placed 2.0 g (5.2 mmol) of tetracyclone (1), 0.50 g (7.7 mmol) of potassium cyanide, 60 mL of benzene, and 60 mL of dimethyl sulfoxide (Me<sub>2</sub>SO). This mixture was stirred at room temperature (27 °C) for 5 hrs and was then placed into an ice-water bath for an additional 30 min. The reaction was then quenched with 50 mL of a 1 M HCl solution previously cooled to 0 °C. The benzene layer was then separated, washed three times with 50-mL portions water, and dried over anhydrous magnesium sulfate. Removal of the benzene on a rotary evaporator afforded a yellow oil which was dissolved in 10 mL of hot benzene, and treated with 20 mL of petroleum ether (bp 30-60 °C) . This afforded 1.58 g (3.84 mmol, 75%) of the *cis*-cyano ketone in the form of white needles: mp 174-176 °C ; IR (CCl<sub>4</sub>) 2260 cm<sup>-1</sup> (CN), 1720 cm<sup>-1</sup> (C = O); <sup>1</sup>H NMR (CDCl<sub>3</sub>) δ 6.6-7.8 (m, 20 H), 4.81 (s, 1 H); <sup>13</sup>C NMR (CDCl<sub>3</sub>) δ 120.4 (CN); mass spectrum, *m/z* 411 (M<sup>+</sup>). Anal. Calcd for C<sub>30</sub>H<sub>21</sub>NO: C, 87.56; H, 5.14; N, 3.40. Found: C, 87.80; H, 5.43; N, 3.15.

***trans*-2,3,4,5-tetraphenyl-4-cyano-2-cyclopenten-1-one (40a).** Into a 250-mL three-necked flask equipped with a magnetic stirring bar and nitrogen inlet were placed 2.0 g (5.2 mmol) of tetracyclone (1), 0.50 g (7.7 mmol) of potassium cyanide, 60 mL of benzene, and 60 mL of dimethyl sulfoxide (Me<sub>2</sub>SO). This mixture was stirred at room temperature (27 °C) for 5 hrs followed by the dropwise addition of concentrated HCl until the color changed from deep red to light yellow. The resulting mixture was allowed to stir at room temperature for 18 hrs. The contents of the flask were then transferred to a separatory funnel containing 50 mL of water; the benzene layer was separated, washed twice with 50 mL portions of water, and dried over magnesium sulfate. Removal of the solvent on a rotary evaporator afforded a yellow oil which was dissolved in 10 mL of hot benzene and treated with 20 mL of petroleum ether (bp 30-60 °C). This afforded 1.4 g (3.40 mmol, 65%) of a mixture of the *cis* and *trans* isomers. The off-white, denser-packed crystals of the *trans* isomer were separated from the slightly yellow needles of the *cis* isomer by hand. This afforded 1.1 g (2.67 mmol, 51%) of the *trans*-cyano ketone which upon recrystallization from benzene/petroleum ether (1/2) gave the analytically pure isomer: mp 195-197 °C; IR (CCl<sub>4</sub>) 2260 cm<sup>-1</sup> (CN), 1720 cm<sup>-1</sup> (C=O); <sup>1</sup>H NMR (CDCl<sub>3</sub>) δ 6.6-7.8 (m, 20 H), 4.16 (s, 1 H); <sup>13</sup>C NMR (CDCl<sub>3</sub>) δ 118.0 (CN); mass spectrum, *m/z* 411 (M<sup>+</sup>). Anal. Calcd for C<sub>30</sub>H<sub>21</sub>NO: C, 87.56; H, 5.14; N, 3.40. Found: C, 87.68; H, 5.36; N, 3.40.

***cis*-2,3,4,5-tetraphenyl-4-cyano-5-methyl-2-cyclopenten-1-one (41).** Into a 250-mL three-necked flask equipped with a magnetic stirring bar and nitrogen inlet were placed 2.0 g (5.2 mmol) of tetracyclone (1), 0.50 g (7.7 mmol) of potassium cyanide, 60 mL of benzene, and 60 mL of dimethyl sulfoxide (Me<sub>2</sub>SO). The mixture was stirred at room temperature (27 °C) for 5 hrs followed by the addition of 2 mL of methyl iodide to the deep red solution of the enolate. The resulting pale yellow solution was stirred for an additional 30 min then transferred to a separatory funnel containing 50 mL of water. The benzene layer was separated and dried over anhydrous magnesium sulfate. Removal of the solvent on a rotary evaporator afforded a yellow oil which was dissolved in 8 mL of hot benzene and treated with 16 mL of petroleum ether (bp 30-60 °C). This afforded 1.58 g (3.7 mmol, 71%) of the *cis* isomer in the form of off-white crystals: mp 198-199 °C; IR (CCl<sub>4</sub>) 2260 cm<sup>-1</sup> (CN), 1720 cm<sup>-1</sup> (C=O); <sup>1</sup>H NMR (CDCl<sub>3</sub>) δ 6.8-7.5 (m, 20 H);



2.17 (s, 3 H); mass spectrum,  $m/z$  425 ( $M^+$ ). Anal. Calcd for  $C_{31}H_{23}NO$ : C, 87.50; H, 5.45; N, 3.29. Found: C, 87.44; H, 5.70; N, 3.30.

*cis*- (39b) and *trans*-2,3,4,5-tetraphenyl-4-methoxy-2-cyclopenten-1-one (40b). Into a 250-mL three-necked flask equipped with a magnetic stirring bar and nitrogen inlet were placed 2.0 g (5.2 mmol) of tetracyclone(1), 60 mL of benzene, and 60 mL of  $Me_2SO$ . To this solution was added 4 mL of a 40% solution of benzyltrimethylammonium hydroxide in methanol (Triton B). The resulting red solution of the enolate 38b was stirred at 27 °C for 50 min followed by the addition of 5 mL of concentrated HCl. The contents of the flask were transferred to a separatory funnel containing 50 mL of water; the benzene layer was separated, washed twice with 50-mL portions of water and dried over anhydrous magnesium sulfate. Removal of the solvent on a rotary evaporator afforded a pink oil which was dissolved in 10 mL of hot benzene and treated with 20 mL of petroleum ether (bp 30-60 °C). Within 1 hr at room temperature the *cis* isomer (39b) began crystallizing in the form of fine white needles, and after 2 hrs the crystals were filtered and washed with cold petroleum ether to afford 0.91 g (2.18 mmol, 42%) of the *cis* isomer: mp 208-210 °C *dec* (lit.<sup>30</sup> mp 193-203 °C *dec*); IR ( $CCl_4$ ) 1720  $cm^{-1}$  (C=O);  $^1H$  NMR ( $CDCl_3$ )  $\delta$  6.8-7.8 (m, 20 H), 4.63 (s, 1 H), 3.35 (s, 3 H); mass spectrum,  $m/z$  416 ( $M^+$ ). Anal. Calcd for  $C_{30}H_{24}O_2$ : C, 86.51; H, 5.81. Found: C, 86.51; H, 5.99.

Allowing the mother liquor to stand overnight at room temperature afforded white salt-like crystals which were filtered and washed with cold petroleum ether affording 0.23 g (0.55 mmol, 11%) of the *trans* isomer (40b): mp 126-130 °C *dec*; IR ( $CCl_4$ ) 1720  $cm^{-1}$  (C=O);  $^1H$  NMR ( $CDCl_3$ )  $\delta$  6.8-7.8 (m, 20 H), 4.27 (s, 1 H), 3.07 (s, 3 H); mass spectrum,  $m/z$  416 ( $M^+$ ). Anal. Calcd for  $C_{30}H_{24}O_2$ : C, 86.51; H, 5.81. Found: C, 86.62; H, 6.04.

**1,3-Dimethoxy-1,2,4,5-tetraphenyl-2,4-cyclopentadiene (42).** Into a 250-mL three-necked flask equipped with a magnetic stirring bar and nitrogen inlet were placed 2.0 g (5.2 mmol) of tetracyclone (1), 60 mL of benzene, and 60 mL of  $Me_2SO$ . To this solution was added 4 mL of a 40% solution of benzyltrimethylammonium hydroxide in methanol (Triton B). The resulting red solution of the enolate 38b was stirred at 27 °C for 50 min followed by the addition of 2 mL of methyl iodide. The resulting solution was stirred at room temperature for an additional 45 min then

transferred to a separatory funnel containing 50 mL of water. The benzene layer was separated, washed twice with 50 mL-portions of water, and dried over anhydrous magnesium sulfate. Removal of the solvent on a rotary evaporator afforded a dark red oil which was dissolved in 20 mL of absolute ethanol. The crystals obtained were filtered and washed with cold 95% ethanol affording 1.77 g (4.1 mmol, 79%) of slightly impure material which upon recrystallization from absolute ethanol produced the analytically pure compound in the form of dazzling yellow needles: mp 160-161 °C; IR (CCl<sub>4</sub>) 1650 cm<sup>-1</sup> (C = COCH<sub>3</sub>), 1085 cm<sup>-1</sup> (COC); <sup>1</sup>H NMR (CDCl<sub>3</sub>) δ 6.9-7.6 (m, 20 H), 3.51 (s, 3 H), 3.32 (s, 3 H); mass spectrum, *m/z* 430 (M<sup>+</sup>). Anal. Calcd for C<sub>31</sub>H<sub>26</sub>O<sub>2</sub>: C, 86.48; H, 6.09. Found: C, 86.31; H, 6.23.

**Tables XXX + XXXI.** The data reported in the tables were obtained using the following procedures:

**Formation of Enolate 38a.** Into a 25-mL three-necked flask equipped with a magnetic stirring bar and nitrogen inlet were placed 100 mg of tetracyclone (1), 25 mg of potassium cyanide, 7.5 mL of benzene, and 7.5 mL of Me<sub>2</sub>SO (or 15 mL of N,N-dimethylformamide) and the reaction was stirred at 27 °C for 3 hrs.

**Formation of Enolate 38b.** Into a 25-mL three-necked flask equipped with a magnetic stirring bar and nitrogen inlet were placed 100 mg of tetracyclone (1), 7.5 mL of benzene and 7.5 mL of Me<sub>2</sub>SO. To this solution was added 0.2 mL of 1.2 M potassium methoxide in methanol and the resulting solution was stirred at 27 °C for 15 min.

**Kinetic Protonation of Enolates 38a and 38b.** Approximately 5 min prior to protonation, the temperature of the flask containing the enolate was adjusted to the desired level (0 °C by using an ice-water bath or 90 °C by refluxing the solvent) and at this point, 5 drops of concentrated HCl were rapidly added. The contents of the flask were then transferred to a separatory funnel containing 10 mL of benzene and 10 mL of water; the benzene layer was separated, washed twice with 20-mL portions of water, and dried over anhydrous magnesium sulfate. Removal of the solvent on a rotary evaporator afforded a yellow oil which was dissolved entirely in CDCl<sub>3</sub> and analyzed by <sup>1</sup>H NMR. The *cis-trans* ratios were determined by proton integration and recorded in Table XXX.

**Equilibration of Isomers 5 and 6.** Into a 25-mL three-necked flask equipped with a magnetic stirring bar were placed 100 mg of the starting isomer (either **5** or **6**), 7.5 mL of benzene, and 7.5 mL of Me<sub>2</sub>SO. Once the sample had dissolved (ca. 5 min), the particular mode isomerization mode was employed: (a) Base (for **39a** and **40a**). One drop of a saturated solution of potassium cyanide in Me<sub>2</sub>SO was added to the above mixture, the solution was stirred at 27 °C for the amount of time indicated in Table XXXI, then transferred to a separatory funnel containing 10 mL of benzene and 10 mL of water. The benzene layer was separated, washed twice with 20-mL portions of water, and dried over anhydrous magnesium sulfate. Removal of the solvent on a rotary evaporator afforded a yellow oil which was dissolved entirely in CDCl<sub>3</sub> and analyzed by <sup>1</sup>H NMR. The *cis-trans* ratios were determined by proton integration and recorded in Table XXXI. (b) Base (for **39b** and **40b**). One drop of a base solution, prepared by adding 5 drops of Triton B to 1 mL of Me<sub>2</sub>SO, was added to the above solution to be equilibrated and the solution was stirred at 27 °C for 2 hr, then transferred to a separatory funnel containing 10 mL of benzene and 10 mL of water. The benzene layer was separated, washed twice with 20-mL portions of water, and dried over anhydrous magnesium sulfate. Removal of the solvent on a rotary evaporator afforded a yellow oil which was dissolved entirely in CDCl<sub>3</sub> and analyzed by <sup>1</sup>H NMR. The *cis-trans* ratios were determined by proton integration and recorded in Table XXXI. (c) Acid. Three drops of concentrated HCl were added to the solution to be equilibrated and the solution was stirred at the temperature and the time indicated in Table XXXI. The solution was then transferred to a separatory funnel containing 10 mL of benzene and 10 mL of water. The benzene layer was separated, washed twice with 20-mL portions of water, and dried over anhydrous magnesium sulfate. Removal of the solvent on a rotary evaporator afforded a yellow oil which was dissolved entirely in CDCl<sub>3</sub> and analyzed by <sup>1</sup>H NMR. The *cis-trans* ratios were determined by proton integration and recorded in Table XXXI. (d) Thermal. The solution to be equilibrated was refluxed (ca. 90 °C) for the time specified in Table XXXI. The solution was then transferred to a separatory funnel containing 10 mL of benzene and 10 mL of water. The benzene layer was separated, washed twice with 20-mL portions of water, and dried over anhydrous magnesium sulfate. Removal of the solvent on a rotary evaporator afforded a yellow oil which was dissolved entirely in CDCl<sub>3</sub> and

analyzed by  $^1\text{H}$  NMR. The *cis-trans* ratios were determined by proton integration and recorded in Table XXXI.

### ***Reactions with sodium azide***

**7-Substituted-1,5,8-triphenyl-2,3,4-triazabicyclo [3.3.0] octa-2,7-dien-6-one (45a, R = Ph; 45b, R = Me).** Into a 250-mL round bottom flask equipped with a magnetic stirring bar were placed 2.6 mmol of the cyclopentadienone (1.0 g of **1**, 0.84 g of **43**), 1.2 g ( 18.5 mmol) of sodium azide, 75 mL of N,N-dimethylformamide (DMF), and 0.3 mL of concentrated  $\text{H}_2\text{SO}_4$ . The mixture was gradually heated to  $80\text{ }^\circ\text{C}$  during which time the color changed from dark purple (**1**) or dark reddish-brown (**43**) to a cloudy white or light yellow color (ca. 25 min for **1**, 35 min for **43**). At this time, 60 mL of benzene was added to the flask. The solution was cooled in an ice-water bath then transferred to a separatory funnel containing 75 mL of water. The benzene layer was immediately separated and dried over anhydrous magnesium sulfate. The benzene was removed on a rotary evaporator and the residual DMF was removed under vacuum. The resulting off-white residue was dissolved in 75 mL of hot benzene followed by the addition of 85 mL of petroleum ether (bp  $30\text{-}60\text{ }^\circ\text{C}$  ). This afforded 1.0 g (2.34 mmol, 90%) of **45a** or 0.77 g (2.39 mmol, 92%) of **45b** in the form of white cotton-like fibers. **45a**: mp  $183\text{-}184\text{ }^\circ\text{C}$  (dec); IR ( $\text{CHCl}_3$ )  $3455\text{ cm}^{-1}$  (N-H),  $1725\text{ cm}^{-1}$  (C=O);  $^1\text{H}$  NMR ( $\text{CDCl}_3$ )  $\delta$  8.8 (s, 1 H), 6.8-8.2 (m, 20 H); mass spectrum, *m/z* 399 ( $\text{M}^+ - 28$ ). Anal. Calcd for  $\text{C}_{29}\text{H}_{21}\text{N}_3\text{O}$ : C, 81.48; H, 4.95; N, 9.83. Found: C, 81.53; H, 5.13; N, 9.44. **45b**: mp  $183.5\text{-}184\text{ }^\circ\text{C}$  (dec); IR ( $\text{CDCl}_3$ )  $3470\text{ cm}^{-1}$  (N-H),  $1730\text{ cm}^{-1}$  (C=O);  $^1\text{H}$  NMR ( $\text{CDCl}_3$ )  $\delta$  8.7 (s, 1 H), 6.6-7.9 (m, 15 H), 2.2 (s, 3 H); mass spectrum, *m/z* 337 ( $\text{M}^+ - 28$ ). Anal. Calcd for  $\text{C}_{24}\text{H}_{19}\text{N}_3\text{O}$ : C, 78.88; H, 5.24; N, 11.50. Found: C, 79.11; H, 5.44; N, 11.41.

**3-Substituted-4,5,6-triphenyl-2(1H)-pyridinone (44a, R = Ph; 44b, R = Me).** From **1** or **43**. Into a 250-mL round-bottom flask equipped with a magnetic stirring bar and reflux condenser were placed 2.6 mmol of the cyclopentadienone (1.0 g of **1**, 0.84 g of **43**), 1.2 g ( 18.5 mmol) of sodium azide, 75 mL of N,N-dimethylformamide (DMF), and 0.3 mL of concentrated  $\text{H}_2\text{SO}_4$ . The mixture

was gradually heated to 80 °C during which time the color changed from dark purple (1) or dark reddish-brown (43) to a cloudy white or light yellow color (ca. 25 min for 1, 35 min for 43). At this time, 50 mL of glacial acetic acid was then added to the flask and the solution was refluxed for 15 min. The solution was then transferred to a 500-mL Erlenmeyer flask and 200 mL of water was added. After cooling to room temperature, the flask was placed in an ice-water bath. Suction filtration followed by washing with 15 mL of cold absolute ethanol afforded 0.94 g (2.34 mmol, 90%) of **44a** or 0.61 g (1.81 mmol, 70%) of **44b** in the form of a white powder. **44a**: mp 272-273 °C (lit. mp 271-273 °C<sup>38</sup> ; 262-267 °C<sup>39</sup> ; 273-275 °C<sup>40</sup> ; 264-267 °C<sup>41</sup> ); IR (CDCl<sub>3</sub>) 3455 cm<sup>-1</sup> (N-H), 1650 cm<sup>-1</sup> (C=O); <sup>1</sup>H NMR (CDCl<sub>3</sub>) δ 11.6 (br s, 1 H), 6.5-7.5 (m, 20 H); mass spectrum, *m/z* 399 (M<sup>+</sup>). Anal. Calcd for C<sub>29</sub>H<sub>21</sub>NO: C, 87.19; H, 5.30; N, 3.51. Found: C, 87.26; H, 5.52; N, 3.23. **44b**: mp 297-299 °C ; IR (CDCl<sub>3</sub>) 3440 cm<sup>-1</sup> (N-H), 1650 cm<sup>-1</sup> (C=O); <sup>1</sup>H NMR (CDCl<sub>3</sub>) δ 10.5 (br s, 1 H), 6.6-7.4 (m, 15 H), 1.98 (s, 3 H); mass spectrum, *m/z* 337 (M<sup>+</sup>). Anal. Calcd for C<sub>24</sub>H<sub>19</sub>NO: C, 85.43; H, 5.68; N, 4.15. Found: C, 85.46; H, 5.77; N, 4.11.

**3-Substituted-4,5,6-triphenyl-2(1H)-pyridinone (44a, R = Ph; 44b, R = Me). From 45.** Into a 50-mL round bottom flask equipped with a magnetic stirring bar and reflux condenser were placed 1.2 mmol of **45** (0.51 g of **45a**, 0.44 g of **45b**) and 25 mL of glacial acetic acid. At this time, 0.1 mL of concentrated H<sub>2</sub>SO<sub>4</sub> was slowly added at room temperature. The resulting yellow solution was refluxed for 20 min, cooled slightly and then transferred to a 250-mL Erlenmeyer flask. Upon addition of 100 mL of water, the flask was placed in an ice-water bath. Suction filtration followed by washing with 20 mL of cold absolute ethanol afforded 0.39 g (0.98 mmol, 82%) of **44a** or 0.31 g (0.92 mmol, 77%) of **44b** in the form of a white powder. Both compounds were identical to the pyridinones described above.

**2-Methoxy-3,4,5,6-tetraphenylpyridine (46a) and 1-Methyl-3,4,5,6-tetraphenyl-2(1H)-pyridinone (47a).** From **44a**. Into a 250-mL round bottom flask equipped with a magnetic stirring bar were placed 1.16 g (2.9 mmol) of **44a**, 100 mL of DMF and 0.5 g (4.5 mmol) potassium *tert*-butoxide. The solution was stirred for 5 min at room temperature then placed in an ice-water bath for an additional 10 min. To the light yellow solution was added 1 mL (2.3 g, 16 mmol) of methyl iodide. The resulting colorless solution was stirred for 10 min followed by the addition of

75 mL of benzene then transferred to a separatory funnel containing 100 mL of water. The benzene layer was washed three times with 100-mL portions of water and dried over anhydrous magnesium sulfate. Removal of the solvent on a rotary evaporator afforded an oil which was redissolved in 8 mL of hot benzene and treated with 15 mL of petroleum ether (bp 30-60 °C). This resulted in 0.83 g (2.0 mmol, 69%) of white crystals which contained 92% of the N-methyl derivative according to <sup>1</sup>H NMR integration. Recrystallization from benzene/petroleum ether (1/2) afforded the pure N-methyl-pyridinone **47a**: mp 230-232 °C (lit.<sup>42</sup> mp 232-234 °C) ; IR (CDCl<sub>3</sub>) 1645 cm<sup>-1</sup> (C=O); <sup>1</sup>H NMR (CDCl<sub>3</sub>) δ 6.4-7.5 (m, 20 H), 3.38 (s, 3 H); mass spectrum, *m/z* 413 (M<sup>+</sup>). Anal. Calcd for C<sub>30</sub>H<sub>23</sub>NO : C, 87.14; H, 5.61; N, 3.39. Found: C, 87.36; H, 5.80; N, 3.23. Evaporation of the original mother liquor afforded 0.25 g (0.60 mmol, 21%) of white crystals containing 85% of the O-methyl isomer (<sup>1</sup>H NMR integration). Recrystallization from benzene/petroleum ether (1/2) produced the pure methoxypyridine **46a**: mp 196.5-197.5 °C; IR (CDCl<sub>3</sub>) 1245 cm<sup>-1</sup> and 1030 cm<sup>-1</sup> (C-O-C); <sup>1</sup>H NMR (CDCl<sub>3</sub>) δ 6.5-7.5 (m, 20 H), 3.98 (s, 3 H); mass spectrum, *m/z* 413 (M<sup>+</sup>). Anal. Calcd for C<sub>30</sub>H<sub>23</sub>NO : C, 87.14; H, 5.61; N, 3.39. Found: C, 87.22; H, 5.74; N, 3.32.

**2-Methoxy-3-methyl-4,5,6-triphenylpyridine (46b) and 1,3-Dimethyl-4,5,6-triphenyl-2(1H)-pyridinone (47b).** From **44b**. Into a 50-mL round bottom flask equipped with a magnetic stirring bar were placed 0.67 g (2.0 mmol) of **44b**, 35 mL of DMF and 0.3 g (2.7 mmol) of potassium *tert*-butoxide. The solution was stirred for 10 min at room temperature then placed in an ice-water bath for an additional 10 min. To the pale yellow solution was added 1 mL (2.3 g, 16 mmol) of methyl iodide. The resulting colorless solution was stirred for 10 min followed by the addition of 50 mL of benzene. The contents of the flask were transferred to a separatory funnel containing 50 mL of water. The benzene layer was washed three times with 50-mL portions of water and dried over anhydrous magnesium sulfate. Removal of the solvent on a rotary evaporator afforded a white solid which contained 75% of the N-methyl derivative and 25% of the O-methyl isomer (<sup>1</sup>H NMR integration). The solid was redissolved in 6 mL of hot benzene then treated with 12 mL of petroleum ether (bp 30-60 °C). This afforded 0.39 g (1.1 mmol, 55%) of **47b** in the form of white crystals: mp 221-223 °C ; IR (CDCl<sub>3</sub>) 1645 cm<sup>-1</sup> (C=O); <sup>1</sup>H NMR (CDCl<sub>3</sub>) δ 6.4-7.4 (m, 15 H), 3.37 (s, 3 H), 2.06 (s, 3 H); mass spectrum, *m/z* 351 (M<sup>+</sup>). Anal. Calcd for C<sub>25</sub>H<sub>21</sub>NO: C,

85.44; H, 6.02; N, 3.99. Found: C, 85.76; H, 6.19; N, 3.97. Evaporation of the mother liquor afforded a solid which was recrystallized from absolute ethanol to yield 0.07 g (0.2 mmol, 10%) of **46b** in the form of clear crystals: mp 156-157 °C; IR (CDCl<sub>3</sub>) 1255 and 1035 cm<sup>-1</sup> (C-O-C); <sup>1</sup>H NMR (CDCl<sub>3</sub>) δ 6.5-7.4 (m, 15 H), 4.07 (s, 3 H), 2.03 (s, 3 H); mass spectrum, *m/z* 351 (M<sup>+</sup>). Anal. Calcd for C<sub>25</sub>H<sub>21</sub>NO: C, 85.44; H, 6.02; N, 3.99. Found: C, 85.40; H, 6.16; N, 3.93.

**3,4,5,6-Tetraphenyl-2(1H)-pyridinone (44a) and 2-Methoxy-3,4,5,6-tetraphenylpyridine (46a).**

**From 45a.** Into a 100-mL three-necked flask equipped with a magnetic stirring bar, reflux condenser and fritted-glass gas inlet tube were placed 0.86 g (2.0 mmol) of **45a** and 50 mL of anhydrous methanol. The flask was gently warmed (ca. 40 °C) and HCl gas (generated in a second flask by the addition of H<sub>2</sub>SO<sub>4</sub> to NaCl) was bubbled into the solution for 10 min. After refluxing for 30 min the solvent was removed on a rotary evaporator. The residue was redissolved in 20 mL of hot benzene and treated with 25 mL of petroleum ether (bp 30-60 °C). This afforded 0.54 g (1.4 mmol, 70%) of **44a** in the form of a white powder. This compound was identical in all respect to the tetraphenylpyridinone described above. The mother liquor was removed on a rotary evaporator and the residue was recrystallized in 10 mL of methanol. Cooling to 0 °C afforded 0.14 g (0.34 mmol, 17%) of **46a** in the form of white crystals which was identical in all respects to the 2-methoxytetraphenylpyridine described above.

**3-Methyl-4,5,6-triphenyl-2(1H)-pyridinone (44b) and 2-Methoxy-3-methyl-4,5,6-triphenylpyridine (46b).** **From 45b.** Into a 100-mL three-necked flask equipped with a magnetic stirring bar, reflux condenser and fritted-glass gas inlet tube were placed 1.0 g (2.7 mmol) of **45b** and 50 mL of anhydrous methanol. The flask was gently warmed (ca. 50 °C) and HCl gas (generated in a second flask by the addition of H<sub>2</sub>SO<sub>4</sub> to NaCl) was bubbled into the solution for 20 min. After refluxing for 10 additional min, 50 mL of benzene was added and the contents of the flask were transferred to a separatory funnel containing 200 mL of water and 150 mL of benzene. The benzene layer was washed once with 200 mL of water and dried over anhydrous magnesium sulfate. Removal of the solvent on a rotary evaporator afforded a pale yellow solid which contained about 65% of the pyridinone **44b** and 35% of the methoxypyridine **46b** (<sup>1</sup>H NMR integration). Dissolution of the crude material in 60 mL of hot benzene and addition of 65 mL of petroleum ether (bp

30-60 °C) followed by suction filtration afforded 0.51 g (1.5 mmol, 56%) of **44b** in the form of white crystals. This compound was identical in all respects to the methyltriphenylpyridinone described above. Evaporation of the mother liquor afforded an oil which was recrystallized from absolute ethanol to yield 0.20 g (0.57 mmol, 21%) of **46b** in the form of white crystals which were identical in all respects to the methoxypyridine described above.

**7-substituted-4-methyl-1,5,8-triphenyl-2,3,4-triazabicyclo [3.3.0] octa-2,7-dien-6-one (48a, R = Ph; 48b, R = Me).** Into a 100-mL round bottom flask equipped with a magnetic stirring bar were placed 2.2 mmol of **45** (0.94 g of **45a** or 0.80 g of **45b**), 35 mL of benzene and 35 mL of dimethyl sulfoxide (DMSO). After the solid had dissolved, 1 mL (2.3 g, 16 mmol) of methyl iodide was added and the solution was stirred for 5-10 min. At this time, 0.4 g (3.6 mmol) of potassium *tert*-butoxide was added to the flask. The solution was stirred for 45 min then transferred to a separatory funnel containing 50 mL of water. The benzene layer was separated, washed twice with 50-mL portions of water and dried over anhydrous sulfate. Removal of the solvent on a rotary evaporator afforded a pale yellow residue which was redissolved in 50 mL of hot benzene and treated with 60 mL of petroleum ether (bp 30-60 °C). Suction filtration resulted in recovery of unreacted starting material **45** (**45a**, 0.43 g, 1.0 mmol, 45%; **45b**, 0.44 g, 1.2 mmol, 55%). Evaporation of the mother liquor on a rotary evaporator afforded an off-white residue which was recrystallized from methanol to produce the desired N-methyl derivative **48**. **48a** (0.34 g, 0.77 mmol, 35%): mp 186-187 °C (dec); IR (CDCl<sub>3</sub>) 1720 cm<sup>-1</sup> (C=O); <sup>1</sup>H NMR (CDCl<sub>3</sub>) δ 6.5-7.8 (m, 20 H), 3.34 (s, 3 H); <sup>13</sup>C NMR (CDCl<sub>3</sub>) δ 199.3 (C=O), 33.3 (CH<sub>3</sub>); mass spectrum, *m/z* 413 (M<sup>+</sup>-28). Anal. Calcd for C<sub>30</sub>H<sub>23</sub>N<sub>3</sub>O: C, 81.61; H, 5.25; N, 9.52. Found: C, 81.47; H, 5.40; N, 9.28. **48b** (0.28 g, 0.74 mmol, 34%): mp 185-187 °C (dec); IR (CDCl<sub>3</sub>) 1725 cm<sup>-1</sup> (C=O); <sup>1</sup>H NMR (CDCl<sub>3</sub>) δ 6.6-7.9 (m, 15 H), 3.33 (s, 3 H), 2.18 (s, 3 H); mass spectrum, *m/z* 351 (M<sup>+</sup>-28). Anal. Calcd for C<sub>25</sub>H<sub>21</sub>N<sub>3</sub>O: C, 79.13; H, 5.58; N, 11.07. Found: C, 79.01; H, 5.60; N, 10.65.

**3-substituted-1-methyl-4,5,6-triphenyl-2(1H)-pyridinone (47a, R = Ph; 47b, R = Me).** From **6**. Into a 100-mL three-necked flask equipped with a magnetic stirring bar, reflux condenser and a fritted-glass gas inlet tube were placed 0.55 mmol of **6** (0.24 g of **48a**, 0.21 g of **48b**) and 60 mL of anhydrous methanol. The flask was gently warmed (ca. 50 °C) and HCl gas (generated in a



second flask by the addition of H<sub>2</sub>SO<sub>4</sub> to NaCl) was bubbled into the solution for 50 min. After refluxing for an additional hour, the solvent was removed on a rotary evaporator. The residue was redissolved in 30 mL of benzene, placed in a separatory funnel, washed three times with 25-mL portions of water and dried over anhydrous magnesium sulfate. Removal of the benzene on a rotary evaporator afforded a white solid which was recrystallized from 3 mL of hot benzene and 8 mL of petroleum ether (bp 30-60 °C). This afforded 0.18 g (0.44 mmol, 80%) of **47a** or 0.14 g (0.40 mmol, 73%) of **47b** in the form of white crystals. Both compounds were identical in all respects to the N-methylpyridinines described above.

### Crystallographic Analysis

Crystals of **40a** formed in symmetry space group  $P\bar{1}$  with  $a = 14.428(3)$  Å,  $b = 15.954(1)$  Å,  $c = 10.609(4)$  Å,  $\alpha = 104.40(2)^\circ$ ,  $\beta = 109.48(2)^\circ$ , and  $\gamma = 84.16(1)^\circ$  for  $Z = 4$ . An automatic four circle diffractometer equipped with Cu radiation ( $\lambda$  1.5418 Å) was used for data collection. Of the 6021 reflections measured with  $2\theta \leq 114^\circ$ , 4970 were observed and corrected for Lorentz and polarization effects. A multi-solution tangent formula approach with recycling of initially found fragments gave positions for a majority of the non-hydrogen atoms. The function  $\sum \omega(|F_o| - |F_c|)^2$  with  $\omega = (1/\sigma F_o)^2$  was minimized to give an unweighted residual of 0.045. Figure 54 is a perspective drawing showing one of the independent molecules of **40a**; the other molecule has essentially the same conformation. There are no close intermolecular contacts. The phenyl groups at C2 and C3 in Figure 54 are trans to one another and, because of crowding, the five-membered rings are somewhat distorted from planarity.

Suitable crystals of **41** for X-ray diffraction studies were formed from an ethyl alcohol solution. The space groups symmetry was  $P2_1/c$  with  $a = 8.983(1)$  Å,  $b = 16.254(2)$  Å,  $c = 15.988(2)$  Å, and  $\beta = 98.22(1)^\circ$  for  $Z = 4$ . Of the 3105 reflections measured with an automatic four circle diffractometer equipped with Cu radiation, 2199 were observed ( $I > 3\sigma I$ ). The structure was solved with a multi-solution tangent formula approach and difference Fourier analysis and refined

with full-matrix least-squares techniques. Hydrogens were assigned isotropic temperature factors corresponding to their attached atoms. The function  $\sum \omega(|F_o| - |F_c|)^2$  with  $\omega = (1/\sigma F_o)^2$  was minimized to give an unweighted residual of 0.039. Figure 55 is a perspective drawing showing one of the independent molecules of **41**; the other molecule has essentially the same conformation. Appendix L-Q contains the fractional coordinates, bond distances and bond angles for **40a** and **41**.

Suitable crystals of **45b** ( $C_{19}H_{24}N_3O$ ) for X-ray diffraction studies were formed from acetone and have a space group symmetry of  $P2_1$  and cell constants of  $a = 11.936(2)$  Å,  $b = 6.795(3)$  Å,  $c = 12.005(2)$  Å, and  $\beta = 99.92(1)^\circ$  for  $Z = 2$ . and a calculated density of 1.265 g/cm<sup>3</sup>. Of the 1413 reflections measured with an automatic four circle diffractometer equipped with Cu radiation, 1342 were observed ( $I \geq 3\sigma I$ ). The structure was solved with a multi-solution tangent formula approach and difference Fourier analysis and refined using full-matrix least-squares techniques. Hydrogens were assigned isotropic temperature factors corresponding to their attached atoms. The function  $\sum \omega(|F_o| - |F_c|)^2$  with  $\omega = (1/\sigma F_o)^2$  was minimized to give an unweighted residual of 0.037. No abnormally short intermolecular contacts were noted. Appendix R-T contains the final fractional coordinates, bond distances and bond angles. Figure 56 is a computer generated perspective drawing of **45b** from the final X-ray coordinates showing the relative stereochemistry.

## Literature Cited

1. Youssef, A.K.; Ogliaruso, M.A. *J. Org. Chem.* **1972**, *37*, 2601.
2. Oldaker, G.B.; Perfetti, T.A.; Ogliaruso, M.A. *J. Org. Chem.* **1980**, *45*, 3910.
3. Brubaker, W.F.; Ph.D. Dissertation, Virginia Polytechnic Institute & State University, 1982.
4. Allen, C.F.H.; VanAllan, J.A. *J. Am. Chem. Soc.* **1943**, *65*, 1384.
5. Dufraisse, C.; Rio, G.; Ranjon, A. *C. R. Acad. Sci.* **1961**, 253, 244.
6. Woodward, R.B.; Hoffmann, R. "The Conservation of Orbital Symmetry"; Academic Press Inc.: New York, 1970.
7. March, J. "Advanced Organic Chemistry", 2<sup>nd</sup> Ed., McGraw-Hill, Inc.: New York, 1977, pp. 1037-1045.
8. Gilchrist, T.L.; Stork, R.C. "Organic Reactions and Orbital Symmetry"; Cambridge University Press: London, 1972, p. 204.
9. Carey, F.A.; Sundberg, R.J. "Advanced Organic Chemistry", Part A; Plenum Press: New York, 1977, p. 425.
10. Morrison, R.T.; Boyd, R.N. "Organic Chemistry", 3<sup>rd</sup> Ed., Allyn and Bacon, Inc.: Boston, 1973, p. 955.
11. Youssef, A.K.; Ogliaruso, M.A. *J. Org. Chem.* **1973**, *38*, 487.
12. Miller, L.L.; Greisinger, R.; Boyer, R.F. *J. Am. Chem. Soc.* **1969**, *91*, 1578.
13. McLean, S.; Haynes, P. *Tetrahedron* **1965**, *21*, 2329.
14. Breslow, R.; Hoffman, J.H.; Perchonock, C. *Tetrahedron Lett.* **1973**, 3723.
15. Schembelov, G.A.; Ustynuk, Y.A. *J. Am. Chem. Soc.* **1974**, *96*, 4189.
16. Youssef, A.K.; Ph.D. Dissertation, Virginia Polytechnic Institute & State University, 1973.
17. Berg, R.G.; Ogliaruso, M.A.; McNair, H.M. *J. Chromatographic Sci.* **1975**, *13*, 69.

18. Davis, D.M.; Ph.D. Dissertation, Virginia Polytechnic Institute & State University, 1985.
19. Lowery, T.H.; Richardson, K.T. "Mechanism and Theory in Organic Chemistry", 2<sup>nd</sup> Ed.; Harper & Row, Publishers: New York, 1981, p. 280.
20. Cutshaw, R.C.; Ph.D. Dissertation, Virginia Polytechnic Institute & State University, 1980.
21. Youssef, A.K.; Ogliaruso, M.A. *J. Org. Chem.* **1973**, *38*, 3998.
22. Beak, P.; Yamamoto, J.; Upton, C.J. *J. Org. Chem.* **1975**, *40*, 3053.
23. Daniels, F.; Alberty, R.A. "Physical Chemistry", 4<sup>th</sup> Ed., John Wiley & Sons, Inc.: New York, 1975, pp. 300-322.
24. Field, P.E. "Physical Methods in Chemistry", Virginia Polytechnic Institute & State University: Blacksburg, Va, 1978, pp 1-6.
25. Nebergall, W.H.; Schmidt, F.C.; Holtzclaw, H.F., Jr. "College Chemistry", 5<sup>th</sup> Ed., D.C. Heath and Company: Lexington, MA, 1976, p. 89.
26. Daniels, F.; Alberty, R.A. "Physical Chemistry", 4<sup>th</sup> Ed., John Wiley & Sons, Inc.: New York, 1975, p. 57.
27. Eagan, R.L.; Ogliaruso, M.A.; Arison, B.H.; Springer, J.P. *J. Org. Chem.* **1984**, *49*, 4248.
28. Silverstein, R.M.; Bassler, G.C.; Morrill, T.C. "Spectrometric Identification of Organic Compounds", 4<sup>th</sup> Ed., John Wiley & Sons, Inc.: New York, 1981, pp. 184-189.
29. X-ray crystallographic analyzes were performed by Dr. James P. Springer at Merck, Sharp and Dohme Research Laboratories, Rahway, NJ.
30. Muckenstrum, B. *Tetrahedron* **1975**, *31*, 1933.
31. Eagan, R.L.; Ogliaruso, M.A.; Springer, J.P. *J. Org. Chem.* **1986**, *51*, 1544.
32. March, J. "Advanced Organic Chemistry"; McGraw-Hill, Inc.: New York, 1977; pp 1006-1008.
33. For a review, see: Biffin, Miller, and Paul in "The Chemistry of the Azido Group", Patai, E., Ed., Interscience Publishers: New York, 1971; pp 122-130.
34. For a review, see: Povarov *Russ. Chem. Rev.* **1965**, *34*, 639-656.
35. Gordon, A.J.; Ford, R.A. "The Chemist's Companion"; John Wiley and Sons: New York, 1972; pp 430-436.
36. Johnson, J.R.; Grummitt, O. *Organic Syntheses*; Wiley: New York, 1953; Collect. Vol. III, p 806.
37. Allen, C.F.H.; VanAllan, J.A. *J. Am. Chem. Soc.* **1950**, *72*, 5165.
38. Wajon, J.F.M.; Arens, J.F. *Recl. Trav. Chim. Pays-Bas* **1957**, *76*, 65.
39. Jagt, J.C.; Van Leusen, A.M. *Recl. Trav. Chim. Pays-Bas* **1973**, *92*, 1343.
40. Abramovitch, R.A.; Knaus, G.N. *J. Org. Chem.* **1975**, *40*, 883.
41. Martin, D.; Bauer, M. *Z. Chem.* **1980**, *20*, 53.
42. Hons, P.; Yamazaki, H. *Synthesis* **1977**, 50.

## Appendix

### A: Derivation of the rate constant (k) for a first-order reaction

$$-\frac{d[A]}{dt} = k[A]$$

$$-\frac{d[A]}{[A]} = k dt$$

$$-\int_{[A]_1}^{[A]_2} \frac{d[A]}{[A]} = k \int_{t_1}^{t_2} dt$$

$$-(\ln[A]_2 - \ln[A]_1) = k(t_2 - t_1)$$

$$\ln[A]_2 - \ln[A]_1 = -k(t_2 - t_1)$$

$$\ln([A]_2 / [A]_1) = -k(t_2 - t_1)$$

If  $t_1 = 0$

$$\ln([A]_2 / [A]_1) = -k t_2$$

$$2.303 \log([A]_2 / [A]_1) = -k t_2$$

$$\log([A]_2 / [A]_1) = -\frac{k}{2.303} t_2$$

$$\log[A]_2 - \log[A]_1 = -\frac{k}{2.303} t_2$$

$$\log[A]_2 = -\frac{k}{2.303} t_2 + \log[A]_1$$

If  $[A]_1 = 100\%$

$$\log[A]_2 = -\frac{k}{2.303} t_2 + \log[100]$$

$$\log[A]_2 = -\frac{k}{2.303} t_2 + 2.00$$

Plotting  $\log[A]_2$  versus  $t_2$

$$\text{slope} = -\frac{k}{2.303}$$

$$k = -2.303 (\text{slope})$$

$$y_{\text{intercept}} = 2.00$$

### B: Derivation of the activation energy ( $E_a$ ) from the Arrhenius equation

$$k = A e^{-E_a/RT}$$

$$\log k = \log A + \log (e^{-E_a/RT})$$

$$\log k = \log A - \frac{E_a}{2.303 R T}$$

Plotting  $\log k$  versus  $\frac{1}{T}$

$$\text{slope} = -\frac{E_a}{2.303 R}$$

$$E_a = -2.303 (R) (\text{slope})$$

$$E_a = -2.303 (1.987 \text{ cal mol}^{-1} \text{ K}^{-1}) (\text{slope})$$

$$E_a = -4.576 \text{ cal mol}^{-1} \text{ K}^{-1} (\text{slope})$$

**C: Derivation of the enthalpy ( $\Delta H^\ddagger$ ) and entropy ( $\Delta S^\ddagger$ ) of activation from the Eyring equation**

$$k = \frac{R T}{N_A h} e^{\Delta S^\ddagger/R} e^{-\Delta H^\ddagger/RT}$$

where

$$R = 1.987 \text{ cal mol}^{-1} \text{ K}^{-1}$$

$$N_A = 6.022 \times 10^{23} \text{ mol}^{-1}$$

$$h = 1.584 \times 10^{-34} \text{ cal sec}$$

thus

$$k = 2.083 \times 10^{10} T e^{\Delta S^\ddagger/R} e^{-\Delta H^\ddagger/RT}$$

$$\frac{k}{T} = 2.083 \times 10^{10} e^{\Delta S^\ddagger/R} e^{-\Delta H^\ddagger/RT}$$

$$\log\left(\frac{k}{T}\right) = \log(2.083 \times 10^{10}) + \log(e^{\Delta S^\ddagger/R}) + \log(e^{-\Delta H^\ddagger/RT})$$

$$\log\left(\frac{k}{T}\right) = 10.32 + \frac{\Delta S^\ddagger}{2.303 R} - \frac{\Delta H^\ddagger}{2.303 R T}$$

Plotting  $\log\left(\frac{k}{T}\right)$  versus  $\frac{1}{T}$

$$\text{slope} = -\frac{\Delta H^\ddagger}{2.303 R}$$

$$\Delta H^\ddagger = -2.303 R (\text{slope})$$

$$\Delta H^\ddagger = -2.303 (1.987 \text{ cal mol}^{-1} \text{ K}^{-1}) (\text{slope})$$

$$\Delta H^\ddagger = -4.576 \text{ cal mol}^{-1} \text{ K}^{-1} (\text{slope})$$

$$y_{\text{intercept}} = \frac{\Delta S^\ddagger}{2.303 R} + 10.32$$

$$\Delta S^\ddagger = 2.303 R (y_{\text{intercept}} - 10.32)$$

$$\Delta S^\ddagger = 2.303 (1.987 \text{ cal mol}^{-1} \text{ K}^{-1}) (y_{\text{intercept}} - 10.32)$$

$$\Delta S^\ddagger = 4.576 \text{ cal mol}^{-1} \text{ K}^{-1} (y_{\text{intercept}} - 10.32)$$

**D: Calculation of the  $E_a$ ,  $\Delta H^\ddagger$  and  $\Delta S^\ddagger$  for the [1,5]-sigmatropic rearrangement of 1,2,3,4,5-pentaphenyl-2,4-cyclopentadien-1-ol (55).**

Temperature		$k$	$1/T$	$\log k$	$\log(k/T)$
$^\circ\text{C}$	$^\circ\text{K}$	$\text{sec}^{-1}$	$^\circ\text{K}^{-1}$		
175.0	448.15	$6.30 \times 10^{-5}$	$2.231 \times 10^{-3}$	-4.201	-6.852
190.0	463.15	$2.07 \times 10^{-4}$	$2.159 \times 10^{-3}$	-3.684	-6.350
205.0	478.15	$5.86 \times 10^{-4}$	$2.091 \times 10^{-3}$	-3.232	-5.912

$E_a$

Plotting  $\log k$  versus  $1/T$

$$\text{slope} = -6.93 \times 10^3$$

$$E_a = -4.576 \text{ cal mol}^{-1} \text{ K}^{-1} \text{ (slope)}$$

$$y_{\text{intercept}} = 11.25$$

$$E_a = 31.7 \pm 1.4 \text{ kcal mol}^{-1}$$

$$\text{corr} = -1.000$$

$\Delta H^\ddagger$  &  $\Delta S^\ddagger$

Plotting  $\log(k/T)$  versus  $1/T$

$$\text{slope} = -6.71 \times 10^3$$

$$\Delta H^\ddagger = -4.576 \text{ cal mol}^{-1} \text{ K}^{-1} \text{ (slope)}$$

$$y_{\text{intercept}} = 8.14$$

$$\Delta H^\ddagger = 30.7 \pm 1.4 \text{ kcal mol}^{-1} \text{ K}^{-1}$$

$$\text{corr} = -1.000$$

$$\Delta S^\ddagger = 4.576 \text{ cal mol}^{-1} \text{ K}^{-1} \text{ (} y_{\text{intercept}} - 10.32 \text{)}$$

$$\Delta S^\ddagger = -10.0 \pm 3.1 \text{ cal mol}^{-1} \text{ K}^{-1}$$



**E: Calculation of the  $E_a$ ,  $\Delta H^\ddagger$  and  $\Delta S^\ddagger$  for the [1,5]-sigmatropic rearrangement of 1-(1-naphthyl)-2,3,4,5-tetraphenyl-2,4-cyclopentadien-1-ol (55).**

Temperature		$k$	$1/T$	$\log k$	$\log(k/T)$
$^\circ\text{C}$	$^\circ\text{K}$	$\text{sec}^{-1}$	$^\circ\text{K}^{-1}$		
205.0	478.15	$6.24 \times 10^{-5}$	$2.091 \times 10^{-3}$	-4.205	-6.884
220.0	493.15	$1.97 \times 10^{-4}$	$2.028 \times 10^{-3}$	-3.706	-6.398
235.0	508.15	$5.37 \times 10^{-4}$	$1.968 \times 10^{-3}$	-3.270	-5.976

**$E_a$**

Plotting  $\log k$  versus  $1/T$

$$\text{slope} = -7.60 \times 10^3$$

$$E_a = -4.576 \text{ cal mol}^{-1} \text{ K}^{-1} \text{ (slope)}$$

$$y_{\text{intercept}} = 11.70$$

$$E_a = 34.8 \pm 1.3 \text{ kcal mol}^{-1}$$

$$\text{corr} = -1.000$$

**$\Delta H^\ddagger$  &  $\Delta S^\ddagger$**

Plotting  $\log(k/T)$  versus  $1/T$

$$\text{slope} = -7.39 \times 10^3$$

$$\Delta H^\ddagger = -4.576 \text{ cal mol}^{-1} \text{ K}^{-1} \text{ (slope)}$$

$$y_{\text{intercept}} = 8.56$$

$$\Delta H^\ddagger = 33.8 \pm 1.4 \text{ kcal mol}^{-1} \text{ K}^{-1}$$

$$\text{corr} = -1.000$$

$$\Delta S^\ddagger = 4.576 \text{ cal mol}^{-1} \text{ K}^{-1} (y_{\text{intercept}} - 10.32)$$

$$\Delta S^\ddagger = -8.0 \pm 3.0 \text{ cal mol}^{-1} \text{ K}^{-1}$$

**F: Calculation of the  $E_a$ ,  $\Delta H^\ddagger$  and  $\Delta S^\ddagger$  for the [1,5]-sigmatropic rearrangement of 1-(2-pyridyl)-2,3,4,5-tetraphenyl-2,4-cyclopentadien-1-ol (55).**

Temperature		$k$	$1/T$		
$^\circ\text{C}$	$^\circ\text{K}$	$\text{sec}^{-1}$	$^\circ\text{K}^{-1}$	$\log k$	$\log(k/T)$
145.0	418.15	$5.78 \times 10^{-5}$	$2.391 \times 10^{-3}$	-4.238	-6.859
160.0	433.15	$1.87 \times 10^{-4}$	$2.309 \times 10^{-3}$	-3.728	-6.365
175.0	448.15	$6.33 \times 10^{-4}$	$2.231 \times 10^{-3}$	-3.199	-5.850

$E_a$

Plotting  $\log k$  versus  $1/T$

$$\text{slope} = -6.49 \times 10^3$$

$$E_a = -4.576 \text{ cal mol}^{-1} \text{ K}^{-1} \text{ (slope)}$$

$$y_{\text{intercept}} = 11.28$$

$$E_a = 29.7 \pm 1.8 \text{ kcal mol}^{-1}$$

$$\text{corr} = -1.000$$

$\Delta H^\ddagger$  &  $\Delta S^\ddagger$

Plotting  $\log(k/T)$  versus  $1/T$

$$\text{slope} = -6.29 \times 10^3$$

$$\Delta H^\ddagger = -4.576 \text{ cal mol}^{-1} \text{ K}^{-1} \text{ (slope)}$$

$$y_{\text{intercept}} = 8.21$$

$$\Delta H^\ddagger = 28.8 \pm 1.8 \text{ kcal mol}^{-1} \text{ K}^{-1}$$

$$\text{corr} = -1.000$$

$$\Delta S^\ddagger = 4.576 \text{ cal mol}^{-1} \text{ K}^{-1} \text{ (} y_{\text{intercept}} - 10.32 \text{)}$$

$$\Delta S^\ddagger = -9.7 \pm 4.2 \text{ cal mol}^{-1} \text{ K}^{-1}$$

**G: Calculation of the  $E_a$ ,  $\Delta H^\ddagger$  and  $\Delta S^\ddagger$  for the [1,5]-sigmatropic rearrangement of 1-(2-furyl)-2,3,4,5-tetraphenyl-2,4-cyclopentadien-1-ol (55).**

Temperature		$k$	$1/T$		
$^\circ\text{C}$	$^\circ\text{K}$	$\text{sec}^{-1}$	$^\circ\text{K}^{-1}$	$\log k$	$\log(k/T)$
175.0	448.15	$4.35 \times 10^{-5}$	$2.231 \times 10^{-3}$	-4.362	-7.013
190.0	463.15	$1.49 \times 10^{-4}$	$2.159 \times 10^{-3}$	-3.827	-6.493
205.0	478.15	$4.60 \times 10^{-4}$	$2.091 \times 10^{-3}$	-3.337	-6.017

**$E_a$**

Plotting  $\log k$  versus  $1/T$

$$\text{slope} = -7.32 \times 10^3$$

$$E_a = -4.576 \text{ cal mol}^{-1} \text{ K}^{-1} \text{ (slope)}$$

$$y_{\text{intercept}} = 11.98$$

$$E_a = 33.5 \pm 1.6 \text{ kcal mol}^{-1}$$

$$\text{corr} = -1.000$$

**$\Delta H^\ddagger$  &  $\Delta S^\ddagger$**

Plotting  $\log(k/T)$  versus  $1/T$

$$\text{slope} = -7.12 \times 10^3$$

$$\Delta H^\ddagger = -4.576 \text{ cal mol}^{-1} \text{ K}^{-1} \text{ (slope)}$$

$$y_{\text{intercept}} = 8.86$$

$$\Delta H^\ddagger = 32.6 \pm 1.6 \text{ kcal mol}^{-1} \text{ K}^{-1}$$

$$\text{corr} = -1.000$$

$$\Delta S^\ddagger = 4.576 \text{ cal mol}^{-1} \text{ K}^{-1} (y_{\text{intercept}} - 10.32)$$

$$\Delta S^\ddagger = -6.7 \pm 3.5 \text{ cal mol}^{-1} \text{ K}^{-1}$$

**H: Calculation of the  $E_a$ ,  $\Delta H^\ddagger$  and  $\Delta S^\ddagger$  for the [1,5]-sigmatropic rearrangement of 1-(2-thienyl)-2,3,4,5-tetraphenyl-2,4-cyclopentadien-1-ol (55).**

Temperature		$k$	$1/T$		
$^\circ\text{C}$	$^\circ\text{K}$	$\text{sec}^{-1}$	$^\circ\text{K}^{-1}$	$\log k$	$\log(k/T)$
175.0	448.15	$6.46 \times 10^{-5}$	$2.231 \times 10^{-3}$	-4.190	-6.841
190.0	463.15	$2.16 \times 10^{-4}$	$2.159 \times 10^{-3}$	-3.666	-6.331
205.0	478.15	$6.38 \times 10^{-4}$	$2.091 \times 10^{-3}$	-3.195	-5.875

$E_a$

Plotting  $\log k$  versus  $1/T$

$$\text{slope} = -7.11 \times 10^3$$

$$E_a = -4.576 \text{ cal mol}^{-1} \text{ K}^{-1} \text{ (slope)}$$

$$y_{\text{intercept}} = 11.67$$

$$E_a = 32.5 \pm 1.6 \text{ kcal mol}^{-1}$$

$$\text{corr} = -1.000$$

$\Delta H^\ddagger$  &  $\Delta S^\ddagger$

Plotting  $\log(k/T)$  versus  $1/T$

$$\text{slope} = -6.90 \times 10^3$$

$$\Delta H^\ddagger = -4.576 \text{ cal mol}^{-1} \text{ K}^{-1} \text{ (slope)}$$

$$y_{\text{intercept}} = 8.56$$

$$\Delta H^\ddagger = 31.6 \pm 1.6 \text{ kcal mol}^{-1} \text{ K}^{-1}$$

$$\text{corr} = -1.000$$

$$\Delta S^\ddagger = 4.576 \text{ cal mol}^{-1} \text{ K}^{-1} (y_{\text{intercept}} - 10.32)$$

$$\Delta S^\ddagger = -8.1 \pm 3.6 \text{ cal mol}^{-1} \text{ K}^{-1}$$

**I: Calculation of the  $E_a$ ,  $\Delta H^\ddagger$  and  $\Delta S^\ddagger$  for the [1,5]-sigmatropic rearrangement of 1-phenylethynyl-2,3,4,5-tetraphenyl-2,4-cyclopentadien-1-ol (55).**

Temperature		$k$	$1/T$	$\log k$	$\log(k/T)$
$^\circ\text{C}$	$^\circ\text{K}$	$\text{sec}^{-1}$	$^\circ\text{K}^{-1}$		
145.0	418.15	$7.38 \times 10^{-5}$	$2.391 \times 10^{-3}$	-4.132	-6.753
160.0	433.15	$2.72 \times 10^{-4}$	$2.309 \times 10^{-3}$	-3.565	-6.202
175.0	448.15	$9.70 \times 10^{-4}$	$2.231 \times 10^{-3}$	-3.013	-5.665

$E_a$

Plotting  $\log k$  versus  $1/T$

$$E_a = -4.576 \text{ cal mol}^{-1} \text{ K}^{-1} \text{ (slope)}$$

$$E_a = 32.0 \pm 1.4 \text{ kcal mol}^{-1}$$

$$\text{slope} = -6.99 \times 10^3$$

$$y_{\text{intercept}} = 12.59$$

$$\text{corr} = -1.000$$

$\Delta H^\ddagger$  &  $\Delta S^\ddagger$

Plotting  $\log(k/T)$  versus  $1/T$

$$\Delta H^\ddagger = -4.576 \text{ cal mol}^{-1} \text{ K}^{-1} \text{ (slope)}$$

$$\Delta H^\ddagger = 31.1 \pm 1.4 \text{ kcal mol}^{-1} \text{ K}^{-1}$$

$$\Delta S^\ddagger = 4.576 \text{ cal mol}^{-1} \text{ K}^{-1} (y_{\text{intercept}} - 10.32)$$

$$\Delta S^\ddagger = -3.7 \pm 3.2 \text{ cal mol}^{-1} \text{ K}^{-1}$$

$$\text{slope} = -6.80 \times 10^3$$

$$y_{\text{intercept}} = 9.50$$

$$\text{corr} = -1.000$$

**J: Calculation of the  $E_a$ ,  $\Delta H^\ddagger$  and  $\Delta S^\ddagger$  for the [1,5]-sigmatropic rearrangement of 1-vinyl-2,3,4,5-tetraphenyl-2,4-cyclopentadien-1-ol (55).**

Temperature		$k$	$1/T$		
$^\circ\text{C}$	$^\circ\text{K}$	$\text{sec}^{-1}$	$^\circ\text{K}^{-1}$	$\log k$	$\log(k/T)$
90.0	363.15	$2.82 \times 10^{-5}$	$2.754 \times 10^{-3}$	-4.550	-7.110
105.0	378.15	$1.10 \times 10^{-4}$	$2.644 \times 10^{-3}$	-3.959	-6.536
120.0	393.15	$5.18 \times 10^{-4}$	$2.544 \times 10^{-3}$	-3.286	-5.880

**$E_a$**

Plotting  $\log k$  versus  $1/T$

$$\text{slope} = -6.01 \times 10^3$$

$$E_a = -4.576 \text{ cal mol}^{-1} \text{ K}^{-1} \text{ (slope)}$$

$$y_{\text{intercept}} = 11.97$$

$$E_a = 27.5 \pm 1.5 \text{ kcal mol}^{-1}$$

$$\text{corr} = -0.998$$

**$\Delta H^\ddagger$  &  $\Delta S^\ddagger$**

Plotting  $\log(k/T)$  versus  $1/T$

$$\text{slope} = -5.85 \times 10^3$$

$$\Delta H^\ddagger = -4.576 \text{ cal mol}^{-1} \text{ K}^{-1} \text{ (slope)}$$

$$y_{\text{intercept}} = 8.97$$

$$\Delta H^\ddagger = 26.8 \pm 1.2 \text{ kcal mol}^{-1} \text{ K}^{-1}$$

$$\text{corr} = -0.998$$

$$\Delta S^\ddagger = 4.576 \text{ cal mol}^{-1} \text{ K}^{-1} (y_{\text{intercept}} - 10.32)$$

$$\Delta S^\ddagger = -6.2 \pm 3.2 \text{ cal mol}^{-1} \text{ K}^{-1}$$

**K: Calculation of the  $E_a$ ,  $\Delta H^\ddagger$  and  $\Delta S^\ddagger$  for the [1,5]-sigmatropic rearrangement of 1-*tert*-butyl-2,3,4,5-tetraphenyl-2,4-cyclopentadien-1-ol (55).**

Temperature		$k$	$1/T$		
$^\circ\text{C}$	$^\circ\text{K}$	$\text{sec}^{-1}$	$^\circ\text{K}^{-1}$	$\log k$	$\log(k/T)$
145.0	418.15	$5.01 \times 10^{-5}$	$2.391 \times 10^{-3}$	-4.300	-6.922
160.0	433.15	$1.59 \times 10^{-4}$	$2.309 \times 10^{-3}$	-3.799	-6.435
175.0	448.15	$4.83 \times 10^{-4}$	$2.231 \times 10^{-3}$	-3.316	-5.968

$E_a$

Plotting  $\log k$  versus  $1/T$

$$\text{slope} = -6.14 \times 10^3$$

$$E_a = -4.576 \text{ cal mol}^{-1} \text{ K}^{-1} \text{ (slope)}$$

$$y_{\text{intercept}} = 10.40$$

$$E_a = 28.1 \pm 2.2 \text{ kcal mol}^{-1}$$

$$\text{corr} = -1.000$$

$\Delta H^\ddagger$  &  $\Delta S^\ddagger$

Plotting  $\log(k/T)$  versus  $1/T$

$$\text{slope} = -5.97 \times 10^3$$

$$\Delta H^\ddagger = -4.576 \text{ cal mol}^{-1} \text{ K}^{-1} \text{ (slope)}$$

$$y_{\text{intercept}} = 7.33$$

$$\Delta H^\ddagger = 27.3 \pm 2.3 \text{ kcal mol}^{-1} \text{ K}^{-1}$$

$$\text{corr} = -1.000$$

$$\Delta S^\ddagger = 4.576 \text{ cal mol}^{-1} \text{ K}^{-1} (y_{\text{intercept}} - 10.32)$$

$$\Delta S^\ddagger = -13.7 \pm 5.2 \text{ cal mol}^{-1} \text{ K}^{-1}$$

L: Fractional Coordinates<sup>a,b</sup> for 40a.

Atom	X	Y	Z
C1	1.0547(1)	1.0134(1)	0.3794(2)
C2	1.1522(1)	0.9674(1)	0.3753(2)
C3	1.2291(1)	1.0404(1)	0.4489(2)
C4	1.1653(1)	1.1239(1)	0.4529(2)
C5	1.0697(1)	1.1076(1)	0.4294(2)
O6	0.9781(1)	0.9754(1)	0.3406(1)
C7	1.1441(1)	0.9210(1)	0.2285(2)
C8	1.1216(2)	0.9657(1)	0.1252(2)
C9	1.1101(2)	0.9220(2)	-0.0084(2)
C10	1.1204(2)	0.8349(2)	-0.0415(2)
C11	1.1429(2)	0.7900(1)	0.0587(2)
C12	1.1542(1)	0.8330(1)	0.1945(2)
C13	1.2974(1)	1.0414(1)	0.3706(2)
N14	1.3503(1)	1.0419(1)	0.3123(2)
C15	1.2887(1)	1.0277(1)	0.5927(2)
C16	1.3815(1)	0.9883(1)	0.6202(2)
C17	1.4277(2)	0.9674(1)	0.7454(2)
C18	1.3835(2)	0.9861(1)	0.8454(2)
C19	1.2938(2)	1.0273(2)	0.8214(2)
C20	1.2460(1)	1.0485(1)	0.6964(2)
C21	1.2091(1)	1.2085(1)	0.4796(2)
C22	1.3005(2)	1.2302(1)	0.5725(2)
C23	1.3396(2)	1.3097(2)	0.5929(3)
C24	1.2909(2)	1.3671(1)	0.5191(3)
C25	1.2020(2)	1.3453(1)	0.4200(2)
C26	1.1607(2)	1.2671(1)	0.4006(2)
C27	0.9906(1)	1.1703(1)	0.4526(2)
C28	1.0113(1)	1.2464(1)	0.5542(2)
C29	0.9374(2)	1.3032(2)	0.5791(2)
C30	0.8413(2)	1.2854(2)	0.5041(2)
C31	0.8190(1)	1.2103(1)	0.4071(2)
C32	0.8921(1)	1.1526(1)	0.3806(2)
H2	1.165(1)	0.925(1)	0.430(1)
H8	1.112(1)	1.027(1)	0.151(2)
H9	1.098(1)	0.955(1)	-0.077(2)
H10	1.109(1)	0.801(1)	-0.137(2)
H11	1.149(1)	0.731(1)	0.039(2)
H12	1.169(1)	0.802(1)	0.266(2)
H16	1.409(1)	0.975(1)	0.548(1)
H17	1.489(1)	0.940(1)	0.763(2)
H18	1.421(1)	0.969(1)	0.935(2)
H19	1.263(1)	1.043(1)	0.891(2)
H20	1.184(1)	1.077(1)	0.680(2)
H22	1.335(1)	1.190(1)	0.629(2)
H23	1.396(1)	1.325(1)	0.666(2)
H24	1.317(1)	1.427(1)	0.539(2)
H25	1.169(1)	1.388(1)	0.365(2)



L: Continued

Atom	X	Y	Z
H26	1.094(1)	1.249(1)	0.326(2)
H28	1.079(1)	1.257(1)	0.612(2)
H29	0.956(1)	1.356(1)	0.647(2)
H30	0.789(1)	1.328(1)	0.522(2)
H31	0.754(1)	1.197(1)	0.355(2)
H32	0.875(1)	1.101(1)	0.313(2)

<sup>a</sup>The standard deviations of the least significant figures are given in parentheses.

<sup>b</sup>Hydrogens are assigned the same numbers as the heavy atoms to which they are bonded.

M: Bond distances<sup>a</sup> in Angstroms (Å) of 40a.

Bond	Distance (Å)	Bond	Distance (Å)
C1 - C2	1.528(3)	C15 - C16	1.390(3)
C1 - C5	1.477(3)	C15 - C20	1.390(3)
C1 - O6	1.210(2)	C16 - C17	1.379(3)
C2 - C3	1.560(2)	C17 - C18	1.370(4)
C2 - C7	1.519(2)	C18 - C19	1.364(3)
C3 - C4	1.541(3)	C19 - C20	1.384(3)
C3 - C13	1.489(3)	C21 - C22	1.373(2)
C3 - C15	1.533(2)	C21 - C26	1.389(3)
C4 - C5	1.359(3)	C22 - C23	1.380(3)
C4 - C21	1.472(3)	C23 - C24	1.342(4)
C5 - C27	1.480(3)	C24 - C25	1.371(3)
C7 - C8	1.385(3)	C25 - C26	1.377(3)
C7 - C12	1.367(3)	C27 - C28	1.390(3)
C8 - C9	1.378(3)	C27 - C32	1.391(2)
C9 - C10	1.352(4)	C28 - C29	1.379(3)
C10 - C11	1.361(4)	C29 - C30	1.367(3)
C11 - C12	1.395(3)	C30 - C31	1.358(3)
C13 - N14	1.133(3)	C31 - C32	1.381(3)

<sup>a</sup>The standard deviations of the least significant figures of each distance are given in parentheses.

N: Bond angles<sup>a</sup> in Degrees of 40a.

Bond	Angle (deg)	Bond	Angle (deg)
C2 - C1 - C5	109.6(2)	C3 - C13 - N14	179.2(2)
C2 - C1 - O6	122.7(2)	C3 - C15 - C16	122.0(2)
C5 - C1 - O6	127.6(2)	C3 - C15 - C20	119.5(2)
C1 - C2 - C3	103.6(1)	C16 - C15 - C20	118.2(2)
C1 - C2 - C7	109.8(1)	C15 - C16 - C17	120.6(2)
C3 - C2 - C7	117.7(2)	C16 - C17 - C18	120.7(2)
C2 - C3 - C4	103.4(1)	C17 - C18 - C19	119.4(2)
C2 - C3 - C13	112.0(1)	C18 - C19 - C20	120.9(2)
C2 - C3 - C15	109.5(2)	C15 - C20 - C19	120.2(2)
C4 - C3 - C13	110.0(2)	C4 - C21 - C22	122.8(2)
C4 - C3 - C15	112.6(1)	C4 - C21 - C26	119.4(1)
C13 - C3 - C15	109.2(1)	C22 - C21 - C26	117.5(2)
C3 - C4 - C5	111.8(2)	C21 - C22 - C23	121.0(2)
C3 - C4 - C21	120.7(2)	C22 - C23 - C24	120.9(2)
C5 - C4 - C21	127.4(2)	C23 - C24 - C25	119.4(2)
C1 - C5 - C4	108.9(2)	C24 - C25 - C26	120.4(2)
C1 - C5 - C27	123.1(2)	C21 - C26 - C25	120.5(2)
C4 - C5 - C27	128.0(2)	C5 - C27 - C28	121.3(2)
C2 - C7 - C8	121.5(2)	C5 - C27 - C32	121.4(2)
C2 - C7 - C12	120.1(2)	C28 - C27 - C32	117.1(2)
C8 - C7 - C12	118.4(2)	C27 - C28 - C29	121.3(2)
C7 - C8 - C9	120.6(2)	C28 - C29 - C30	120.3(2)
C8 - C9 - C10	120.8(2)	C29 - C30 - C31	119.4(2)
C9 - C10 - C11	119.5(2)	C30 - C31 - C32	121.0(2)
C10 - C11 - C12	120.6(2)	C27 - C32 - C31	120.7(2)
C7 - C12 - C11	120.2(2)		

<sup>a</sup>The standard deviations of the least significant figures of each angle are given in parentheses.

O: Fractional Coordinates<sup>a,b</sup> for 41.

Atom	X	Y	Z
C1	0.4500(3)	0.1964(1)	1.0610(1)
C2	0.3278(2)	0.2056(1)	0.9849(1)
C3	0.4265(2)	0.2181(1)	0.9115(1)
C4	0.5780(2)	0.1785(1)	0.9471(1)
C5	0.5926(2)	0.1726(1)	1.0321(1)
O6	0.4294(2)	0.2018(1)	1.1343(1)
C7	0.2507(3)	0.1209(2)	0.9787(2)
C8	0.2126(2)	0.2730(1)	0.9913(1)
C9	0.2271(3)	0.3302(2)	1.0560(1)
C10	0.1160(3)	0.3883(2)	1.0613(2)
C11	-0.0091(3)	0.3910(2)	1.0018(2)
C12	-0.0238(3)	0.3364(2)	0.9364(2)
C13	0.0850(3)	0.2778(2)	0.9309(1)
C14	0.3591(3)	0.1732(1)	0.8348(1)
N15	0.3055(3)	0.1371(1)	0.7774(1)
C16	0.4491(2)	0.3093(1)	0.8903(1)
C17	0.5458(3)	0.3584(2)	0.9443(1)
C18	0.5661(3)	0.4397(2)	0.9264(2)
C19	0.4901(3)	0.4743(2)	0.8531(2)
C20	0.3952(3)	0.4269(2)	0.8000(2)
C21	0.3739(3)	0.3443(2)	0.8177(1)
C22	0.6860(2)	0.1529(1)	0.8910(1)
C23	0.6938(3)	0.1914(1)	0.8141(1)
C24	0.7939(3)	0.1648(2)	0.7621(1)
C25	0.8865(3)	0.0993(2)	0.7852(2)
C26	0.8793(3)	0.0595(2)	0.8604(2)
C27	0.7801(3)	0.0859(1)	0.9127(1)
C28	0.7243(3)	0.1504(1)	1.0946(1)
C29	0.7065(3)	0.0959(2)	1.1599(1)
C30	0.8265(3)	0.0787(2)	1.2215(1)
C31	0.9638(3)	0.1153(2)	1.2197(1)
C32	0.9831(3)	0.1688(2)	1.1554(1)
C33	0.8646(3)	0.1860(1)	1.0932(1)
H7A	0.322(2)	0.074(1)	0.970(1)
H7B	0.209(2)	0.111(1)	1.033(1)
H7C	0.172(2)	0.117(1)	0.931(1)
H9	0.311(2)	0.328(1)	1.100(1)
H10	0.135(2)	0.432(1)	1.109(1)
H11	-0.079(2)	0.431(1)	1.006(1)
H12	-0.115(2)	0.337(1)	0.896(1)
H13	0.074(2)	0.237(1)	0.885(1)
H17	0.602(2)	0.335(1)	0.992(1)
H18	0.630(2)	0.476(1)	0.963(1)
H19	0.512(2)	0.535(1)	0.846(1)
H20	0.344(2)	0.448(1)	0.750(1)
H21	0.308(2)	0.310(1)	0.778(1)
H23	0.634(2)	0.238(1)	0.797(1)

O: Continued

Atom	X	Y	Z
H24	0.795(2)	0.193(1)	0.711(1)
H25	0.955(2)	0.080(1)	0.750(1)
H26	0.942(2)	0.014(1)	0.877(1)
H27	0.776(2)	0.057(1)	0.965(1)
H29	0.612(2)	0.070(1)	1.160(1)
H30	0.809(2)	0.038(1)	1.265(1)
H31	1.048(2)	0.105(1)	1.263(1)
H32	1.080(2)	0.196(1)	1.155(1)
H33	0.878(2)	0.224(1)	1.051(1)

<sup>a</sup>The standard deviations of the least significant figures are given in parentheses.

<sup>b</sup>Hydrogens are assigned the same numbers as the heavy atoms to which they are bonded.

**P: Bond distances<sup>a</sup> in Angstroms (Å) of 41.**

Bond	Distance (Å)	Bond	Distance (Å)
C1 - C2	1.525(3)	C16 - C17	1.387(3)
C1 - C5	1.474(3)	C16 - C21	1.380(3)
C1 - O6	1.215(3)	C17 - C18	1.370(4)
C2 - C3	1.582(3)	C18 - C19	1.389(4)
C2 - C7	1.538(3)	C19 - C20	1.354(4)
C2 - C8	1.520(3)	C20 - C21	1.390(4)
C3 - C4	1.539(3)	C22 - C23	1.390(3)
C3 - C14	1.479(3)	C22 - C27	1.391(3)
C3 - C16	1.540(3)	C23 - C24	1.379(4)
C4 - C5	1.349(3)	C24 - C25	1.369(4)
C4 - C22	1.473(3)	C25 - C26	1.374(4)
C5 - C28	1.481(3)	C26 - C27	1.375(4)
C8 - C9	1.383(3)	C28 - C29	1.396(3)
C8 - C13	1.392(3)	C28 - C33	1.390(3)
C9 - C10	1.385(4)	C29 - C30	1.381(3)
C10 - C11	1.366(4)	C30 - C31	1.374(4)
C11 - C12	1.364(4)	C31 - C32	1.377(4)
C12 - C13	1.377(4)	C32 - C33	1.378(3)
C14 - N15	1.137(3)		

<sup>a</sup>The standard deviations of the least significant figures of each distance are given in parentheses.

Q: Bond angles<sup>a</sup> in Degrees of 41.

Bond	Angle (deg)	Bond	Angle (deg)
C2 - C1 - C5	109.5(2)	C11 - C12 - C13	120.5(2)
C2 - C1 - O6	124.8(2)	C8 - C13 - C12	121.1(2)
C5 - C1 - O6	125.5(2)	C3 - C14 - N15	178.0(3)
C1 - C2 - C3	100.9(2)	C3 - C16 - C17	120.5(2)
C1 - C2 - C7	103.2(2)	C3 - C16 - C21	121.5(2)
C1 - C2 - C8	115.9(2)	C17 - C16 - C21	118.3(2)
C3 - C2 - C7	111.3(2)	C16 - C17 - C18	121.0(2)
C3 - C2 - C8	114.6(2)	C17 - C18 - C19	120.2(2)
C7 - C2 - C8	110.2(2)	C18 - C19 - C20	119.2(2)
C2 - C3 - C4	103.4(2)	C19 - C20 - C21	121.0(2)
C2 - C3 - C14	110.2(2)	C16 - C21 - C20	120.3(2)
C2 - C3 - C16	113.1(2)	C4 - C22 - C23	122.1(2)
C4 - C3 - C14	109.6(2)	C4 - C22 - C27	119.9(2)
C4 - C3 - C16	110.3(2)	C23 - C22 - C27	117.9(2)
C14 - C3 - C16	110.1(2)	C22 - C23 - C24	120.7(2)
C3 - C4 - C5	110.8(2)	C23 - C24 - C25	120.3(2)
C3 - C4 - C22	121.2(2)	C24 - C25 - C26	120.0(3)
C5 - C4 - C22	128.0(2)	C25 - C26 - C27	120.0(2)
C1 - C5 - C4	109.5(2)	C22 - C27 - C26	121.0(2)
C1 - C5 - C28	119.9(2)	C5 - C28 - C29	119.6(2)
C4 - C5 - C28	130.6(2)	C5 - C28 - C33	121.8(2)
C2 - C8 - C9	122.9(2)	C29 - C28 - C33	118.5(2)
C2 - C8 - C13	119.6(2)	C28 - C29 - C30	120.0(2)
C9 - C8 - C13	117.5(2)	C29 - C30 - C31	120.7(2)
C8 - C9 - C10	120.8(2)	C30 - C31 - C32	119.9(2)
C9 - C10 - C11	120.5(2)	C31 - C32 - C33	120.1(2)
C10 - C11 - C12	119.5(2)	C28 - C33 - C32	120.9(2)

<sup>a</sup>The standard deviations of the least significant figures of each angle are given in parentheses.

R: Fractional Coordinates<sup>a,b</sup> for 45b.

Atom	X	Y	Z
C1	1.0674(3)	0.3141(0)	0.1114(3)
C2	1.1852(3)	0.2179(6)	0.1313(2)
C3	1.2253(3)	0.2427(5)	0.2615(2)
C4	1.1362(3)	0.3790(5)	0.2978(2)
C5	1.0498(2)	0.4178(6)	0.2131(2)
O6	0.9989(2)	0.2944(4)	0.0245(2)
C7	1.2587(3)	0.2964(6)	0.0507(2)
C8	1.2477(3)	0.4916(7)	0.0150(3)
C9	1.3132(4)	0.5627(9)	-0.0604(3)
C10	1.3885(3)	0.4449(10)	-0.1012(3)
C11	1.4011(3)	0.2527(10)	-0.0668(3)
C12	1.3360(3)	0.1780(7)	0.0102(3)
N13	1.1716(2)	0.0039(5)	0.1245(2)
N14	1.1717(3)	-0.0769(5)	0.2275(2)
N15	1.2041(2)	0.0399(5)	0.3070(2)
C16	1.3466(3)	0.3032(6)	0.3014(2)
C17	1.3778(3)	0.5002(6)	0.3016(3)
C18	1.4911(3)	0.5532(7)	0.3360(3)
C19	1.5710(3)	0.4154(8)	0.3724(4)
C20	1.5404(3)	0.2211(8)	0.3736(4)
C21	1.4295(3)	0.1651(6)	0.3376(3)
C22	1.1473(2)	0.4461(6)	0.4163(2)
C23	1.1928(3)	0.3227(6)	0.5061(3)
C24	1.1963(3)	0.3852(8)	0.6161(3)
C25	1.1581(3)	0.5688(9)	0.6393(3)
C26	1.1163(3)	0.6940(8)	0.5510(3)
C27	1.1115(3)	0.6337(6)	0.4409(3)
C28	0.9436(3)	0.5330(7)	0.2120(3)
H8	1.193(2)	0.568(6)	0.040(2)
H9	1.308(3)	0.697(6)	-0.085(3)
H10	1.430(3)	0.483(6)	-0.156(3)
H11	1.454(3)	0.153(6)	-0.094(3)
H12	1.347(2)	0.035(6)	0.039(2)
H13	1.139(2)	-0.058(5)	0.060(2)
H17	1.323(2)	0.606(5)	0.276(2)
H18	1.512(2)	0.691(6)	0.336(2)
H19	1.649(2)	0.447(5)	0.393(2)
H20	1.590(2)	0.123(5)	0.407(2)
H21	1.408(2)	0.036(5)	0.339(2)
H23	1.222(2)	0.195(5)	0.489(2)
H24	1.228(2)	0.293(6)	0.676(2)
H25	1.160(3)	0.612(5)	0.718(2)
H26	1.090(2)	0.823(6)	0.563(2)
H27	1.085(2)	0.717(5)	0.380(2)



**R: Continued**

Atom	X	Y	Z
H28A	0.925(2)	0.541(5)	0.282(2)
H28B	0.946(2)	0.658(5)	0.189(2)
H28C	0.885(2)	0.459(5)	0.165(2)

<sup>a</sup>The standard deviations of the least significant figures are given in parentheses.

<sup>b</sup>Hydrogens are assigned the same numbers as the heavy atoms to which they are bonded.

S: Bond distances<sup>a</sup> in Angstroms (Å) of 45b.

Bond	Distance (Å)	Bond	Distance (Å)
C1 - C2	1.532(4)	C10 - C11	1.370(9)
C1 - C5	1.456(4)	C11 - C12	1.401(6)
C1 - O6	1.217(3)	N13 - N14	1.353(4)
C2 - C3	1.563(4)	N14 - N15	1.251(4)
C2 - C7	1.511(5)	C16 - C17	1.390(6)
C2 - N13	1.464(5)	C16 - C21	1.378(5)
C3 - C4	1.529(5)	C17 - C18	1.392(5)
C3 - N15	1.519(5)	C18 - C19	1.354(6)
C3 - C16	1.502(4)	C19 - C20	1.370(7)
C4 - C5	1.344(4)	C20 - C21	1.374(5)
C4 - C22	1.477(4)	C22 - C23	1.400(5)
C5 - C28	1.488(5)	C22 - C27	1.393(6)
C7 - C8	1.393(6)	C23 - C24	1.381(5)
C7 - C12	1.375(6)	C24 - C25	1.373(8)
C8 - C9	1.381(6)	C25 - C26	1.383(6)
C9 - C10	1.356(7)	C26 - C27	1.375(5)

<sup>a</sup>The standard deviations of the least significant figures of each distance are given in parentheses.

T: Bond Angles<sup>a</sup> in Degrees of 45b.

Bond	Angle (deg)	Bond	Angle (deg)
C2 - C1 - C5	109.7(2)	C7 - C8 - C9	120.0(4)
C2 - C1 - O6	123.3(3)	C8 - C9 - C10	121.0(5)
C5 - C1 - O6	126.8(3)	C9 - C10 - C11	119.9(4)
C1 - C2 - C3	102.9(3)	C10 - C11 - C12	120.0(5)
C1 - C2 - C7	111.7(3)	C7 - C12 - C11	120.2(5)
C1 - C2 - N13	108.9(2)	C2 - N13 - N14	111.7(3)
C3 - C2 - C7	119.4(3)	N13 - N14 - N15	113.0(3)
C3 - C2 - N13	100.1(3)	C3 - N15 - N14	110.5(3)
C7 - C2 - N13	112.8(3)	C3 - C16 - C17	120.5(3)
C2 - C3 - C4	104.0(2)	C3 - C16 - C21	121.0(3)
C2 - C3 - N15	102.7(3)	C17 - C16 - C21	118.5(3)
C2 - C3 - C16	117.4(3)	C16 - C17 - C18	119.7(4)
C4 - C3 - N15	106.3(3)	C17 - C18 - C19	120.7(4)
C4 - C3 - C16	115.0(3)	C18 - C19 - C20	119.7(4)
N15 - C3 - C16	110.1(3)	C19 - C20 - C21	120.5(4)
C3 - C4 - C5	112.6(3)	C16 - C21 - C20	120.7(4)
C3 - C4 - C22	120.7(2)	C4 - C22 - C23	121.0(3)
C5 - C4 - C22	126.7(3)	C4 - C22 - C27	120.5(3)
C1 - C5 - C4	109.7(3)	C23 - C22 - C27	118.5(3)
C1 - C5 - C28	119.5(2)	C22 - C23 - C24	119.8(4)
C4 - C5 - C28	130.7(3)	C23 - C24 - C25	121.1(4)
C2 - C7 - C8	119.9(3)	C24 - C25 - C26	119.5(4)
C2 - C7 - C12	121.3(4)	C25 - C26 - C27	120.2(4)
C8 - C7 - C12	118.8(4)	C22 - C27 - C26	120.9(3)

<sup>a</sup>The standard deviations of the least significant figures of each angle are given in parentheses.

**U: Retention Times and Mobile Phases for the 1-Substituted Alcohols.**

Alcohol	Retention Time	Mobile Phase
Phenyl (2)	11.1 min	99% Hexane / 1% MeOH
1-Naphthyl (24)	10.4 min	98% Hexane / 2% MeOH
2-Pyridyl (25)	7.6 min	94% Hexane / 3% MeOH 2% <i>i</i> -PrOH / 1% Acetic Acid
2-Furyl (26)	9.4 min	98% Hexane / 2% MeOH
2-Thienyl (27)	9.1 min	98% Hexane / 2% MeOH
Phenylethynyl (28)	11.4 min	98% Hexane / 2% MeOH
Vinyl (29)	9.4 min	98% Hexane / 2% MeOH
<i>tert</i> -Butyl (30)	9.0 min	99% Hexane / 1% MeOH

**The vita has been removed from  
the scanned document**